ENGINEERING GEOLOGICAL APPRAISAL OF KISHAU DAM PROJECT, GARHWAL HIMALAYA

A THESIS

submitted in fulfilment of the requirements for the award of the degree of

DOCTOR OF PHILOSOPHY

in

EARTH SCIENCES

By

TARUN KUMAR RAGHUVANSHI

DEPARTMENT OF EARTH SCIENCES
UNIVERSITY OF ROORKEE
ROORKEE-247 667 (INDIA)

MARCH, 1996

Gratis

CANDIDATE'S DECLARATION

I hereby certify that the work which is being presented in the thesis entitled **ENGINEERING GEOLOGICAL APPRAISAL OF KISHAU DAM PROJECT, GARHWAL HIMALAYA** in fulfilment of the requirement for the award of the Degree of Doctor of Philosophy and submitted in the **DEPARTMENT OF EARTH SCIENCES** of the University is an authentic record of my own work carried out during a period from **October, 1990** to **March, 1996** under the supervision of **Dr. R. ANBALAGAN** and **PROFESSOR S.S. SRIVASTAVA**.

The matter presented in this thesis has not been submitted by me for the award of any other degree of this or any other University.

Tarun Raghuvanshi

TARUN KUMAR RAGHUVANSHI

This is to certify that the above statement made by the candidate is correct to the best of our knowledge.

26/3/96

DR. R. ANBALAGAN
Lecturer
Department of Earth Sciences
University of Roorkee
ROORKEE - 247 667
INDIA

26/3/96

DR. S.S SRIVASTAVA
Professor
Department of Earth Sciences
University of Roorkee
ROORKEE - 247 667
INDIA

Date :

The Ph.D Viva-Voce examination of **Mr. Tarun Kumar Raghuvanshi** Research Scholar, has been held on 11.4.99

11/4/99

Signature of Supervisor(s)

11/4/99

Signature of H.O.D.

11.4.99

Signature of External Examiner

ACKNOWLEDGEMENT

I express my feelings of profound gratitude to my supervisor and guide **Dr. R. Anbalagan**. His immense interest in my work, constant counselling, unflinching support, meaningful help and scholarly suggestions were of immense help in completing this research work. Besides, he extended financial support from his research grants at his disposal.

I do not have adequate words to express my feelings of gratitude to **Prof. S.S. Srivastava** whose benevolent guidance and constant encouragement during the present investigation could help me to complete my work. He is the person who has always appreciated my work and encouraged me.

The unrestricted, prompt & generous help, constructive criticism and valuable technical suggestions extended by **Prof. Bhawani Singh** is very heartily acknowledged. I must appreciate his most cordial attitude in helping me, whenever, I approached him despite his many pre-occupations.

I wish to express my sincere thanks to Late **Prof. R.K. Goel** whose constant encouragement and fruitful advice made me strong enough to do my work with full confidence.

I am grateful to **Prof. S.K. Upadhyay**, Head of the Department and **Prof. A.K. Jain** (Ex-Head of the Department), Department of Earth Sciences, University of Roorkee, Roorkee for their help, constant encouragement and cooperation, which gave me strength for carrying out this investigation.

Unrestricted and continued encouragement imparted by **Prof. A.K. Awasthi, Prof. Ramesh Chander, Prof. V.N. Singh, Prof. Brahm Parkash, Dr. D.C.Srivastava and Dr. A.K. Saraf** is heartily acknowledged. I am also grateful to all other teaching faculty members and staff of Earth Sciences Department, from whom I have learnt and got benefited immensely during my stay.

A man of substance and knowledge who has encouraged me constantly is my respected **Prof. R.C. Bhatnagar**. I am emotionally indebted to him.

A friend in need is a friend indeed- (Dr.) **Sanjeev Sharma** (Sanju) my only best friend, who stood like a light house and he not only enlightened my path with his immense knowledge but he also put me to the right path. Few words cannot express my feelings for his greatness. Still, I am trying to acknowledge the great job that he has done for me. Mrs. Meenakshi, his wife, with her billion dollar smile and cups & cups of tea always encouraged me. I am emotionally indebted and grateful to her. I am heartily indebted for the caring and silent help extended to me by Malivika.

A caring and daring man who happens to be my friend, **Jay Ram Sahoo** (Motu), has helped me a lot, inspite of his own research activities and busy schedule. I heartily acknowledge the brotherly support offered by him.

I am obliged to the support provided to me by Pankaj Sir. The help and encouragement provided by Mrs. Neelam is also duly acknowledged.

I am further obliged for the help provided to me, from time to time, by Mr. S. Maheshwari. The help extended by him in the early stage of this research work is duly acknowledged. The love & affection shown by Master Rishu helped me a lot during the course of this work, thanks for his silent help.

Thanks are also due to my colleagues, for whom, I have no words appropriate enough to express my feelings; Anurag Khanna (Khanna ji), Dr. L.P. Singh, Dr. Sandeep Singh, Dr. H.N. Sinha, Dr. P.K.S. Chauhan, Dr. Vineet, Dr. (Mrs) Kalpna, Dr. Irfan Ullah, Dr. A.K. Seth, Dr. B.K. Bhadra, Tamal Sir, Semwal ji, Poojari, Thomas, Ajay, Sundaram, Miss Anupma, Tyagi ji, Pushpendra, Premanand, Debi, N.C.N. Srivastava, Bhisham, Pramod, Atanu, Anirban, Vikrant, Bhawani, Biswal, Prabeer and many others.

I am further obliged to Mr. A.R.J.G. Nair (Nair ji) for his brotherly cooperation and extraordinary help offered in finalising this research work.

I am thankful to Mr. Kamesh Gupta, from whom, I have learned the language of lines and was able to draft all the drawings myself, presented in this thesis.

Thanks are also due to M/s Atul Printers, Mr. Rajpal, Basant, Kishan ji and Sukhram for the silent help that they have extended to me.

I would be failing in my duties without acknowledging the willing cooperation of the Kishau Dam project authorities, especially Dr. K.N. Mutreja, Mr. M.N. Yadav and Mr. Shivpujan Singh, for providing all logistic support during several field visits.

I am also thankful to the officials and staff of P.W.D. and Forest Department for providing accommodation in various guest houses during my field visits.

The Jaunsaris, people of my study area have helped me a lot during my field work. The strength to bear the toughness of the Himalaya, I have learnt from them. I am thankful to them for the love and affection they have showed during my field work.

I offer my special thanks to respected Srivastava Aunti who has been a source of constant encouragement and inspiration to me.

I owe special thanks to respected Mrs. Anbalagan, Mrs. Bhatnagar, Mr. H.K. Sharma & Aunti, Dr. Suman Batra & Mrs Batra, Mrs. & Mr.Virmani who have been a constant source of encouragement.

Thanks are also due to respected Dr. Indrajeet Singh, Mrs. Reeta, Mr. Gaurav & Mr. Shailendra along with their wives, dear Anshu & Summi, dear Raju & Anita for the love and encouragement they have shown to me.

Words cannot express the feelings which I have for my parents in particular. I am highly indebted to them for their blessings, guidance, advice, encouragement, caring and moral support.

Thanks are also due to my only younger brother Mr. Shailendra (Vinky), for his continuous support and encouragement.

My in-laws, particularly my father-in-law Dr. S. K. Rajput, do deserve a special mention for their perennial encouraging blessings and moral support.

Behind every **man** there stands a **woman** telling that you are right or wrong - **Meenakshi,** my wife, who not only encouraged me but spared me from all homely responsibilities. Thanks are due to her for the sacrifices and patience that she has shown adequately.

Lastly, but not the least, I am grateful to the caring smiles and cries of my five months old daughter **Goli** (Shubha) who gave me immense strength in the final phase of this work.

Tarun Raghuvanshi

TARUN K. RAGHUVANSHI

ABSTRACT

With the increasing demand for power, the activities on river valley projects have been accelerated in the recent times. The Himalaya, which holds an enormous hydro-electric power potential provides many favourable sites for the construction of river valley projects. Number of schemes have already been implemented to harness the vast power and irrigation potential in this region and many more are under planning and construction.

Kishau dam project, one of the major river valley projects, envisages the construction of a 236m high concrete gravity dam, across the river Tons with a surface power house of 600 MW of peak power. The dam site is located near village Samberkhera (30° 39' 39" : 77° 46' 55") in Dehradun District of Uttar Pradesh, India.

The present research work is aimed to evaluate the engineering geological problems which may arise during or after the construction of Kishau dam. The study has been carried out under three broad heads.

a) Engineering geological evaluation of suitability of the dam foundation
b) Engineering geological evaluation of suitability of the power house site.
c) Assessment of stability of hill slopes around the dam reservoir.

On the basis of the surface and sub-surface investigations carried out at the dam site, an evaluation of the dam foundation condition has been presented. The dam foundation area has been mapped on 1:2000 scale. In the river section of the foundation of the dam, quartzitic slates with interbands of purple quartzites are present. Purple quartzite and white quartzite are exposed on the dam abutments. The rocks at the dam site are folded into an assymetrical upright anticlinal fold. The dam foundation falls on the hinge zone of the assymetrical anticlinal

fold. The foundation rocks are highly fractured due to folding. The Tons thrust, a major structural feature of the area cuts across the right bank at the dam site between El. 845 m to 850 m and enters into the adjoining Meera river valley. It dips at 15° to 25° in Southwesterly direction and is associated with large scale shearing. The thrust will be submerged under the maximum reservoir level of 860 m. The interpretation of the drill hole data has revealed that the fluvial overburden in the river bed section ranges from 3.65 m to 11.8 m. On the basis of limited water pressure test data, it is estimated that the foundation rocks are semipervious to pervious in nature. The stability analysis of abutments has revealed that the left abutment slope is kinematically unstable for plane mode of failure. The plane failure analysis for right abutment slope has been carried out by modifying the analytical technique of Hoek & Bray, where the effects of inclined upper slope surface and tension crack have been incorporated. In order to improve the overall foundation condition, suitable remedial measures have been evolved.

The Kishau dam project envisages the construction of a surface power house with an installed capacity of 600 MW of peak power, on the left bank of Tons river. For housing the power units, a terrace (22 x 70 m) has to be created by excavating the adjoining hill slopes. The stability analysis of hill slopes adjoining the power house site has revealed that the slopes are stable. Based on the stability analysis, a cut slope design has been suggested in addition to suitable stability measures. In view of the problems arising due to Jamar stream flowing in the centre of the site, an alternate site has been identified about 75 m downstream of the present one.

The reservoir area has been mapped on 1:15,000 scale. The rocks belonging to Dharagad Group (Limestone, Quartzite and Slate), Deoban Group (Limestone, Slates and Quartzite), Simla Group (Quartzite and Quartzitic slates) and Jaunsar Group (Slates) are exposed in the reservoir area. For the stability analysis, the data pertaining to structural discontinuities, mainly joints, has been collected from 100 localities. In the entire reservoir area 70 potentially unstable slopes have been identified for detailed stability analysis. A computer program ROSS has been developed to identify the possible plane and wedge mode of failures. Besides, four slopes, having rotational mode of failure, have also been studied. The detailed analysis has been carried out for both natural and water impoundment conditions. An attempt has been made to study the possible impacts of these unstable slopes on the stability of dam in the event of failures.

CONTENTS

LIST OF TABLES

CHAPTER IV

CHAPTER V

LIST OF FIGURES

CHAPTER IV

LIST OF PLATES

CHAPTER IV

CHAPTER V

CHAPTER I

INTRODUCTION

Power plays a vital role in imparting momentum to the economic development of any nation. It plays a crucial role in industry, agriculture and domestic sector. Among the three major sources of electricity generation namely thermal, hydroelectric and nuclear, hydroelectric power is the cheapest and renewable with minimum environmental hazards to the mankind.

Though, the power production in India has made significant and impressive strides since independence, it has not been able to bridge the demand supply gap. Therefore, with increasing demand of power, the activities on river valley projects have been accelerated in recent times.

1.1 HYDRO ELECTRIC POWER DEVELOPMENT IN INDIA

The total installed capacity of the country as on March, 1993 was 72319.46 MW. While the hydro electric power accounts for 19568.76 MW (27%), the major share of power generation was through thermal source, which accounted for 50,745.7 MW (70%). The total estimated potential for hydro electric power is about 84,044 MW at 60% load factor. Out of this potential, only 19568.76 MW was developed by March, 1993. (The Hindustan Times June, 28, 1993). India holds an enormous hydro electric power potential through its great river systems. The major river basins are divided into six groups namely, the Indus, the Bramhaputra, the Ganga,

West flowing peninsular rivers, Central Indian rivers and East flowing peninsular rivers. The hydro power schemes operating over these river basins have, so far harnessed only about 14.14 percent of the estimated potential.

In order to harness the enormous untapped water resources of Himalaya, a number of schemes have already been implemented. Many more are under planning and construction. The various schemes operating or in planning and construction stages in the Tons and the Yamuna valleys are listed in Table 1.1.

TABLE 1.1 HYDRO POWER DEVELOPMENT IN THE TONS AND THE YAMUNA VALLEYS

S.No.	Project Name	Type of Project	Installed Capacity	River
Under Operation				
1.	Chibro	ROR	240 MW	Tons
2.	Khodri	ROR	120 MW	Tons
3.	Dhakrani	ROR	84 MW	Yamuna
4.	Dhalipur	ROR	51 MW	Yamuna
5.	Kulhal	ROR	65 MW	Yamuna
6.	Khara	ROR	160 MW	Yamuna
Under Construction				
7.	Lakhwar Vyasi I	SD	300 MW	Yamuna
8.	Lakhwar Vyasi II	ROR	120 MW	Yamuna
Under Planning				
9.	Chami Naingaon	SD	126 MW	Yamuna
10.	Kishau	SD	600 MW	Tons
11.	Tiuni Plasu	ROR	50 MW	Tons
ROR - Run of the River , SD - Storage Dam				

The Yamuna river and its major tributary the Tons, holds a vast hydro power and irrigation potential. The river Yamuna runs through the states of Uttar Pradesh, Himachal Pradesh and Haryana. The river Yamuna descends into the plains near Dakpathar and traverses through the fertile plains of Uttar Pradesh and Haryana, where, it is essentially responsible for the irrigation. Delhi, the capital of India, and Agra are two important cities which are dependent on the Yamuna for domestic water supply. During lean seasons, particularly, during summers,

the water discharge gets considerably reduced causing acute problems for irrigation and domestic water supply. Moreover, during flood seasons, the low lying colonies of Delhi, often get submerged. Hence, the construction of Kishau Dam and Lakhwar dam would not only help to augment the electricity production, but also regulate the water discharge in the down reaches to avoid the adverse effects of draught and floods.

1.2 GENERAL ENGINEERING GEOLOGICAL PROBLEMS OF HYDRO POWER DEVELOPMENT IN HIMALAYA

Though the Himalaya holds an enormous hydroelectric potential, still much of it is yet to be harnessed because of the complicated engineering geological problems, generally, associated with the Himalayan terrain.

Himalaya, represents the abduction zone, where, the under thrusting is still in progress. The area, often, experiences high order seismic activities. Moreover, the tectonically active Himalayan terrain consists of fragile rocks which have been traversed by many sets of structural discontinuities, as many as , four sets of discontinuities, in addition to random ones at many places. Moreover, it is commonly observed that the rocks are alternatively banded with competent beds and incompetent beds. A combination of all these factors result in extensive foundation treatments, while constructing hydro development projects. In addition to this, stability problems of the rock slopes are to be properly studied and evaluated before taking up the construction activities.

1.3 SEISMICITY

The study area falls in the Zone IV of the Seismic zoning map of India, prepared by the Bureau of Indian Standards. The Kishau dam area falls within the Rossi-Forrel intensity VIII isoseismal of Kangra earthquake of 1905. The secondary epicentre of Kangra earthquake was in the Mussoorie-Dehradun region. However, no published records of the damage caused by this earthquake in the study area are available.

Another strong earthquake of 6.6 intensity occurred in Uttarkashi on 20th October, 1991. Due to this earthquake, some of the poorly built houses, in the villages Samberkhera, Kota, Manjgaon were damaged, causing minor cracks on the walls of the houses. Besides these two strong earthquakes many small magnitude earthquakes have also been reported in the

adjoining areas. In view of the above fact, the stability analysis for slopes, in the study area, have been carried out, incorporating the horizontal acceleration induced by the earthquake, as an equivalent static force αW, where `α' is the horizontal acceleration (α = 0.15 g) and W is the weight of the rock block.

1.4 PROFILE OF THE STUDY AREA

The study area forms a part of the Jaunsar-Bawar region, a name well known since British times. The Tons and the Yamuna rivers form the Western and Eastern extremities of this region respectively. This region falls in the Dehradun District of Uttar Pradesh. The Jaunsar-Bawar region is a land of pine clad slopes, lofty snow covered peaks and above all, the long narrow V-shaped Tons and Yamuna Valleys, which attract a large number of tourists every year. These rivers, which hold an enormous hydroelectric power potential, provide favourable sites for river valley projects.

1.4.1 LOCATION

The Kishau dam is being planned across the Tons river, near Samberkhera village (Plate 1) defined by the coordinates (30° 39' 39" : 77°46'55"), about 45 km upstream of Dakhpathar in Dehradun District of Uttar Pradesh (Plate 1.1).

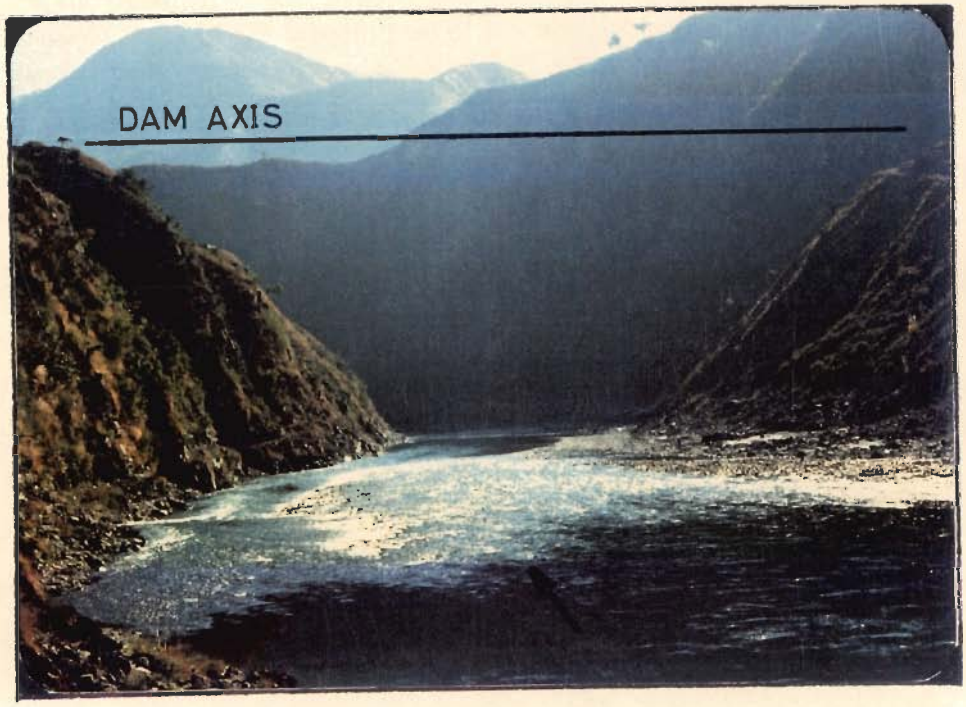

PLATE 1.1 DOWNSTREAM VIEW OF DAM SITE

The location of the Dam site is shown in Fig.1.1. The 45 km long reservoir of the Kishau dam extends over the boundary of the Dehradun district and the Sirmaur district of Uttar Pradesh and Himachal Pradesh respectively. The study area falls in the Survey of India toposheet Nos.53 F/9, 53 F/10, 53 F/13 and 53 F/14. The reservoir area is shown in Fig.1.1

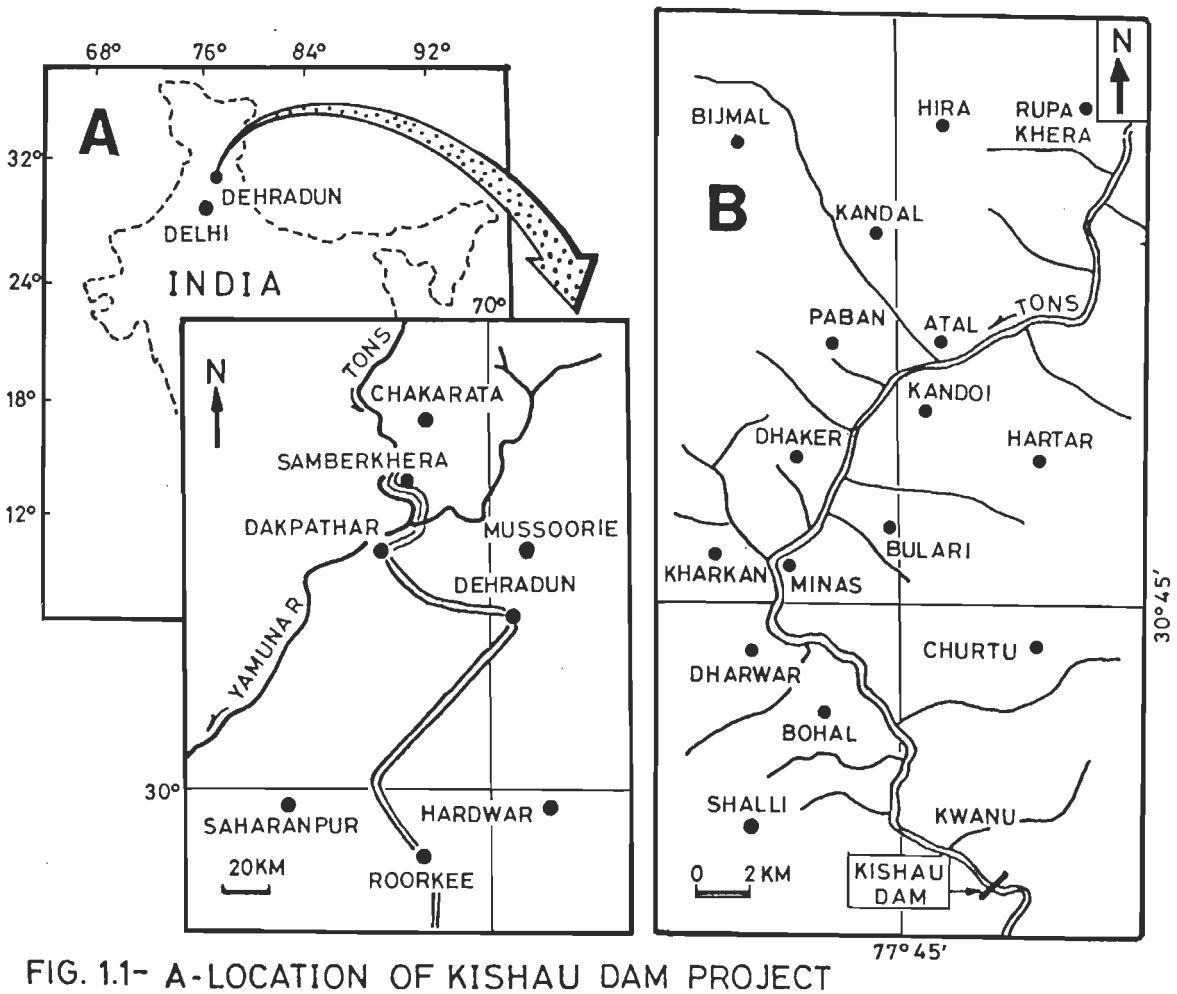

FIG. 1.1- A-LOCATION OF KISHAU DAM PROJECT
B-AREA OF STUDY

1.4.2 ACCESSIBILITY

The dam site is accessible from Dakhpathar by a 45 km long motorable road along the left bank of the Tons river. Besides, the dam site is also accessible by a 18 km unmetalled motorable road from Sahiya, which is connected to Dehradun by an all weather motorable road (Fig.1.1)

1.4.3 HISTORY OF THE PROJECT

The Kishau Dam Project was planned in 1940 and the preliminary investigations were initiated by the then Punjab Government during the period 1944-46. Initially, the dam site was selected at a narrow gorge near Kishau village about 38 km upstream of Dakpathar. However, the survey and investigations were abandoned in 1946. The surveys were resumed later, by the Uttar Pradesh Government in 1962. A preliminary Project, in favour of a double curvature type of dam with a power house of 500 MW installed capacity was proposed in the year 1964. Later, a detailed project was planned favouring a medium thick arch dam with a power house of 750 MW installed capacity. However, the detailed investigations revealed several geological weaknesses at the Kishau Site, rendering it unfavourable for the construction of a high arch dam. Moreover, the inundation of the site by the reservoir of Ichari dam, which came up downstream in the mean time, added to the existing problems of the Kishau site. Therefore, this site was rejected and an alternative site, near village Samberkhera was selected. The detailed investigation for a concrete gravity Dam at Samberkhera site were initiated in 1979 and are in progress.

1.4.4 TOPOGRAPHY

The topography of the area is highly rugged, characterised by high peaks, deep valleys and steep slopes (Fig.1.2). The major ridges in the study area, roughly trend North-South, while the minor cross ridges, originating from the main North-South trending ridges, generally trend East-West. The rectangular pattern of drainage discernible in this area indicates a structural control. Several peaks formed by the intersection of the major and minor ridges, have elevations varying between 1000 m to 2753 m , on the right bank, while 1230 m to 2530 m on the left bank of the Tons river. The highest peak on the right bank is 2753 m and located North of the Sainj Village. Similarly, the highest peak on the left bank is 2530 m and is located South-East of the Baila village. A part of ridge, originating from dam site area and extending upto the Shallai town, is shown through Plate 1.2.

1.4.5 RIVER SYSTEM

The Tons river originates from the confluence of the Lupin and the Supin rivers near village Sankri. The Tons river is the major tributary of the river Yamuna. The Tons river system consists of three major sub-basins, namely the Pabar,Bhangal and Meera rivers. Out of these, only the Minas river forms a part of the reservoir. Besides, the Bhangal, Shalongad and

PLATE 1.2 A PART OF RIDGE ORIGINATING FROM DAM SITE AREA AND EXTENDING UPTO THE SHALLAI TOWN

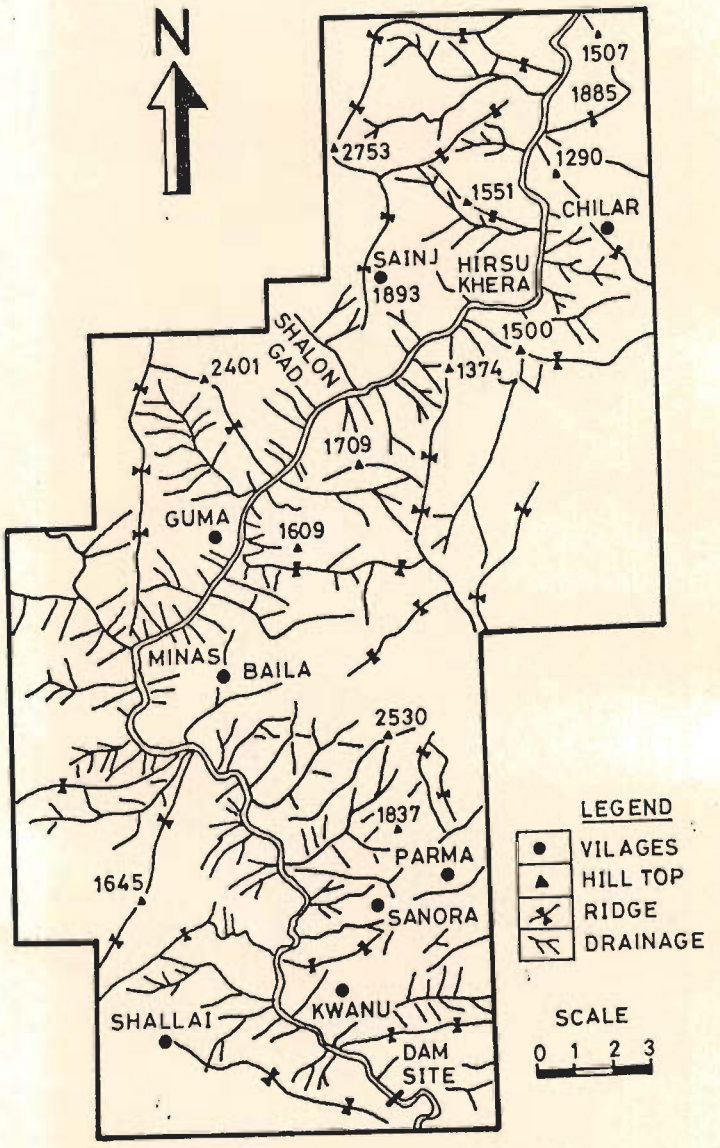

FIG. 1.2 TOPOGRAPHIC MAP OF THE STUDY AREA.

Daragad streams are also a part of the Tons river system. The confluence of these streams with the Tons river is shown in Plate 1.3.

The river Tons in the study area, flows roughly towards South. However, at Hirsukhera, it locally changes its course and flows in the Southwest direction upto Minas. Further down, it takes a right angle turn and flows in the Southeast direction upto the dam site, where, it is 80m wide.

PLATE 1.3 THE CONFLUENCE OF THE RIVER TONS WITH -
A - DHARAGAD STREAM B - SHALONGAD STREAM
C - MINAS RIVER

Just after the dam site, the Tons river makes a S-Shaped loop. The valley, just upstream of the dam site is wide and the slopes are relatively gentle.

Meera river, a tributary of the Tons, flowing on Southwestern side joins it about 3 km downstream of the dam axis. The two rivers are separated by a narrow ridge. The river bed levels of the Meera and Tons river along the dam axis are 690m and 641.5m respectively. The general gradient of the Tons river in the reservoir area is 4.78 m/km. The river gradient from the dam site to the reservoir end point is shown in Fig.1.3.

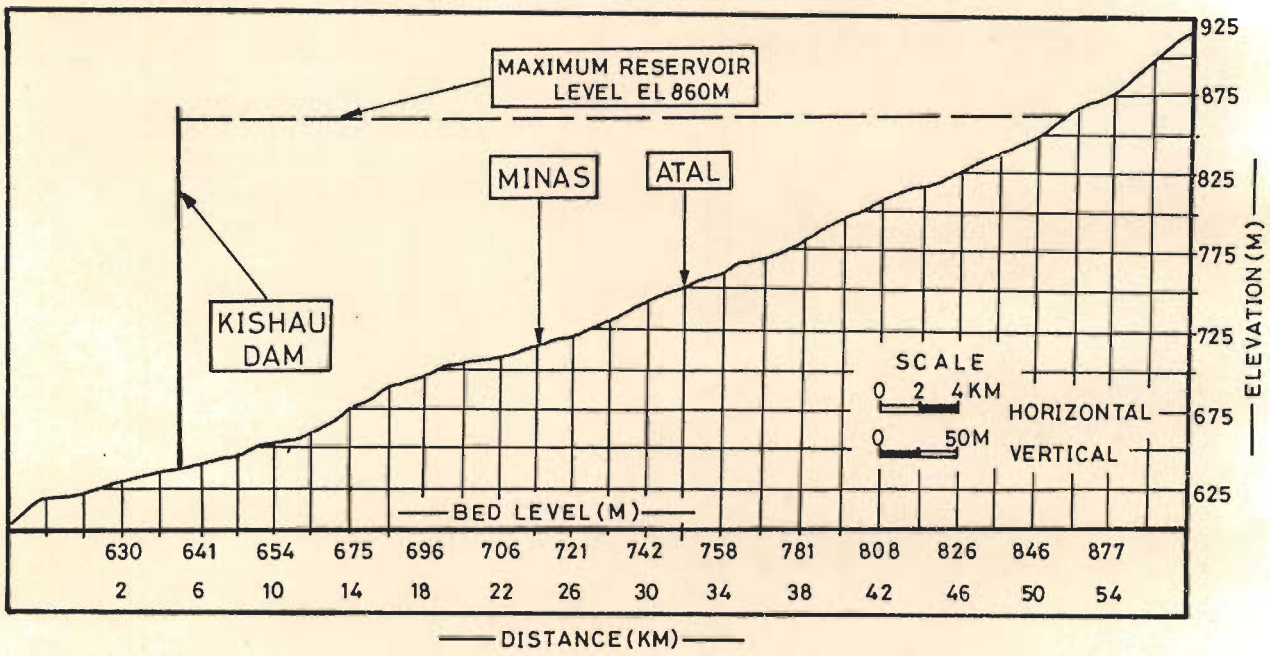

FIG. 1.3 'L' SECTION ALONG TONS RIVER FROM DAM SITE TO RESERVOIR END POINT

1.4.6 CLIMATE

The area of study falls in the Lesser Himalayan zone, which is characterised by the tropical monsoon climate. Long humid summers and cold dry winters are characteristics of the area.

The area receives substantial amount of rainfall, as the South-West monsoon changes its direction to North-West along the NW-SE trending Lesser Himalayan range. Thus, in the process, it looses most of the moisture in the form of rains while moving over the Lesser

Himalayan ranges. In the study area, maximum rainfall occurs between mid June to mid September. However, the normal annual rainfall in the area is about 1650mm. During winter season, the higher peaks receive snow, while low lying areas receive moderate rains between mid December and the month of January.

The average temperature, in the study area remains between 20° C to 30° C. The maximum temperature (35° C) is attained during the months of May-June and a minimum (5° C) during the months of December-January.

1.4.7 FLORA AND FAUNA

The natural vegetation follows a climate altitudinal zonation. The vegetation is characteristic of the Sub-Tropical (below 1200m) to Temperate zone (1200-1800m). Some of the important species in the area are Sal (Shorea robusta), Banj (Quercus incana), Oak (Quercus himalayansis), Chir (Pinus longifolia), Deodar (Cederus deodara). etc.

The hill tops, especially in the reservoir area, are comparatively covered with vegetation, while the valley slopes are generally devoid of vegetation cover. Small patches of shrubs, bushes, wild grasses and thorns are often seen on the valley slopes. On the gentler valley slopes, terraced cultivated fields are present.

The important crops cultivated in the area are wheat, paddy, mustard and maize. The vegetables raised on the terraced fields are potato, tomato, ginger, chilli, palak (Spinacea oleracea) etc.

The wild life in the area comprises fox, jackal, monkeys, bear etc. Among the domestic animals, cows, buffaloes, mules, donkeys, dogs, goats, oxen are the most common.

1.5 GENERAL LAYOUT OF THE PROJECT

The Kishau dam project envisages the construction of a concrete gravity dam across the river Tons and a surface power house of 600 MW of peak power. The general layout of the project is shown in Fig.1.4.

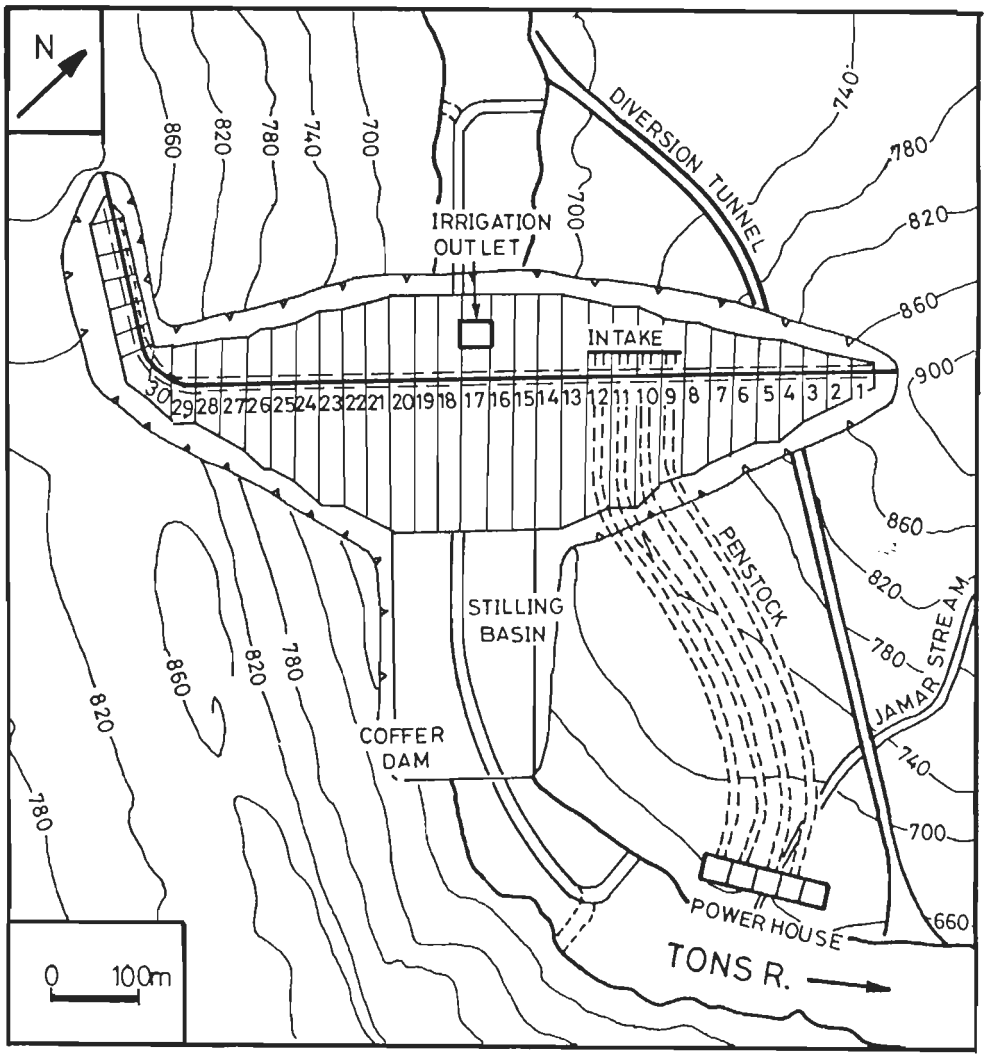

FIG. 1.4 GENERAL LAY OUT OF KISHAU DAM PROJECT

1.5.1 DAM

The concrete gravity dam would be 236 m high above the deepest foundation level. The base width of the dam would be 228 m and the chord length (crest length) would be 680 m. The deepest foundation level is kept at El. 632 m, whereas the top of the dam would be at 868 m. The width at the top of the dam would be 10 m. The cross section of the dam is shown in Fig.1.5.

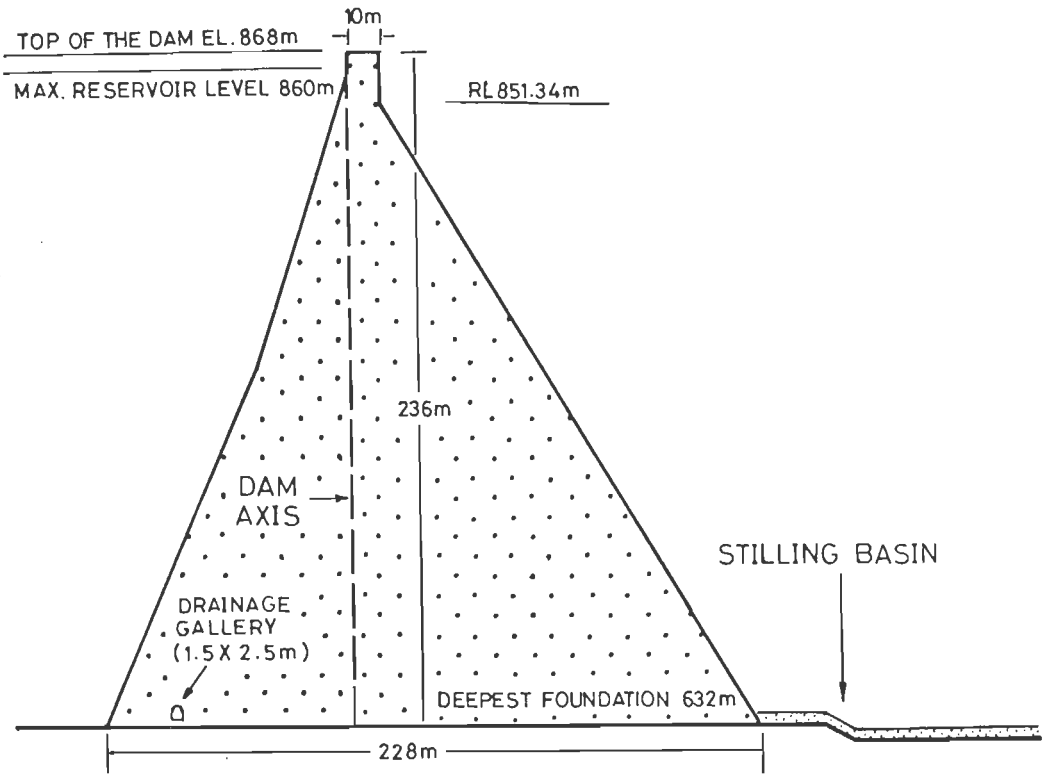

FIG. 1.5 CROSS SECTION OF THE DAM.

1.5.2 POWER HOUSE

For the Kishau dam project a surface power house, on the left bank of the river Tons, about a km downstream from the main dam site, is proposed. The power house would be located on a terrace of 70 x 22 m in dimensions and would have four power generating units of 150 MW each. These power units would be connected to four penstocks of diameter 5.75 m. These penstocks would be connected to the intake structure, located within the body of the dam.

1.5.3 SPILLWAY

A spillway with a total width 127 m would be located in the dam body. The spillway would be provided with 6 nos. of bay each having 17 m clear span. The crest level of spillway would be at El. 841.25 m. The design discharge of the spillway is 23019 cumecs. The each bay of the spillway would be provided with 6 nos. of tainter gates (17 x 19 m) of radial type.

A bridge would be provided over the spillway piers for the road and mounting a 15 tonne crane for lifting and lowering the stop logs. A cross section showing the Tainter gate of spillway is shown in Fig.1.6.

1.5.4 STILLING BASIN

A pool of standing water is necessary for providing a cushion to the jet falling from the flip bucket which would prevent the erosion of the downstream bed of river. For that purpose, a 218 m long and 120 m wide stilling basin would be provided.

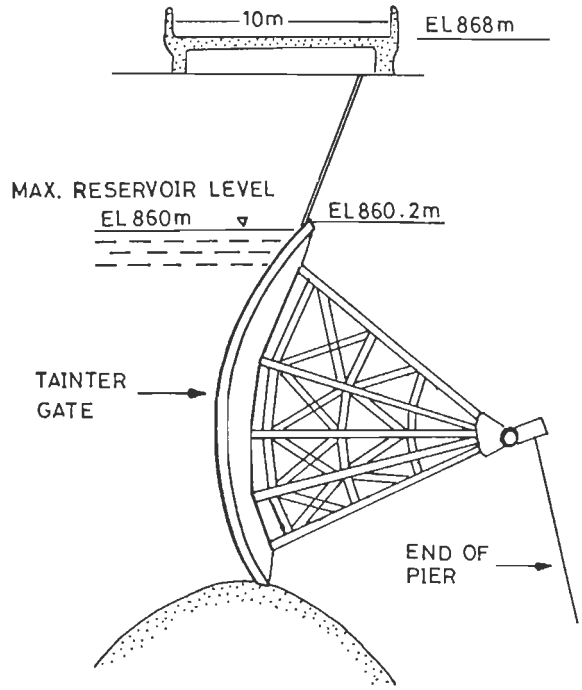

FIG. 1.6 TAINTER GATE OF KISHAU DAM SPILLWAY.

1.5.5 RIVER DIVERSION ARRANGEMENTS FOR CONSTRUCTION WORKS

For the construction works, the river water would be diverted through a 12 m high coffer dam and a tunnel of 7 m in diameter. The maximum non monsoon flood, observed in the year 1982 is of the order of 1200 cumecs. Therefore, the diversion works for non monsoon have been designed for 1200 cumecs. The length of the diversion tunnel would be 850 m and it would be located on the left bank of the river Tons. The intake of the diversion would be located close to the confluence of Samberkhera stream and the river Tons.

1.5.6 SALIENT FEATURES OF THE PROJECT

DAM	
Type of dam	Concrete gravity
Top level of dam	El. 868 m
River bed level	El. 642 m
Expected deepest foundation level	El. 632 m
Maximum height above deepest foundation level	236 m
Crest length of dam	680 m
Base width at foundation level	228 m
Width at top of dam	10 m
Crest level of spillway	El. 841.25 m
Intake location	In the dam body

POWER HOUSE	
Installed capacity	600 MW (4 x 150)
Location	On the left bank of the Tons river about 1km downstream
Penstock diameter and size	5.75 m, Four in no., connected to four intakes
RESERVOIR	
Normal maximum level	El. 860 m
Dead storage level	El. 779 m
Gross storage at El. 860 m	1810 x 10^6 cumecs
Dead storage at El. 779 m	480 x 10^6 cumecs
Live storage	1330 x 10^6 cumecs
Total area of villages likely to be submerged	1329 hectares
i) Cultivated area	512 hectares
ii) Uncultivated area	817 hectares
Persons to be rehabilitated	3972 Nos.
RIVER DIVERSION	
Top of coffer dam	El. 654 m
Diversion tunnel	one, 7 m in diameter on left bank
Average length of diversion tunnel	850 m
HYDROLOGY	
Normal annual rainfall	1650 mm
Maximum annual run-off (1984-85)	2833 x 10^6 cumecs
Maximum recorded monsoon flood (1955)	8210 cumecs
Maximum recorded non-monsoon flood (1978)	1200 cumecs
Source : Kishau Dam Project Authorities	

1.6 OBJECTIVES, METHODOLOGY AND ANALYTICAL TOOLS

1.6.1 OBJECTIVES

The present research program envisages the following major objectives

1. Engineering geological evaluation of suitability of dam foundation
2. Engineering geological evaluation of suitability of power house site.
3. Assessment of the stability of hill slopes around dam reservoir.

1.6.2 METHODOLOGY

In order to achieve the above mentioned objectives, the following methodology has been adopted:

1. Engineering geological evaluation of suitability of dam foundation:
   - i) Mapping of the dam site on 1:2000 scale.
   - ii) Subsurface exploration of foundation through,
     - a) Interpretation of 3-D logging of drifts in foundation rocks.
     - b) Interpretation of drill hole data.
   - iii) Assessment of permeability of foundation rocks.
   - iv) Slope stability analysis of the abutments.
   - v) Identification of possible remedial measures.

2. Engineering geological evaluation of suitability of power house site
   - i) Mapping of the power house site on 1:500 scale.
   - ii) Stability analysis of the slopes adjoining to power house site, proposed by the project authorities.
   - iii) Selection of an alternative site for the power house.
   - iv) Stability analysis of the slopes adjoining to alternative site.
   - v) Safe design and suitable remedial measures for the excavated slopes.

3. Assessment of stability of hill slopes around the dam reservoir:
   - i) Mapping of the reservoir area on 1:15,000 scale.
   - ii) Identification of potentially unstable slopes in the reservoir area.
   - iii) Determination of Factor of Safety for critical slopes under natural and water impoundment conditions.
   - iv) Determination of height of the water waves, generated by the possible slides, in the reservoir.

1.6.3 ANALYTICAL TOOLS

In the present study, the slopes having plane mode of failure have been analysed by modifying the analytical technique of Hoek and Bray (1981). Moreover, rotational and wedge failure analyses have been carried out by using computer programs. These computer programs and the modified technique for plane failure analysis, are based on the limit equilibrium methods. Besides, Geomechanics classification and empirical relations have also

been used to estimate the strength parameters of the rocks. The structural data, collected from the field, have been stereographically analysed.

1.7 SCHEME OF PRESENTATION

The research investigations carried out are presented in six chapters. A brief outline of each chapter is given below

Chapter I, **Introduction**: covers the hydro electric power development in India and General Engineering Geological problems of hydro power development in Himalaya. The profile of the study area includes location, accessibility, topography, river system, climate, flora & fauna and seismicity. Besides, objectives, methodology, analytical tools used, history of the project, general layout of the project and significance of the study are also presented in this Chapter.

Chapter II, **Geological Set Up**: mainly covers the regional geology and the geology around the study area. Besides, geology of the reservoir area and the dam site is also presented in this Chapter.

Chapter III, **Engineering Geological Studies of Dam Foundation**: includes exploratory drifting, drilling, assessment of permeability, engineering properties of rocks, stability analysis of abutments and finally, evaluation of foundation conditions and foundation treatments.

Chapter IV, **Engineering Geological Investigations of Power House Site**: covers the field investigations, engineering properties of rocks, stability analysis of the slopes adjoining the power house and the cut slope design for open excavation for power house. Besides, the investigations for an alternative site for power house are also covered in this Chapter.

Chapter V, **Slope Stability Studies of Reservoir Area**: mainly includes the stability analysis of the slopes around the reservoir. The stability analysis of potentially unstable slopes have been carried out for natural, as well as, for water impoundment conditions. The earthquake effect has also been incorporated in stability analysis. In addition, the height of wave, generated by the possible slide in the reservoir area and the effect of these waves on the stability of dam has also been presented in this Chapter.

Chapter VI, **Conclusions**: mainly include the discussion of the results and the conclusions drawn from these results.

CHAPTER II

GEOLOGICAL SET UP

2.1 REGIONAL GEOLOGY

The Himalaya has drawn the attention of a large number of investigators for over a century who endeavoured to work out the structural and tectonic patterns in this region. The results of these investigations have added to the knowledge and understanding of the complex geology of the Himalayan terrain.

The Himalaya is broadly divided into four principal East-West trending linear tectonic belts (Fig.2.1) on the basis of their characteristic geologic attributes (Shankar et al., 1989, Kumar et al., 1989). The Karakorum Belt is the Northern most (Table 2.1) which is followed in the south by the Ophiolitic melange and the plutonic zone of the Indus-Shyok Belt, followed in the south by the Main Himalayan Belt which has been further sub divided into two viz., Lesser Himalaya and Higher Himalaya. The Frontal Fold Belt is the Southern most Belt which consists essentially of the Tertiary rocks of the foreland basin.

On the basis of lithological assemblages, grade of metamorphism, limited radiometric data, emplacement of granites, presence of diagnostic sedimentary structures and presence of unconformities, eleven different stacks of sedimentary cycles have been identified (Shankar et al., 1989).

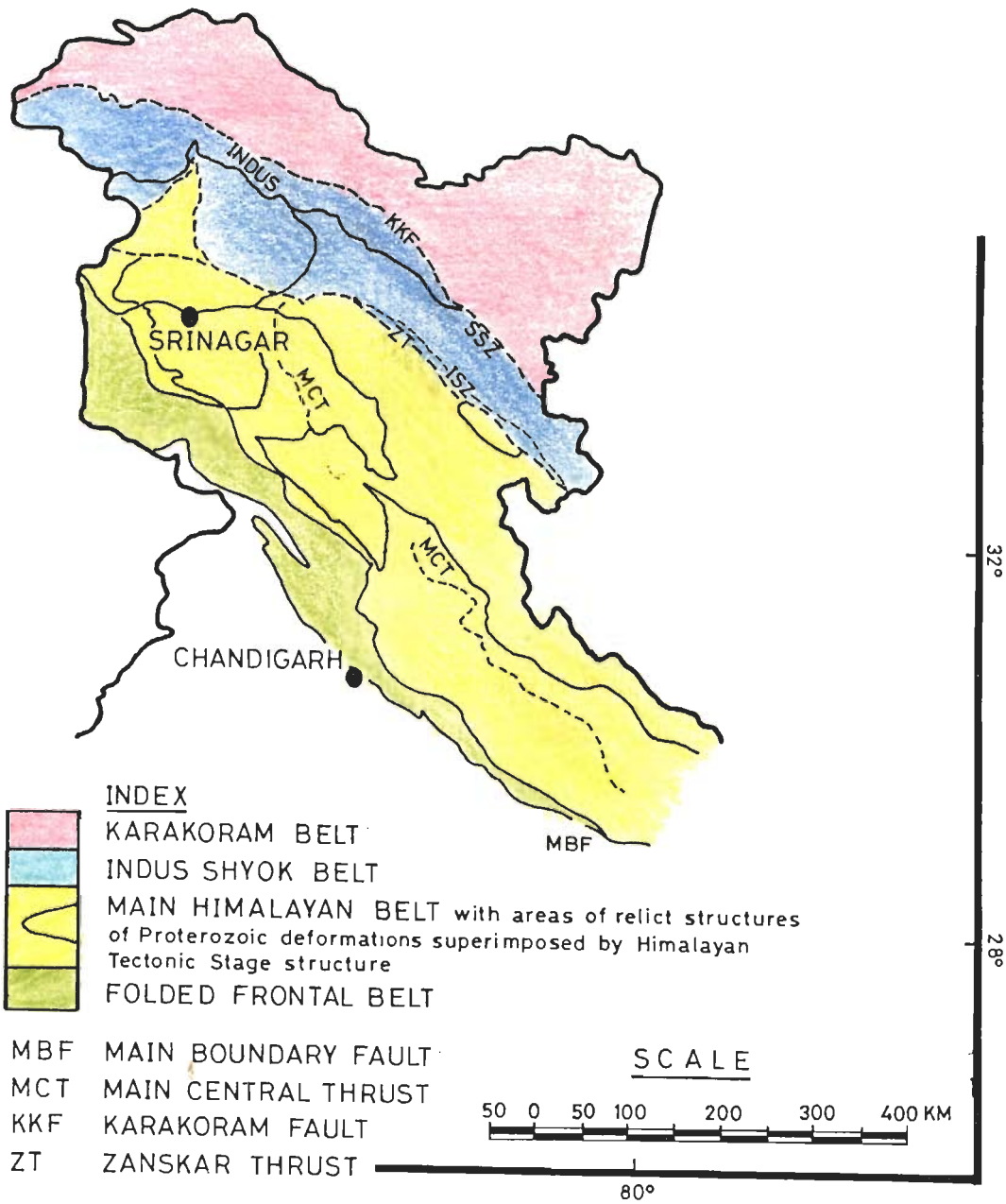

FIG. 2.1 MAP OF THE WESTERN HIMALAYA SHOWING TECTONO LITHOSTRATIGRAPHIC BELTS. (Kumar et al, 1989)

A brief description of each belt is given below:

2.1.1 FRONTAL FOLD BELT (FFB)

It is the Southern most tectonic belt and is made up essentially of Tertiary and Quaternary sediments, consisting the Subathu, the Murree and the Siwalik Group rocks overlain by alluvium. The former three sequences rest on the Proterozoic basement. This belt is separated from Main Himalayan Belt by tectonic surface known as Murree thrust in Jammu region, Krol thrust in the Eastern and Western part of Himachal Pradesh and Uttar Pradesh respectively, and the Main Boundary Thrust (MBT)/ Main Boundary Fault (MBF) in parts of Garhwal and Kumaon in U.P., Nepal, Bhutan and Arunachal Pradesh (Kumar et al, 1989).

TABLE 2.1 THE HIMALAYAN TECTONIC BELTS
(Kumar et al., 1989)

North
Karakorum Belt (KB)
----------Shyok Suture----------
Indus Shyok Belt (ISB) & Lohit Complex Belt (LCB)
----------Indus-Tsangpo/Tidding Suture----------
Main Himalayan Belt (MHB)
----------Main Boundary Thrust/Fault----------
Frontal Fold Belt (FFB)
South

2.1.2 MAIN HIMALAYAN BELT

This is the most complex tectonic belt which occurs between the FFB in the South and the ISB in the North. It abuts in the east against the Lohit Complex along the Tidding Suture, whereas in the west it continues upto Pakistan. This belt itself can be divided into two zones (Shankar et al. 1989) - Lesser Himalayan Zone and Higher Himalayan Zone

Lesser Himalayan Zone

The Lesser Himalayan zone is composed of the late Precambrian-Eocene rocks. The Murree, Krol Thrust, and MBT/MBF marks the Southern boundary with the Frontal Folded Belt

whereas, the Main Central Thrust (MCT) separates it from the Higher Himalaya.

Higher Himalayan Zone

This represents a zone of greatest vertical uplift. The Main Cental Thrust (MCT) marks the boundary between the Lesser and the Higher Himalaya whereas the Indus Suture Zone (ISZ) marks the upper boundary. This zone is characterised by low to high grade metamorphic rocks.

2.1.3 INDUS SHYOK BELT

This belt is sandwitched between the Karakoram Belt in the North and the Main Himalayan Belt in the South. It is essentially made up of early to late Cretaceous to Tertiary Sediments and associated ultramafic, mafic, intermediate and acid magmatic rocks. However, imprints of earlier geologic history are also known in parts of this belt. This belt can also be divided into three Zones (Kumar et. al, 1989) i.e.

i) Zone I - Indus Suture Zone
ii) Zone II - Ladakh Granitoid with Indus Group & Khardung Volcanics
iii) Zone III - Shyok Suture Zone

2.1.4 KARAKORUM BELT

It is the Northern most lithotectonic belt on which very limited information is available. The Karakorum fault marks its Southern boundary.

2.2 GEOLOGY OF THE STUDY AREA

The present study area lies within the Lesser Himalayan Zone of Main Himalayan Belt (MHB) in the Western parts of Himachal Himalaya in H.P. and the Eastern parts of Garhwal Himalaya in U.P. The foundation of the stratigraphy of the lesser Himalaya has been laid down by the Medlicott (1864) followed by Oldham (1883,88), Middlemiss (1890) Pilgrim and West (1928) etc. However, it is the work of Auden (1934) and Heim & Gansser (1934) which initiated a new era of lithostratigraphical and structural studies in the Lesser Himalaya. Thereafter, considerable research activities have been carried out by many workers such as Pascoe (1959), Dutta &Kumar (1964), Bhargava (1969,72,76) Jain (1971,81, Srikantia and Sharma (1971) Pachauri (1972), Srikantia & Bhargava (1974), Ganesan & Verma (1974,81) Valdiya

(1976,80), Ganesan & Thussu (1978), Sharkar et. al (1989), Kumar et. al (1989) and many others. With every passing year, the volume of literature is growing, and along with it the welter of questions are also increasing. However, the regional geology of the study area described herein is based mainly on the work done by Bhargava (1969, 72,76), Srikantia & Bhargava (1974), Ganesan & Verma (1974,81) and Ganesan & Thussu (1978).

Two major lithotectonics units, namely Inner Krol Belt (Bhargava, 1972) and Deoban Structural Belt (Ganesan & Verma, 1981) is exposed in and around the study area (Tons Valley, Yamuna Valley and parts of Himachal Pradesh). A brief description of each Belt is as follows.

2.2.1 DEOBAN STRUCTURAL BELT

The Deoban Belt is a WNW-ESE trending autochthonous belt and exposes some of the oldest sediments of the Lesser Himalaya (Fig.2.2). This belt is exposed over a distance of 70 km. between the Katlai Stream in H.P. to Bangaon in the U.P. (Ganesan & Verma, 1981). This belt can be further sub-divided into three district lithostratigraphic Groups (Table 2.2).

TABLE 2.1 STRATIGRAPHIC SUCCESSION OF THE DEOBAN BELT
(After Ganessan and Verma, 1981)

Southern and Central Part		Northern and Northwestern Part	
Subathu Group			
----------Unconformity----------			
Simla Group		Jaunsar Group	Nagthat Formation Chandpur Formation Mandhali Formation
----------Contact disconformable----------		------- Contact para to unconformable------	
Deoban Group	Ambota Formation Bohar Formation Tiontar Formation	Deoban Group	Ambota Formation Bohar Formation Tiontar Formation
----------Contact angular unconformity----------			
Dharagad Group		Kanda Formation Nimga Formation Atoll Formation	

Dharagad Group

This represents the oldest exposed sediments in the Lesser Himalaya as well as in the Deoban Structural Belt. This group is mainly exposed in the central parts of Deoban Belt in the Dharagad-Barnigad anticlinal core in the Tons and Yamuna valleys.

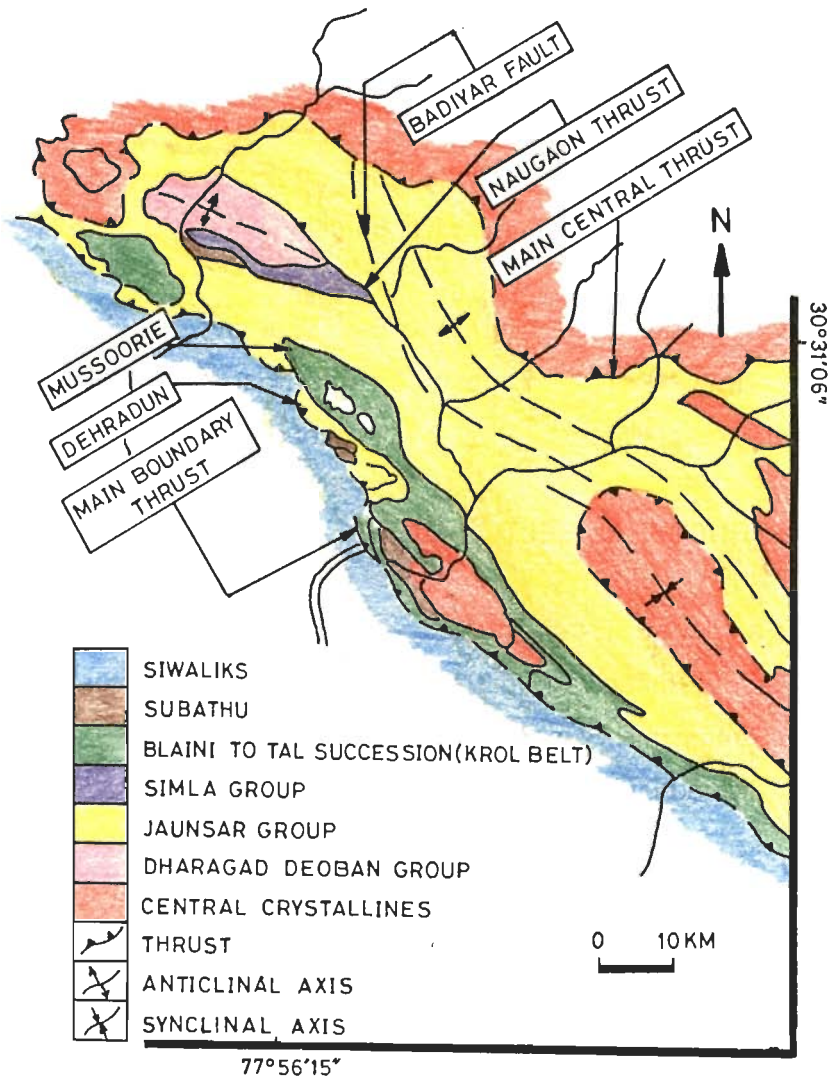

FIG. 2.2 GEOLOGICAL MAP OF THE DEOBAN BELT AND IT'S ADJOINING AREA. (GANESAN AND VERMA, 1981)

Deoban Group

This group succeeds the Dharagad Group with a prominent irregular unconformity. This Group is further divided into three Formations (Table 2.2).

i) Tiontar Formation - An association of shale with thin beds of quartzite. This formation is not developed in the Southern parts of the Tons valley (Ganesan & Verma, 1981)

ii) Bohar Formation - This is the best developed Formation of this Group. The bluish grey algal limestone consisting of colonies of stromatolite is the characteristic feature of this formation.

iii) Ambota Formation - This Formation is well exposed in Southern and Central part of the Deoban Structural Belt, whereas, it is absent in the Northern part of this belt.

Simla Group

The Simla along with in-folded outlier of the Subathu Group forms a narrow belt, occupying the southern fringe of the Deoban structural Belt (Fig.2.2). Its maximum extension is further Northwest, in the Simla Himalaya. The Simla Group exposed in this belt mainly belongs to the Chhaosa Formation of Srikantia and Sharma (1971). This Group is folded into an isoclinal syncline overturned North with its Southern limb sheared by the Tons thrust.

Jaunsar Group

This group is exposed in the Southern and Northern part of the Deoban structural Belt (Fig.2.2) and mainly pertains to the autochthonous Jaunsar Group. To the South of Deoban Belt, the Jaunsar Group is tectonically resting over the Deoban and Simla Groups along the Tons Thrust and forms a part of the Inner Krol Belt (Bhargava, 1972).

2.2.2 INNER KROL BELT

The Inner Krol Belt (Fig.2.3) represents the major tectonic unit of the Krol rocks in the Lesser Himalaya. The Inner Krol Belt consists of the sequence ranging from Mandhali Formation to Subathu Formation (Table 2.3).

TABLE 2.3 LITHOSTRATIGRAPHY OF INNER KROL BELT (After Bhargava, 1969)

<table>
<tr><th>Formation</th><th>Thickness (m)</th><th colspan="2">Age (After Azmi & Joshi, 1983)</th></tr>
<tr><td>Subathu</td><td></td><td colspan="2">L. Palaeocene to M. Eocene</td></tr>
<tr><td>Tal</td><td>2180</td><td colspan="2">Ordovician-Devonian (500-350 m.y.)</td></tr>
<tr><td>Krol</td><td>1265</td><td colspan="2" rowspan="2">Cambrian</td></tr>
<tr><td>Infra Krol</td><td>600</td></tr>
<tr><td>Blaini</td><td>60</td><td>Eocambrian (650-570 m.y.)</td><td rowspan="4">Late Precambrian</td></tr>
<tr><td>Nagthat</td><td>1550</td><td rowspan="2"></td></tr>
<tr><td>Chandpur</td><td>1250</td></tr>
<tr><td>Mandhali</td><td>800</td><td>Early Up. Riphean (950±50 m.y.)</td></tr>
<tr><td colspan="4">Base Deoban-Dharagad Group</td></tr>
</table>

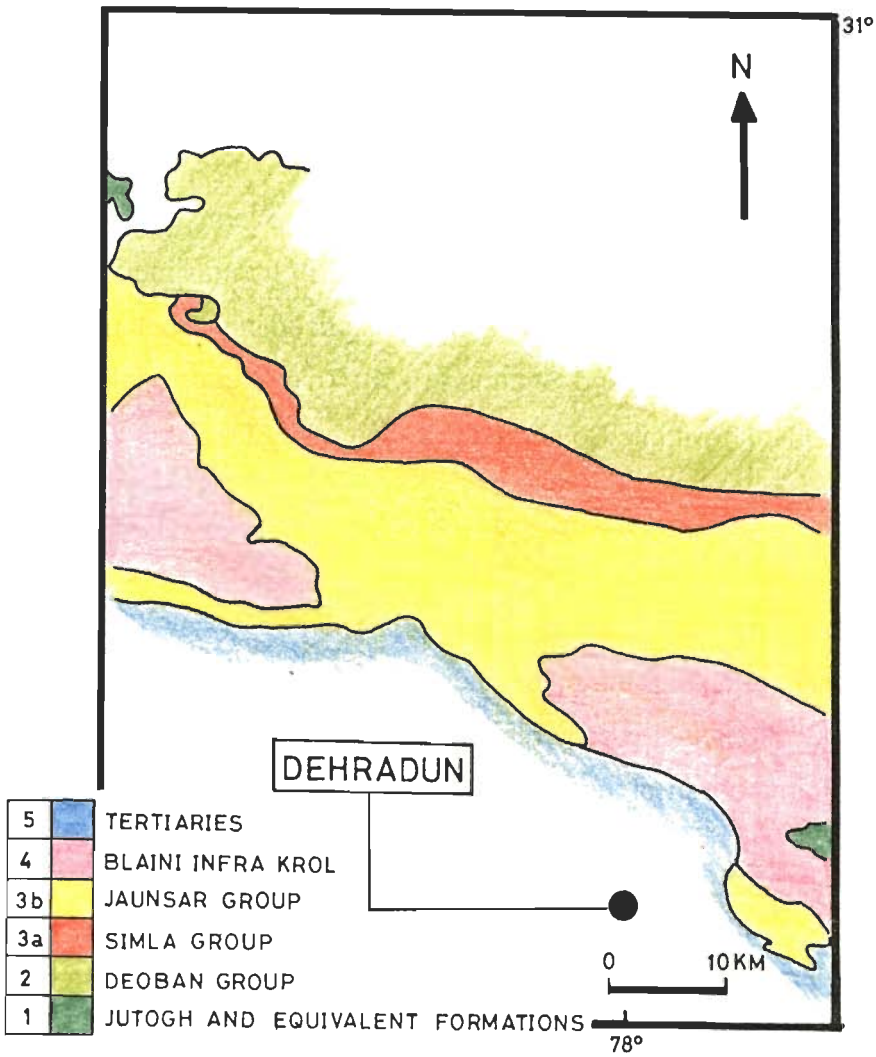

FIG. 2.3 GEOLOGICAL MAP OF PARTS OF THE SIMLA AND THE GARHWAL HIMALAYAS (SRIKANTIA AND BHARGAVA,1974)

The belt extends from Halog in the Simla area to Nainital in Kumaun over a distance of 350 km. This belt strikes NW-SE at Halog and swerves until it strikes E-W at Rainka, then it reverses its curvature near Mussoorie (Bhargava, 1972).

The Inner Krol Belt is a thrust bound synform along the northerly dipping Chail thrust (Krol thrust of Auden, 1934) and southernly dipping Tons thrust. This belt in outer region rests over the Simla Group with Eocene outliers and the Outer Krol Belt. It is thrust over the Subathu and even Siwaliks in Mussoorie-Nainital area (Bhargava, 1972).

2.3 GEOLOGY OF RESERVOIR

The rocks of mainly Deoban Belt are exposed in the reservoir area. The Tons thrust, as discussed earlier also, marks the Southern boundary of this belt. The Mandhali Formation of Inner Krol Belt is also exposed in the South and Southwestern part of the reservoir.

The geological mapping of reservoir area has been carried out on 1 :15,000 scale on the basis of a number of traverses on both banks of river Tons (Fig.2.4). The rock types forming the reservoir area belong to the Simla Group, Deoban Group, Dharagad Group and Jaunsar Group (Table 2.4). The description of various Formations is given below:

2.3.1 DHARAGAD GROUP

The Dharagad Group represents the oldest exposed sedimentary rocks in the Lesser Himalaya. It comprises of three Formations, namely, Atoll, Nimga and Kanda. In the reservoir area, only Atoll Formation is exposed.

Atoll Formation

The rock types belonging to Atoll Formation are quartzite, limestone, minor slates and interbedded thick basic flows. The quartzites are grey to pink in colour, medium to coarse grained. The limestone is pink to purple in colour, while slates are greenish grey in colour. The basic rocks are greenish to greenish grey in colour, vesicular to non-vesicular in nature. The rocks of Atoll formation are well exposed in between Atoll village and reservoir end point.

The contact of Dharagad Group with the overlying Deoban Group is marked by an angular unconformity, which is well exposed near village Gumma.

2.3.2 DEOBAN GROUP

The Deoban Group is divided into three mappable Formations - the lower Tiontar, the middle Bohar and the upper Ambota Formations.

Tiontar Formation

It comprises mainly quartzite. On the right bank of the Tons river, the rocks of this Formation

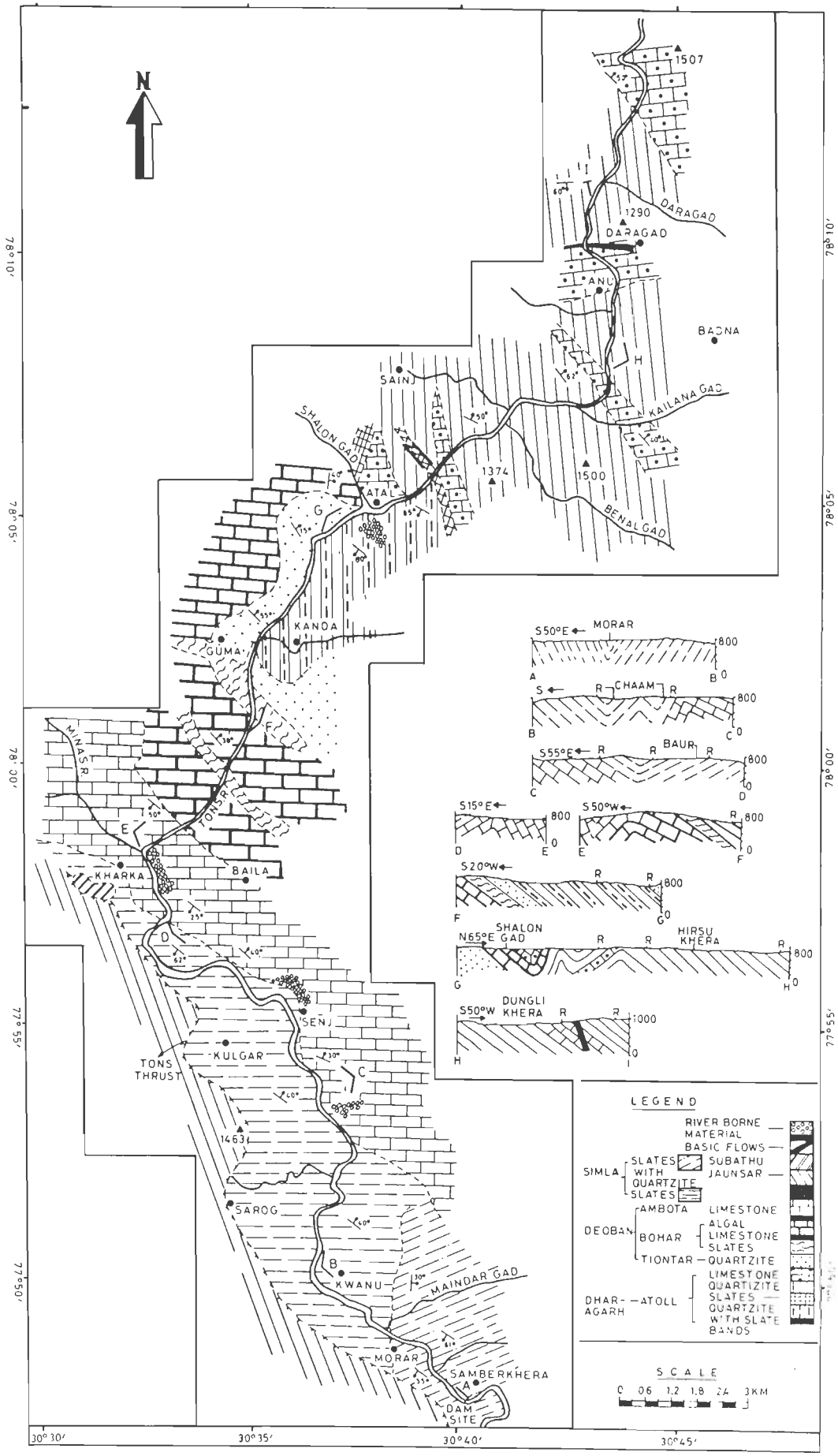

FIG. 2.4 GEOLOGICAL MAP OF KISHAU DAM RESERVOIR AREA

are well exposed in between Gumma village and Shalon Gad stream. A band of this Formation is also exposed on the left bank, Southeast of Gumma village. The Tiontar Formation is succeeded by Bohar Formation.

TABLE 2.4 STRATIGRAPHIC SUCCESSION IN THE KISHAU DAM RESERVOIR AREA

Inner Krol Belt	Deoban Belt
Jaunsar Group	Subathu Group ---------- Unconformity---------- Simla Group
---------- disconformity ----------	
Deoban Group	Ambota Formation Bohar Formation Tiontar Formation
---------- angular unconformity ----------	
Dharagad Group	Atoll Formation

Bohar Formation

This Formation comprises mainly pale grey to grey stromatolitic limestone (Plate 2.1) and minor dark coloured slates. In the reservoir area, this Formation is well exposed in between Shalon Gad stream and Northwest of Baila village.

Ambota Formation

The Bohar Formation is succeeded by Ambota Formation. It comprises bluish grey limestone, dolomite and oolitic limestone. This Formation is well exposed from Kharkan village to North of Amtiar Gad stream.

The contact of Deoban with the overlying Simla Group is marked by disconformity.

2.3.3 SIMLA GROUP

The Simla Group contains mainly grey quartzitic slates and purple to white quartzite. The rocks of Simla Group are well exposed from dam site to Northwest of Baila village. In the Southern part of the reservoir area, the Simla Group is lying tectonically below the allochthonous Jaunsar Group along the Tons thrust.

PLATE 2.1 STROMATOLITIC LIMESTONE OF BOHAR FORMATION

2.3.4 JAUNSAR GROUP

The rocks exposed in the reservoir area, belonging to Jaunsar Group, are mainly grey to black calcareous slates and phyllite. The rocks of this Group are present on the right bank of Tons river between the dam site and South of Kharkan village.

2.3.5 SUBATHU GROUP

The Subathu Group occurs as infolded outlier in the Simla Group. It consists of olive green shale and lenses of bluish grey fossiliferous limestone yielding Nummulite sp. These rocks are exposed South of Kharkan village. The contact of the Subathu with the underlying Simla Group is an unconformity.

2.3.6 STRUCTURE

Tons Thrust

The Tons Thrust is the major tectonic structure in the reservoir area and it separates the autochthonous Simla Group from allochthonous Jaunsar Group. It is a NW-SE to WNW-ESE

trending, low angle (15° to 25°) thrust dipping in S to SW direction. In the reservoir area, the trace of the thrust is seen on right bank of river Tons, between dam site and South of Kharkan village.

The Tons thrust has caused tremendous crushing and deformation as seen along the Rohnat-Shallai road near village Sayasu. Here the overridden Subathu is meshed up into gaugy mass. Likewise the Slates of Jaunsar Group and Simla Group rocks are crushed and folded.

Folding

It has been observed that the rocks have been folded into a number of antiforms and synforms in the reservoir. Due to this effect, the attitude of bedding planes vary frequently. Although the folding is persistent throughout the reservoir area, but the rocks of the Deoban Group are more affected. Different types of folds have been observed in the rocks of Deoban Group (Plate 2.2). Besides these structures, some minor sedimentary structures have also been observed, such as ripple marks (Plate 2.2) in Atoll Formation, load and cast structure in Simla Group .

2.4 GEOLOGY OF THE DAM SITE

At the dam site, the river Tons flows in a Southeasterly direction through a valley having moderate slopes. The river takes a sharp Northeasterly turn about 300 m down stream of the dam axis (Plate 2.3). Its tributary the river Meera flowing on its Southern side, joins it about 3 km downstream of dam axis . The ridge, which separates the two rivers, is very narrow with the steep slopes on the Tons river side.

For the present study, detailed geological mapping (Fig.2.5) on 1 : 2000 scale, covering an area of 1.5 sq km has been carried out to study the various rock types and other structural details in and around the dam site. The mapping has revealed that rocks belonging to Chhaosa Formation of Simla Group occupy the major parts of dam area, and Mandhali slates of Jaunsar Group are exposed relatively over a small area on the ridge separating the Tons and Meera river. A description of various rock types exposed at the dam site is given below:

PLATE 2.2 A - DIFFERENT TYPES OF FOLDS AS OBSERVED IN DEOBAN GROUP
B - RIPPLE MARKS IN QUARTZITE ROCK OF ATOLL FORMATION, NEAR ANU

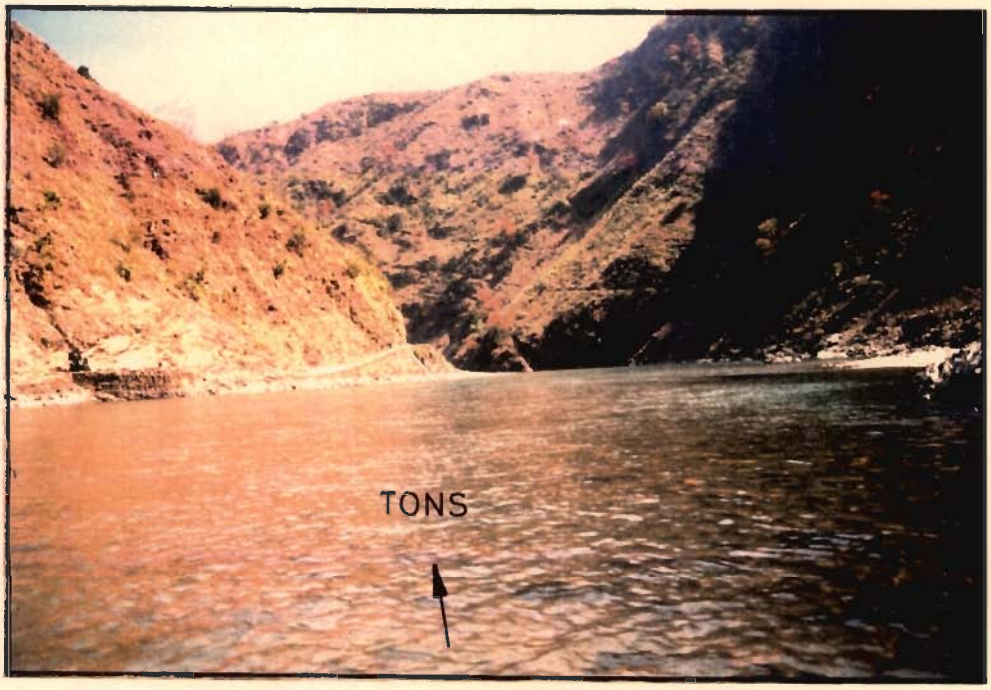

PLATE 2.3 DOWNSTREAM VIEW OF THE TONS VALLEY, AT DAM SITE

2.4.1 CHHAOSA FORMATION

At the dam site three lithounits of Chhaosa Formation, belonging to Simla Group. have been recognised, which are;

Unit III White quartzite
Unit II Purple quartzite with subordinate sandstone
Unit I Grey quartzitic slate with intercalations of quartzite

UNIT I

This unit is composed of quartzitic slates with intercalated bands of quartzite. The rocks belonging to Unit I are exposed along the river bed from 400 m upstream to 600 m downstream of the dam axis. The rocks are exposed upto 680m elevation on the left bank slope and upto 700 m elevation on the right bank slope.

The quartzitic slates are occasionally phyllitic in nature and grade into grey coloured quartzite. The strike of the bedding ranges between S30°-60°E to N30°-60°W and dip at 30° to 50° in

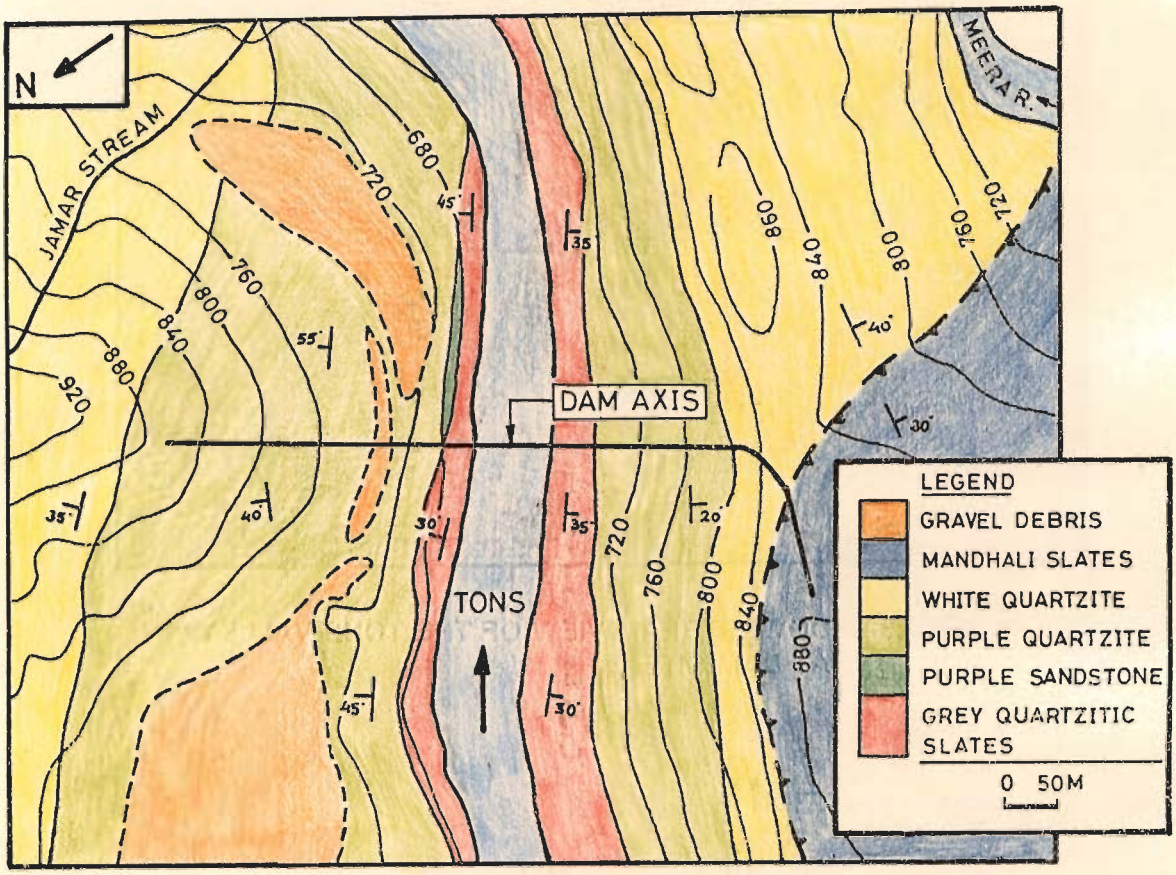

FIG. 2.5 GEOLOGICAL MAP OF THE DAM SITE AREA.

N30° to 60°E direction on the left bank. On the right bank the bedding plane strikes at N20°-35°W - S20°-35°E and dips at 50° to 70° in S55°-70°W direction.

The joint sets as observed in Unit I on both the banks are given below

Joint Set No.	On Left Bank		On Right Bank	
	Dip Amount	Dip Direction	Dip Amount	Dip Direction
BJ	30°-50°	N30°-60°E	50°-70°	S55°-70°W
J_1	65°-75°	N25°-35°W	25°-35°	S35°-40°W
J_2	70°-85°	S25°-45°W	60°-80°	N30°-50°W
J_3	60°-70°	S35°-45°E	30°-45°	N40°-50°E

UNIT II

The rocks of unit I are overlain by purple sandstone and quartzite of Unit II. The contact of the grey quartzitic slate and overlying purple quartzite is very sharp (Plate 2.4).

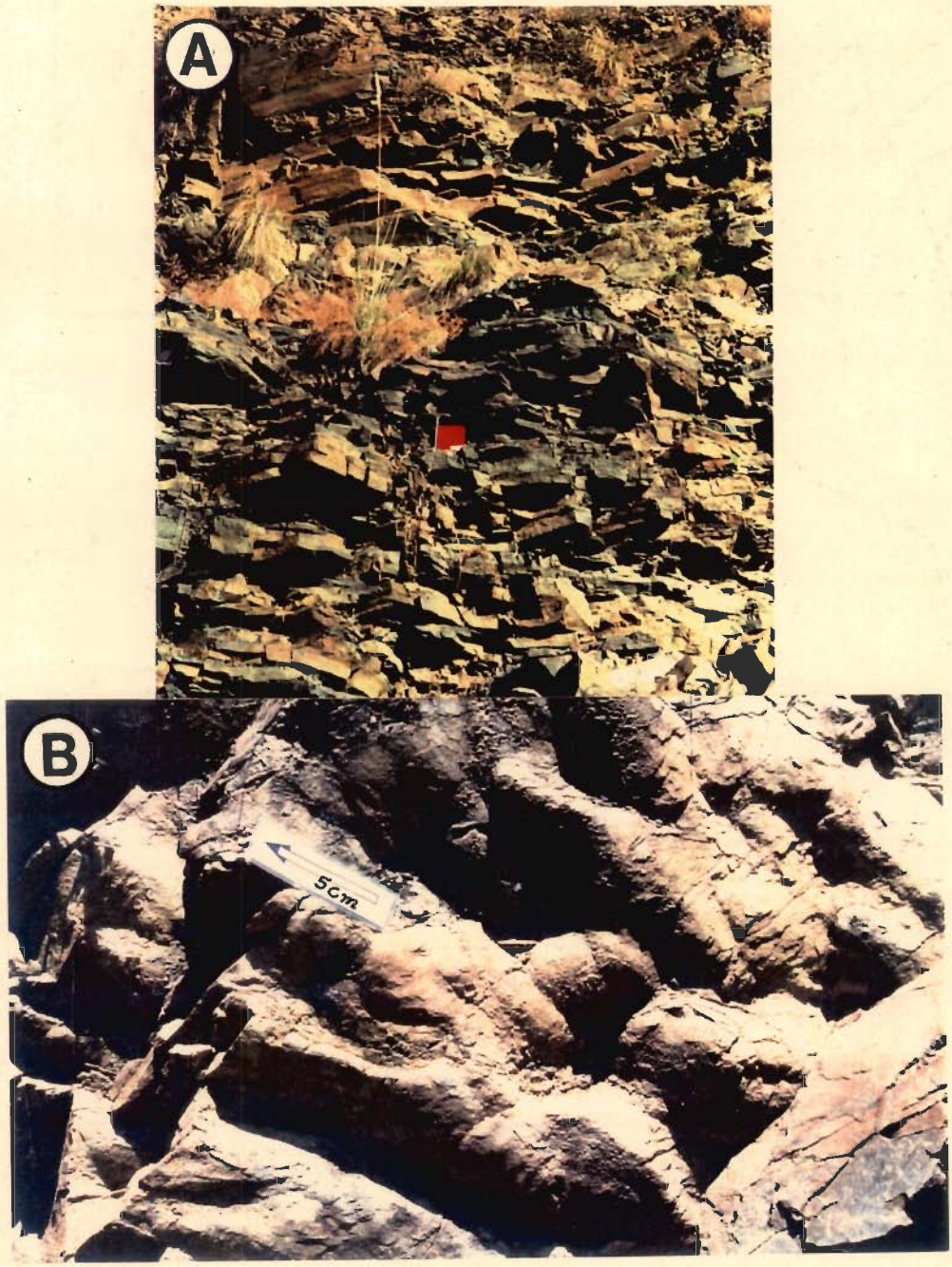

PLATE 2.4 A - CONTACT OF GREY QUARTZITIC SLATE AND PURPLE QUARTZITE, ON LEFT ABUTMENT
B - LOAD AND CAST STRUCTURES IN QUARTZITE ROCK OF SIMLA GROUP, NEAR DAM AXIS ON LEFT ABUTMENT

A mappable band of purple sandstone exists on the left abutment above El. 680 m which otherwise is present as intercalations with purple quartzite. The rocks of Unit II are exposed from El. 680 m to the crest level of the dam on left abutment and from El. 700 m to about El. 800 m on right abutment. The major area of the dam site is covered by this unit only. Shear zones are more predominantly developed in this unit than in the underlying unit. The contact between this unit and the overlying white quartzite is marked by the presence of a sheared purple shale band. Close to the contact, the purple quartzite, at places, shows the convex surfaces of the load casts (Plate 2.4). In the Chhaosa formation, Load costs are widespread sedimentary structures usually found at the contact of shale and quartzite (Bhargava, 1976). On the left bank slope, 200 m upstream and 50 m down stream, a terrace comprising of Gravel and debris is present. This terrace has been formed over the rocks of Unit I. The upstream terrace is known as Samberkhera terrace on which the village Samberkhera is located. The bedding planes, in general, dips at 25°-35° in N45°-60°E direction on the left bank and 55°-70° in S50°-60°W direction on the right bank.

The attitude of joints as observed in rocks of Unit II on both the banks are given below:

Joint Set No.	On Left Bank		On Right Bank	
	Dip Amount	Dip Direction	Dip Amount	Dip Direction
BJ	25°-35°	N40°-60°E	60°-80°	S55°-65°W
J_1	50°-70°	S20°-35°W	20°-30°	S40°-50°W
J_2	50°-70°	N55°-70°W	55°-75°	N35°-55°W
J_3			75°-85°	N50°-60°E

UNIT III

The purple quartzite of Unit II are overlain by the rocks of Unit III. It comprises dull white to white, medium to coarse grained micaceous quartzite. The rocks of this unit are exposed from El. 870 m to the higher elevations on the left abutment and from El 800 m to El 850 m on the right abutment.

On the left bank the rocks of this unit seeps down to lower levels and crosses the Tons river near to the Jamar stream. The bedding planes, in general, are dipping at angles 40° - 55° in N30° to 60°E direction on the left bank and 50°-70° in s 50° to 60°E direction on the right bank. The attitude of joints as observed in rocks of Unit III on both the banks are given

hereunder

Joint Set No.	On Left Bank		On Right Bank	
	Dip Amount	Dip Direction	Dip Amount	Dip Direction
BJ	40°-55°	N30°-60°E	50°-70°	S50°-60°E
J_1	55°-60°	N20°-30°W	75°-85°	N50°-60°E
J_2	35°-65°	N65°-70°W	20°-35°	N45°-50°W
J_3	40°-55°	S25°-35°E	Vertical	Strike E-W

2.4.2 MANDHALI FORMATION

The rocks belonging to Mandhali Formation are mainly slates. These rocks are exposed from El. 850 m to the higher elevations on the right bank only. The Mandhali slates are crushed and sheared and thinly foliated. These have been brought over the rocks of Simla Group by the Tons thrust. Close to the dam axis the slates seeps down into the Meera river valley.

2.4.3 STRUCTURE

Joints

The rocks exposed at the dam site are moderate to highly jointed. The folding and thrusting may have resulted into intensely jointed rocks. For studying the pattern of jointing at the dam site, about 600 reading, 300 on either bank have been recorded. The poles of the attitude of these joints have been plotted on equal angle Wulff's stereonet and later, contoured (Fig.2.6) to get preferred orientation of the joints.

Thrust

The Tons thrust which separates the rocks of Mandhali Formation and the Simla Group is present on the right bank, between the El. 845 m and 850 m (Fig.2.5). The thrust is dipping 15° - 25° towards SW direction into the adjoining Meera river valley. The trace of the thrust just upstream of dam axis runs just below the maximum reservoir level between El 845 m to 850 m. Further upstream the thrust takes an upward turn towards higher elevations. However, the thrust takes a sharp turn toward West to enter into the Meera river valley close to the dam axis. The rocks adjoining to thrust are intensely sheared and crushed at places, Mandhali slates, are much affected due to thrusting than the competent white quartzite of Simla Group.

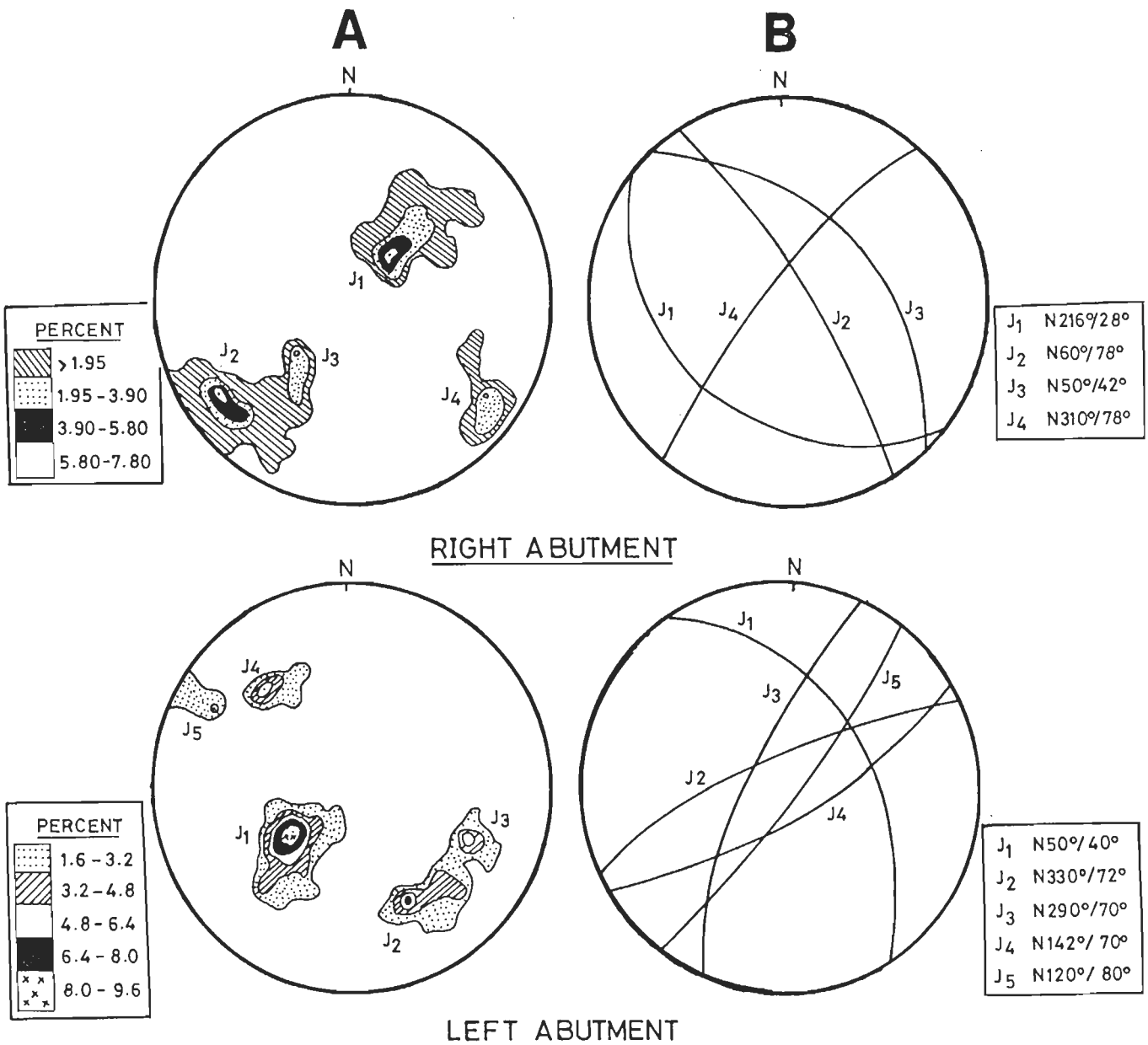

FIG. 2.6 A - DENSITY PLOT OF JOINT POLES ON LEFT AND RIGHT ABUTMENT.
B - ATTITUDE OF STRUCTURAL DISCONTINUITIES ON LEFT AND RIGHT ABUTMENT

Folding

At the dam site, the rocks have been folded into a major asymmetrical upright anticline. The grey quartzitic slates of Unit I are forming the core of this fold. The fold axis trends N45°W - S45°E, (Fig.2.7) almost parallel to the river flow direction.

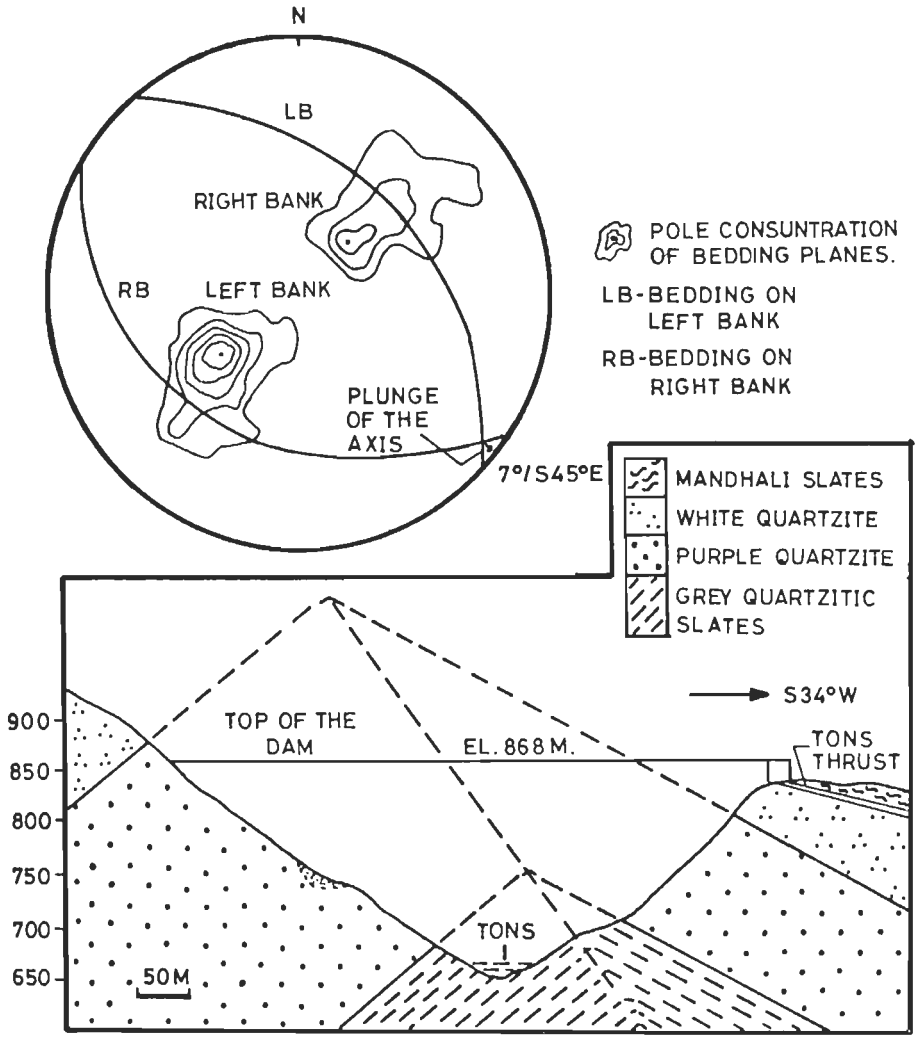

FIG. 2·7 GEOLOGICAL CROSS SECTION ALONG DAM AXIS

The axial plane of this major fold is dipping towards the right abutment and the axis is plunging 7° in S45°E direction.Small scale folds have also been noticed in the drifts on both the banks. As a result of this intense folding the competent quartzitic slates show bedding shears.

CHAPTER III

ENGINEERING GEOLOGICAL STUDIES OF DAM FOUNDATION

Foundation of the dam includes the area of the abutments and the river bed on which the dam rests at the general level of fresh rocks.

The safety and stability of major engineering structures, such as `dams', are to a large extent dependent on the foundation conditions. Weaknesses , if any, in the foundation characteristics may lead to unequal settlement of the structure. Hence, the stress deformation properties of the rocks constituting the foundation are to be evaluated in detail, so as to adequately account for them in the design.

The Himalayan rocks are generally characterised by multiple jointing due to shearing, faulting and folding in addition to high in-situ stresses. Since the attitude of these discontinuities have got an important bearing on the stability of the abutments and that of the superstructure, the data pertaining to discontinuities at the Kishau dam site has been collected in detail and analysed. The seepage properties of the foundation rocks are mainly dependent on the inter connected pattern of joints.

Engineering geological investigations of the Kishau dam site have been carried out mainly to evaluate the overall foundation conditions and to suggest proper foundation treatments. The foundation investigations mainly include;

- Detailed mapping of the dam site area
- Preparation of cross sections
- Three Dimensional mapping of the drifts.
- Interpretation of drill hole data.
- Determination of engineering properties of foundation rocks.
- Assessment of permeability of foundation rocks
- Stability analysis of dam abutments, and
- To suggest proper foundation treatments.

3.1 GEOLOGY OF THE DAM SITE

For the present study, detailed geological mapping on 1 : 2000 scale has been carried out to study the various rock types and other structural details in and around the dam site. The mapping has revealed that rocks belonging to Chhaosa Formation of Simla Group occupies the major parts of the dam area and Mandhali slates of Jaunsar Group are exposed relatively over a smaller area. However, the geology of the dam site has already been discussed in detail in section 2.4 of Chapter II.

3.2 EXPLORATORY DRIFTING

At Kishau dam site eleven drifts, 8 on right bank and 3 on left bank have been excavated for sub-surface exploration of the foundation. The total length of the excavated drifts is 956 meters. The details of these exploratory drifts are given in Table 3.1.

For the present study seven drifts, along dam axis have been studied in detail (Fig.3.1), since other drifts in the vicinity have collapsed and no useful information could be obtained. Four drifts on the right abutment and three on the left abutment have been 3 Dimensionally mapped on 1:100 scale. The mapping of these drifts have been mainly done:

- to know the sub-surface geological conditions
- to assess the lateral depth of weathering
- to identify the lateral depth upto which the glide cracks extend
- to estimate the lateral depth of stripping.

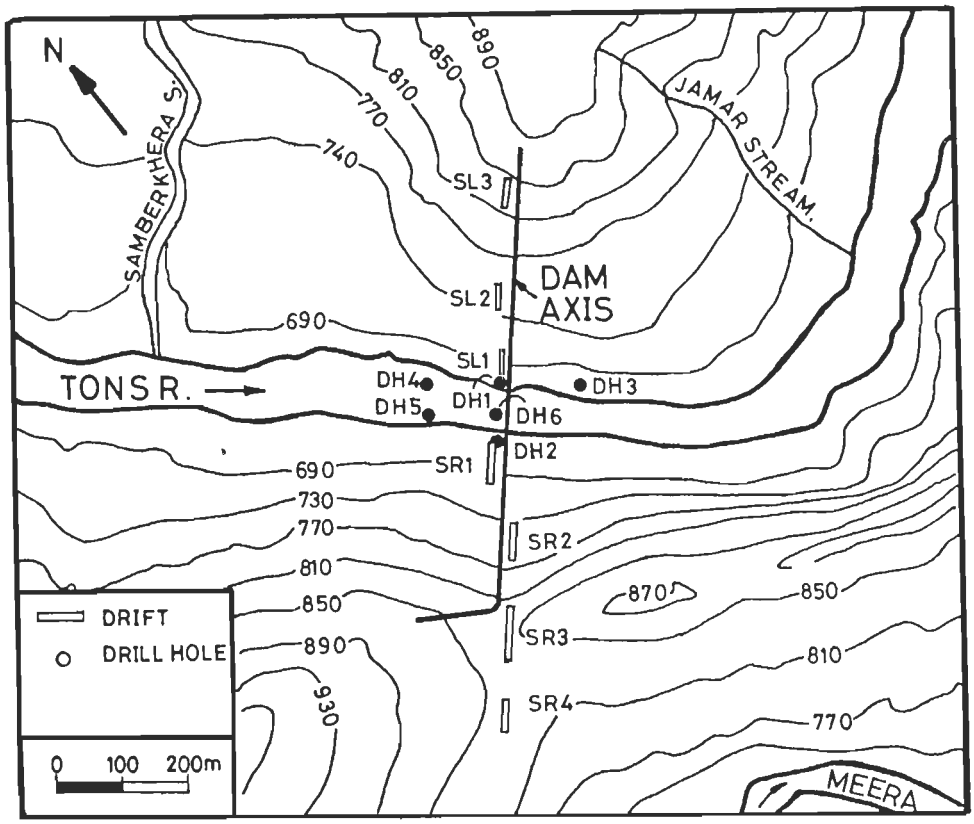

FIG. 3.1 LOCATION OF DRIFTS AND DRILL HOLES IN DAM FOUNDATION AREA.

3.2.1 DRIFTS ON LEFT ABUTMENT

1. Drift SL1

Location : Dam Axis
Elevation : 670.5 m
Bearing : N30°E
Mapped Length : 40 m

This drift has been excavated through purple quartzite and bands of quartzitic slates (Fig.3.2) weathered rocks are encountered upto R.D.15m. Open cracks filled with clay has been noticed upto R.D. 3m. A 50 to 90cm thin shear zone is encountered between R.D. 33 and R.D. 34. The bedding planes dip at 35° to 55° in N30° to 60°E direction. The following joint sets are encountered in drift SL1.

Joint Set	Strike	Dip Amount	Dip Direction
B_J	N30°to 60°W - S30°to 60°E	35°-55°	N30°-60°E
J_1	N55°to 65°E - S55°to 65°W	65°-75°	N25°-35°W
J_2	N45°to 65°W - S45°to 65°E	70°-85°	S25°-45°W
J_3	N45°to 55°E - S45°to 55°W	60°-70°	S35°-45°E

The rocks are highly jointed upto RD 34 m with few open joints indicating glide cracks. The rocks are fresh and massive inside. On the basis of above observations, the lateral depth of striping limit has been estimated to extends upto 34 m from the portal.

TABLE 3.1: DETAILS OF EXPLORATORY DRIFTS AT KISHAU DAM SITE

S.No	Drift No.	Location	Elevation (m)	Bearing	Length (mtr)
1	SL1	Left bank of Tons river,at dam axis	670.5	N30°E	40
2	SL2	Left bank of Tons river,at dam axis	744.7	N35°E	55
3	SL3	Left bank of Tons ,40m u/s of dam axis	815.7	N40°E	40
4	SR1	Right bank of Tons river,at dam axis	667.0	S34°W	100
5	SR2	Right bank of Tons river,at dam axis	748.0	S34°W	56
6	SR3	Right bank of Tons river,at dam axis	817.0	S30°W	180
7	SR4	Right bank of Tons river,from Meera river side in the direction of dam axis	817.0	N34°E	120
8	SR5	Right bank of Tons ,200m u/s of dam axis	818.6	S51°W	85
9	SR6	Right bank of Tons ,150m u/s of dam axis	748.0	S51°W	65
10	SR7	Right bank of Tons ,150m u/s of dam axis	695.0	S51°W	135
11	SR8	Right bank of Tons ,300m u/s of dam axis	827.5	S30°W	80

After Kishau Dam Project Authorities

2. Drifts SL2

Location : Dam axis
Elevation : 744.7 m
Bearing : N35°E
Mapped Length : 55 m

The drift is excavated through purple quartzite and slates (Fig.3.2). The drift is supported with wooden planks and back filled with stone blocks upto RD 9m. Open joints with opening 1 to

5 cm are observed upto RD18m. The rocks are fresh further inside. However, the rocks are crushed between RD 27 m and RD 39 m. The bedding planes dip at 25° to 35° in N40° to 60° E direction. The following joint sets are encountered.

Joint Set	Strike	Dip Amount	Dip Direction
B_J	N30° to 50° W - S30° to 50° E	25°-35°	N40°-60° E
J_1	N55° to 70° W - S55° to 70° E	50°-70°	S20°-35° W
J_2	N20° to 35° E - S20° to 35° W	50°-70°	N55°-70° W

On the basis of above observations, the lateral depth of stripping limit has been estimated to extend upto 18m from the portal.

3. Drift SL3

Location : Dam Axis
Elevation : 815.7 m
Bearing : N40° E
Mapped Length : 40 m

The drift has been excavated through purple quartzite (Fig.3.2). Rocks are highly jointed and crushed upto RD21m, though they are fresh and massive further inside. The rocks show small scale folds between RD36 m and RD40 m. Open cracks are occasionally observed. The crown of the drift is supported by wooden planks upto RD 25 m. The bedding planes are dipping 40° to 55° in N30° to 60° E The following joint sets are encountered in the drift.

Joint Set	Strike	Dip Amount	Dip Direction
B_J	N30° to 60° W - S30° to 60° E	40°-55°	N30°-60° E
J_1	N60° to 70° E - S60° to 70° W	55°-60°	N20°-30° W
J_2	N20° to 25° E - S20° to 25° W	35°-65°	N65°-70° W
J_3	N55° to 65° E - S55° to 65° W	40°-55°	S25°-35° E

On the basis of above observations the lateral depth of stripping limit has been estimated to extend upto 22m from the portal.

Fig.3.2 shows the 3-D logs of drifts of left abutment.

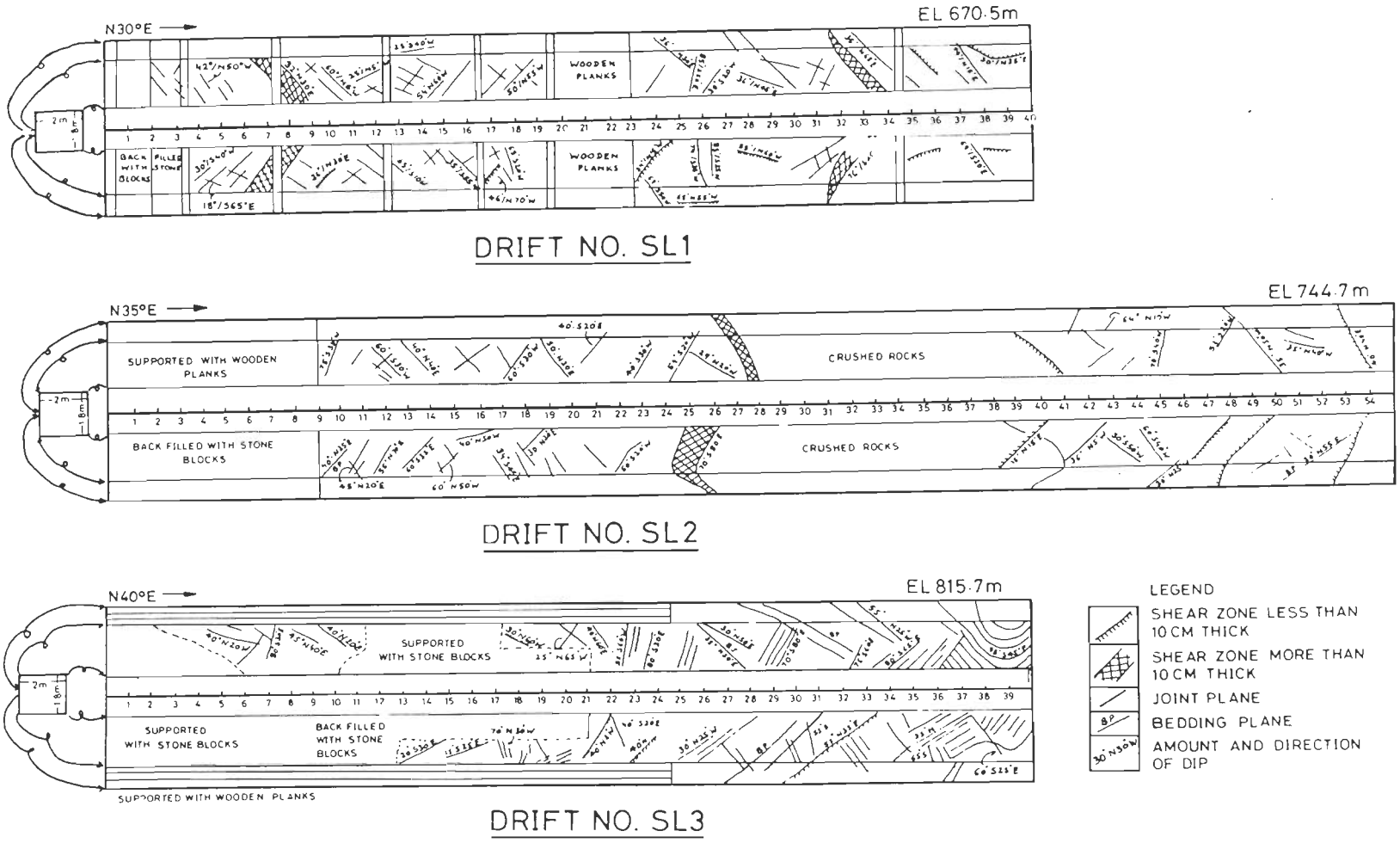

FIG. 3.2 3D GEOLOG OF DRIFTS ON LEFT ABUTMENT

3.2.2 DRIFTS ON RIGHT ABUTMENT

1. Drifts SR1

Location : Dam Axis
Elevation : 667 m
Bearing : S34°W
Mapped Length : 50 m

The drift is excavated through highly disturbed quartzitic slates (Fig.3.3). The rocks are tightly folded leading to shattering. The rocks are weathered upto RD16 m. The rocks are fresh further inside. However, the rocks are sheared and crushed between RD 27 m and RD 41 m. The rocks from RD 16 m to RD 27 m are shattered due to a series of closely spaced small scale folding. The dripping conditions prevail from RD 7 m to RD 16 m, beyond which crown and walls are wet upto RD 36 m. The bedding planes in general dip 50° to 70° in S55° - 70°W direction.

The following joint sets are present in the drift.

Joint Set	Strike	Dip Amount	Dip Direction
B_J	N20°to 35°W - S20°to 35°E	50°-70°	S55°-70°W
J_1	N50°to 55°W - S50°to 55°E	25°-35°	S35°-40°W
J_2	N40°to 60°E - S40°to 60°W	60°-80°	N30°-50°W
J_3	N40°to 50°W - S40°to 50°E	30°-45°	N40°-50°E

On the basis of above observations the lateral depth of stripping limit has been estimated to extend upto 45 m from the portal.

2. Drift SR2

Location : Dam Axis
Elevation : 748 m
Bearing : S34°W
Mapped Length : 56 m

The drift is excavated through purple quartzite (Fig.3.3). The drift is supported with wooden planks and back filled with stone blocks from portal to RD 4 m. The rocks are thrown into minor folds but the intensity of folding is much less as compared to the drift SR1. The rocks show weathering effects upto RD 19 m. The joints at places are open upto RD 25 m. The bedding planes dip at 60° to 80° in S55° to 65°W direction.

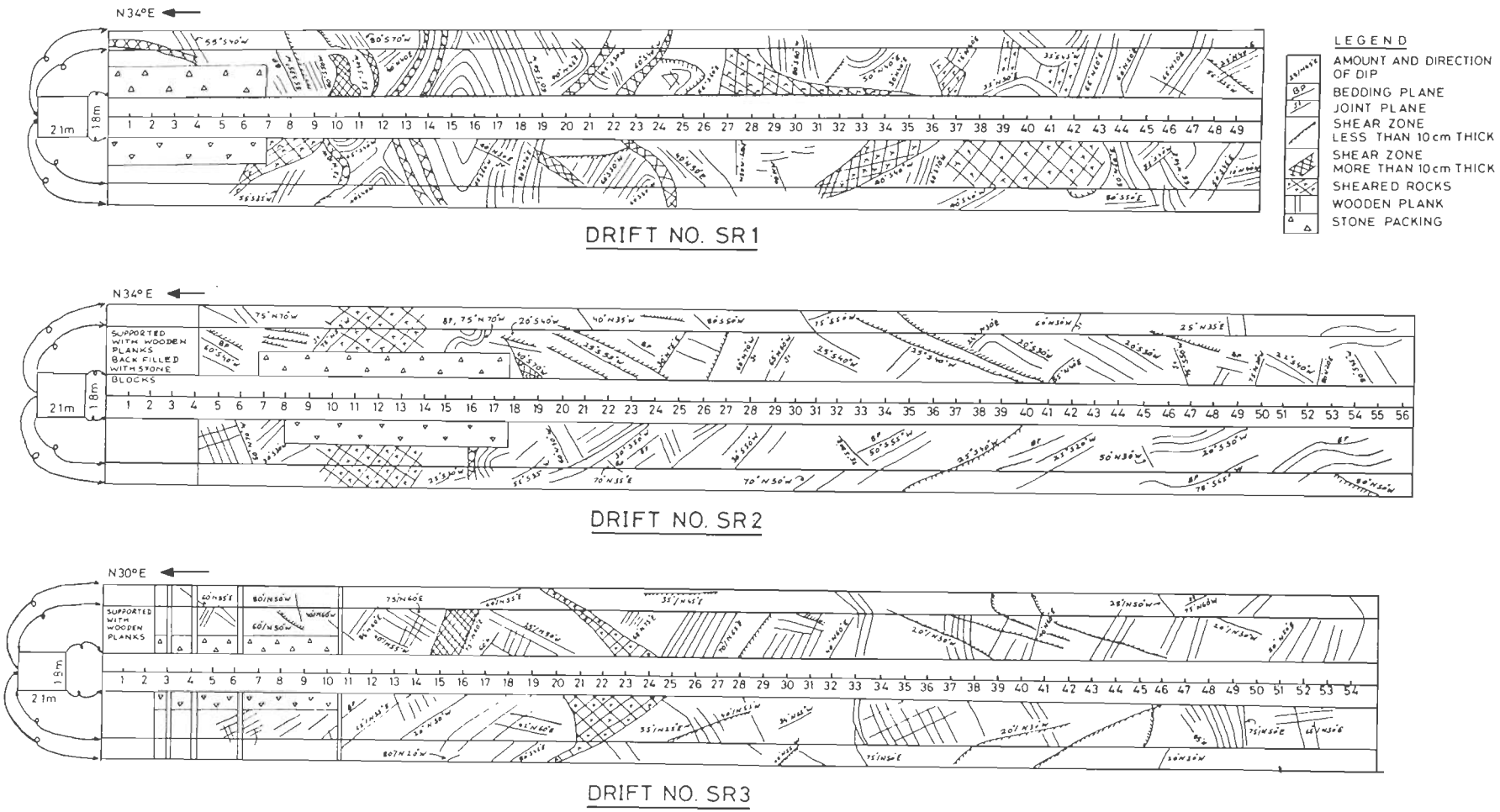

FIG. 3.3 3D GEOLOG OF DRIFTS ON RIGHT ABUTMENT

The following joint sets are present in drift SR2.

Joint Set	Strike	Dip Amount	Dip Direction
B_J	N25°to 35°W - S25°to 35°E	60°-80°	S55°-65°W
J_1	N40°to 50°W - S40°to 50°E	20°-30°	S40°-50°W
J_2	N35°to 55°E - S35°to 55°W	55°-75°	N35°-55°W

On the basis of above observations a minimum lateral depth of stripping limit has been estimated to extend upto 26 m from the portal.

3. Drift SR3

Location : Dam Axis
Elevation : 817 m
Bearing : S30°W
Mapped Length : 55 m

The drift has been excavated through purple quartzite (Fig.3.3) upto RD 19 m and through white quartzite in the remaining reaches. The rocks are shattered upto RD 25 m. The rocks are fresh further inside.

A shear zone is present at RD 21 m which has a maximum thickness of 200 cm. The following joint sets are present in the drift;

Joint Set	Strike	Dip Amount	Dip Direction
B_J	N30°to 40°E - S30°to40°W	50°-70°	S50°-60°E
J_1	N30°to 40°W - S30°to 40°E	75°-85°	N50°-60°E
J_2	N40°to 45°E - S40°to 45°W	20°-35°	N45°-50°W
J_3	N - S		Vertical

The dripping conditions are prevailing upto RD 35 m. The drift is moist to dry further inside. On the basis of above observations a minimum lateral depth of stripping limit has been estimated to extend upto 25 m from the portal.

As discussed above, fresh rocks are present after RD 25 m and they remained fresh and massive upto RD 55 m, though bedding shears are seen at several places. Moreover, possibility of crushed and sheared rocks to appear further inside can not be ruled out. As

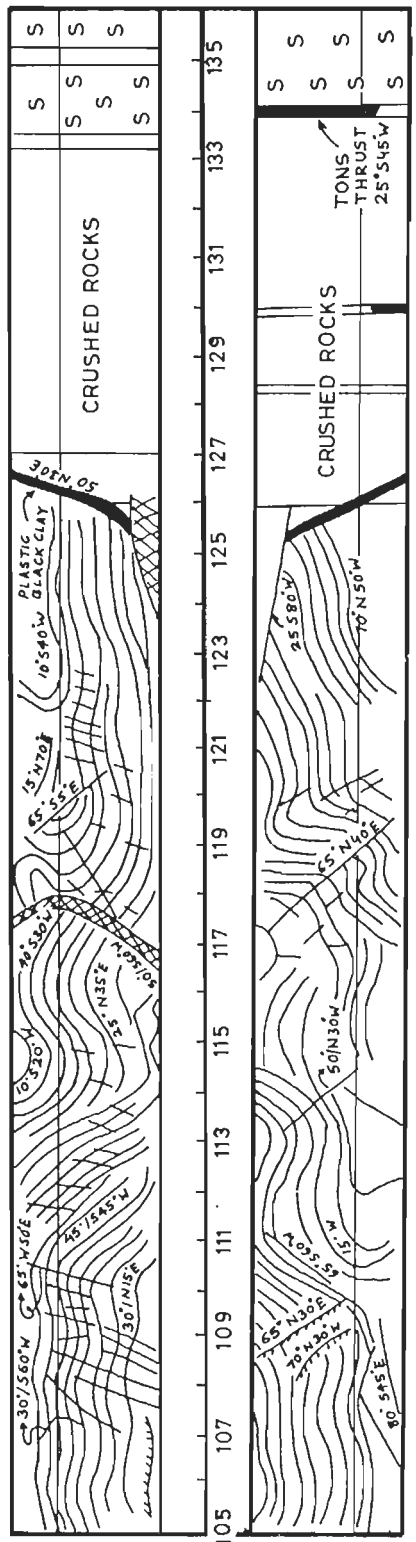

FIG. 3.4 3D GEOLOG OF PART OF DRIFT SR 3 (105m TO 136m FROM PORTAL)
(After Kishau Dam Project Authorities.)

discussed earlier in chapter II, under section Geology of the dam site, the surface traces of Tons thrust are observed on right bank between elevation 845 m and 850 m and the thrust is dipping 15° to 25° towards south westerly direction. Therefore, if projected from this level into the drift SR3, Tons thrust may appear around RD 140 -150 m. This fact has been further verified by the 3D log of this drift, obtained from the project authorities. In this log the Tons thrust is present between RD 125 m and RD 134 m from the portal.(Fig.3.4).

4. Drift SR4

Location : Dam Axis from the river Meera side
Bearing : N34°E
Elevation : 817 m
Mapped Length : 15 m

The drift is excavated through Mandhali Slates. From the portal to RD 15 m the roof and walls are supported by wooden planks and stone packing. The rocks as visible in between the planks are weathered, crushed and sheared. The drift is choked completely at RD15 m. The possibility of presence of Tons thrust at depth is indicated by the crushed and highly sheared rocks present upto RD 15 m.

The 3D logs of drifts on right abutment are shown in Fig.3.3.

Discussion

From the subsurface explorations through drifting, the following deductions are made:

a. The glide cracks on the left abutment extend upto 18 m of lateral depth, whereas, on the right abutment they extend upto 25 m of lateral depth.

b. On the left abutment a shear zone of 1m thickness, has been encountered between RD 33 m and 34 m in drift SL1 . The shear zone dips 70° in N15°E direction. Though this will be removed at drift level, but will be encountered at the foundation in lower elevations. Crushed rocks are present in between RD 27 m and 39 m in drift SL2. On the basis of general observation in the drifts, it is inferred that the shear zones ranging in thickness 0.5 to 1.5 m are likely to be present at foundation level of the dam.

c. The lateral depth of weathering ranges from 22 to 34m on the left abutment and this range varies from 16 to 25m on the right abutment.

Thus on the basis of the above observations, the lateral depth of the stripping on the left abutment ranges between 22 m in the upper reaches and 34 m in the lower reaches. The lateral depth of stripping on right abutment ranges between 25 m in the upper elevations and 45 m in the lower elevations. The stripping limit marked over the cross section, along dam axis, is shown in Fig.3.5.

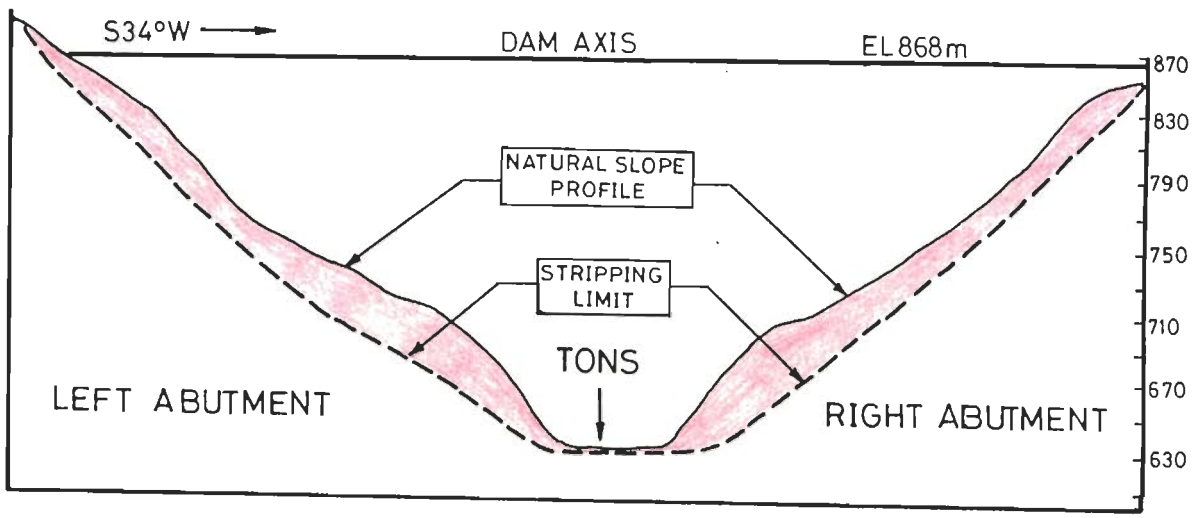

FIG. 3.5 CROSS SECTION SHOWING THE STRIPPING LIMIT

3.3 EXPLORATORY DRILLING

The exploratory drilling at the dam site is conducted mainly,

- to establish correlation of lithounits.
- to evaluate the physical conditions of rocks such as rock quality designation
- to collect samples of various rock units for laboratory tests
- to carry out water pressure tests.

A total of 16 drill holes have been drilled in the dam area by the project authorities. The cumulative length of exploratory drilling is about 1000 m. The details of these exploratory drill holes are presented in Table 3.2 and the locations of these drill holes are shown in Fig.3.1.

TABLE 3.2 : DETAILS OF EXPLORATORY DRILLING IN AND AROUND KISHAU DAM SITE

S. No	Drill Hole No.	Location	Collar Elevation (mtr)	Angle/ Bearing	Depth (mtr)
1	DH-1	Left abutment,at dam axis	656.8	60°/S34°W	98.07
2	DH-2	Right abutment,at dam axis	657.3	60°/N34°E	96.01
3	DH-3	Left abutment,100m d/s of dam axis	650.5	60°/S34°W	91.57
4	DH-4	River bed,100m u/s of dam axis	647.1	90°	91.74
5	DH-5	Right abutment,100m u/s of dam axis	647.1	60°/N51°E	14.63
6	DH-6	River bed,100m u/s of dam axis	645.0	90°	65.07
7	DH-7	Right bank,100m d/s of dam axis	650.0	60°/N51°E	44.65
8	DH-8	Right bank,dam axis	718.5	90°	38.09
9	DH-9	Right bank, u/s of dam axis	690.0	90°	20.42
10	DH-10	Samberkhera stream	709.0	90°	51.91
11	DH-11	Right bank,50m d/s of dam axis	700.0	90°	56.99
12	DH-12	Power house site	645.0	90°	36.57
13	DH-13	Right bank, opposite Samberkhera stream	702.0	90°	86.80
14	DH-14	Left bank, dam axis	725.0	90°	30.48
15	DH-15	River bed near Samberkhera stream	709.6	90°	-
16	DH-16	Meera river bed	692.5	90°	70.00

After Kishau Dam Project Authorities

In the present study, the drill holes located in the foundation of the dam, namely DH1, DH2,DH3,DH4 and DH5, have been studied to explore the foundation conditions in the dam area. The summarised logs of these drill holes are presented in Annexure I

Discussion

A perusal of the summarised logs of drill holes in the foundation of the dam, reveal the following:

1) The depth of fluvial fill in the river section ranges from 3.65 m to 11.88 m

2) In the river section, bed rock is encountered at El. 635.2 m.
3) The percent core recovery varies generally from 25 to 75, though it broadly ranges from 7% to 100%.
4) In the river bed section alternating bands of grey quartzitic slate and purple quartzite are encountered.
5) In general, the thickness of grey quartzitic slate bands varies from 2 to 6m, but at a depth of 36 m (El 611 m) in DH5 grey quartzitic slate rock continuously encountered upto a depth of 92 m (El. 555 m).
6) The thickness of purple quartzite in river section varies from 2 to 7 m.
7) The foliations in grey quartzitic slates dip at 20° to 60° and the bedding planes of purple quartzite dip 35° to 70°.

3.4 ASSESSMENT OF PERMEABILITY OF FOUNDATION ROCKS

The water pressure test have been conducted in drill hole DH2 only, located on right bank of dam axis. This is the only quantitative data available at the dam site.

The water pressure test data for drill hole DH2 reveals that the foundation rocks in the dam area have permeability values ranging from 9 to 63 lugeons. However, the reliability of this data can only be demonstrated after more water pressure tests are conducted in the dam area. An attempt has been made to qualitatively assess the permeability of foundation rocks.

The dam at deepest level would rest on the hinge zone of a major asymmetrical anticline. The intense tension fracturing in the hinge zone may considerably increase the permeability of the foundation rocks. Moreover, due to folding, the water under high pressure may seep into the adjoining valleys.

The percent core recovery of 25 to 75 in the river bed section indicates that the foundation rocks are moderately jointed and thus they may be semipervious to pervious in nature (< 5 lugeons). The percent core recovery increases with depth, as indicated by the drill hole data. It implies that the intensity of jointing is less at depth. Hence, the permeability values may decrease with depth. Since the rocks in general are well jointed the permeability upto the one-third height of dam may be more than 5 Lugeons and thereby indicating the necessity of a grout curtain.

3.5 ENGINEERING PROPERTIES OF ROCKS

The important parameters on which the design and construction of a dam depends are the engineering properties of the rocks such as shear strength, the deformability character of the foundation rocks, uniaxial compressive strength and rock density.

These engineering properties are determined by the in-situ tests and the tests conducted in the laboratory. In addition to these, the rock mass classifications are also widely used for estimating these properties. In the present study, the in-situ test data have been obtained from the Project Authorities. Besides, a number of laboratory tests have also been carried out. The geomechanical classification has been used to estimate the strength parameters.

3.5.1 IN-SITU TESTS

Data pertaining to in situ tests, performed in drifts in the foundation, has been utilised to determine the shear strength properties and the value of modulus of deformation.

Modulus of Deformation

The in-situ test data on modulus of deformation has been obtained from the project authorities. These tests have been performed in the drifts SL1,SL2,SL3 and SR1 using Uniaxial plate load test. The results are presented in Table 3.3.

TABLE 3.3 : MODULUS OF DEFORMATION OF ROCK AS COMPUTED FROM THE IN-SITU ROCK TEST CONDUCTED IN THE DRIFTS ON LEFT ABUTMENT

S. No	Drift No.	Rock Type	Chainage (mtr)	Dire-ction	E_e (kg/cm^2)	E_d (kg/cm^2)	Ratio $R=E_e/E_d$
1	SL1	QSL	18.0	H	$2.27*10^5$	$0.69*10^5$	3.29
2	SL1	QSL	20.0	V	$1.34*10^5$	$0.27*10^5$	4.94
3	SL1	QSL	38.9	H	$1.09*10^5$	$0.18*10^5$	6.06
4	SL1	QSL	38.0	V	$2.68*10^5$	$0.29*10^5$	8.99
5	SL1	QSL	27.5	H	$3.68*10^5$	$0.75*10^5$	4.97
6	SL1	QSL	23.5	V	$1.47*10^5$	$0.40*10^5$	3.70
7	SL2	Q-SZ	27.8	H	$0.67*10^5$	$0.10*10^5$	6.20
8	SL2	Q-SZ	27.8	V	$1.40*10^5$	$0.11*10^5$	12.3

S. No	Drift No.	Rock Type	Chainage (mtr)	Dire-ction	E_e (kg/cm^2)	E_d (kg/cm^2)	Ratio $R=E_e/E_d$
9	SL2	Q	42.2	H	$1.55*10^5$	$0.13*10^5$	11.7
10	SL2	Q	41.7	V	$1.64*10^5$	$0.21*10^5$	7.5
11	SL2	Q	53.6	H	$2.26*10^5$	$0.33*10^5$	6.8
12	SL2	Q	46.3	V	$1.96*10^5$	$0.41*10^5$	4.7
13	SL3	Q	30.5	H	$0.35*10^5$	$0.16*10^5$	2.19
14	SL3	Q	37.7	V	$2.27*10^5$	$0.30*10^5$	7.6
15	SL3	Q	22.4	H	$0.49*10^5$	$0.28*10^5$	1.8
16	SL3	Q	29.5	V	$0.98*10^5$	$0.22*10^5$	4.5
17	SL3	Q	20.4	H	$0.21*10^5$	$0.06*10^5$	3.78
18	SL3	Q	22.3	V	$1.84*10^5$	$0.22*10^5$	8.1
19	SR1	QSL	38.29	H	$1.64*10^5$	$0.26*10^5$	6.2
20	SR1	QSL	37.27	V	$0.98*10^5$	$0.29*10^5$	3.3
21	SR1	QSL	48.6	H	$0.87*10^5$	$0.35*10^5$	2.5
22	SR1	QSL	48.6	V	$1.09*10^5$	$0.19*10^5$	5.6
23	SR1	QSL	57.9	H	$1.34*10^5$	$0.21*10^5$	6.5
24	SR1	QSL	59.2	V	$0.75*10^5$	$0.22*10^5$	3.3
25	SR1	QSL	77.8	H	$0.58*10^5$	$0.29*10^5$	1.85
26	SR1	QSL	77.9	V	$0.57*10^5$	$0.23*10^5$	2.51
27	SR1	QSL	98.2	H	$1.40*10^5$	$0.23*10^5$	6.1
28	SR1	QSL	96.9	V	$2.27*10^5$	$0.39*10^5$	5.85

E_e = Modulus of Elastic Deformation
E_d = Modulus of Total Deformation
Q = Quartzite
QSL = Quartzitic Slate
Q-SZ = Quartzite (Shear Zone)

After Kishau Dam Project Authorities

A perusal of Table 3.3 indicates that in case of quartzitic slates the modules of elastic deformation (E_e) and total deformation (E_d) varies in between 0.57 x 10^5 kg/cm^2 to 3.68 x 10^5 kg/cm^2 and 0.18 x 10^5 kg/cm^2 to 0.75 x 10^5 kg/cm^2 respectively. The modulus of elastic deformation (E_e) for quartzite varies between 0.21 x 10^5 kg/cm^2 to 2.27 x 10^5 kg/cm^2 and the total deformation (E_d) varies from 0.16 x 10^5 kg/cm^2 to 0.41 x 10^5 kg/cm^2 . These values have shown the ratio E_e/E_d varying between 2.19 to 8.1.

In case of quartzitic slates, the average values of modulus of elastic deformation and total deformation are 1.49 x 10^5 kg/cm^2 and 0.32 x 10^5 kg/cm^2 respectively. The ratio of E_e and E_d is 4.65. Similarly, in case of quartzite rock the average values of E_e and E_d are 1.3 x 10^5 kg/cm^2 and 0.21 x 10^5 kg/cm^2 respectively.

If all the 28 nos. of tests are taken into consideration, the average values of E_e and E_d comes out to be 1.41 x 10^5 kg/cm^2 and 0.27 x 10^5 kg/cm^2 respectively. However, the median value of in-situ modulus of deformation comes out to be 0.27 x 10^5 kg/cm^2.

Shear Strength

The in-situ shear test data has been obtained from the project authorities in the form of normal and shear stresses. These tests have been performed between rock to concrete in drifts SL1 ,SL2,SL3 and SR1. In drifts SL1 and SR1 these tests have been performed at three locations whereas in drifts SL2 and SL3 these tests are carried out in four locations. The in-situ shear test data is presented in Table 3.4.

TABLE 3.4 : IN SITU SHEAR TEST DATA FOR ROCK TO CONCRETE IN DRIFTS AT DAM SITE

S.No.	Drift No.	Chainage (mtr)	Normal Stress kg/cm^2	Shear Stress kg/cm^2
1.	SL1	28.3	8.8	13.8
2.	SL1	32.0	17.1	25.6
3.	SL1	39.0	23.26	33.5
4.	SL2	41.0	6.72	9.86
5.	SL2	36.0	13.44	19.71
6.	SL2	28.6	20.17	29.57
7.	SL2	25.0	25.31	33.51
8.	SL3	20.0	8.3	11.8
9.	SL3	23.7	14.5	23.7
10.	SL3	27.3	25.3	33.5
11.	SL3	37.3	20.2	29.6
12.	SR1	52.0	7.25	11.83
13.	SR1	63.0	12.92	17.74
14.	SR1	77.3	19.64	27.6

The shear strength parameters have been calculated by adopting Mohr-Coulomb failure criteria which can be expressed as,

$$\tau = C + \sigma \tan \phi \quad \ldots \quad 3.1$$

Where, τ = Shear Stress
σ = normal stress
C = Cohesion
ϕ = Angle of internal friction

This equation can be expressed in the general form;

$$Y = a + bx$$

The constants a and b can be determined by linear regression analysis as given below

$$a = \Sigma y/n - b\,\Sigma x/n \quad \ldots \quad 3.2$$

$$b = \frac{\Sigma xy - \Sigma x \Sigma y/n}{\Sigma x^2 - (\Sigma x)^2/n} \quad \ldots \quad 3.3$$

Where, x = Normal stress
y = Shear stress
n = Total number of test points
a = Cohesion (C)
b = Tan (ϕ)

Thus, the values of cohesion and angle of internal friction, as calculated from the data of each drift, is presented in Table 3.5.

TABLE 3.5 : SHEAR STRENGTH PARAMETERS AS OBTAINED BY LINEAR REGRESSION ANALYSIS

S.No.	Drift No.	Rock Type	Cohesion, C kg/cm^2	Angle of Internal Friction, ϕ
1.	SL 1	Quartzitic Slate	1.93	53.7°
2.	SL 2	Quartzite	1.83	52.6°
3.	SL 3	Quartzite	3.14	51.5°
4.	SR 1	Quartzitic Slate	2.06	51.9°

The average values of cohesion and angle of internal friction between quartzitic slate and concrete in natural conditions are 1.9 kg/cm^2 and 52.8° respectively. However, in case of quartzite rock the values of cohesion and angle of internal friction are 2.48 kg/cm^2 and 52° respectively.

3.5.2 LABORATORY TESTS

For the determination of engineering properties of rocks in the laboratory, lump samples and rock cores have been used. Important engineering properties such as uniaxial compressive strength and rock density have been determined by using the standard techniques.

Uniaxial Compressive Strength

Two rock core samples of each rock type, constituting the foundation of the dam, has been tested to determine the uniaxial compressive strength. To calculate the uniaxial compressive strength of the rock following formula has been used.

$$q_c = P/A$$

Where, q_c = Uniaxial Compressive Strength (kg/cm^2)
P = Load at failure in kg
A = Cross sectional area of sample in cm^2

The uniaxial compressive strength of different rock types, as obtained from laboratory testing is presented in Table 3.6.

TABLE 3.6 UNIAXIAL COMPRESSIVE STRENGTH OF FOUNDATION ROCKS

S.No.	Rock Type	Cross Sectional Area of Sample (cm^2)	Load at Failure,P (kg)	Uniaxial Compressive Strength (kg/cm^2)	Average (kg/cm^2)
1.	Quartzitic Slate	22.05	17507.7	794	780
2.	Quartzitic Slate	22.05	16890.3	766	
3.	Quartzite	22.05	43328.2	1965	2050
4.	Quartzite	22.05	47076.7	2135	

Thus, the average uniaxial compressive strength of quartzitic slates and quartzite rock comes out to be 780 kg/cm^2 and 2050 kg/cm^2 respectively.

Rock Density

Density of the rock types exposed at the dam site have been determined following the standard practice. The test results are presented in Table 3.7.

TABLE 3.7 : DENSITY OF ROCK TYPES EXPOSED AT DAM SITE

S.No.	Rock Type	Locality from where sample was taken	Rock Density T/m^3
1.	Quartzitic Slate	Left Bank at Dam Axis	2.72
2.	Quartzite	Left Bank near Drift SL2	2.78

3.5.3 ESTIMATION OF SHEAR STRENGTH PARAMETERS BY EMPIRICAL APPROACH

An attempt has been made to estimate the shear strength parameters of the rocks exposed at the dam site by using the geomechanics classification. For that purpose, the rock mass rating (RMR) system of Bieniawski (1973) and modified by Bureau of Indian standard (BIS : 13365, part II) has been used.

In this modified approach, the adjustment of RMR for adverse orientation of discontinuities with respect to orientation of slope has been eliminated. The parameters used in the geomechanics classification are:

Strength of intact rock material,
Rock quality designation,
Spacing of discontinuities,
Condition of discontinuities, and
Groundwater conditions

In the present study, the data pertaining to rock mass rating system has been collected from both the abutments and in the drifts located along the dam axis. In all, the data has been collected from 10 locations (Fig.3.6). For rock mass rating, uniaxial compressive strength of the intact rock has been determined in the laboratory. The spacing and the condition of discontinuities as well as groundwater conditions have been visually estimated. The rock quality designation (RQD) has been obtained by using Palmstom (1981)correlation,

$$RQD = 115 - 3.3\ J_v \quad \ldots\ 3.4$$

Where, J_v is the total number of joints in a cube of 1 m of rock mass.

The J_v values and corresponding RQD's at different localities are presented in Table 3.8.

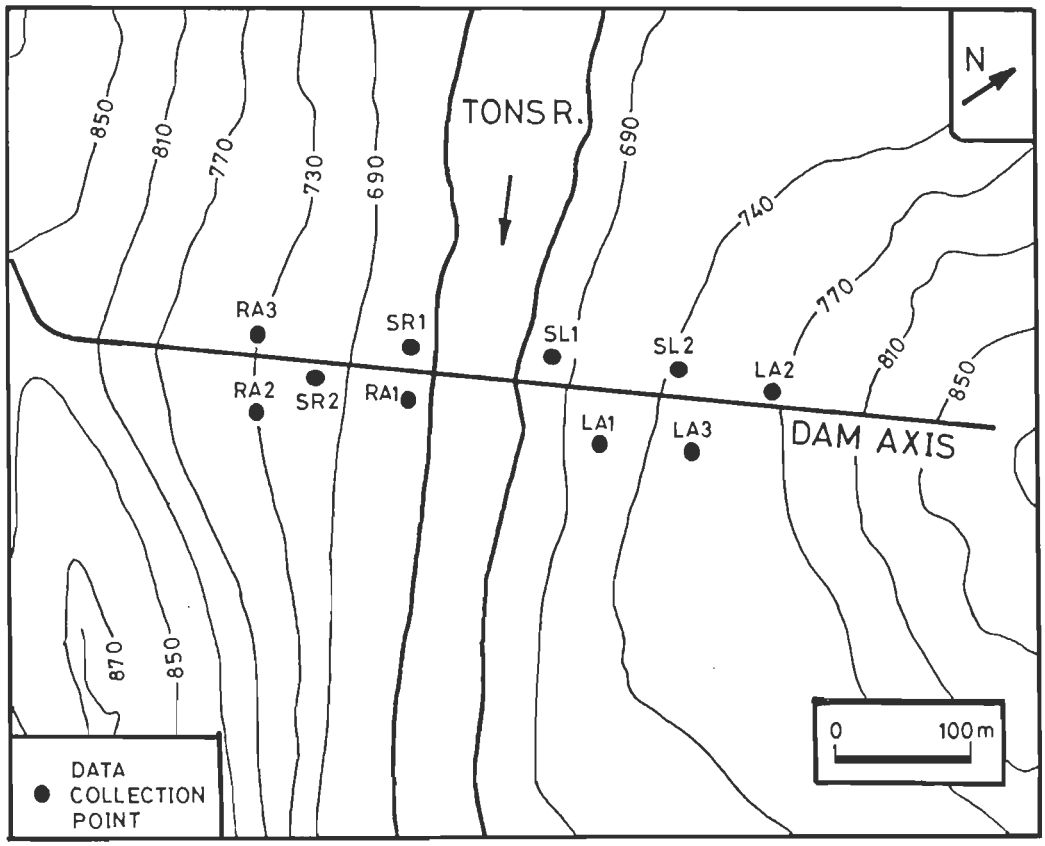

FIG. 3.6 LOCATIONS OF RMR DATA COLLECTION POINTS.

TABLE 3.8 : ESTIMATED ROCK QUALITY DESIGNATION AT DIFFERENT LOCALITIES ON THE ABUTMENTS

Location		Rock Type	J_v Value	RQD	Rating Allocated
Left Abutment	LA1	QSL	17	58.9	13
	LA2	Q	13	72.1	13
	LA3	Q	11	78.7	17
Right Abutment	RA1	QSL	18	55.6	13
	RA2	Q	14	68.8	13
	RA3	Q	13	72.1	13
In Drift on Left Abutment	SL1	QSL	17	58.9	13
	SL2	Q	13	72.1	13

Location		Rock Type	J_v Value	RQD	Rating Allocated
In Drift on Right Abutment	SR1	QSL	18	55.6	13
	SR2	Q	14	68.8	13

QSL - Quartzitic Slates
Q - Quartzite
J_v - Total number of discontinuities in a cube of 1m of rock mass
RQD - Rock quality designation

Thus, the various parameters as estimated in the field and in laboratory are awarded ratings using the RMR classification (Table 3.9). A perusal of the Table 3.9 indicates that the quartzite rock mass falls in good quality and quartizitic slates falling in fair category, except at locality LA1 where it is good in quality.

TABLE 3.9 : GEOMECHANICS CLASSIFICATION OF ROCK MASS AT ABUTMENTS

Location		Parameters						Class	Classification
		UCS	RQD	SP.	GWC	COD	RMR		
Left Abutment	LA1	7	13	8	15	20	63	II	Good
	LA2	12	13	8	15	20	68	II	Good
	LA3	12	17	8	15	15	67	II	Good
Right Abutment	RA1	7	13	8	10	20	58	III	Fair
	RA2	12	13	8	12	20	65	II	Good
	RA3	12	13	8	15	20	68	II	Good
In Drift on Left Abutment	SL1	7	13	8	15	17	60	III	Fair
	SL2.	12	13	8	15	20	68	II	Good
In Drift on Right Abutment	SR1	7	13	8	10	17	55	III	Fair
	SR2	12	13	8	10	20	63	II	Good

UCS - Uniaxial compressive strength
RQD - Rock quality designation
SP. - Spacing of discontinuities
GWC - Ground water condition
COD - Condition of discontinuities
RMR_B - Rock mass rating (Basic)

The shear strength parameters corresponding to rock mass ratings of various localities are presented in Table 3.10. To calculate the shear strength parameters of the rock mass, relation

given by Bieniawski (1989) has been used which is as follows

$$\phi = 0.5 \times RMR + 5 \quad \ldots 3.5$$
$$C = 0.05 \times RMR \text{ (KPa)} \quad \ldots 3.6$$

Where, ϕ = Angle of internal friction
C = Cohesion
RMR = Rock Mass Rating

TABLE 3.10 : SHEAR STRENGTH PARAMETERS OF THE ROCK MASS AT VARIOUS LOCALITIES ON THE ABUTMENTS

Location		RMR	Corresponding Class		Cohesion, C (kg/cm^2)	Friction Angle, ϕ (Deg)
			Cohesion (kg/cm^2)	Friction angle (Deg)		
Left Abutment	LA1	63	3-4	35-45	3.15	36.5
	LA2	68	3-4	35-45	3.40	39.0
	LA3	67	3-4	35-45	3.35	38.5
Right Abutment	RA1	58	2-3	25-35	2.90	34.0
	RA2	65	3-4	35-45	3.25	37.5
	RA3	68	3-4	35-45	3.40	39.0
In Drift on Left Abutment	SL1	60	2-3	25-35	3.00	35.0
	SL2	68	3-4	35-45	3.40	39.0
In Drift on Right Abutment	SR1	55	2-3	25-35	2.75	32.5
	SR2	63	3-4	35-45	3.15	36.5

3.5.4 ESTIMATION OF IN-SITU MODULUS OF DEFORMATION OF FOUNDATION ROCKS BY ROCK MASS RATING

The in-situ modulus of deformation of foundation rocks has been estimated by empirical approaches of Bieniawski (1978), Serafim & Pereira (1983) and Agarwal et al. (1991). Bieniawski established a relationship between RMR and in-situ modulus of deformation which is given by:

$$E_d = 2RMR - 100 \quad \ldots 3.7$$

Where, E_d is the in-situ modulus of deformation in GPa.

Another relation proposed by Serafim& Pereira (1983) between RMR and in-situ modulus of deformation is given by:

$$E_d = 10^{(RMR\ -10)/\ 40} \quad \ldots\ 3.8$$

Where, E_d is the in-situ modulus of deformation in GPa.

Similarly, Agarwal et al. (1991) established a relation between RMR and modulus of deformation and found good agreement between measured and predicted values of in-situ deformation. It is given by:

$$E_d = 10^{(RMR\ -30)/\ 50} \quad \ldots\ 3.9$$

Where, E_d is the in-situ modulus of deformation in GPa.

Thus, a comparison of values of in-situ modules of deformation, estimated through different empirical approaches, is presented in Table 3.11 and is shown in Fig.3.7.

TABLE 3.11 : COMPARISON OF IN-SITU MODULUS OF DEFORMATION OF FOUNDATION ROCKS OBTAINED BY EMPIRICAL APPROACHES

Location	Rock Type	RMR	In-Situ Modulus of Deformation, E_d (kg/cm^2)		
			Bieniawski Relation	Serafim & Pereira Relation	Agarwal et al. Relation
LA1	QSL	63	$2.6*10^5$	$2.1*10^5$	$0.4*10^5$
LA2	Q	68	$3.6*10^5$	$2.8*10^5$	$0.5*10^5$
LA3	Q	67	$3.4*10^5$	$2.6*10^5$	$0.5*10^5$
RA1	QSL	58	$1.6*10^5$	$1.5*10^5$	$0.3*10^5$
RA2	Q	65	$3.0*10^5$	$2.3*10^5$	$0.5*10^5$
RA3	Q	68	$3.6*10^5$	$2.8*10^5$	$0.5*10^5$
SL1	QSL	60	$2.0*10^5$	$1.7*10^5$	$0.3*10^5$
SL2	Q	68	$3.6*10^5$	$2.8*10^5$	$0.5*10^5$
SR1	QSL	55	$1.0*10^5$	$1.3*10^5$	$0.3*10^5$
SR2	Q	63	$2.6*10^5$	$2.1*10^5$	$0.4*10^5$

A perusal of Table 3.11 indicates that the values of in-situ modulus of deformation obtained by empirical approaches of Bieniawski and Serafim & Pereira are much higher than the in-situ

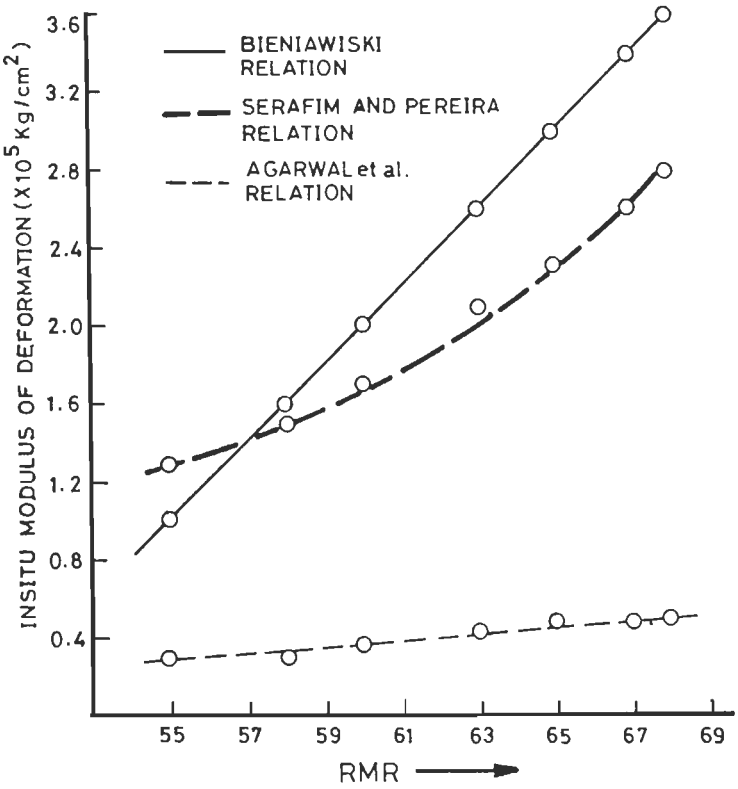

FIG. 3.7 COMPARISON OF IN-SITU MODULUS OF DEFORMATION OF FOUNDATION ROCKS OBTAINED BY EMPIRICAL APPROACHES.

tested values, as given in Table 3.3. Moreover, the values obtained by Agarwal et.al relation are in close agreement with the in-situ tested values of modulus of deformation.

The average value of the in-situ modulus of deformation, as determined from the Agarwal et al. relation is 0.39 x 10^5 kg/cm^2.

3.6 STABILITY ANALYSIS OF AUBTMENTS

Design of stable cut slope is a prerequisite for the safe construction of a dam. Potential instability of abutment slopes may pose problems during construction works. Therefore, it is essential to recognise the potential stability problems in the early stage of planning so that a safe and economic structure could be designed.

3.6.1 FIELD INVESTIGATIONS

During field investigations, a detailed geological mapping on 1:2000 scale covering an area of 1.5 sq km has been carried out to obtain the lithological and structural data in and around the dam site. The rocks exposed on the abutments are mainly quartzites and quartzitic slates of Simla Group. The quartzites are exposed over a larger area while quartzitic slates are exposed relatively over smaller areas on both the abutments. Detailed description of geology of the dam site and adjoining areas has already been given in Chapter II. However, a geological cross section along the dam axis is shown in Fig.3.8.

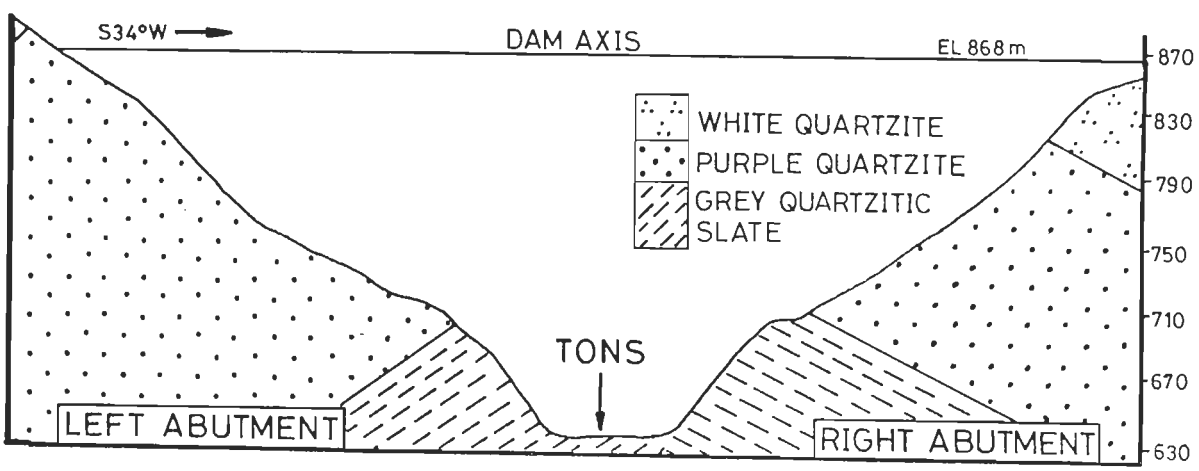

FIG. 3.8 GEOLOGICAL CROSS SECTION OF BOTH THE ABUTMENTS, ALONG DAM AXIS.

Data pertaining to structural discontinuities, mainly joints has been collected from both left and right abutments (300 nos. each). The poles of the attitude of joints, as observed in the field have been plotted on the stereonet for both the abutments separately. These poles have been contoured and the predominant clusters have been identified. The attitude of maxima of the structural discontinuities, thus obtained are presented in Fig.3.9.

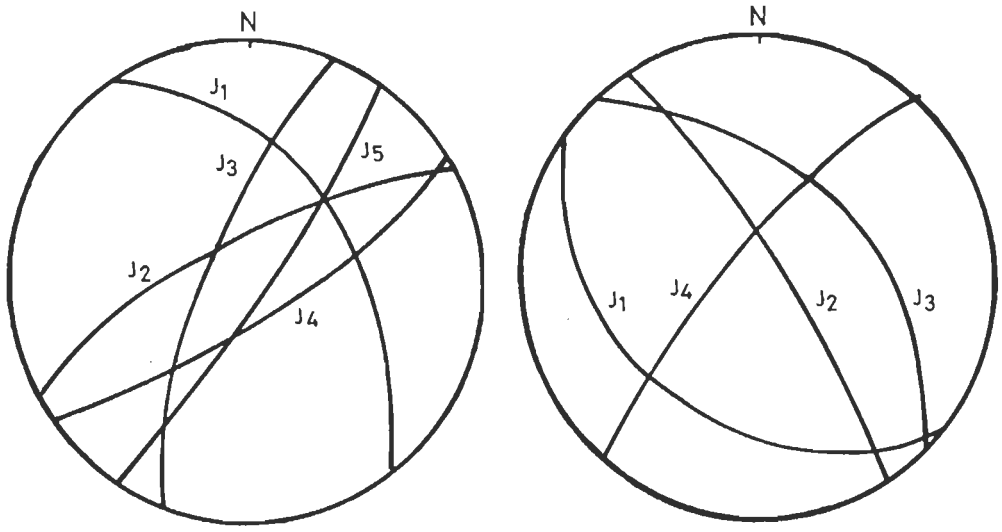

LEFT ABUTMENT

J_1	N50°E/40°
J_2	N30°W/72°
J_3	N70°W/70°
J_4	S38°E/70°
J_5	S60°E/80°

RIGHT ABUTMENT

J_1	S36°W/28°
J_2	N60°E/78°
J_3	N50°E/42°
J_4	N50°W/78°

FIG. 3.9 ATTITUDE OF STRUCTURAL DISCONTINUITIES ON LEFT AND RIGHT ABUTMENT

3.6.2 GEOMETRY OF ABUTMENT SLOPES

Left Abutment

The left abutment slope has an uneven slope profile with varying slope angles from the river bed to the ridge top (Plate 3.1). The slope section close to the river bed and the section above El. 770 m have steep angles of about 50° and 45° respectively, whereas the slope section, forming the middle portion of the abutment has a moderate angle (28°).

For the purpose of stability analysis, the left abutment slope has been sub-divided into three segments in such a manner that the slope angle within a segment is consistent.These slope segments are designated as LA1, LA2 and LA3 . The heights and angles of these segments are given in Fig.3.10. The stability analysis has been carried out for all the three segments separately.

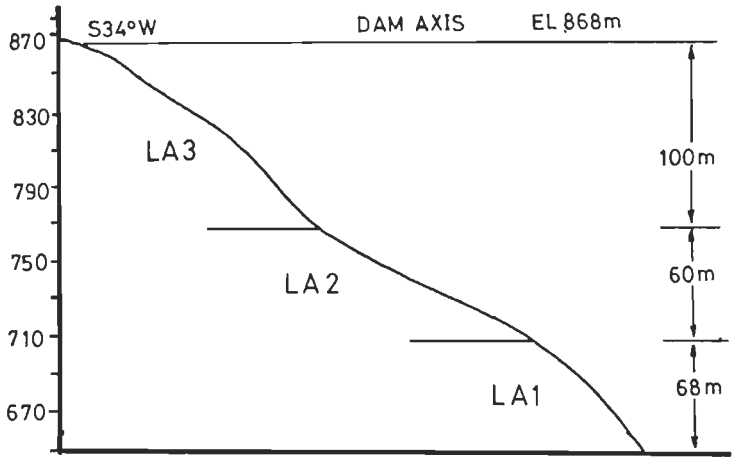

SLOPE SEGMENT	SLOPE HEIGHT	SLOPE ANGLE
LA1	68m	50°
LA2	60m	28°
LA3	100m	45°

FIG. 3.10 SLOPE GEOMETRY OF LEFT ABUTMENT.

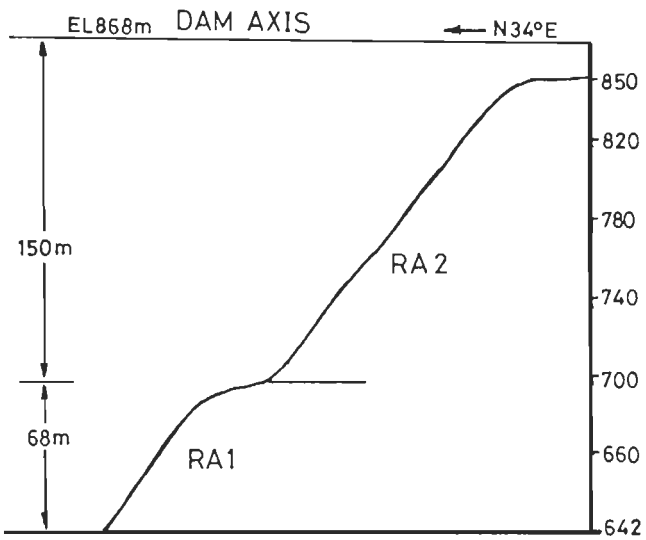

SLOPE SEGMENT	SLOPE HEIGHT	SLOPE ANGLE
RA1	68m	52°
RA2	150m	50°

FIG. 3.11 SLOPE GEOMETRY OF RIGHT ABUTMENT.

Right Abutment

The right abutment slope angle is more or less consistent from the river bed to the ridge top with a local terrace extending for about 10m at El. 710 m (Plate 3.2). Accordingly the slope has been subdivided into two major segments namely RA1and RA2. The stability analysis has been carried out for these two slope segments, separately. A cross section of right abutment slope is shown in Fig 3.11.

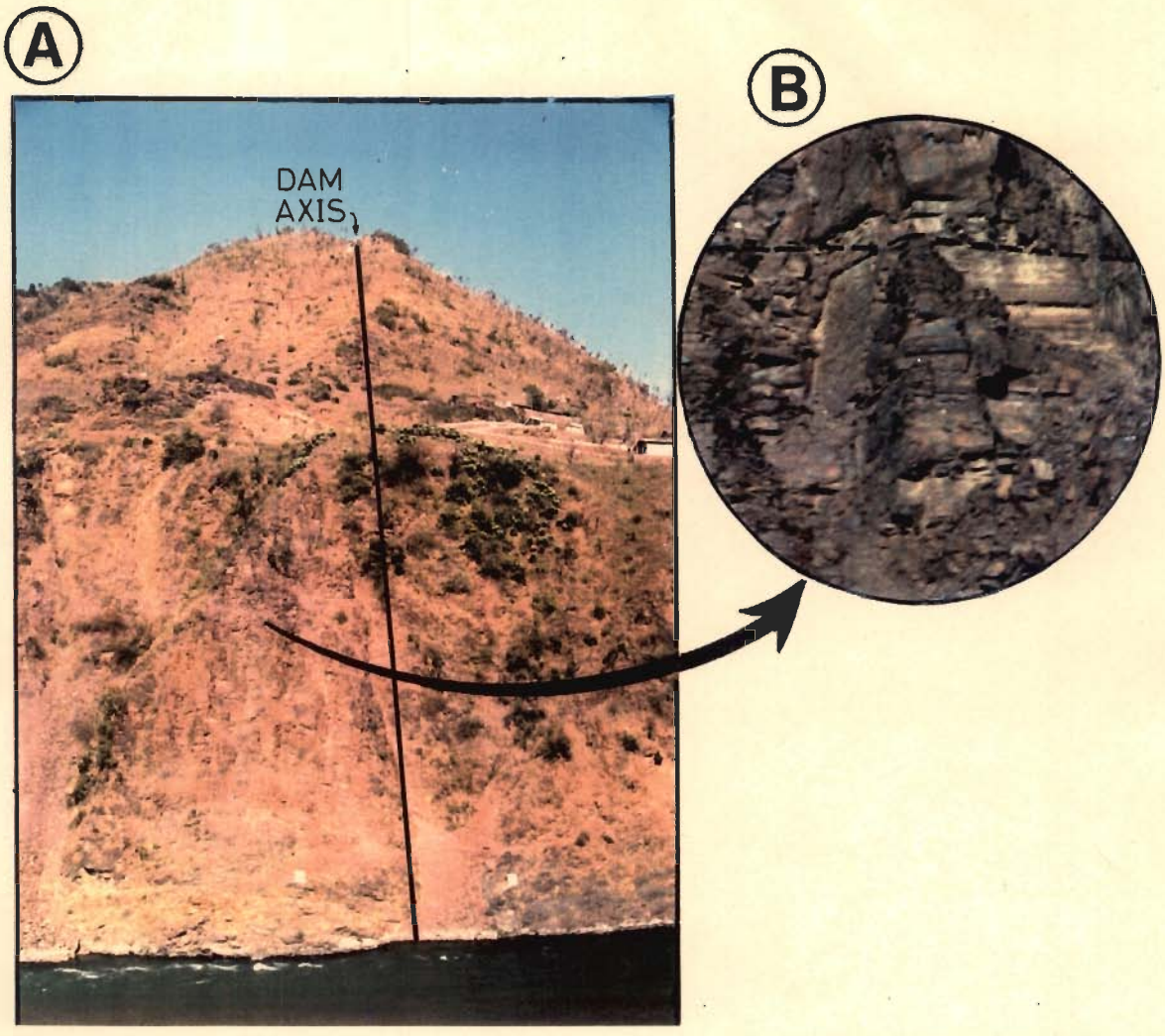

PLATE 3.1 **A - A VIEW OF LEFT ABUTMENT SHOWING DAM AXIS**
B - CONTACT OF QUARTZITIC SLATE AND PURPLE QUARTZITE ON LEFT ABUTMENT

3.6.3 POSSIBLE MODE OF FAILURE

In order to identify the possible mode of failure on abutment slopes, the Markland test has been applied. According to Markland test the following conditions should be satisfied for the failure to occur.

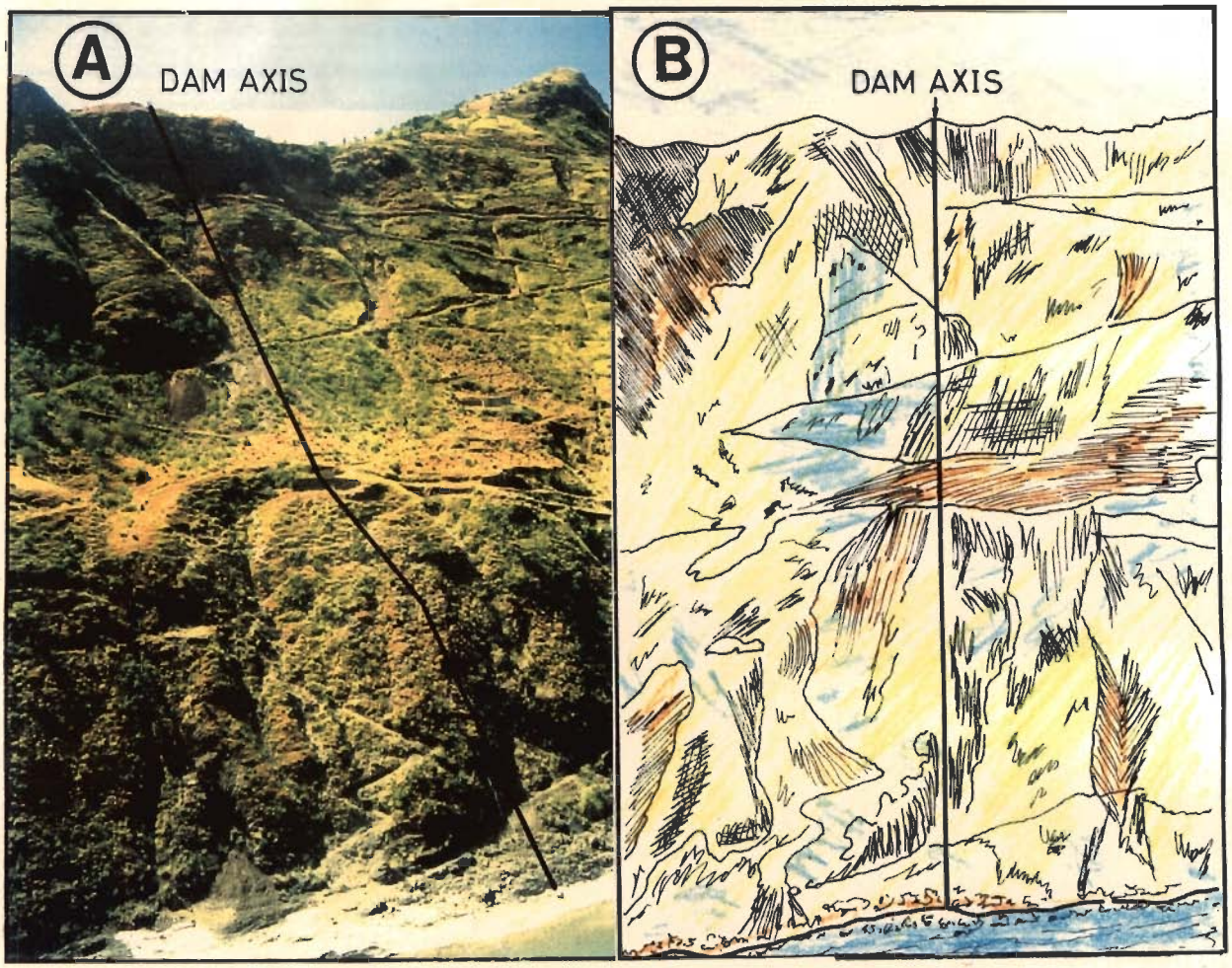

PLATE 3.2 A - A VIEW OF RIGHT ABUTMENT SHOWING DAM AXIS
B - A SKETCH OF RIGHT ABUTMENT

Markland Condition		
For Plane Failure - $\alpha_s > \alpha_p > \phi$ For Wedge Failure - $\alpha_s > \alpha_i > \phi$	Where,	α_s = Slope face inclination α_p = Failure plane inclination α_i = Plunge of line of intersection ϕ = Angle of internal friction

Stereographic projections are the simple and meaningful method to identify the possible mode of failures. For that purpose, the structural discontinuity planes and the great circle representing the slope face are plotted over the stereonet. Also, a friction circle corresponding

to angle of shearing resistance is plotted over it . The angle of internal friction (ϕ) obtained by the rock mass rating has bean used in Markland test to identify the possible mode of failure. For that purpose the mid value of the angle of internal friction class corresponding to class in which rock mass rating falls has been adopted.

A perusal of Fig.3.12 indicates that although many wedges are formed on left abutment by the

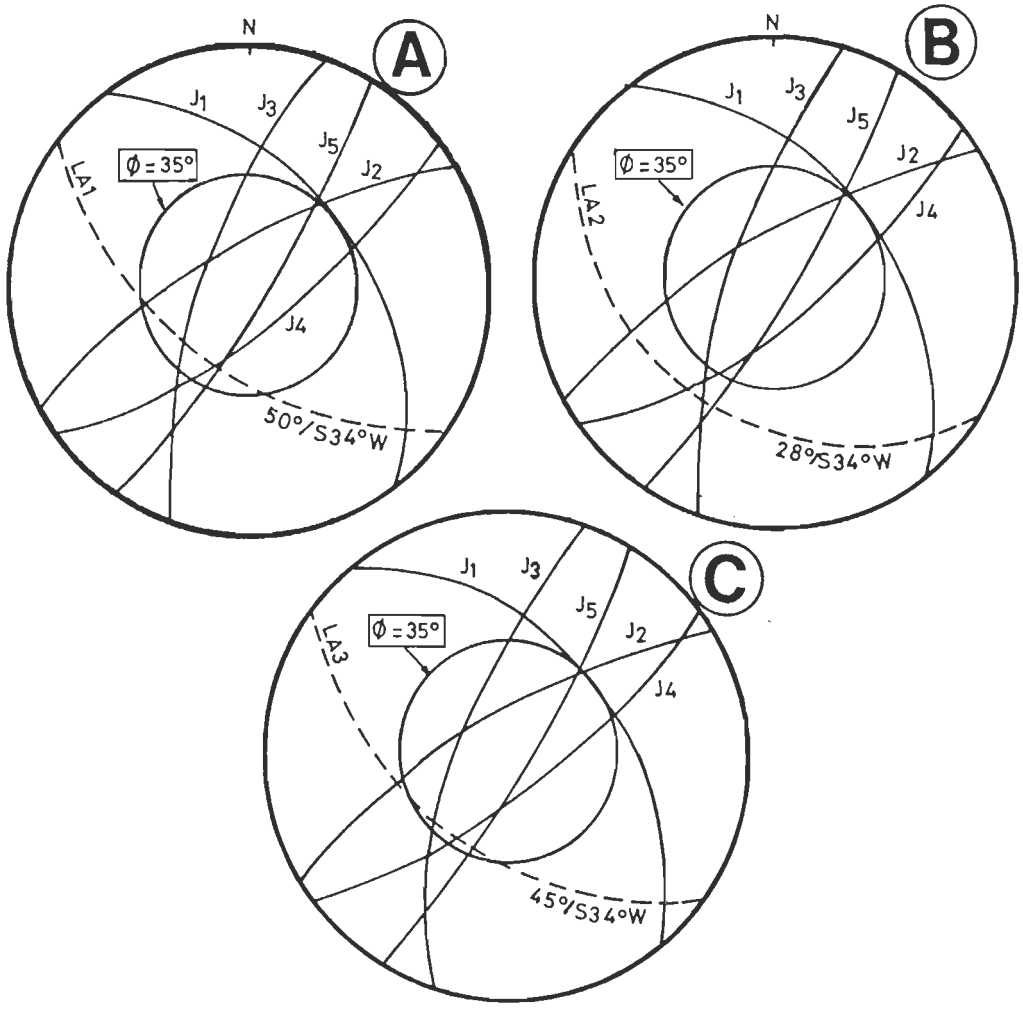

FIG. 3.12 KINEMATIC CHECK FOR LEFT ABUTMENT SLOPE - A-LA1 SEGMENT, B-LA2 SEGMENT, C-LA3 SEGMENT.

intersection of structural discontinuities, but none is kinematically unstable. It may be noted from the stereoplot of left abutment that no wedge or plane is falling in the zone, defined by the great circle of the slope face and the ϕ circle. Therefore, no wedge or plane satisfies the Markland test. Hence, it can be concluded that no wedge or plane is kinematically unstable

on left abutment slope.

From the stereoplots of RA1 and RA2 slope segments of right abutment (Fig.3.13) it may be

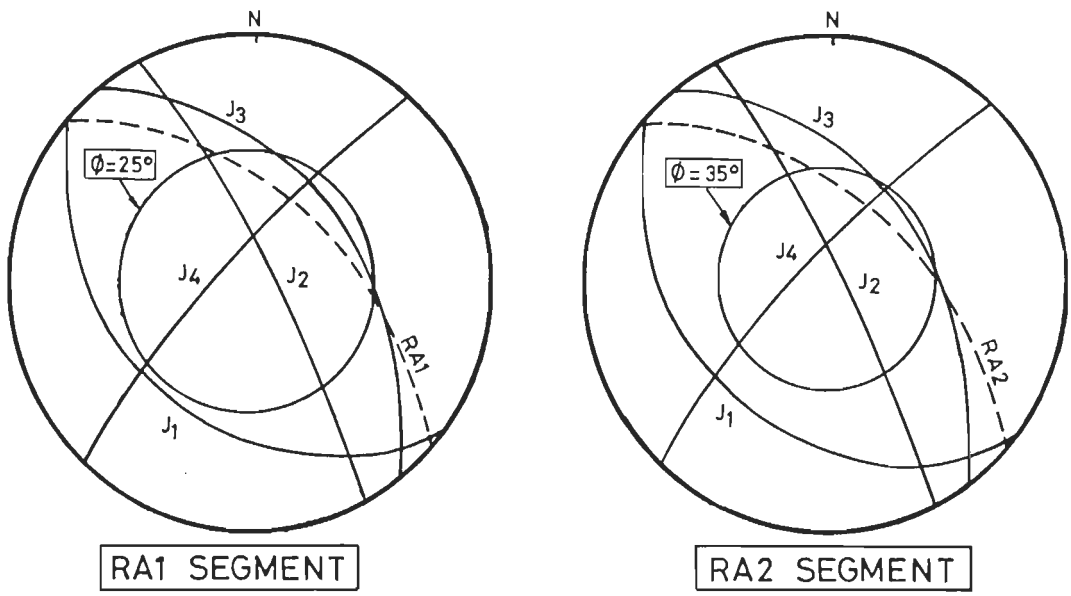

FIG. 3.13 KINEMATIC CHECK FOR RIGHT ABUTMENT SLOPE.

noted that in both the cases a wedge formed by the discontinuities J_3 and J_4 and the plane J_3 are falling in the unstable zone marked by the slope and the ϕ circle. It means that both the slope segments (RA1 & RA2) are kinematically unstable for wedge and plane mode of failure. It may also be noted from both the stereoplotes that joint J_4 is more or less perpendicular to the slope and joint J_3 is involved in both, plane and wedge failures. Therefore, the possible failure in both the slope segments would follow plane mode of failure. The Joint J_4 would contribute its presence as a lateral boundary to the block sliding along joint J_3.

3.6.4 SHEAR STRENGTH PARAMETERS FOR JOINT J_3

On the right abutment slope, as discussed earlier, Joint J_3 is kinematically unstable for RA1 and RA2 slope segments. Therefore, an attempt has been made to estimate the shear strength along Joint J_3. The shear strength of this joint surface has been estimated by using empirical law of friction, for rock joints (Barton, 1977). The empirical equation used to determine the shear strength of the joint surface is given below:

$$\tau = \sigma_n \times \text{Tan} [\phi_b + \text{JRC} \log_{10} (\text{JCS}/\sigma_n)] \quad \ldots \quad 3.10$$

τ = Peak Shear Strength
σ_n = Effective Normal Stress
JRC = Joint Roughness Coefficient
JCS = Joint Compressive Strength
ϕ_b = Basic Friction Angle

Although, the three basic parameters JRC, JCS and ϕ_b, used in the empirical equation can be determined in the field or in the laboratory, but they can still be estimated by standard tables when no laboratory or field data is available

However, for the present study, the basic friction angle has been estimated through the table given by Barton & Choubey (1977). The joint roughness coefficient has been estimated by the figure given by Barton & Choubey (1977). The joint compressive strength of weathered surface has been taken as one fourth of the compressive strength of unweathered rock (Barton, 1973). The effective normal stress acting on the joint surface has been calculated by using the equation 3.11

$$\sigma = W \text{ Cos } \alpha_p / A \quad \ldots \quad 3.11$$

Where, α_p is the dip of the failure plane
W is the weight of the sliding block
A is the area of the failure plane

The equations to calculate the weight (W) and the area (A) are given later in this Chapter.

The input data required to estimate the shear strength of Joint J_3 is given in Table 3.12. The value of total friction angle of Joint J_3 has also been obtained by the plot drawn in between the normal stress and the shear stress (Fig.3.14).

Thus, the total friction angle of Joint J_3 , as estimated by the Barton's empirical equation comes out to be 35° and 45° for RA1 and RA2 slope segments, respectively. The estimated values of total friction angle for Joint J3 by Barotn's empirical equation are in close agreement with the tested values of various quartzites and slates (Barton, 1973; Hoek & Bray 1981).

The J_3 joints are well developed having continuity ranging upto 10m and occasionally upto 20 m. The joint surfaces are slickensided and moderately weathered at places. Due to these reasons, a slightly lower total friction angle of 30° and 40° have been used in stability analysis of RA1 and RA2 slope segments, respectively, instead of the values 35° and 45°, as obtained by empirical law of friction.

TABLE 3.12 : ESTIMATION OF SHEAR STRENGTH OF JOINT J_3 ON RIGHT ABUTMENT SLOPE

Parameters	Slope Segment	
	RA1	RA2
Effective normal stress acting on the joint surface, σ_n	2.46 kg/cm^2	3.9 kg/cm^2
Basic friction angle, ϕ_b	30°	35°
Joint roughness coefficient, JRC	2.9	5
Joint compressive strength, JCS	195 kg/cm^2	512.5 kg/cm^2
Compressive strength of intact rock, σ_c	780 kg/cm^2	2050 kg/cm^2
$\tau = \sigma * \text{Tan} [\phi_b + \text{JRC} \log_{10}(\text{JCS}/\sigma_n)]$ ... 3.10 $\text{Tan}^{-1} (\tau/\sigma_n)$ Total friction angle for discontinuity J_3	35.36°	45.58°

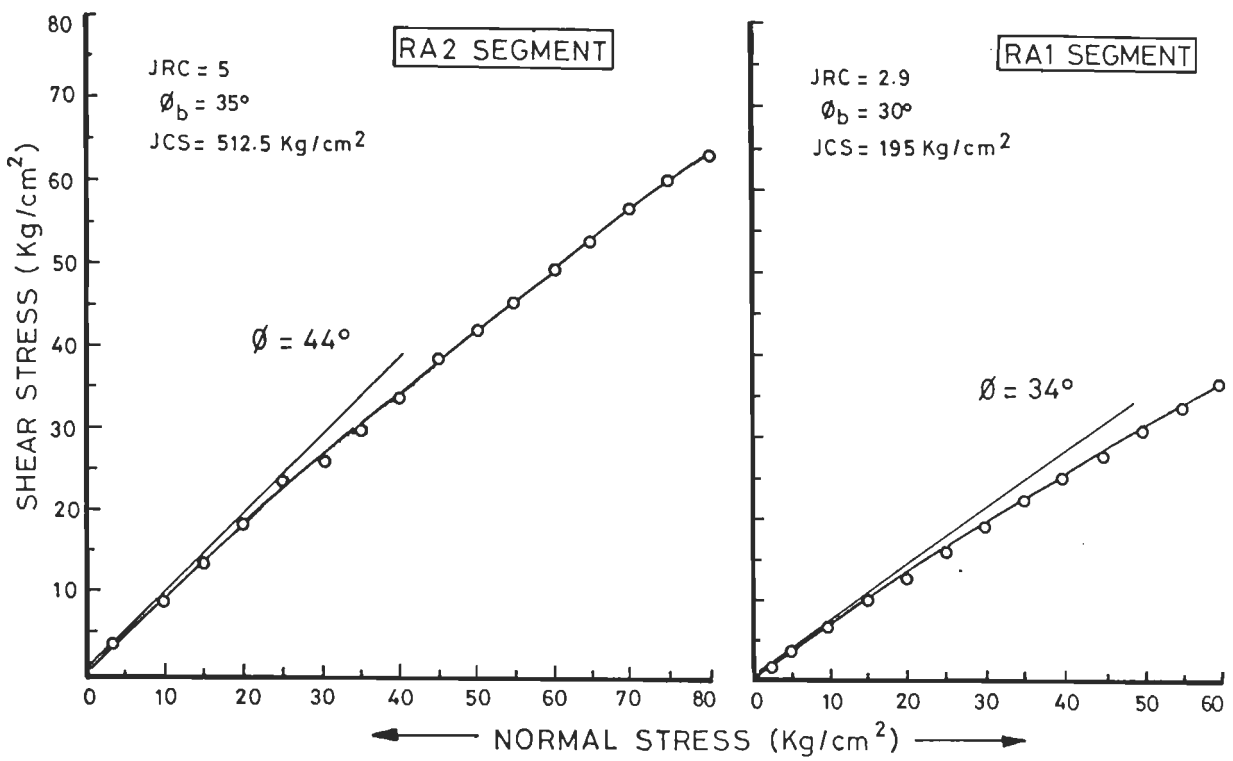

FIG. 3.14 ESTIMATION OF SHEAR STRENGTH OF JOINT J_3 ON RIGHT ABUTMENT

In order to estimate the cohesion (C) along the surface of Joint J3, back analysis of failed slopes (2 nos.) in the same rock has been carried out. Details of these failed slopes are given in Table 3.13. The likely mobilised cohesion (C) effective on these failed slopes has been back calculated by the following equation.

$$C = \frac{F\,[W(\sin\alpha_p + \alpha\cos\alpha_p) + V\cos\alpha_p] - [W(\cos\alpha_p - \alpha\sin\alpha_p) - U - V\sin\alpha_p]\tan\phi}{A} \quad \ldots 3.12$$

The various symbols used in the above equation and the derivation are given later in this Chapter.

TABLE 3.13 : BACK ANALYSIS FOR COHESION OF FAILED SLOPES

Input Data	Back Analysis for RA1 Slope	Back Analysis for RA2 Slope
Slope Angle, α_t	70°	75°
Dip of Failure Plane, α_p	42°	42°
Dip of Upper Slope Surface, α_s	0°	0°
Dip of Tension Crack, α_t	78°	78°
Height of Slope, h	30	30
Angle of Internal Friction, ϕ	30°	45°
Unit Weight of Rock, γ	2.72 T/m^3	2.75 T/m^3
Unit Weight of Water, γ_w	1.00 T/m^3	1.00 T/m^3
Horizontal Earthquake Acceleration, α	0.15	0.15
Height of Water in Tension crack, Z_w	1/2 Z_L*	1/2 Z_L*
Factor of Safety, FOS	1.0	1.0
Calculated Cohesion, C	15.59 T/m^2	16.01 T/m^2
* Z_L - Depth of tension crack		

3.6.5 CALCULATION OF FACTOR OF SAFETY

The left abutment slope, as discussed earlier, is Kinematically stable. However, on the right abutment, both the slope segments (RA1 and RA2) have been identified as kinematically unstable for plane mode of failure. Therefore, the calculation of factors of safety of these segments has been carried out by adopting a modified technique of plane failure analysis.

3.6.6 MODIFIED TECHNIQUE OF PLANE FAILURE ANALYSIS

Plane failure in rock slopes occur, when a geological discontinuity strikes parallel or nearly parallel to the slope face and dips at an angle greater than the angle of internal friction. Hoek and Bray(1981) gave an analytical solution for the plane failure mode in rock slopes. In this analysis, it was assumed that the upper slope surface is horizontal and the tension crack is

vertical. However, this method does not account for those rock slopes in which the upper slope surface and tension crack are not vertical and inclined at some angle. During the field work, it has been observed that most of the slopes have inclined upper slope surfaces. Moreover, it is difficult to trace out the tension crack on the upper slope surface. Thus, keeping these observations in mind, an attempt has bean made to modify the technique of Hoek & Bray (1981).

General Conditions and Assumptions

In the present analysis, the general conditions as assumed by Hoek and Brey (1981) remain the same for plane failure except that the upper slope surface and tension crack are inclined. Hence, the following general conditions must be satisfied.

1) The failure plane must strike parallel or nearly parallel (Approximately ± 20°) to the slope face.
2) The dip of the failure plane must be smaller than the dip of the slope face ($\alpha_p < \alpha_f$).
3) The angle of internal friction (ϕ) of the failure plane must be smaller than the dip of the failure plane ($\phi < \alpha_p$).
4) The upper slope surface and tension crack may be inclined.
5) The dip of the upper slope must be smaller than the dip of the failure plane ($\alpha_s < \alpha_p$).
6) The tension crack must be present on the upper slope surface.

The following assumptions are made in this analysis

1) It is presumed that there is no resistance to sliding at the lateral boundaries of the slide.
2) The tension crack is filled with water to a vertical depth of Z_w. The water from tension crack seeps along the failure surface and escapes out on the slope face where the failure surface daylights.
3) It is assumed that any pre existing discontinuity, vertical or dipping towards valley, act as the tension crack.

Geometry of the Slope

The geometry of the slope considered in the present analysis is defined in Fig.3.15. The various symbols used in this figure are:

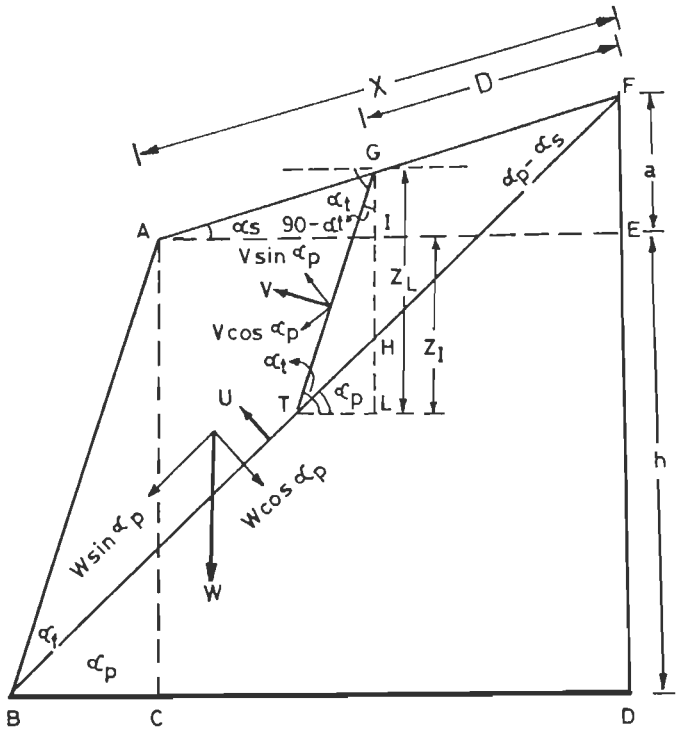

GEOMETRY OF THE SLOPE CONSIDERED IN THE ANALYSIS

FIG. 3.15

α_f - Slope face angle
α_s - Upper slope surface angle
α_p - Dip of potential failure plane
α_t - Angle of tension crack
h - Height of slope
Z_L - Height of tension crack
W - Weight of Sliding block
U - Uplift water force acting on the block
V - Water force in the crack, acting on the rear face of the block

Area of the Sliding Block

The area of the sliding surface, A is represented by the length of the surface visible in a cross section drawn through the slope. Hence, from Fig.3.15

$$\text{Area, } A = (h - Z_l)\ \text{Cosec}\ \alpha_p \quad \ldots\ 3.13$$
$$b_c = AI = h\ [\ \sqrt{(\ \text{Cot}\ \alpha_f * \text{Cot}\ \alpha_p\ )} - \text{Cot}\ \alpha_f\ ]\ \ldots\ 3.14$$
$$Z_c = IH = h\ [1 - \sqrt{(\ \text{Cot}\ \alpha_f * \text{Tan}\ \alpha_p\ )}\ ] \quad \ldots\ 3.15$$

Equations 3.14 & 3.15 are equivalent to those given by Hoek & Bray (1981). Also from Fig.3.15

$$AG = b_c / \text{Cos}\ \alpha_s \quad \ldots\ 3.16$$
$$IG = b_c / \text{Cot}\ \alpha_s \quad \ldots\ 3.17$$

Substituting the value of b_c from Eq. 3.14 into Eq. 3.17

$$IG = h [\sqrt{(Cot \alpha_f * Cot \alpha_p)} - Cot \alpha_f] / Cot \alpha_s \quad ... \quad 3.18$$

From Fig.3.15

$$Z = GH = IG + IH$$

Thus, from Eq. 3.15 & 3.18

$$Z = h [(1 - (Cot \alpha_f / Cot \alpha_s) + (\sqrt{} Cot \alpha_f / \sqrt{}Cot \alpha_p) * (Cot \alpha_p / Cot \alpha_s - 1)] \quad ... \quad 3.19$$

Again from Fig.3.15

$$Z_L = GL = Z Sin \alpha_f / [Sin \alpha_f - (Tan \alpha_p * Cos \alpha_f)] \quad ... \quad 3.20$$
$$Z_I = IL = GL - IG$$

Thus, from equation 3.18 & 3.20

$$Z_I = IL = [Z Sin \alpha_f / \{Sin \alpha_f - (Tan \alpha_p * Cos \alpha_f)\}] - b_c * Tan \alpha_s \quad ... \quad 3.21$$

By substituting the value of Z_I from Eq. 3.21 into Eq. 3.13, the area of the sliding surface is calculated

Weight of the Sliding Block

The weight of the sliding block is obtained by the product of unit weight of rock (γ) and the volume of the sliding block.

$W = \frac{1}{2} \gamma [(h + a) X - D Z_L]$ ... 3.22
Where, γ is the unit weight of the rock, X and D are the distance AF and GF respectively, and a is the height EF as shown in Fig.3.15
$X = [h (Cot \alpha_f / Cos \alpha_s)] * [(Tan \alpha_p - Tan \alpha_f) / (Tan \alpha_s - Tan \alpha_p)]$ ... 3.23 $D = Z / [Tan \alpha_p * Cos \alpha_s) - Sin \alpha_s]$ ... 3.24 and $a = [h (Tan \alpha_s / Tan \alpha_f)] * [(Tan \alpha_p - Tan \alpha_f) / (Tan \alpha_s - Tan \alpha_p)]$ ... 3.25

Horizontal Water Force

The horizontal force, V, due to water pressure in the tension crack, acting on the rear face of the block (as shown in Fig.3.16) is derived from

$$V = \frac{1}{2} \gamma_w Z_w^2 \sin^2\alpha_t \quad \ldots \quad 3.26$$

Where, γ_w is the unit weight of water, and
Z_w is the height of the water column in the tension crack.

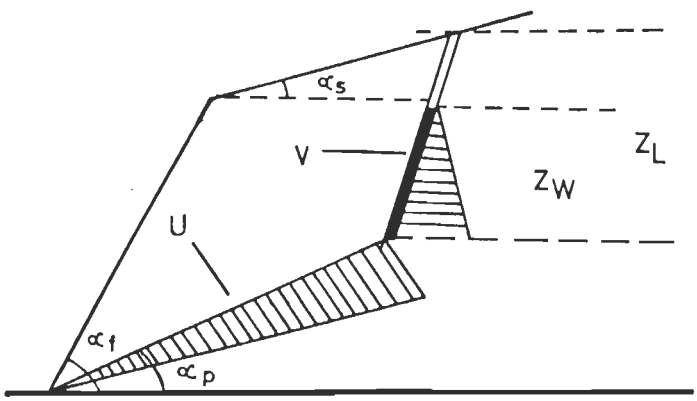

FIG. 3.16 WATER PRESSURE DISTRIBUTION ALONG THE TENSION CRACK AND THE BASE OF THE SLIDING BLOCK.

Uplift Water Force

The water seeps through the tension crack into the sliding surface and results in an uplift force, U, as shown in Fig.3.16. This uplift force is calculated from

$$U = \frac{1}{2} \gamma_w Z_w \sin \alpha_t (h - Z_t) * \text{Cosec } \alpha_p \quad \ldots \quad 3.27$$

Thus, substituting the value of Z_t from Eq. 3.21 the uplift water force acting on the sliding block is computed.

Factor of Safety Under Static Condition

The factor of safety under static condition is derived from the equation 3.28

$$F = \frac{CA + [\,W\cos\alpha_p - U - V\sin\alpha_p]\tan\phi}{W\sin\alpha_p + V\cos\alpha_p} \quad \ldots 3.28$$

Where, C is the Cohesion along the failure plane and,
ϕ is the angle of internal friction along the failure plane

Factor of Safety Under Dynamic Condition

The factor of safety under dynamic condition is obtained from the equation 3.29

$$F = \frac{CA + [W(\cos\alpha_p - \alpha\sin\alpha_p) - U - V\sin\alpha_p]\tan\phi}{W(\sin\alpha_p + \alpha\cos\alpha_p) + V\cos\alpha_p} \quad \ldots 3.29$$

Where, α is the horizontal earthquake acceleration.

In the Eq. 3.28 & 3.29, the water pressure distribution along the tension crack (V) and the area of base of the sliding block (U) are required for a meaningful calculation. But in the field it is not easy to measure the depth of water in tension crack (Z_w). Hence, the factor of safety cannot be calculated without knowing the depth of water in the tension crack. Therefore, the value of Z_w can be varied from a minimum to the maximum depth of tension crack during the stability analysis. The depth of water in tension crack for which the factor of safety matches with the existing slope conditions, is considered as the representative value of Z_w.

Validity of the Technique

In the present study the technique of Hoek and Bray (1981) which assumes a horizontal upper slope and vertical tension crack has been modified to account for the inclined upper slope surface and tension crack in nature.

To prove the validity of the modified technique, the values of upper slope surface angle (α_s) and tension crack inclination (α_t) have been taken as 0° and 90° respectively. By substituting these values in the modified equations, they would be identical to those given by Hoek & Bray (1981).

Thus, the equations after substituting $\alpha_s = 0$ and $\alpha_t = 90°$ become as such

Area, $A = (h - Z)\ \text{Cosec}\ \alpha_p$

Weight, $W = \frac{1}{2}\ \gamma\ h^2\ [\ \{1 - (Z / h)^2\ \}\ \text{Cot}\ \alpha_p - \text{Cot}\ \alpha_t\ ]$

Uplift water Force, $U = \frac{1}{2}\ \gamma_w . Z_w\ (h - Z)\ \text{Cosec}\ \alpha_p$

Horizontal Water Force, $V = \frac{1}{2}\ \gamma_w . Z_w^2$

Effect of Inclined Upper Slope Surface and Tension Crack on Factor of Safety

To examine the effect of the inclined upper slope surface and tension crack on the factor of safety, an example has been considered with the following data:

Slope Angle, $\alpha_f = 50°$
Dip of Failure Plane, $\alpha_p = 35°$
Dip of Upper Slope Surface, $\alpha_s = 0°$ to $30°$
Dip of Tension Crack, $\alpha_t = 90°$ to $70°$
Height of Slope, $h = 60$ m
Angle of Internal Friction, $\phi = 45°$
Cohesion, $C = 12\ T/m^2$
Unit Weight of Rock, $\gamma = 2.6\ T/m^3$
Unit Weight of Water, $\gamma_w = 1.0\ T/m^3$
Horizontal Earthquake Acceleration, $\alpha = 0.15$
Height of Water in Tension crack, $Z_w = 14$ m

The results are presented in Table 3.14 . A plot of factor of safety against the angle of the upper slope (α_s) is given in Fig.3.17. A perusal of this plot indicates that as the upper slope inclination increases, the factor of safety decreases considerably. For a case where the upper slope is horizontal, the calculated factor of safety is 1.6. If the upper slope angle is increased to 30°, the factor of safety drops to 1.43. This means that if the inclination of the upper slope is not included, the calculated factor of safety will be higher.

TABLE 3.14 : STABILITY ANALYSIS OF SLOPE AT VARYING UPPER SLOPE ANGLE

Case No.	Upper Slope Angle (Deg.)	Area,A (m^2)	Weight,W (Tons)	Horizontal Water Force,V ($T/m^{2)}$	Uplift Water Force,U ($T/m^{2)}$	Factor of Safety,FOS
For an angle of tension crack (α_t) = 70°						
1	0	71.845	2267.68	86.472	472.59	1.60
2	10	70.243	3317.43	86.472	462.05	1.54
3	15	69.382	4433.85	86.472	456.38	1.51
4	20	68.487	6715.23	86.472	450.50	1.48
5	25	67.565	12998.24	86.472	444.43	1.45
6	30	66.505	71425.55	86.472	335.97	1.43

Case No.	Upper Slope Angle (Deg.)	Area,A (m^2)	Weight,W (Tons)	Horizontal Water Force,V ($T/m^{2)}$	Uplift Water Force,U ($T/m^{2)}$	Factor of Safety,FOS
For an angle of tension crack (α_t) = 80°						
1	0	76.72	2340.37	95.044	528.83	1.58
2	10	76.09	3456.77	95.044	524.53	1.53
3	15	75.73	4636.49	95.044	522.00	1.50
4	20	75.38	7032.68	95.044	519.67	1.48
5	25	74.99	13465.16	95.044	516.90	1.45
6	30	74.59	46627.40	95.044	514.14	1.43
For an angle of tension crack (α_t) = 90°						
1	0	80.191	2392.03	98.000	561.267	1.58
2	10	80.191	3558.34	98.000	561.267	1.53
3	15	80.191	4785.03	98.000	561.267	1.50
4	20	80.191	7254.02	98.000	561.267	1.48
5	25	80.191	13932.64	98.000	561.267	1.45
6	30	80.191	47526.01	98.000	561.267	1.43

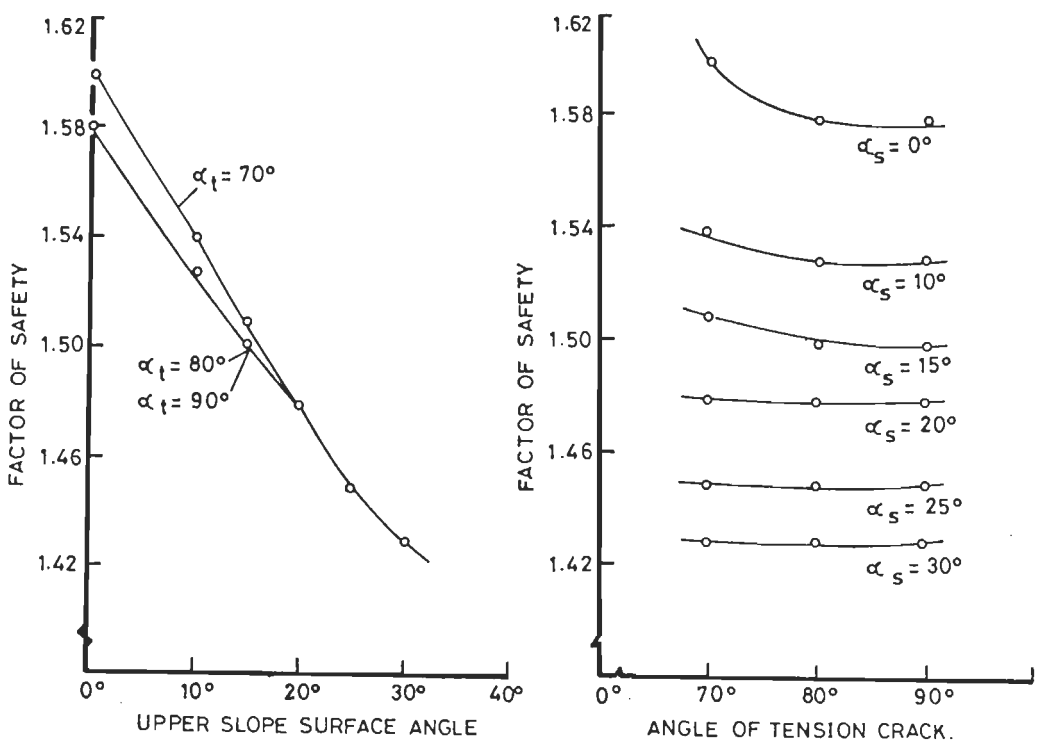

FIG. 3.17 EFFECT OF INCLINED UPPER SLOPE SURFACE AND TENSION CRACK ON FACTOR OF SAFETY.

The impact of the tension crack inclination (α_t) on factor of safety is shown in Fig.3.17. The effect is appreciable for upper slope angles (α_s) up to 20° but has no effect for steeper values. For the range of upper slope angles where it does have an effect (0-20°), the factor of safety actually increases as the angle of the tension crack (α_t) decreases.

3.6.7 PLANE FAILURE ANALYSIS OF RIGHT ABUTMENT SLOPE

It has already been indicated that RA1 and RA2 slope segments of right abutment are kinematically unstable for plane failure (section 3.6.3). The factors of safety of these two slope segments have been calculated by the modified technique described in the previous section. The required input data to calculate factor of safety of right abutment slope is given in Table 3.15.

TABLE 3.15 : INPUT DATA SHEET FOR THE CALCULATION OF FACTOR OF SAFETY OF RIGHT ABUTMENT SLOPE

Input Data	RA1 Slope	RA2 Slope
Slope Angle, α_f	52°	50°
Dip of Failure Plane, α_p	42°	42°
Upper Slope Surface Angle, α_s	13°	10°
Dip of Tension Crack, α_t	78°	78°
Height of Slope, h	68 m	150 m
Cohesion, C	16 T/m^2	16 T/m^2
Angle of Internal Friction, ϕ	30°	40°
Unit Weight of Rock, γ	2.72 T/m^3	2.78 T/m^3
Unit Weight of Water, γ_w	1.00 T/m^3	1.00 T/m^3
Horizontal Earthquake Acceleration, α	0.15	0.15
Height of Water in Tension crack, Z_w	0-1 Z_L	0-1 Z_L
* Z_L is the depth of the tension crack		

The factor of safety has been calculated for static as well as dynamic conditions. The effect of water in tension crack has also been taken into consideration while calculating the factor of safety. However, it is not easy to measure the depth of water (Z_w) in tension crack . Therefore, the value of Z_w has been varied from a minimum to the maximum depth of tension crack (Zw = 0, 1/4 Z_L, ½Z_L, Z_L) during the calculations of factor of safety. The factor of safety, as calculated, for the two slope segments of right abutment are tabulated in Table 3.16.

TABLE 3.16 : FACTOR OF SAFETY OF RA1 AND RA2 SLOPE SEGMENTS OF RIGHT ABUTMENT

Depth of Water in Tension Crack (Z_w)	Factor of Safety			
	RA1 Slope Segment		RA2 Slope Segment	
	Static	Dynamic	Static	Dynamic
Case 1 : No water ($Z_W = 0$)	1.35	1.09	1.37	1.07
Case 2 : Quarter filled ($Z_W = 1/4Z_L$)	1.30	1.05	1.31	1.01
Case 3 : Half filled ($Z_W = 1/2Z_L$)	1.24	1.00	1.23	0.95
Case 4 : Completely filled ($Z_W = Z_L$)	1.10	0.89	1.07	0.81

A perusal of Table 3.16 indicates that both the slope segments are stable in dry condition and even in dynamic condition. The joints, as discussed earlier, are well developed on the right abutment slope and the continuity of these joints is good. Moreover, the upper slope surface in the two slope segments is very gentle. Thus, the water through Joint J_4 (regarded as tension crack) may percolate. Hence, it is reasonable to presume the slope to have half-filled tension crack, as the adverse condition (AC). Further, it is anticipated that during heavy rains if earthquake occurs it would be the worst possible conditions which is termed as anticipated adverse conditions (AAC). The terms adverse condition (AC) and anticipated adverse conditions (AAC) have been used in the same sense in the discussion later in this Chapter. In the stability analysis, earthquake loading effect has also been incorporated by assuming that the acceleration induced by an earthquake can be replaced by an equivalent static force of `αW'. A horizontal acceleration corresponding to 0.15g has been considered for the stability analysis. For Lakhwar dam, the same value has been taken as design value (Chandrasekhran et al., 1981). The Lakhwar dam site and the Kishau dam site fall within the same zone (Zone IV) of the seismic zoning map of India.

Both the slope segments (RA1 & RA2) have been identified to be stable for the adverse condition. However, under anticipated adverse conditions, both the slope segments would be unstable.

3.6.8 EFFECT OF HEIGHT ON FACTOR OF SAFETY

Plane failure in rock slopes occurs, when a geological discontinuity strikes parallel or nearly parallel to the slope face and dips at an angle greater than the angle of internal friction, and

less than the slope angle. This is an essential condition for the failure to occur. For a plane failure, it is also important that the discontinuity must get daylighted on the slope face. For the right abutment slope, it has already been identified that Joint J_3 is kinematically unstable for plane failure. The joint J_3 includes a set of nearly parallel planes present profusely on the entire slope. As a matter of fact any one of these plane, being daylighted on the slope may get mobilise to cause the failure. In view of this, it is more appropriate to vary the height of slope from a minimum to a maximum and study their impact on factor of safety. For that purpose the height has been measured from the ridge top up to the terrace levels (El.710 m) for RA2 segment and from the terrace to the river bed level in RA1 segment. The factors of safety have been calculated for different slope heights under static and dynamic conditions (Table 3.17). The effect of water in tension crack has also been considered during this analysis. The results are also presented diagrammatically in Fig. 3.18. The results indicates that the factor of safety decreases as the height increases, in both the segments.

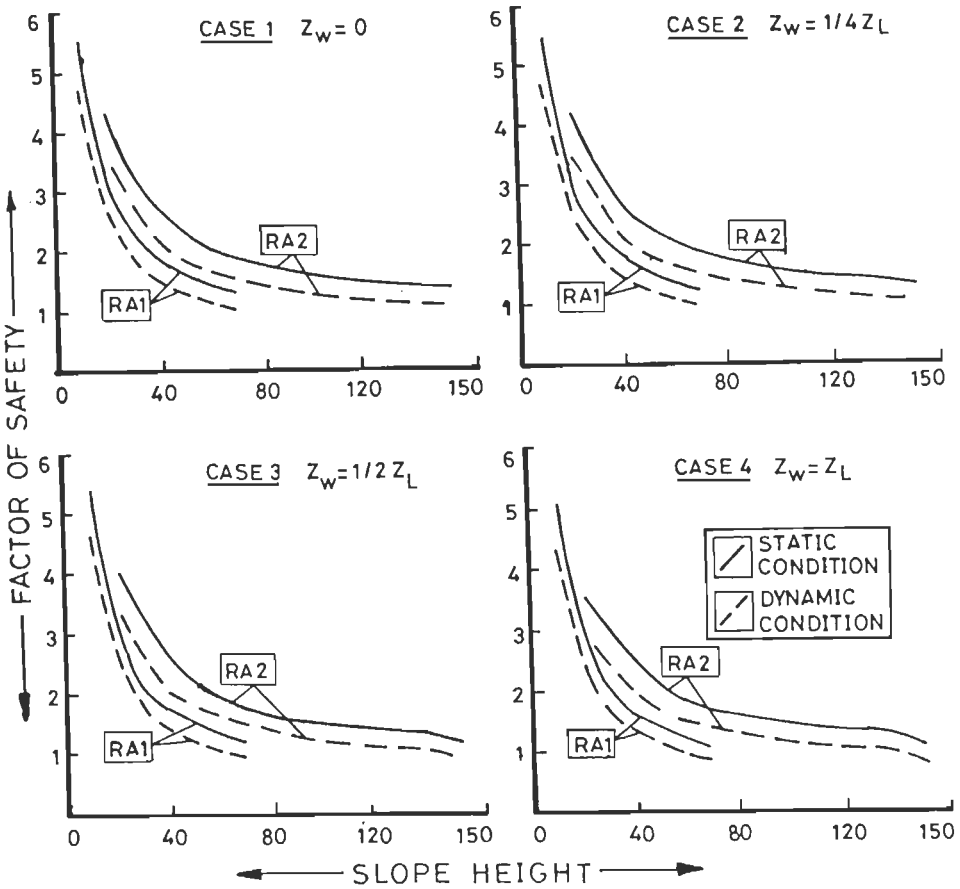

FIG. 3.18 EFFECT OF HEIGHT ON FACTOR OF SAFETY OF RIGHT ABUTMENT SLOPE.

For the anticipated adverse conditions, RA1 slope segment is stable for the top 30 m of the slope. But it is unstable for the remaining height. Similarly, RA2 segment is stable for the top 60 m and unstable for the remaining 90 m. Under adverse conditions RA1 slope segment is stable upto 50 m of height, whereas, RA2 slope is stable for the top 100 m.

TABLE 3.17 : FACTOR OF SAFETY OF RIGHT ABUTMENT SLOPE AT DIFFERENT HEIGHTS.

Slope Height (mtr)	Factor of Safety							
	Case 1		Case 2		Case 3		Case 4	
	ST	DY	ST	DY	ST	DY	ST	DY
RA1 Slope Segment								
10	5.52	4.67	5.48	4.63	5.38	4.56	5.13	4.39
20	3.08	2.57	3.03	2.53	2.95	2.47	2.77	2.34
30	2.26	1.87	2.22	1.83	2.14	1.78	1.98	1.65
40	1.86	1.52	1.81	1.48	1.74	1.43	1.59	1.31
50	1.61	1.31	1.56	1.27	1.50	1.22	1.35	1.10
60	1.45	1.17	1.40	1.13	1.33	1.08	1.19	0.97
68	1.35	1.09	1.30	1.05	1.24	1.00	1.10	0.89
RA2 Slope Segment								
20	4.29	3.57	4.20	3.49	4.08	3.39	3.52	2.93
40	2.63	2.14	2.58	2.10	2.51	2.05	2.33	1.90
60	2.06	1.66	2.03	1.63	1.98	1.59	1.84	1.48
80	1.78	1.42	1.75	1.39	1.71	1.36	1.59	1.27
100	1.61	1.27	1.58	1.25	1.55	1.22	1.45	1.14
120	1.49	1.17	1.47	1.16	1.44	1.13	1.35	1.06
140	1.41	1.10	1.40	1.09	1.37	1.07	1.28	1.00
150	1.37	1.07	1.31	1.01	1.23	0.95	1.07	0.81

ST-Static Condition, DY-Dynamic Condition

Case 1 - No water in tension crack, $Z_W = 0$
Case 2 - One fourth of the tension crack is filled with water, $Z_W = 1/4\ Z_L$
Case 3 - Half of the tension crack is filled with water, $Z_W = 1/2\ Z_L$
Case 4 - Tension crack is fully filled with water, $Z_W = Z_L$

3.6.9 SENSITIVITY ANALYSIS OF RIGHT ABUTMENT SLOPE

The right abutment slope has been identified as unstable for the anticipated adverse conditions. In order to study the influence of different factors on the factor of safety, an analysis of sensitivity on the factor of safety has been carried out by varying each parameter in turn, while keeping the values of other parameters constant.

The analysis has been carried for RA2 slope segment of right abutment. From this analysis, the relative importance of the factors, causing instability of RA2 segment has been evaluated. The probable range of magnitude of functions, causing instability of RA2 slope segment is presented in Table 3.18.

TABLE 3.18 : PROBABLE RANGE OF MAGNITUDE OF VARIOUS PARAMETERS USED IN SENSITIVITY ANALYSIS

Function	Probable Range of Magnitude
Failure Plane Inclination, α_p	38°-46°
Upper Slope Angle, α_s	0°-20°
Water in Tension Crack, Z_W/Z_L	0-1
Cohesion, C	8-24 T/m^2
Angle of Internal Friction, ϕ	35°-45°

The relative sensitivity of factor of safety to variations in magnitudes of each parameter, causing the instability has been evaluated for different heights. For this analysis, it has been considered that the failure plane daylights on the slope face at the heights of 40 m, 80 m, 120 m, and 150 m.

The results, thus obtained are presented in Table 3.19. The relationship between factors of safety and each of the function considered, is shown in Fig.3.19.The main aim of the sensitivity analysis is that it enables the function to be graded in order of their importance with respect to their impact on the factor of safety. The Table 3.20 presents the order of importance of various functions causing instability of RA2 slope segment.

It can be concluded from Table 3.20 that cohesion and failure plane inclination have greater impact on the factor of safety, followed by water in tension crack, upper slope inclination and angle of friction. It can also be noted from the results that the effect of water in tension crack

TABLE 3.19 : SENSITIVITY ANALYSIS OF RA2 SLOPE SEGMENT

Sensitivity of Factor of Safety for Failure Plane Inclination					
Height (mtr)	Failure Plane Inclination, α_p				
	38°	40°	42°	44°	46
	Factor of Safety				
40	1.56	2.01	2.05	2.45	3.45
80	1.10	1.33	1.36	1.47	1.95
120	0.95	1.07	1.13	1.15	1.45
150	0.89	0.95	0.97	1.02	1.25

Sensitivity of Factor of Safety for Upper Slope Angle					
Height (mtr)	Upper Slope Angle, α_s				
	0°	5°	10°	15°	20°
	Factor of Safety				
40	2.42	2.21	2.05	1.74	1.50
80	1.47	1.37	1.36	1.15	1.04
120	1.16	1.09	1.13	0.95	0.88
150	1.03	0.98	0.95	0.87	0.82

Sensitivity of Factor of Safety for Water Pressure					
Height (mtr)	Water in Tension Crack, Z_W/Z_L				
	0	1/4	1/2	3/4	1
	Factor of Safety				
40	2.63	2.58	2.51	2.46	2.33
80	1.78	1.75	1.71	1.66	1.59
120	1.49	1.47	1.44	1.40	1.35
150	1.37	1.31	1.23	1.15	1.07

Sensitivity of Factor of Safety for Cohesion & Friction Angle															
Friction Angle,ϕ	35°					40°					45°				
Cohesion,C	8	12	16	20	24	8	12	16	20	24	8	12	16	20	24
Height (mtr)	Factor of Safety														
40	1.22	1.59	1.95	2.31	2.67	1.33	1.69	2.05	2.41	2.77	1.44	1.80	2.16	2.53	2.8
80	0.89	1.07	1.25	1.43	1.62	1.00	1.18	1.36	1.54	1.72	1.12	1.30	1.48	1.66	1.8
120	0.78	0.90	1.02	1.14	1.26	0.89	1.01	1.13	1.25	1.37	1.02	1.14	1.26	1.38	1.5
150	0.66	0.76	0.85	0.95	1.04	0.76	0.85	0.95	1.04	1.14	0.87	0.96	1.06	1.15	1.2

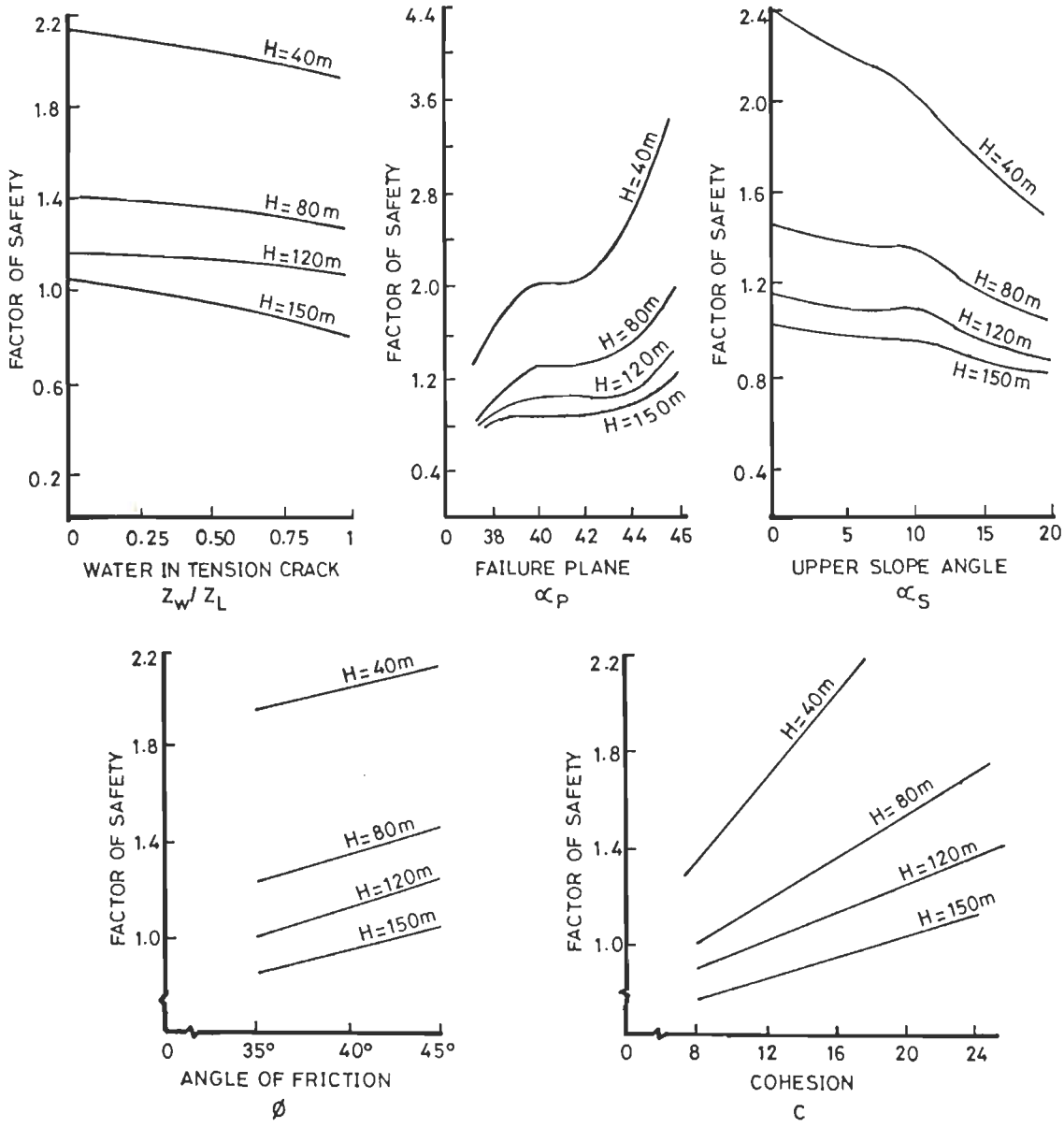

FIG. 3.19 SENSITIVITY OF FACTOR OF SAFETY TO VARIOUS FACTORS CAUSING INSTABILITY OF RA2 SEGMENT OF RIGHT ABUTMENT.

increases as the height of the slope increases. However, all the parameters show nearly uniform impacts on factor of safety upto a height of 120 m. However, for a height of 150 m the cohesion (C) becomes the most important factor influencing the factor of safety (Table 3.20).

TABLE 3.20 : ORDER OF IMPORTANCE OF VARIOUS FUNCTIONS CAUSING INSTABILITY OF RA2 SLOPE SEGMENT

Order of Importance	Height At Which the Failure Plane Daylights on the Slope Face			
	40m	80m	120m	150m
First	α_p	α_p	α_p	C
Second	C	C	C	α_p
Third	α_s	α_s	α_s	Z_W/Z_L
Fourth	Z_W/Z_L	ϕ	ϕ	α_s
Fifth	ϕ	Z_W/Z_L	Z_W/Z_L	ϕ

α_p - Failure Plane Inclination
C - Cohesion
α_s - Upper Slope Angle
Z_w/z_L - Water in Tension Crack
ϕ - Angle of Internal Friction

3.7 EVALUATION OF FOUNDATION CONDITION

An attempt has been made to evaluate the overall foundation condition on the basis of surface investigations and the data obtained from 3D mapping of drifts, drill holes, water pressure tests and the stability analysis of the abutment slopes.

In the river section, quartzitic slates with interbands of purple quartzites are present in the foundation of the dam. Purple quartzites and white quartzites are present on the dam abutments.

The rocks at dam axis are folded into an upright asymmetrical anticlinal fold. The fold axis is trending N45°W-S45°E, which is nearly parallel to the flow direction of the Tons river. The axial plane dips towards right bank and the fold axis has a shallow Southeasterly plunge (about 7°). The dam base would rest on the hinge zone of this major fold.

The rocks in the hinge zone area may have excessive tension fracturing which is indicated by the low to medium core recovery in the river section.

The Tons thrust is present on the right abutment ridge, dipping 15° to 25° in Southwesterly direction into the adjoining Meera river valley. The Tons thrust is present between El. 845 m

and 850 m, close to the dam axis. The trace of the contact of the Tons thrust, because of the topographical effect, shows a swing from WNW-ESE on the upstream side of the dam axis to nearly South on the downstream and veers into the river Meera valley. The thrust, close to the dam axis, would be submerged under the maximum reservoir level of 860 m. This is further confirmed in the top most drift SR3, located at El.817 m on the right abutment, along the dam axis in which the black gaugy materials of the Tons thrust is encountered between RD 125 m - RD134 m from the portal. Further, shattered and disturbed Mandhali slates occur above the thrust. The 3D log of drift SR3 also indicates that 90m wide fresh white quartzite is present along this drift.

The right abutment ridge has a saddle at the elevation of 850m, across the dam axis. The top of the dam being at El 868m. Therefore, to retain the reservoir water a dyke wall over the saddle is planned to be constructed.

The 3D mapping of drifts, located on both the abutments at dam axis, reveals that the lateral depth of weathering ranges from 20 to 34 m on the left abutment and this range varies from 16 to 24m on the right abutment. However, the rocks constituting the right abutment are badly sheared, upto a lateral depth of 20 to 45m along the drifts. Thus, on the basis of the above observations the lateral depth of stripping for left and right abutments has been estimated to be 22 to 34 m, and 25 to 45 m respectively.

The drill hole data indicates that the fluvial overburden in the river bed section is 3.65 to 11.88m and the bed rock is available at El. 635.2 m. In the river bed section alternating bands of grey quartzitic slate and purple quartzite are present.

The percent core recovery in the river section is low to medium which indicates that the foundation rocks are highly fractured due to folding effect. On the basis of limited water pressure test data, it is concluded that the foundation rocks are semipervious to pervious in nature. The median value of in-situ modulus of deformation (E_d) of the foundation rocks is 0.27 x 10^5 kg/cm^2. Whereas, the average value of in-situ modulus of deformation, as estimated from Agarwal et al. relation, is 0.39 x 10^5 kg/cm^2. The average of the tested and the estimated values (Agarwal et al.) has been considered as the design value of the modulus of deformation. The average value comes out to be 0.33 x 10^5 kg/cm^2.

On the basis of in-situ tests, the average values of cohesion and angle of internal friction between rock and concrete are found to be 2.2 kg/cm^2 and 52.4° respectively. Whereas, from

RMR the average values of cohesion and angle of internal friction of rock mass are estimated to be 3.17 kg/cm^2 and 36.7° respectively.

The stability analysis of abutments has revealed that the left abutment slope is stable, while the right abutment slope is kinematically unstable for plane mode of failure. The right abutment slope can be divided into two sub slope segments, the lower RA1 and the upper RA2. Both the slope segments are kinematically unstable for plane mode of failure. The factors of safety for these two slope segments have been calculated by the modified technique, described earlier in this chapter. The analysis shows that both the slope segments are stable for the adverse conditions. Moreover, for the anticipated adverse conditions both the slope segments of right abutment are unstable.

3.8 FOUNDATION TREATMENT

Based on the surface and subsurface investigation carried out to evaluate the dam foundation, the foundation requires ,adequate treatments for improving the strength and control of seepage, in addition to rendering the abutment slope stable while stripping. Accordingly, the following, foundation treatments are suggested.

3.8.1 DESIGN OF ABUTMENT SLOPES

The slope stability analysis of the abutments indicates that the right abutment slope is unstable as well as cohesion and failure plane inclination are two important factors which influence the stability of right abutment. Therefore an analysis has been carried out to obtain a stable cut slope design for the right abutment.

For this analysis, the factor of safety is obtained by assuming different slope angles and slope heights. The factor of safety, as calculated for each combination of slope angle and slope height, is marked over a graph sheet and a contour curve corresponding to factor of safety of 1.5 is drawn (Fig.3.20). Thus, the cut slope angles for different heights are obtained and are shown in Table.3.21.

A perusal of Table 3.21 indicates that cut slope angle is decreasing with depth in the right abutment slope. It implies that the cut slope design following the proposed slope angles would attain a concave shape in section. According to Hoek and Bray (1981) *a significant increase in the factor of safety can be achieved by making the slope face concave in section.*

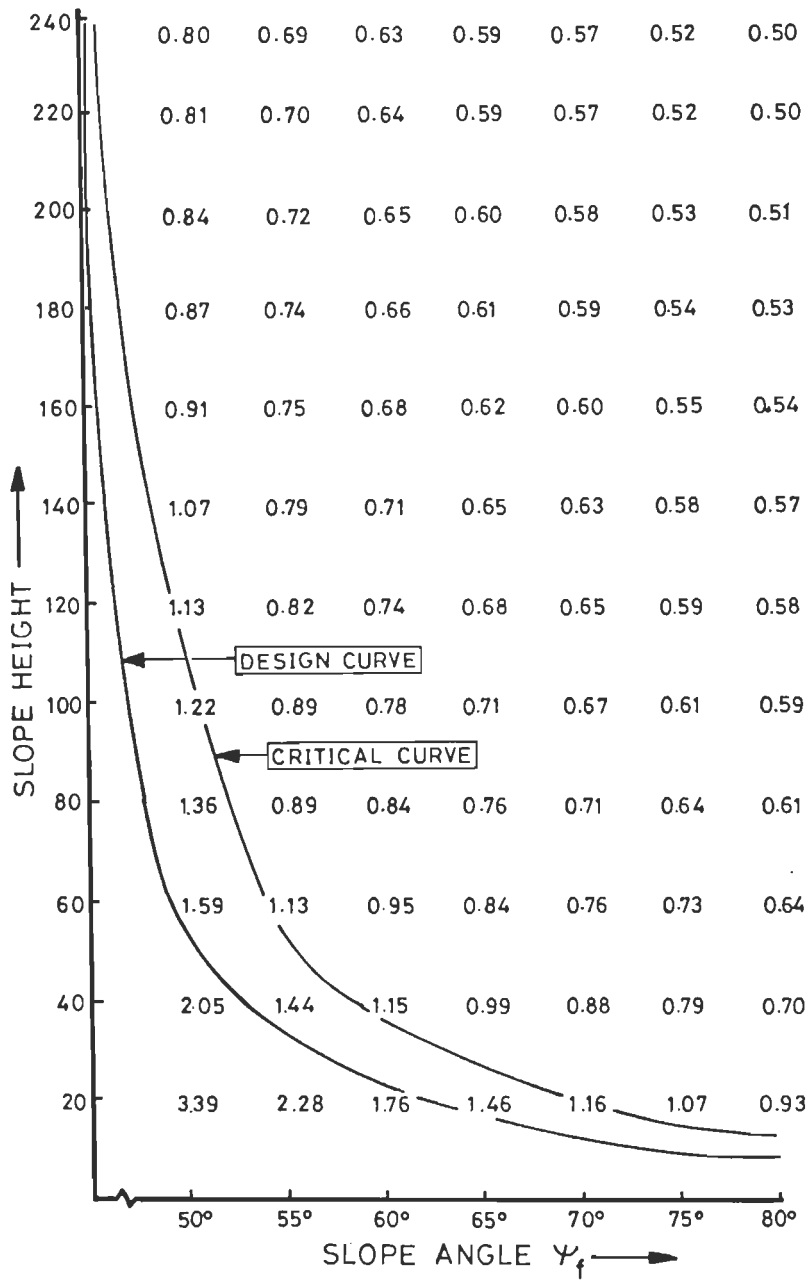

FIG. 3.20 DESIGN CURVE FOR RIGHT ABUTMENT SLOPE.

It is proposed that stripping of the right abutment should be carried out by maintaining the cut slope angles as indicated in Table 3.21. The stripping of left abutment shall be carried out by maintaining the cut slope as far as close to the limit of stripping (indicated in Fig.3.21) with an angle more or less parallel to existing slope.

TABLE 3.21 : CUT SLOPE ANGLES FOR DIFFERENT HEIGHTS OF RIGHT ABUTMENT

Slope Segment	Slope Height (m)	Proposed Cut Slope Angle
RA1	0-20 20-40 40-68	62° 52° 47°
RA2	0-20 20-40 40-60 60-150	63° 54° 50° 46°

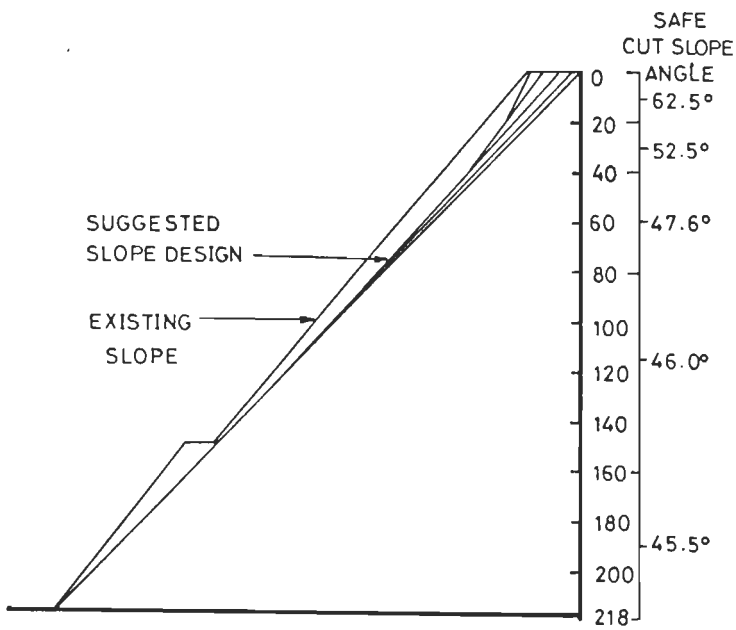

PROPOSED CUT SLOPE ANGLES FOR RIGHT ABUTMENT

The abutment slope should be cut in terraced design by maintaining 5m wide benches. The slope design for both the abutments is shown in Fig.3.21.

Even though the slope are stable at the proposed overall cut slope design, the individual benches having steep slopes locally, during blasting for excavation, the vibrations may tend to create local distressing on the humps of the benches. It may lead to local failures. Hence,

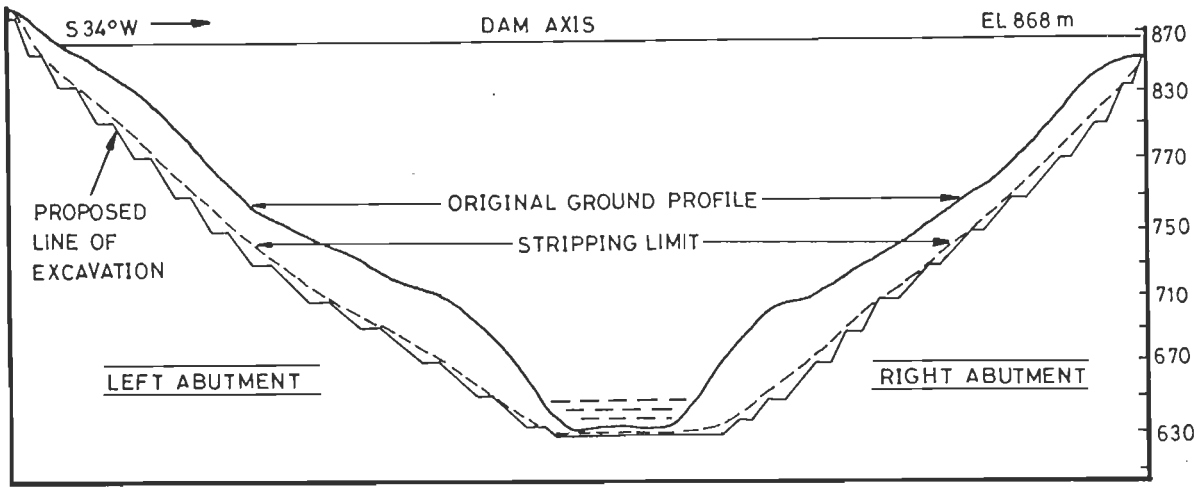

FIG. 3.21 SLOPE DESIGN OF LEFT AND RIGHT ABUTMENT OF THE KISHAU DAM.

it is suggested to provide two rows of grouted anchors to a depth of 5 m at about 45° into the slope at 3 m centre to centre (Fig.3.22). The rows of grouted anchors may be located about 2 m and 6 m below the crest of the benches. These anchors should be installed concurrently as the excavation progresses down.

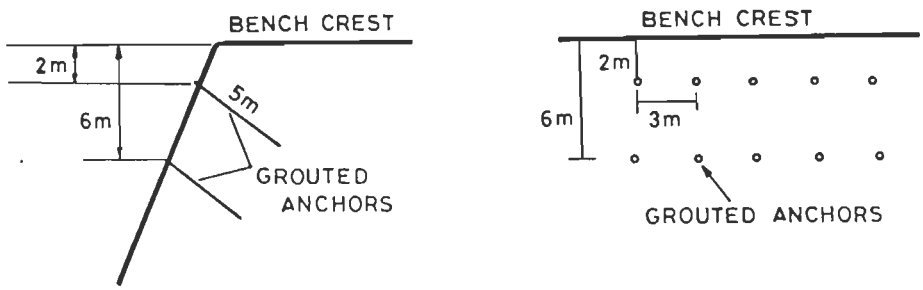

FIG. 3.22 GROUTED ANCHORS TO CONTROL LOCAL FAILURES IN THE BENCHES

3.8.2 DENTAL TREATMENT

In the drifts SL1,SL2,SR1,SR3, shear zones ranging in thickness 0.5 m to 2 m have been encountered. It indicates that these structurally weak features will get exposed at the foundation level during foundation stripping. Such shear zones contain material of low shear strength. They may cause uneven settlement of the dam if not treated properly. Therefore, such shear zones should be removed and back filed by lean concrete by dental treatment,

using the Shasta's formula. The Shasta's formula for dental treatment is as follows:

$$D = 0.00656 \times H \times b + 1.526 \quad \ldots \quad 3.29$$

D = depth of excavation of weak zone below surface adjoining sound rock in meters.
H = height of dam above general foundation level in meters.
b = width of weak zone in meters.

3.8.3 CURTAIN GROUTING

Since the foundation rocks are highly jointed and fractured, water under high pressure may seep through the foundation rocks. From the limited water pressure test data it has been inferred that the foundation rocks are semipervious to pervious in nature. The rocks may be pervious even to a depth of more than one third height of the dam. Hence, in order to control the seepage through the foundation rocks of the dam, a grout curtain in the heel portion of the dam is necessary. The depth of the grout curtain is obtained by using the following relation given by Ewert, 1985

$$D = 1/3\ H + C \quad \ldots \quad 3.30$$

D = Depth of grout curtain
H = Height of Dam
C = Variable constant depending upon foundation condition and dam height. C ranges from 8 to 25.

The variable constant `C' for the present study is taken as 25, because the foundation rocks are highly jointed and fractured. Therefore, a grout curtain upto a minimum depth of 100 m is necessary to control the seepage, in the heel portion of the dam.

Since the foundation rocks are hard and well jointed, the rocks may take good grouting and an effective grout curtain may be created in the heel portion of the dam. This will increase the path of percolation of seepage water which may reduce the velocity of seepage water and thereby reducing the internal erosion of the foundation.

3.8.4 DRAINAGE HOLES

In spite of the effective grout curtain, water may still find its way through the foundation rocks. This water can be intercepted by providing 2 to 3 rows of drainage holes drilled from the

drainage gallery and the water can be pumped back into the reservoir.

3.8.5 CONSOLIDATION GROUTING

Since the rocks are highly jointed and fractured at foundation grade, consolidation grouting in the dam base area is necessary. This would improve the physical properties of the foundation rocks. Consolidation grouting would make the foundation rocks monolithic by fusing the dam base with foundation.

In the river bed area it should be carried out to a depth of 15m and on abutments to a depth of 5 to 10 m. Besides, an extension of consolidation grouting (Fig.3.23) upto b/4 (57 m) beyond the heel and b/3 (76 m) beyond the toe region of the dam should also be carried out (where b is the base width of dam i.e. 228 m). The extension of consolidation grouting in the dam base area is mainly done because under the reservoir full condition, the concentration of stresses is towards the toe region. But for reservoir empty condition, the stress concentration is towards the heel region of the dam (Mistry, 1983).

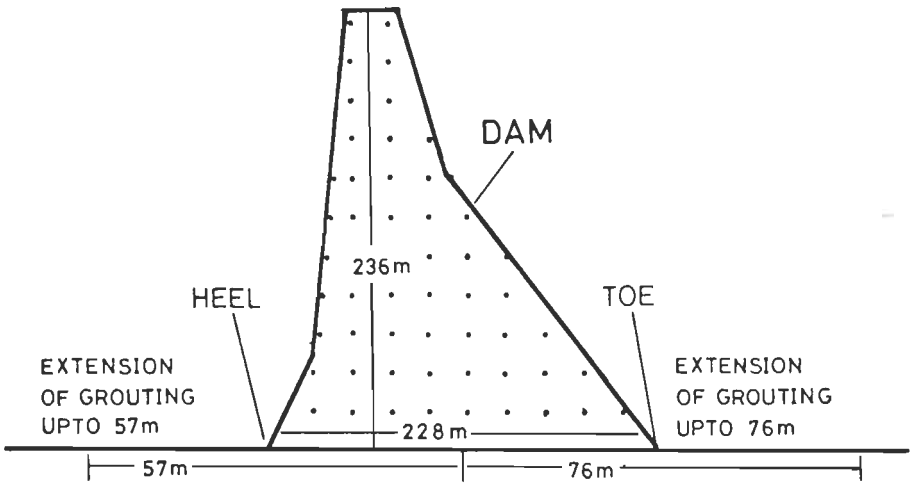

FIG. 3.23 EXTENSION OF CONSOLIDATION GROUTING IN THE HEEL AND THE TOE REGION OF THE DAM.

3.8.6 RCC DIAPHRAGM TO CONTROL SEEPAGE

The Tons thrust is present close to the right abutment ridge between the El. 845 m to 850 m, dipping 15° to 25° towards Southwest direction into the adjoining Meera river valley. The thrust close to the dam axis will be submerged under a maximum reservoir level (El.

860 m). To control the seepage through the thrust a RCC diaphragm, 0.75m wide and 150m long, is proposed. This diaphragm would be founded over the competent white quartzite, just below the Tons thrust. It is proposed that the top of the diaphragm will be kept at El. 860 m. The RCC diaphragm in plane and in section is shown in Fig.3.24.

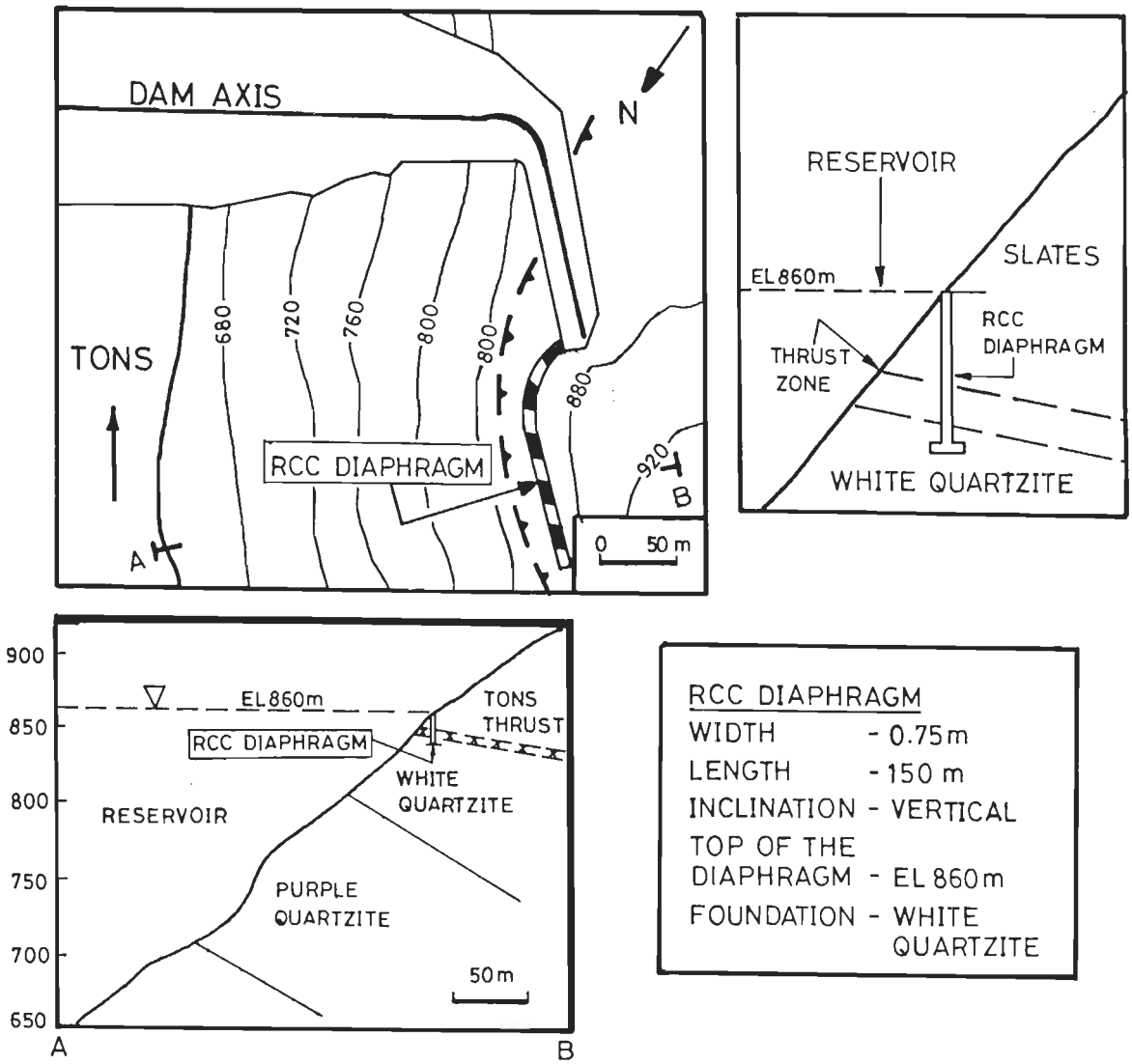

FIG. 3.24 RCC DIAPHRAGM TO CONTROL SEEPAGE

3.8.7 FOUNDATION OF DYKE ON SADDLE

As discussed earlier, the right abutment ridge has a saddle at the elevation of 850 m, across the dam axis. The top of the dam, being at 868 m. A dyke over the saddle has to be constructed to retain the reservoir water at 860 m. The Tons thrust with its highly jointed and sheared zone is exposed between the elevations 845 m and 850 m. Therefore this dyke has to be founded below the Tons thrust zone on the white quartzites of Simla group.

CHAPTER IV

ENGINEERING GEOLOGICAL INVESTIGATIONS OF POWER HOUSE SITE

The hydro electric power house which accommodates the power generating units and other accessory structures is an important appurtenant unit of a dam. The selection of the type of power house and its location are mainly dictated by the topographic and geological considerations. Depending upon the capacity of generating units and the numbers, a certain minimum size of the area is required. In narrow valleys, if the topography is unfavourable for the creation of a terrace of required size, an underground power house may be favoured. The power houses of Tehri and Lakhwar dams were designed underground due to these reasons. However , in wide valleys, the probability of locating a surface power house is very high. At the same time the detailed layout of a power house is more dependent on geological setting mainly from the point of view of stability of cut slopes.

A surface power house is being proposed for the Kishau dam due to favourable topographical and geological conditions with an installed capacity of 600 MW of peak power and is planned to be constructed on the left bank of the Tons river, about a km down stream of the main dam (Plate 4.1). Detailed engineering geological investigations have been carried out to select a suitable location and to evolve suitable cut slope design.

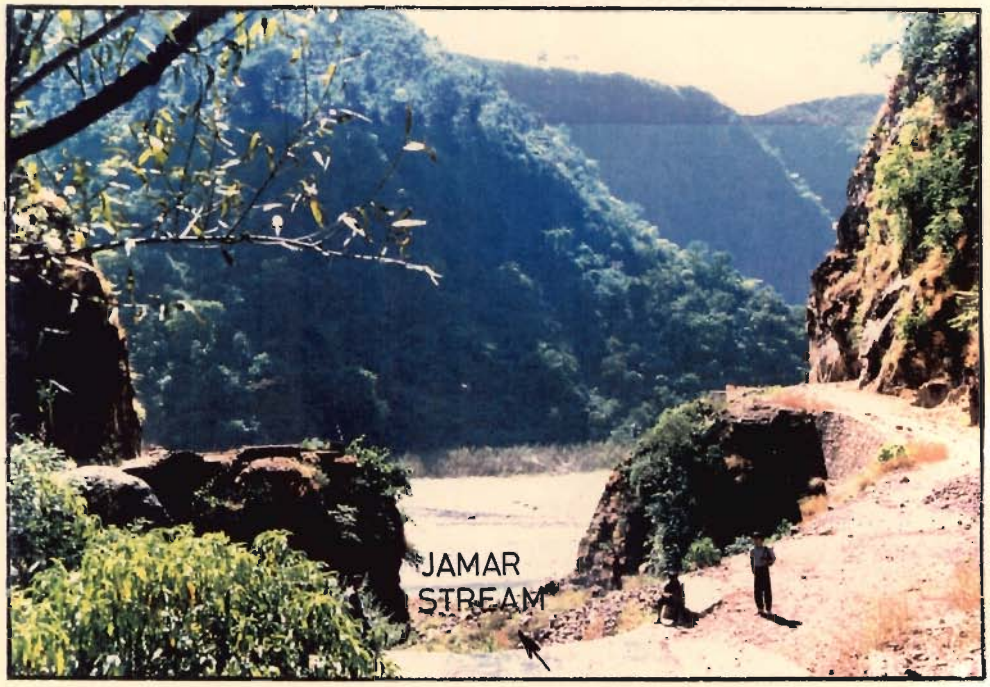

PLATE 4.1 A VIEW OF POWER HOUSE SITE

For detailed stability studies the following investigations have been carried out:

- Mapping of the power house site on 1: 500 Scale and collection of structural data.
- Stability analysis of the power house site proposed by the project authorities.
- Selection of alternative site for power house.
- Stability analysis of the proposed alternative site

The stability study includes the following work component:

- Preparation of detailed plan.
- Preparation of cross sections.
- Determination of shear strength parameters.
- Stability analysis of the slopes.
- Suggestions for safe design and suitable remedial measures for excavated slopes
- A discussion on the merits and demerits of both the sites.

4.1 FIELD INVESTIGATIONS

4.1.1 GEOLOGY OF POWER HOUSE SITE

During field investigations, detailed geological mapping on 1:500 scale has been carried out (Fig.4.1) to study the rock formations exposed in and around the proposed power house site. The rocks exposed are mainly quartzites of the Simla Group. While white quartzite is exposed over a larger area of the power house site, purple coloured quartzite is exposed relatively over a smaller area. The rocks are well jointed with well developed bedding planes. The strike of bedding planes varies from N20° to 30° E - S20° to 30° W and dip 40° to 75° in N60° to 70° W direction. Five prominent joint sets have been observed at the power house site. The attitude and other details of these joint sets are discussed below.

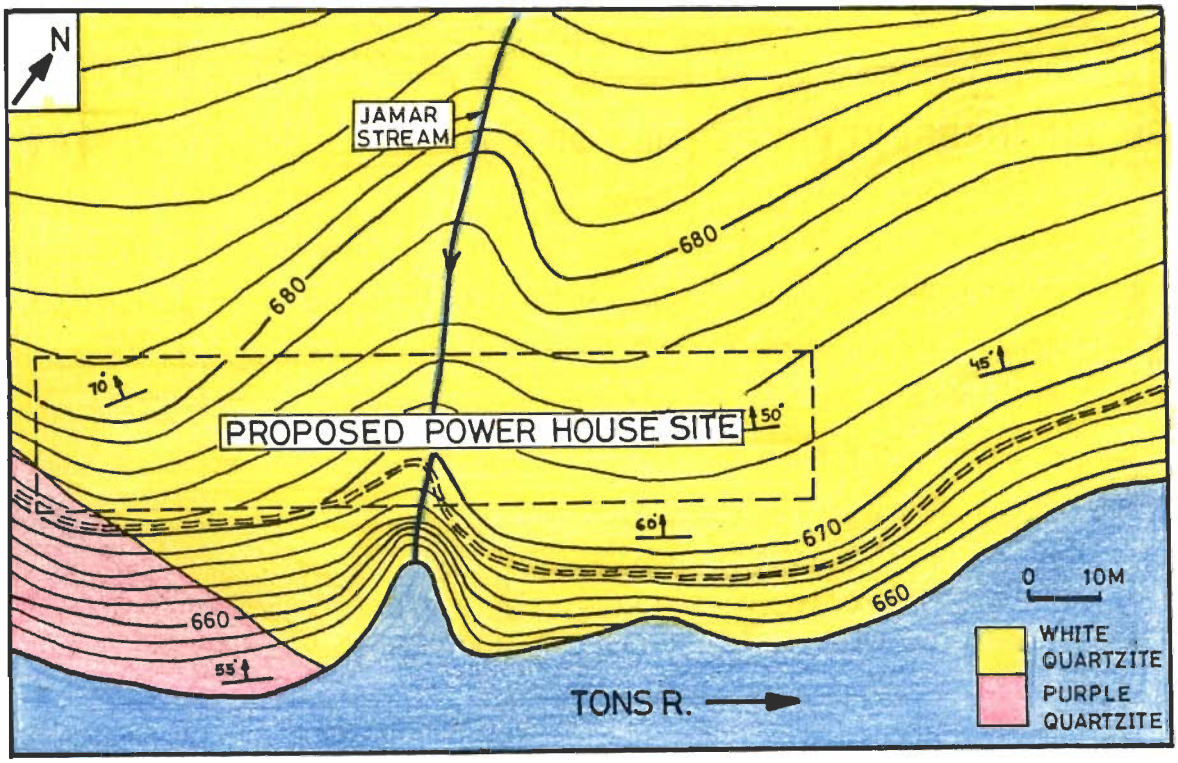

FIG. 4.1 - GEOLOGICAL MAP OF POWER HOUSE SITE

Data pertaining to structural discontinuities, mainly bedding and joints (300 Nos.), have been collected from the power house site and plotted on equal angle stereonet to get the preferred orientation of the discontinuities. For that purpose, the poles of the attitude of joints have been

plotted, contoured and the prominent clusters of the poles have been identified in terms of their predominance. The attitude of the maxima of structural discontinuities, thus obtained, are presented in Table 4.1 and Fig.4.2

TABLE 4.1 ATTITUDE OF STRUCTURAL DISCONTINUITIES AT POWER HOUSE SITE

Joint Set	Dip Direction	Amount of Dip	Strike
Bedding joint J_1	N62°W	71°	N28°E-S28°W
J_2	S77°W	62°	N13°W-S13°E
J_3	S30°E	40°	N60°E-S60°W
J_4	N18°E	32°	N72°W-S72°E
J_5	S82°E	70°	N8°E-S8°W
J_6	S33°W	43°	N57°W-S57°E

4.2 ENGINEERING PROPERTIES OF ROCKS

The important engineering properties of rocks, used in the slope stability studies are uniaxial compressive strength of the intact rock, rock density and the shear strength parameters. For obtaining the uniaxial compressive strength, fresh intact samples from two localities have been collected and cores of NX size have been obtained in the laboratory. These samples have been tested for uniaxial compressive strength following the standard practice (Table 4.2). Similarly the rock density has also been determined in the laboratory (Table 4.2).

TABLE 4.2 UNIAXIAL COMPRESSIVE STRENGTH AND ROCK DENSITY OF QUARTZITE EXPOSED AT POWER HOUSE SITE

Sample No.	Rock Type	Uniaxial Compressive Strength, kg/cm^2	Rock Density gm/cc
PH1	Quartzite (white)	2100	2.75
PH2	Quartzite (pink)	2050	2.75

In order to determine the shear strength parameters of the rocks, data pertaining to geomechanical classification or rock mass rating (RMR) system has been collected from the power house site. The rock mass rating system has already been discussed in Chapter III.

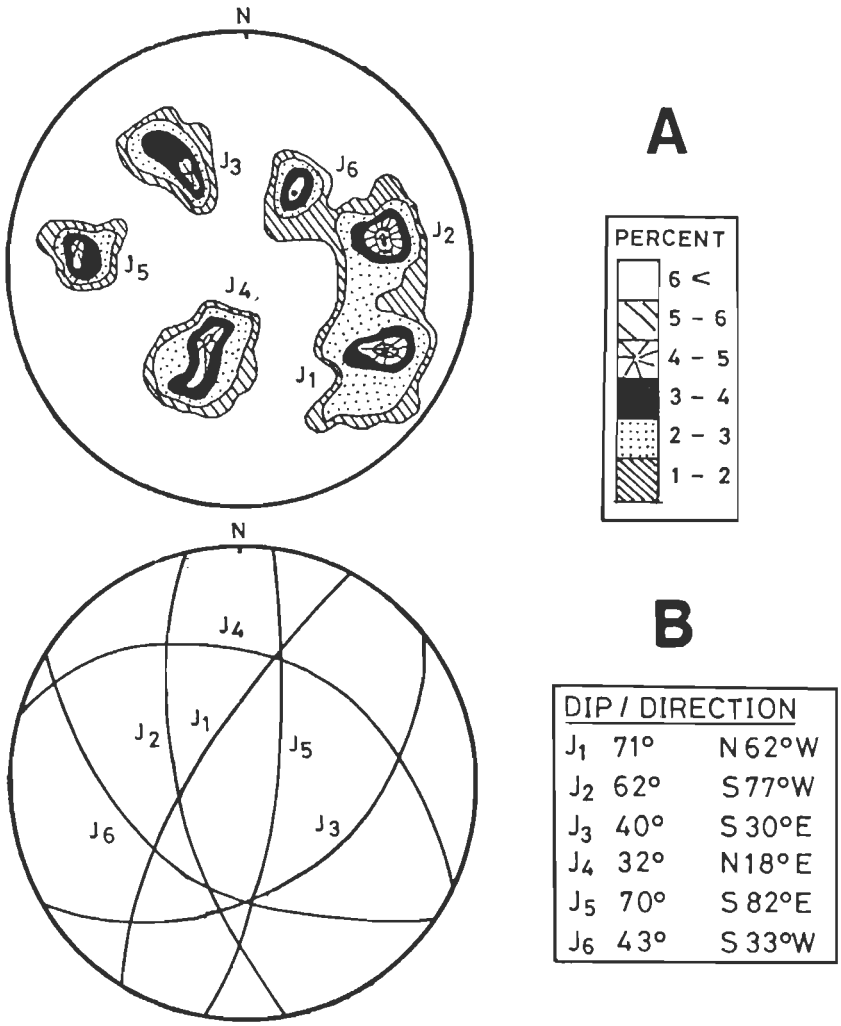

FIG. 4.2 A - DENSITY PLOT OF JOINT POLES
B - ATTITUDE OF STRUCTURAL DISCONTINUITIES AT POWERHOUSE SITE.

For obtaining RMR, the uniaxial compressive strength has been determined in the laboratory, and RQD from the empirical equation given by Palmstorm (1981). The spacing, condition of discontinuities and ground water condition have been visually estimated in the field. The rock mass rating and the corresponding shear strength values for localities at power house site are shown in Table 4.3.

TABLE 4.3 GEOLOGICAL PARAMETERS AND ROCK MASS RATING FOR POWER HOUSE SITE

Slope Section	Rock Type	Geological Parameters and Rock mass rating						Class/ Classification of rock mass	Cohesion (kg/cm^2)	Angle of Internal Friction ϕ (deg)
		UCS	RQD	Sp.	COD	GWC	RMR_B			
PH1	Quartzite (white)	2100	65	0.06-0.2	Slightly Rough and Moderately to Highly Weathered	Dry		II/Good	3-4	35-45
	Rating ➨	12	13	8	20	15	68			
PH2	Quartzite (pink)	2050	70	0.06-0.2	Slightly Rough and Moderately to Highly Weathered	Dry		II/Good	3-4	35-45
	Rating ➨	12	13	8	20	15	68			

UCS = Uniaxial compressive strength (kg/cm^2), RQD = Rock quality designation (%), Sp. = Spacing (meter), COD = Condition of discontinuities, GWC = Ground water condition, RMR_B = Rock mass rating (Basic)

4.3 STABILITY ANALYSIS OF THE SLOPES ADJOINING THE POWER HOUSE

The stability analysis of the slopes adjoining the power house site (Fig.4.3) has been carried out in two stages. Initially, the critical slopes were identified by using *Friction only case* technique and later detailed analysis of these critical slopes has been carried out for calculating the factor of safety for static and dynamic conditions.

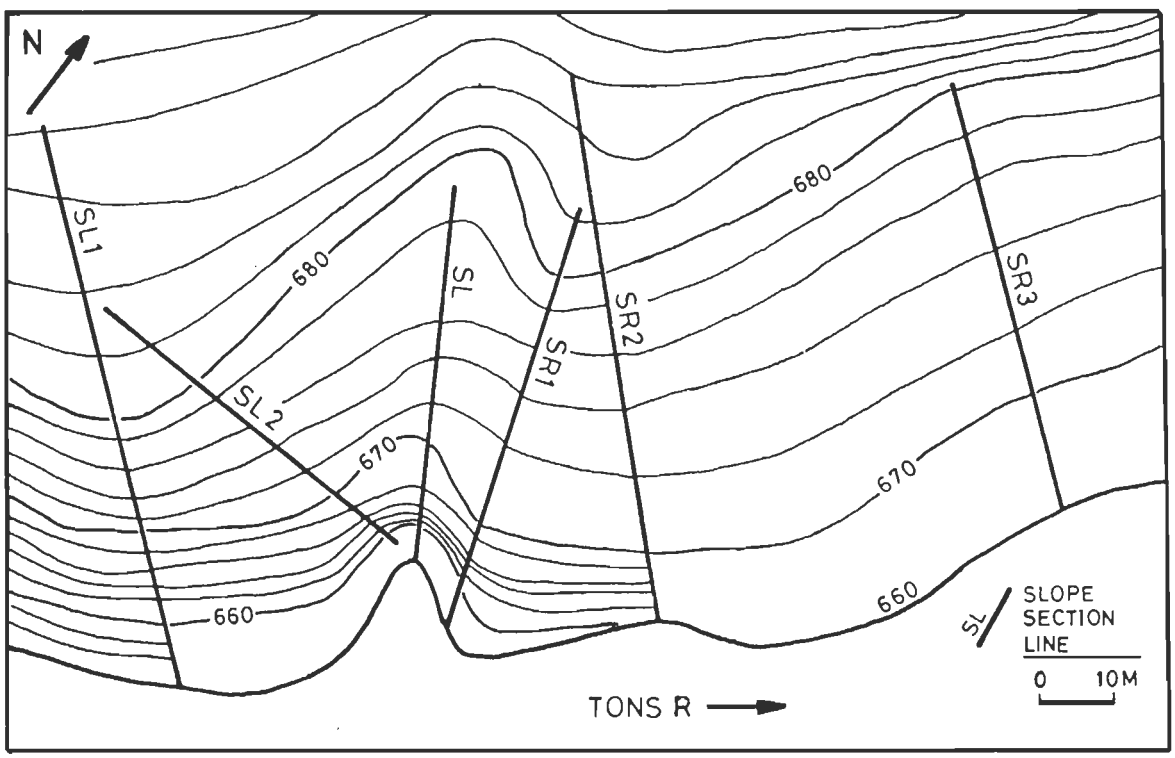

FIG. 4.3 SLOPE SECTIONS AT POWER HOUSE SITE, ALONG WHICH STABILITY ANALYSIS HAS BEEN CARRIED OUT.

4.3.1 IDENTIFICATION OF CRITICAL SLOPES

In order to identify the critical slopes around power house site, *Friction only case* technique (Hoek and Bray, 1977) has been used. The angle of internal friction (ϕ) obtained by rock mass rating has been used in friction only case technique. The slopes adjoining to the power house site falls in RMR range of 61-80, which indicates the values of angle of internal friction ranging between 35°-45°. In view of the importance of the structure, a safer value on lower side (ϕ = 35°) has been used in the analysis.

In this approach, the ϕ circle corresponding to angle of internal friction ($\phi = 35°$) along with all the discontinuities, identified at power house site, have been plotted on the stereonet (Fig.4.4). Further, the factor of safety (FOS) of the wedges, formed by the intersection of discontinuities falling within the ϕ circle has been determined by the equation 4.1

$$F = (A + B) \tan \phi \quad \ldots \quad 4.1$$

where,

$$A = \frac{\cos \Psi_a - \cos \Psi_b \cos \theta_{na.nb}}{\sin \Psi_5 * \sin^2 \theta_{na.nb}}$$

$$B = \frac{\cos \Psi_b - \cos \Psi_a \cos \theta_{na.nb}}{\sin \Psi_5 * \sin^2 \theta_{na.nb}}$$

Ψ_a and Ψ_b are the dips of planes A and B respectively,
Ψ_5 is the plunge of line of intersection of planes A and B, and
$\theta_{na.nb}$ is the angle between the poles of planes A and B

The factor of safety for all the combinations of the discontinuities are given in Table 4.4

TABLE 4.4 FACTOR OF SAFETY OF WEDGES FORMED BY EACH COMBINATIONS OF DISCONTINUITIES AT POWER HOUSE SITE

S.No	Wedge Forming Joints	Ψ_a	Ψ_b	Ψ_5	$\theta_{na\ nb}$	ϕ	A	B	FOS
1	J_1&J_5	70	71	28	105	35	3.049	3.029	4.25
2	J_1&J_4	32	71	32	68	35	1.594	0.017	1.12
3	J_4&J_5	32	70	32	69	35	1.572	0.083	1.15
4	J_1&J_2	62	71	62	40	35	0.603	-0.093	0.35
5	J_3&J_5	40	70	38	51	35	1.480	-0.376	0.77
6	J_1&J_6	43	71	42	73	35	1.040	0.181	0.85
7	J_5&J_6	43	70	37	100	35	1.354	0.803	1.51
8	J_1&J_3	40	71	19	105	35	2.250	0.420	1.86
9	J_3&J_6	40	43	16	42	35	1.800	1.310	2.17
10	J_2&J_6	43	62	42	39	35	1.384	-0.373	0.70
11	J_2&J_3	40	62	32	80	35	1.330	0.657	1.39

Ψ_a = Dip of plane A
Ψ_5 = Plunge of line of intersection
ϕ = Angle of internal friction
$\theta_{na\ nb}$ =Angle between poles of plane A &B

Ψ_b = Dip of plane B
A & B = Dimensionless factor
FOS = Factor of safety

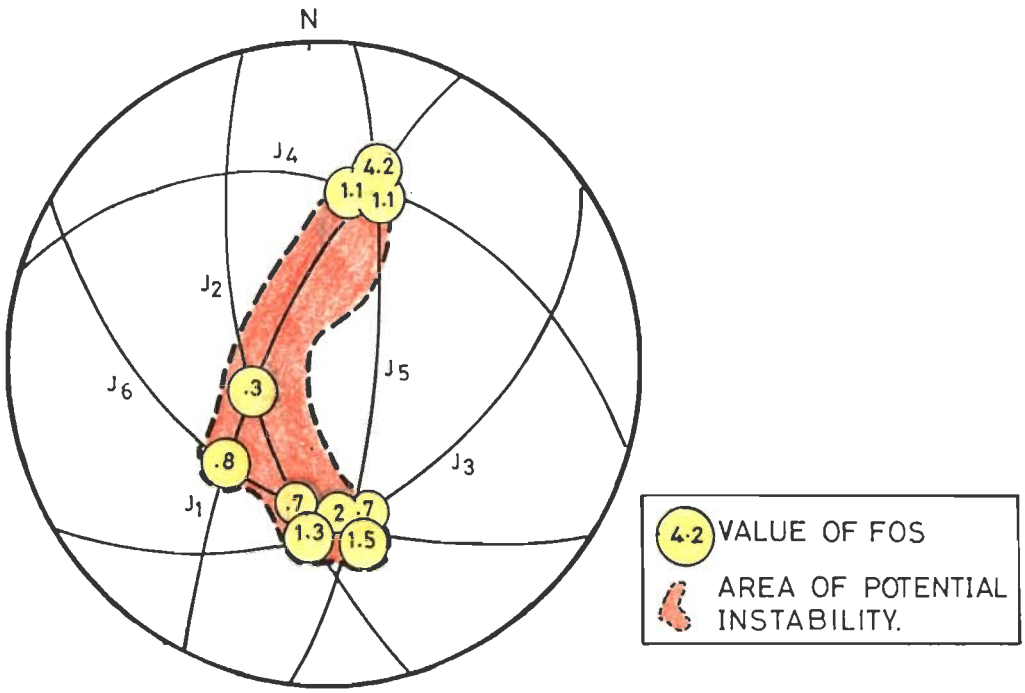

FIG.4.4 STEREOPLOT SHOWING FACTOR OF SAFETY FOR EACH COMBINATION OF DISCONTINUITIES.

It is important to mention that the factor of safety calculated for Friction only case do not take into account the impact of cohesion. Under worst conditions (zero cohesion and maximum water pressure) the value of factor of safety is considerably reduced to nearly half of the value obtained under friction only case. To quote Hoek & Bray (1977) *had the factor of safety for the friction only case been 2.0, the factor of safety for the worst condition would have been 1.0, assuming that the ratio of the factor of safety for the two cases remains constant*. Therefore, a design value corresponding to FOS = 3.0 for the friction only case is considered safe for slopes adjoining the important engineering structures, as FOS = 1.5 is considered safe under worst conditions.

The values of factor of safety, as calculated for each combination of discontinuities, have been marked over the intersection points. A contour corresponding to FOS = 3.0 has been drawn. The area obtained within this contoured line represents the unstable zone (Fig.4.4). It implies that any slope falling within this area would be unstable.

The stability analysis has been carried out for 8 slope sections at power house site. These slopes have moderate to steep angles towards the Southeastern direction. The slopes close to the river bed are generally steep in nature. Geological cross sections as shown in Fig.4.5 have been prepared along the section lines indicated in Fig.4.3.

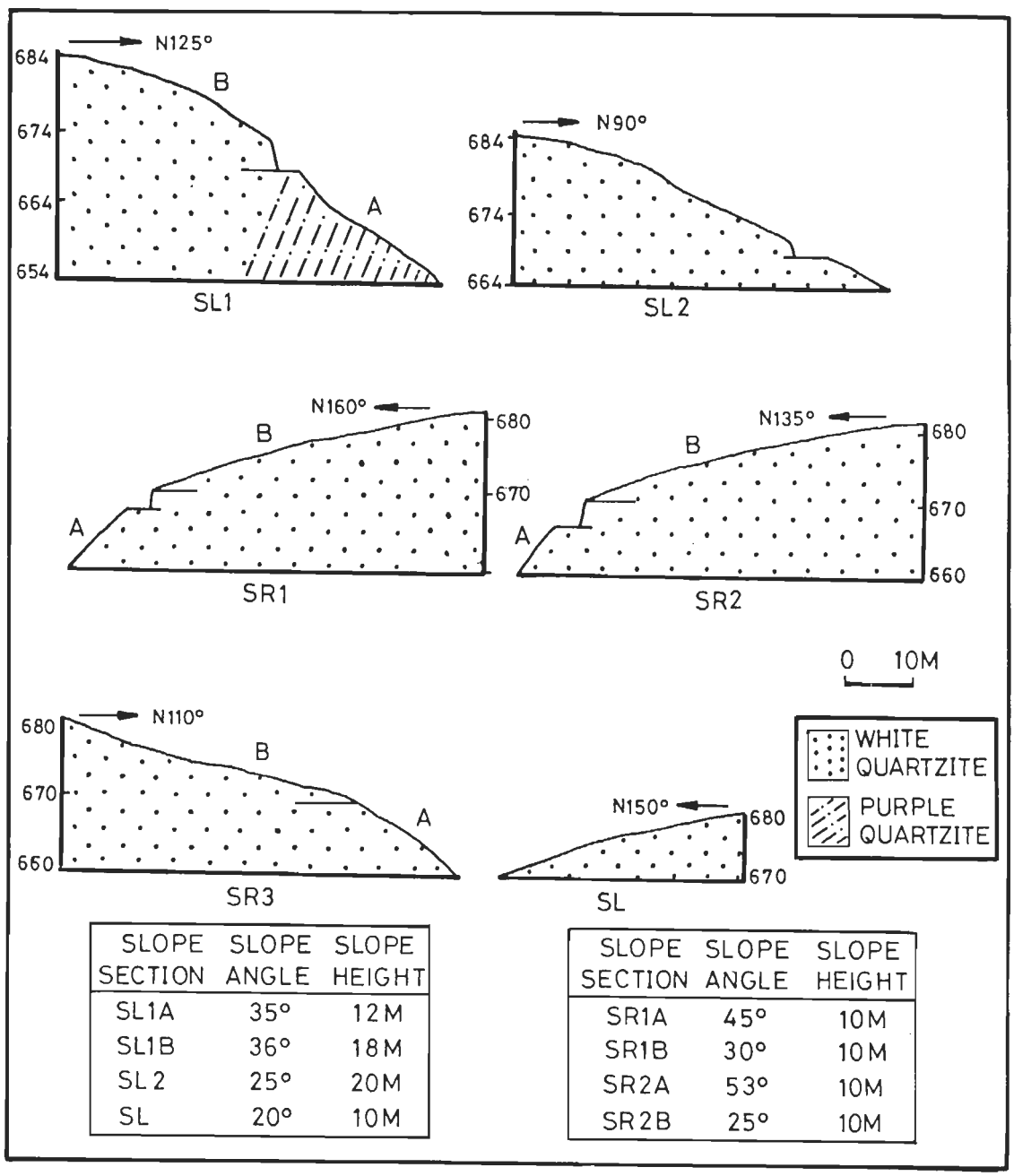

SLOPE SECTION	SLOPE ANGLE	SLOPE HEIGHT
SL1A	35°	12M
SL1B	36°	18M
SL2	25°	20M
SL	20°	10M

SLOPE SECTION	SLOPE ANGLE	SLOPE HEIGHT
SR1A	45°	10M
SR1B	30°	10M
SR2A	53°	10M
SR2B	25°	10M

FIG. 4.5 GEOLOGICAL CROSS SECTIONS OF SLOPES ADJOINING TO POWER HOUSE SITE.

The slope sections are not found to have a uniform slope from the river bed up to the ridge. Therefore, they have been further subdivided into smaller segments. The boundaries of the

subdivisions have been chosen so that the angle of the slope sections is more or less consistent within the segment.

The attitude of the slopes in addition to the unstable zone obtained on the basis of friction only study has been plotted on the stereonet. A perusal of the Fig.4.6 indicates that the slope sections SR1A and SR2A are falling within the unstable zone. Thus, these two slope sections are critical and have been considered for further detailed analysis.

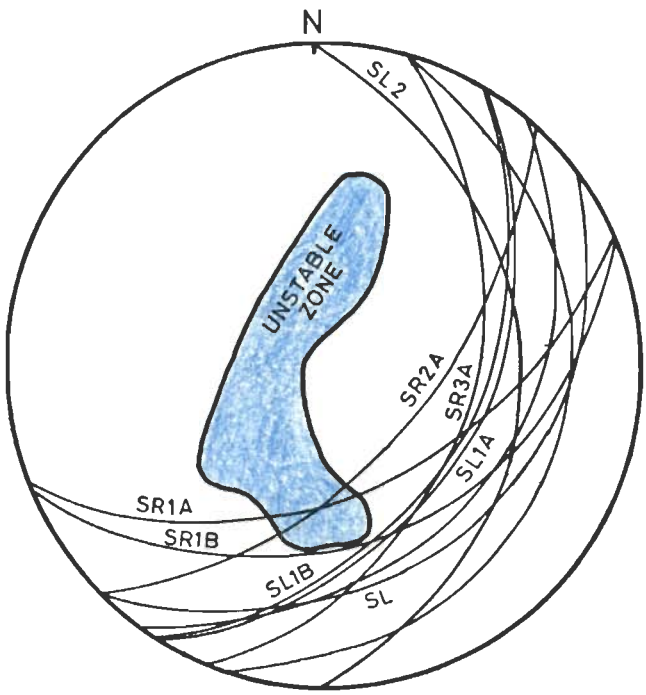

FIG. 4.6 STEREOPLOT SHOWING STABILITY CONDITION OF DIFFERENT SLOPES AT POWER HOUSE SITE.

4.3.2 MODE OF FAILURE

In order to determine the possible mode of failure, the discontinuity planes and the slopes SR1A and SR2A have been plotted on the stereonet. A friction circle corresponding to angle of internal friction ($\phi = 35°$) has also been plotted. A perusal of Fig.4.7 indicates that joint J_3 is falling within the unstable zone, defined by the slope face and the friction circle. It indicates that joint J_3 is kinematically unstable for plane mode of failure for both the slopes.

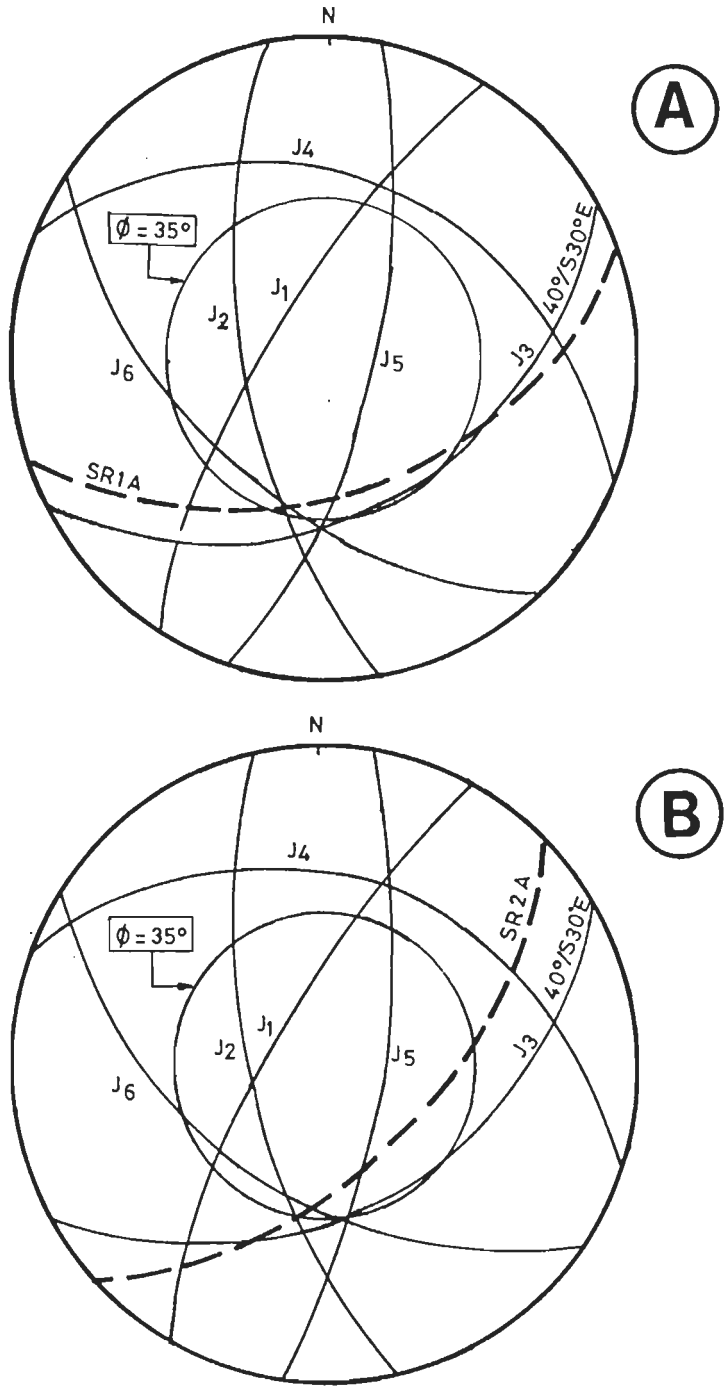

FIG. 4.7 KINEMATIC CHECK FOR CRITICAL SLOPES AT POWER HOUSE SITE. A - FOR SR1A , B - FOR SR2A

The Factors of Safety for both these slopes (SR1A & SR2A) have been obtained for dry, wet as well as dynamic conditions by using the approach given in Chapter III and the results are given later in this Chapter.

4.3.3 ESTIMATION OF SHEAR STRENGTH PARAMETERS FOR JOINT J_3

Since shear strength of a critical joint is one of the important parameters in stability analysis, an attempt has been made to estimate the shear strength of the joint set J_3 by using the empirical law of friction (eq.4.2) for rock joints (Barton, 1977).

$$\tau = \sigma_n \times \text{Tan} (\phi_b + \text{JRC} \log_{10} (\text{JCS}/\sigma_n) \quad \ldots 4.2$$

This has already been discussed in detail in Chapter III. The required input data to estimate the shear strength of joint J_3 is given in the Table 4.5.

The total friction angle, as estimated by the Barton's law, is 42°. However, in the field it has been observed that some joint surfaces are smooth and moderately weathered. Therefore, a conservative value of total friction angle of 35° has been used in the stability analysis.

In order to estimate the value of cohesion for the critical Joint J_3, back analysis of a failed slope has been carried out, where the failure has been guided by the same critical discontinuity J_3. Input data for back analysis is presented in Table 4.6.

TABLE 4.6 BACK ANALYSIS OF A FAILED SLOPE TO ESTIMATE COHESION FOR JOINT J_3

INPUT DATA	
Slope Angle, $\alpha_f = 70°$ Dip of Failure Plane, $\alpha_p = 42°$ Dip of Upper Slope Surface, $\alpha_s = 0°$ Dip of Tension Crack, $\alpha_t = 78°$ Height of Slope, h = 30 m	Angle of Internal Friction, $\phi = 35°$ Unit Weight of Rock, $\gamma = 2.75$ T/m^3 Unit Weight of Water, $\gamma_w = 1.0$ T/m^3 Horizontal earthquake Acceleration = 0.15 Tension Crack is half Filled with Water Factor of Safety = 1.0
EQUATION TO CALCULATE COHESION*	
$F = \dfrac{CA + [W(\text{Cos}\ \alpha_p - \alpha \text{Sin}\ \alpha_p) - U - V\text{Sin}\ \alpha_p] \text{Tan}\ \phi}{W(\text{Sin}\ \alpha_p + \alpha \text{Cos}\ \alpha_p) + V\text{Cos}\ \alpha_p}$ * Derivation of this equation is given in Chapter III	
Value of Cohesion, C as calculated for joint J_3 comes out to be 15.59 T/m^2 say 16 T/m^2	

TABLE 4.5 ESTIMATION OF SHEAR STRENGTH OF JOINT J_3

Basic Friction Angle, ϕ_b^* = 35°
Joint Roughness Coefficient, JRC* = 5
Joint Compressive Strength, JCS** = 512.5 kg/cm^2
Compressive Strength of Intact Rock, σ_c = 2050 kg/cm^2
Effective Normal Stress Acting on the Joint Surface σ_n = 6.49 kg/cm^2
Thus, substituting these values in eq. 4.2, shear stress (τ) acting across the potential failure plane has been obtained. Similarly, for different σ, τ has been calculated by using eq.4.2 and a graph in between normal and shear stress has been plotted.

σ	6.49	10	15	20	25	30	35	40	45	50
τ	6.37	9.5	13.8	18.0	22.1	26.2	30.2	34.2	38.1	42.0

* The values are after Barton & Choubey, 1977
** JCS = σ_c/4 (Barton, 1973)

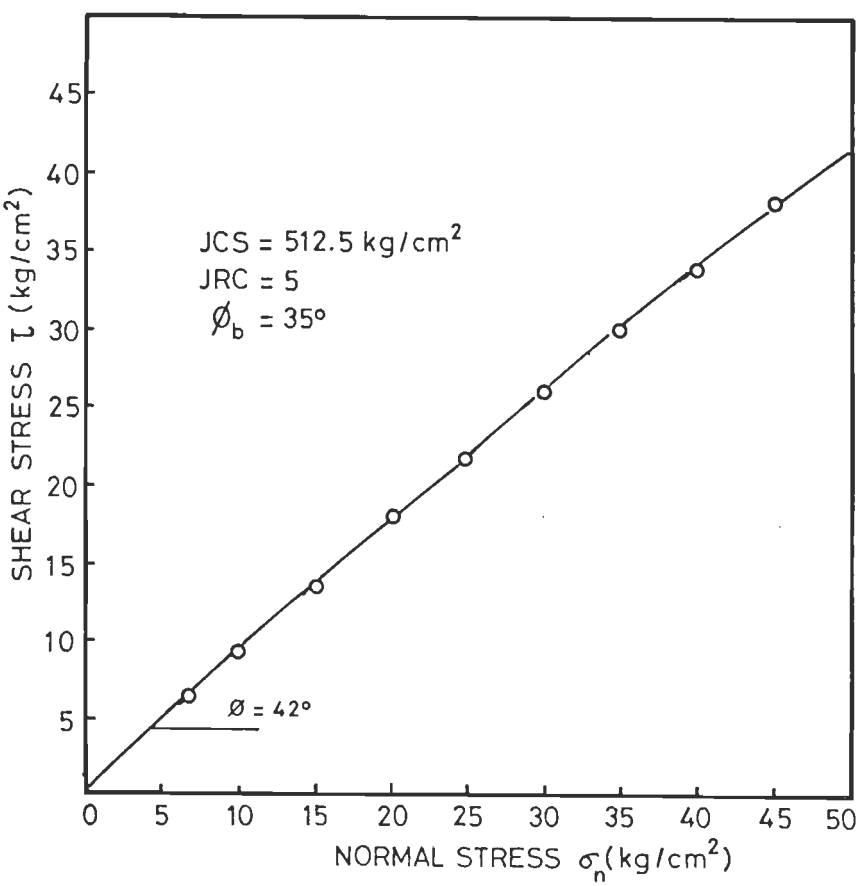

ESTIMATION OF SHEAR STRENGTH OF JOINT J_3

4.3.4 PLANE FAILURE ANALYSIS

As discussed in the previous section, SR1A and SR2A slope sections are kinematically unstable for plane mode of failure. Therefore, these two slopes have been analysed for plane failure by using the approach given in Chapter III.

The factors of safety have been determined for these slopes under static as well as dynamic conditions. The factors of safety have also been determined when the tension crack is dry, fully-filled, half-filled and quarter-filled with water. The input data sheet and the results are given in Table 4.7.

TABLE 4.7 PLANE FAILURE ANALYSIS OF SLOPES AT POWER HOUSE SITE

Input Parameter	Slope Sections	
	SR1A	SR2A
Slope Angle, α_f	45°	53°
Dip of Failure Plane, α_p	40°	40°
Upper Slope Surface Angle, α_s	30°	25°
Dip of Tension Crack, α_t	90°	70°
Height of Slope, h	10 m	10 m
Cohesion, C	16 T/m^2	16 T/m^2
Angle of Internal Friction, ϕ	35°	35°
Unit Weight of Rock, γ	2.75 T/m^3	2.75 T/m^3
Unit Weight of Water, γ_w	1.00 T/m^3	1.00 T/m^3
Horizontal Earthquake Acceleration, α	0.15	0.15
Height of water in Tension crack, Z_w	0-1 Z_L*	0-1 Z_L*

* Z_L is the depth of tension crack

FACTOR OF SAFETY

Depth of Water in Tension Crack	Slope Section			
	SR1A		SR2A	
	Static	Dynamic	Static	Dynamic
Case 1 (No water)	3.76	3.10	2.37	1.92
Case 2 (Quarter filled)	3.74	3.08	2.33	1.88
Case 3 (Half filled)	3.71	3.06	2.26	1.83
Case 4 (Completely filled)	3.64	3.00	2.09	1.70

Discussion

It is anticipated that the worst possible adverse condition of the slope may be defined by half filled tension crack with earthquake loading. However, a perusal of Table 4.7 indicates that both the slope sections are stable in static as well as in dynamic conditions and also for all conditions of different depths of water in tension crack.

4.4 CUT SLOPE DESIGN FOR OPEN EXCAVATION FOR POWER HOUSE

The hill slopes are to be excavated for creating a terrace (22 x 70 m) for housing the power house. The terrace is to be located at El.663 m. The hill slopes adjoining the power house site, as discussed above, are stable.

From the friction only case analysis it has already been mentioned that any slope falling within the unstable zone (Fig.4.6) would be unstable. To avoid this unstable zone, the slopes adjoining the power house site should be excavated by maintaining a maximum cut slope angle of 34°.

A study of the contour plan of the power house site indicates that the slopes are gentle from El. 670 m onwards. Hence, a stable cut slope has been proposed (Fig.4.8 & 4.9) for the hill slopes adjoining the power house terrace. Though the overall cut slope angle of 34° has been maintained, a height of 4m and width of 2m have been proposed for individual benches. Although the cut slopes would remain stable, the slopes would be subjected to continuous vibrations during the operation of power house. These vibrations may tend to destabilise the otherwise stable slopes. Particularly the rock wedges formed in the projecting cut slope benches are more vulnerable.

Hence, some additional stability measures are suggested which include:

a) Two layers of shotcreting on chainlink wiremesh leaving 25 percent surface area available for drainage may be provided.

b) Perfo-anchors of 6 m length at 3 m spacing in staggered fashion may be provided. The free end may be provided with 30 x 30 cm bearing plate. The anchors may be installed after the steel wire mesh is placed so that the anchor heads are concealed under second layer of shotcrete.

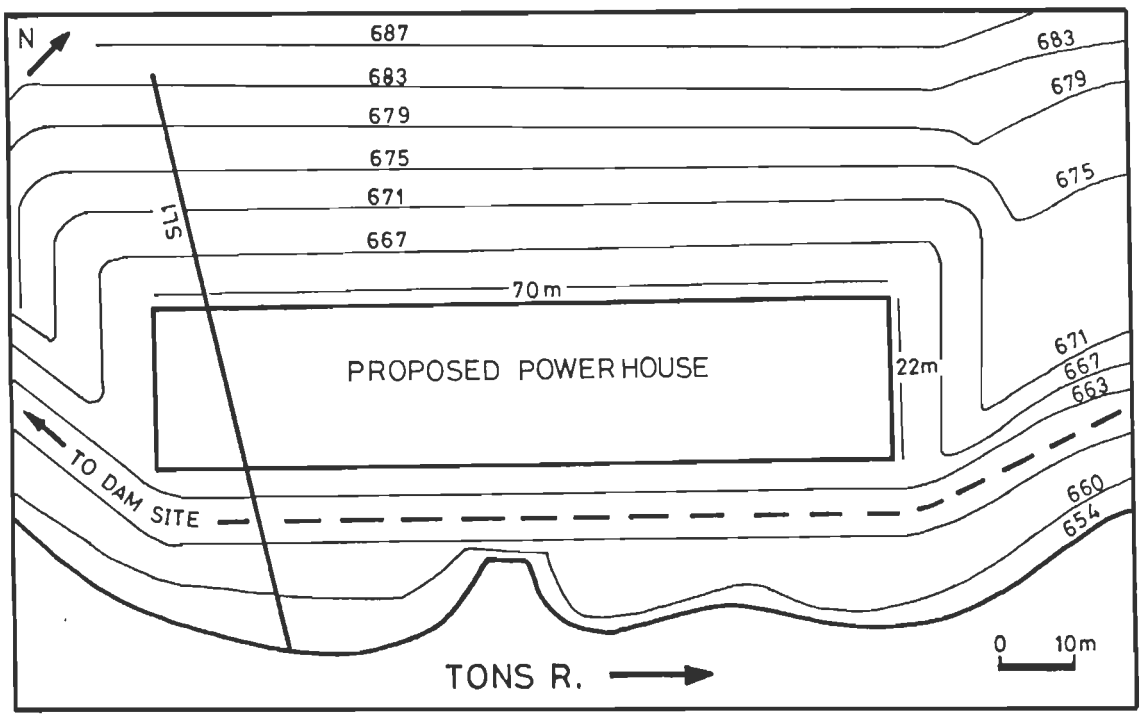

FIG. 4.8 CUT SLOPE DESIGN (IN PLAN) FOR POWER-HOUSE SITE.

c) Lined catch water drain towards the hill side end of benches with proper gradients may be provided. The cut slope design in section is shown in Fig.4.9.

Discussion

Though the power house site will be stable with the proposed cut slope and the treatments. The site incidently falls on a location where a minor perennial Jamar Stream flows in the centre of the site. The Jamar stream course has caused a depression in the general slope profile (Fig.4.1). The Jamar stream is reported to have a heavy discharge during rains. Hence, the most important problem anticipated at this site is to provide a safe and permanent diversion for Jamar stream. Moreover, the excavation for terrace may involve considerable problems to accommodate the Jamar stream course along which the depth of weathering may be more. Hence, it is felt that by shifting the power house site towards East (Fig.4.10) in the downstream direction by about 75 m, the stream course can be avoided completely, though the other conditions remain more or less same.

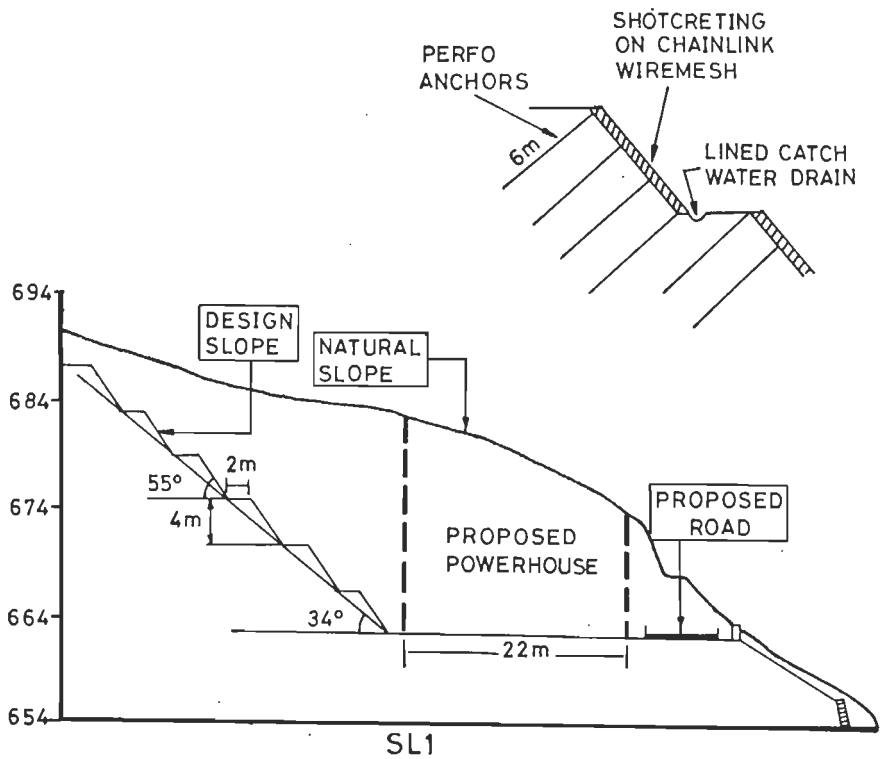

FIG. 4.9 CUT SLOPE DESIGN (IN SECTION) AND STABILITY MEASURES FOR SLOPES ADJOINING TO POWER HOUSE SITE.

4.5 ALTERNATIVE SITE FOR POWER HOUSE

The alternative site for the power house, as shown in Fig.4.10, is located in the same vicinity, where same rocks are exposed. The advantages of this site are:

a) The site is not traversed by any stream course.

b) The slopes at the site has gentle gradients as compared to slopes West of the earlier site.

Since, the hill slopes at this site are more or less uniform, the stability analysis has been carried out only along one section SR3. The perusal of Fig.4.6 indicates that the slope section SR3 do not fall within the unstable zone. Hence, the slope adjoining to the alternative power house site is stable. The cut slope design and other remedial measures suggested for the earlier site are also applicable for this site which has lesser engineering geological problems.

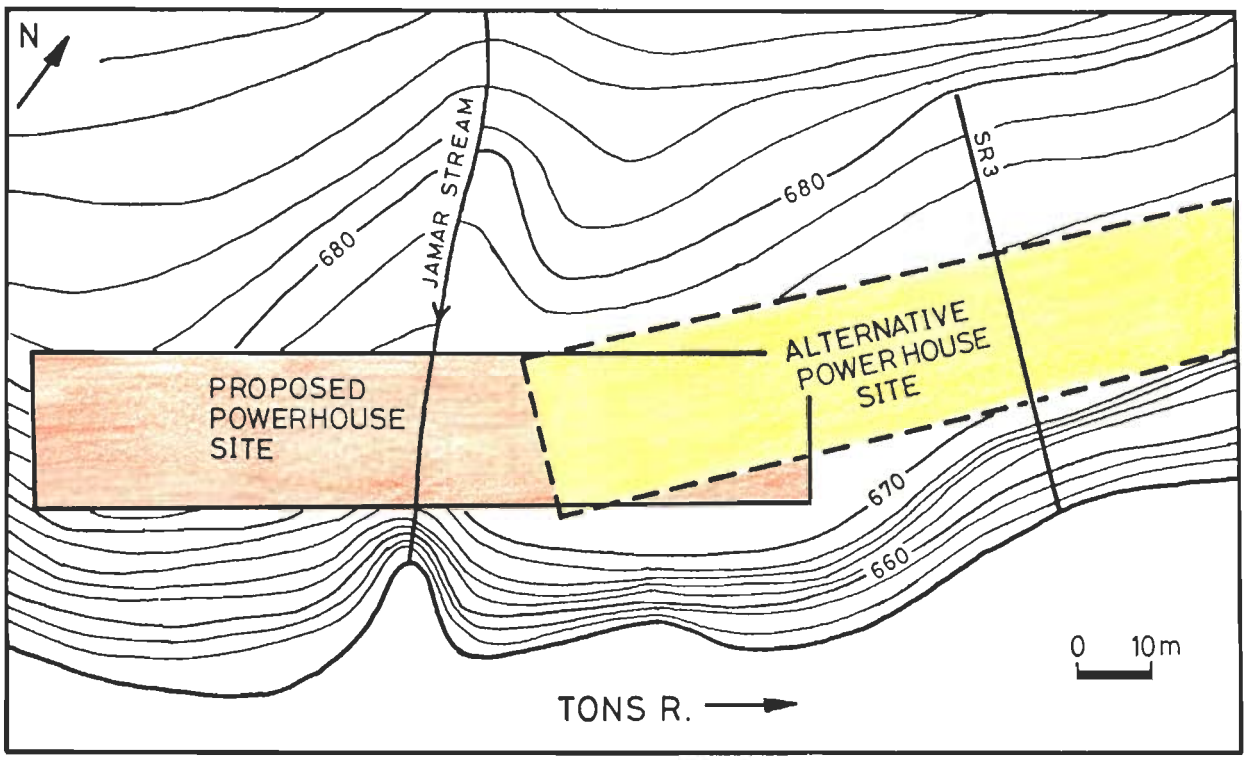

FIG. 4.10 ALTERNATIVE POWER HOUSE SITE FOR KISHAU DAM.

CHAPTER V

SLOPE STABILITY STUDIES OF RESERVOIR AREA

The construction of a dam across the river valley leads to impoundment of water behind it. This trapped water body between the valley slopes and dam is termed as dam reservoir. The engineering geological evaluation of dam reservoir in general includes:

i) Stability studies of the slopes of the reservoir area.
ii) Identification of the weak zones through which water may seep into adjoining valley, and
iii) Siltation problem of the reservoir.

The water seepage and siltation problems have not been considered in the present study due to non-availability of the required data. However, the stability of slopes of the reservoir area has been carried out in detail. Stability of the hill slopes around the reservoir has got an important consideration in the safe functioning of the dam. Major slides in the reservoir can significantly reduce the storage capacity. Slope failures of larger magnitude, if takes place close to the dam body, may generate seiches, causing overtopping of the dam. Vajont Dam, Italy, in 1964 experienced such seiche, generated due to a catastrophic failure in the reservoir area, killing 2000 people in the low lying areas. Therefore , recognition of such potentially unstable slopes bordering the reservoir in the initial stages of investigation may help in evolving possible remedial measures.

In order to identify the potentially unstable slopes bordering the reservoir, the following systematic investigations have been carried out .

i) Reconnaissance survey of the area to identify the potentially unstable slopes
ii) Determination of factor of safety for the critical slopes in dry and wet conditions under static as well as dynamic conditions. Further, the effect of water impoundment on the Factor of Safety of critical slopes have been studied.

Besides, the height of the water wave generated due to a possible potential slide in reservoir area has also been calculated in addition to kinetic energy involved in it.

5.1 GEOLOGY OF THE RESERVOIR AREA

Detailed geological mapping of the reservoir area on 1:15,000 scale has been carried out which has been used as the base map for carrying out systematic stability studies. Mapping was mainly done to study the various rock types exposed and to collect the data of structural discontinuities in the reservoir area. The rocks exposed in the reservoir area fall mainly into three Groups: the lower Dharagad Group, the middle Deoban Group and the upper Jaunsar & Simla Groups. The Geology of the reservoir area has already been discussed in detail in Chapter II.

The data pertaining to structural discontinuities, mainly joints, have been collected from 100 localities on both the banks, in the reservoir area (Fig.5.1). The rocks are intensely jointed and generally have two to four sets of discontinuities.

The distribution of structural data has been studied carefully in order to divide the area into different domains, wherein, the distribution of structural data is more or less uniform. The analysis of structural data, using stereonet, in order to deduce preferred orientation of discontinuities, has been carried out.

For that purpose, the poles of the attitude of joints have been plotted and contoured. The maxima of pole concentrations have been identified in terms of their predominance. The locality-wise attitude of discontinuities for right and left banks are presented in Table 5.1 & Fig.5.2.

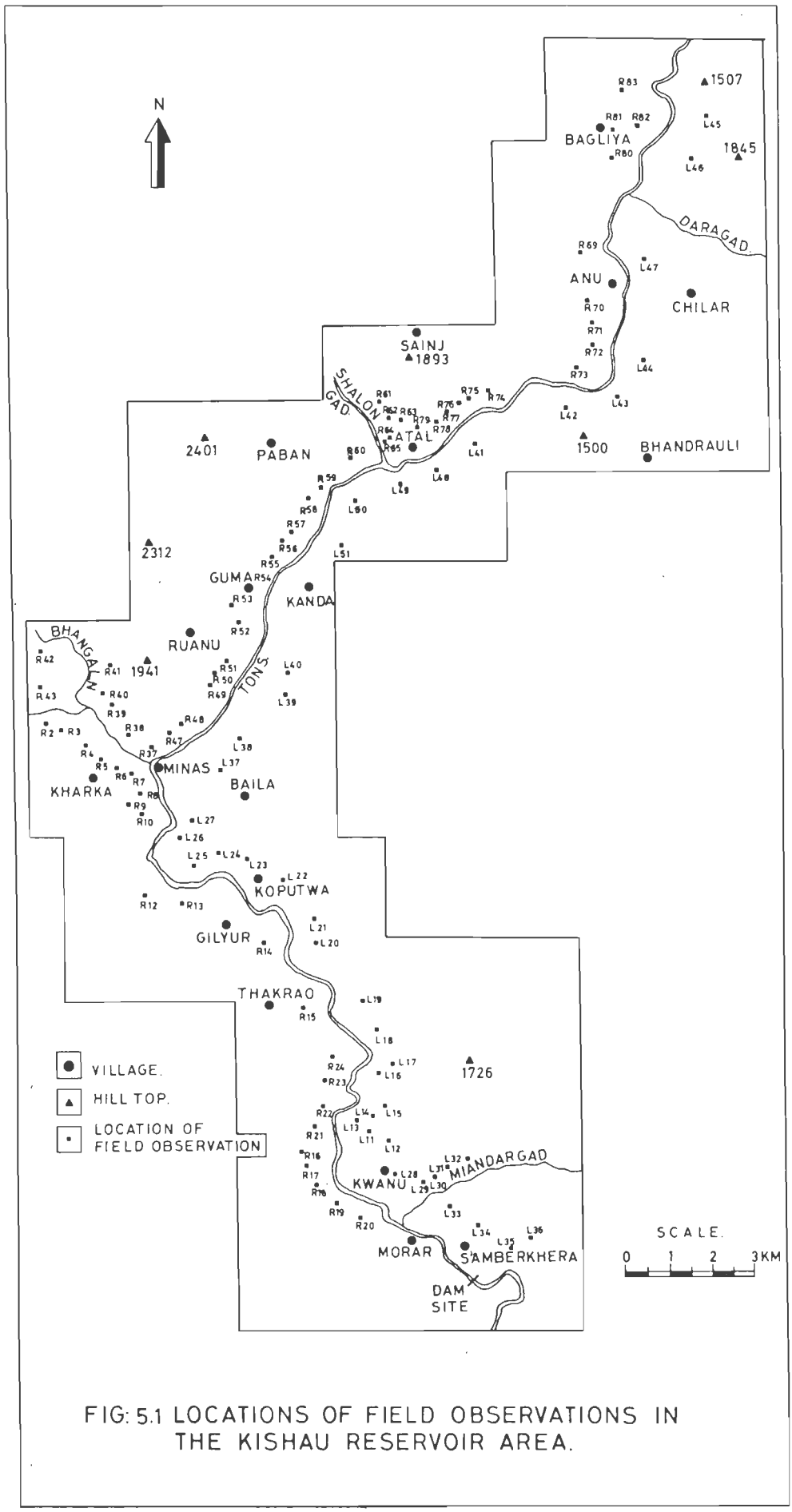

FIG: 5.1 LOCATIONS OF FIELD OBSERVATIONS IN THE KISHAU RESERVOIR AREA.

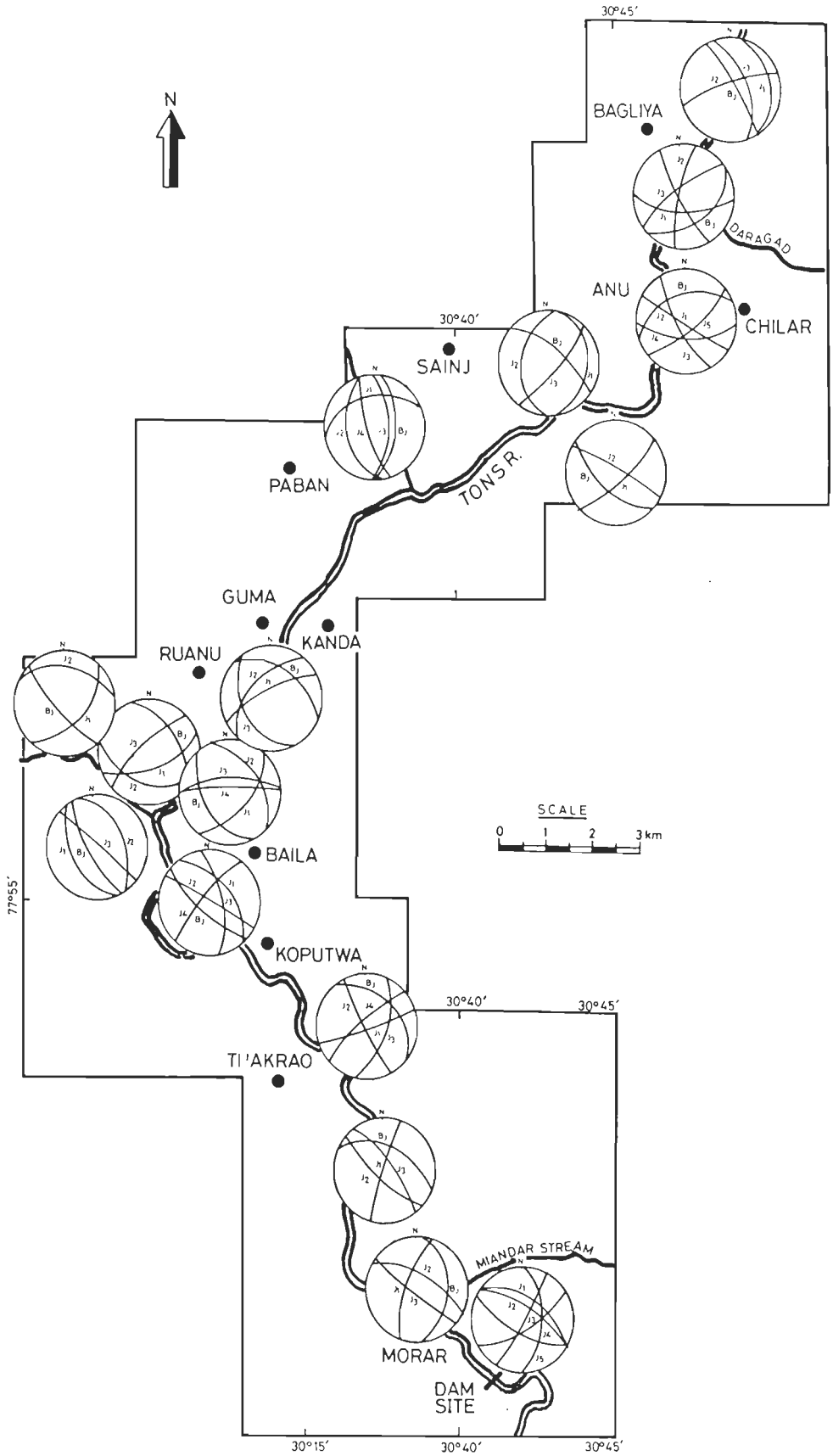

FIG. 5.2 LOCALITY WISE GENERAL TREND OF JOINTS IN RESERVOIR AREA

TABLE 5.1 LOCALITY WISE DESCRIPTION OF DISCONTINUITIES

S. No	Location of Field Observations	Attitude of Discontinuities					
		BJ	J_1	J_2	J_3	J_4	J_5
	Right Bank of Reservoir	Dip Direction/Dip Amount					
1	R_{20}	S85° E/ 24°	N70° W/ 64°	N30° E/ 52°	S40° W/ 80°		
2	R_{13},R_{14},R_{15},R_{16}, R_{17},R_{18},R_{19},R_{21}, R_{22},R_{23},R_{24}	N22° E/ 38°	N73° W/ 84°	S40° W/ 82°	N50° E/ 72°		
3	R_{12},R_{23},R_9,R_{10}	N30° E/ 42°	S70° W/ 42°				
4	R_4,R_6,R_7,R_8	S60° W/ 72°	S60° W/ 30°	N61° E/ 30°	N43° E/ 78°		
5	R_5	S10° E/ 42°	S78° E/ 52°	N50° W/ 52°	N30° W/ 72°		
6	R_1,R_2,R_3	N51° E/ 42°	S38° E/ 30°	N61° E/ 72°			
7	R_{42},R_{43}	S37° E/ 25°	N30° E/ 74°	S50° W/ 80°	N30° W/ 80°		
8	R_{38},R_{39},R_{40},R_{41}	N61° E/ 30°	S20° E/ 54°	S19° W/ 28°	N42° W/ 68°		
9	R_{37}	N61° E/ 52°	N40° W/ 28°	N60° W/ 64°	S2° E/ 54°		
10	R_{47},R_{48},R_{49}	S60° W/ 30°	S48° E/ 42°	N42° E/ 30°	N/62°	N/80°	
11	R_{51},R_{52},R_{53},R_{54}, R_{55},R_{56}	N42° E/ 28°	N30° W/ 72°	N48° W/ 42°	S60° W/ 28°		
12	R_{57},R_{58},R_{59}	N54° E/ 14°	N50° E/ 62°	S79° E/ 64°	S20° W/ 52°	N29° W/ 72°	
13	R_{60},R_{61},R_{62}	S89° E/ 40°	S88° E/ 62°	S80° W/ 28°	N20° W/ 30°	S70° W/ 72°	
14	R_{72},R_{73},R_{74},R_{75}, R_{76}	N41° E/ 52°	S86° E/ 14°	N82° W/ 30°	S49° E/ 63°		
15	R_{69},R_{70},R_{71}	N21° W/ 30°	S29° W/ 80°	S60° W/ 72°	S20° E/ 30°	S2° E 58°	S40° E/ 72°
16	R_{80},R_{81}	S40° E/ 40°	S2° E/ 54°	N71° W/ 80°	N40° W/ 72°	S60° W/ 80°	
17	R_{82},R_{83}	N60° E/ 80°	S86° E/ 14°	N20° W/ 72°	N69° E/ 54°		

S. No	Location of Field Observations	Attitude of Discontinuities					
		BJ	J_1	J_2	J_3	J_4	J_5
	Left Bank of Reservoir	Dip Direction/Dip Amount					
1	$L_{33}, L_{34}, L_{35}, L_{36}$	S29°W/ 63°	N31°E/ 42°	N31°E/ 61°	S61°E/ 79°	S10°E/ 63°	E/41°
2	L_{30}	S/30°	N31°E/ 42°	N58°W/ 28°	S68°E/ 64°	S20°E/ 72°	N79°W/ 64°
3	L_{28}, L_{29}	S85°E/ 24°	N70°W/ 64°	N30°E/ 52°	S40°W/ 80°		
4	$L_{11}, L_{12}, L_{13}, L_{15} L_{16}$	N22°E/ 38°	N73°W/ 84°	S40°W/ 82°	N50°E/ 72°		
5	L_{14}	N30°E/ 42°	S70°W/ 42°				
6	L_{18}	N48°E/ 51°	S60°W/ 62°	N40°W/ 72°			
7	$L_{19}, L_{20}, L_{21}, L_{22} L_{23}, L_{24}$	N41°E/ 28°	S21°E/ 80°	S60°W/ 80°	S70°E/ 42°	N40°W/ 72°	
8	L_{25}	S40°W/ 50°	N50°E/ 41°	N30°E/ 86°	N80°E/ 62°	N49°W/ 72°	
9	L_{37}, L_{38}	S60°W/ 30°	S48°E/ 42°	N42°E/ 30°	N/62°	N/80°	
10	L_{39}, L_{40}	N42°E/ 28°	N30°W/ 72°	N48°W/ 42°	S60°W/ 28°		
11	$L_{41}, L_{42}, L_{48}, L_{49}$ L_{50}, L_{51}	S41°W/ 52°	S38°E/ 72°	N31°E/ 72°			
12	L_{43}	N41°E/ 52°	S86°E/ 14°	N82°W/ 30°	S49°E/ 63°		
13	L_{44}	N21°W/ 30°	S29°W/ 80°	S60°W/ 72°	S20°E/ 30°	S2°E/ 58°	S40°E/ 72°
14	L_{47}	S40°E/ 30°	S2°E/ 54°	N71°W/ 80°	N40°W/ 72°	S60°W/ 80°	
15	L_{45}, L_{46}	N60°E/ 80°	S86°E/ 14°	N20°W/ 72°	N69°E/ 54°		

5.2 ENGINEERING PROPERTIES OF ROCKS

The important Engineering properties used in the slope stability studies are uniaxial compressive strength of the intact rock, rock density and shear strength parameters. The uniaxial compressive strength of the intact rock, for the present study, has been determined in the laboratory. For that purpose, the drill cores of NX size have been obtained from the

fresh intact rock samples brought from the field. These samples were tested using uniaxial compressive testing machine to obtain the strength following the standard procedures. Density of each rock type exposed in the reservoir area has also been determined in the laboratory. Average test values of uniaxial compressive strength of intact rock and rock density are given in Table 5.2.

TABLE 5.2 AVERAGE TEST VALUES OF UNIAXIAL COMPRESSIVE STRENGTH AND ROCK DENSITY OF VARIOUS ROCKS EXPOSED IN THE RESERVOIR AREA.

S.No.	Rock Type	Uniaxial Compressive Strength (kg/cm^2)	Rock Density (gm/cm^3)
1	Simla Slates	752	2.5
2	Simla Quartzite	1956	2.8
3	Ambota Limestone	926	2.4
4	Bohar Limestone	1100	2.6
5	Bohar Slates	715	2.5
6	Tiontar Quartzite	1812	2.8
7	Atoll Limestone	1117	2.6
8	Atoll Slates	750	2.5
9	Atoll Quartzite	1892	2.8

In order to analyse the stability of the slope, shear strength parameters of the discontinuities are to be determined. These parameters are well determined either in field or in laboratory by testing. Since the laboratory testing has its own limitations, the rock mass rating system has been used to account for existing field conditions

The rock mass rating system has been used to determine shear strength parameters. For that purpose, the properties of discontinuities, such as weathering filling, continuity, spacing and separation are evaluated. For Rock Mass Rating, (RMR) System following data is required:

Strength of Intact Rock Material	- UCS
Rock Quality Designation	- RQD
Spacing of Discontinuities	- SP.
Condition of Discontinuities	- COD
Groundwater Condition	- GWC

Rock Mass rating (RMR) system has already been discussed in detail in Chapter III

The data pertaining to RMR system has been collected from all the localities, where, the stability analysis has been planned. Uniaxial compressive strength (UCS) has been determined in laboratory, while RQD is obtained empirically by Palmstorm's correlation (Palmstorm, 1981). Spacing, condition of discontinuity and ground water condition have been visually estimated. The RMR ratings computed for all localities alongwith corresponding shear strength range in terms of cohesion (C) and angle of internal friction (ϕ) are shown in Table 5.3.

The shear strength parameters presented in Table 5.3 correspond to rock mass and not for discontinuities. But, for slope stability analysis, shear strength parameters of discontinuities are required. For that purpose, back analysis of existing failed slopes has been carried out.

From back analysis of an existing failed slope, only one out of the two parameters (C & ϕ) can be determined. In the present study, the angle of internal friction (ϕ) determined by RMR system has been used in back analysis. It may be noted that the value of ϕ determined by RMR corresponds to rock mass and not for discontinuities. However, it can also be used in back analysis for the discontinuities, which are free from soft clay filing, or are not slickensided because the value of internal friction is more or less same for both, the rock mass and the discontinuity. Hence, cohesion `C' has been determined by the back analysis.

Back analysis has only been used for those slopes which are kinematically unstable for plane mode of failure. The geometry of the failed slopes and the computed value of cohesion corresponding to the discontinuity along which the slope failed are shown in Table 5.5, later in this Chapter.

In case of slopes having wedge mode of failure, the value of angle of internal friction determined from RMR has been used for stability analysis. The value of cohesion for both the discontinuities causing the failure have been adopted by considering their continuity. If the continuity is less (<5m) the value of cohesion obtained from RMR has been directly adopted for the stability analysis. But, for those discontinuities which have larger continuity (>5m), lower value of cohesion than the one obtained by RMR has been used, depending upon the site conditions.

TABLE 5.3 LOCALITY WISE ROCK MASS RATING AND SHEAR STRENGTH PARAMETERS IN RESERVOIR AREA

LEFT BANK								
PARAMETER								
ROCK MASS RATING								
Locality No.	UCS	RQD	SP.	COD	GWC	RMR_B	C	ϕ
L_{33}	12	20	8	20	10	70	3-4	35-45
L_{34}	12	17	8	25	15	77	3-4	35-45
L_{35}	12	20	8	20	10	70	3-4	35-45
L_{36}	12	17	8	20	10	67	3-4	35-45
L_{30}	7	8	10	10	15	50	2-3	25-35
L_{28}	7	13	8	14	15	57	2-3	25-35
L_{11}	7	13	8	18	12	56	2-3	25-35
L_{12}	7	13	8	18	12	56	2-3	25-35
L_{15}	7	17	8	17	10	59	2-3	25-35
L_{16}	7	13	8	17	10	59	2-3	25-35
L_{14}	7	17	8	20	15	67	3-4	35-45
L_{18}	7	13	8	12	15	55	2-3	25-35
L_{19}	7	17	8	17	15	64	3-4	35-45
L_{20}	7	17	8	20	15	67	3-4	35-45
L_{21}	7	17	8	20	15	67	3-4	35-45
L_{22}	7	17	8	17	15	64	3-4	35-45
L_{23}	7	17	8	20	15	67	3-4	35-45
L_{24}	7	17	8	17	15	64	3-4	35-45
L_{25}	7	13	8	20	15	63	3-4	35-45
L_{37}	12	20	8	20	15	75	3-4	35-45
L_{38}	12	17	8	25	15	77	3-4	35-45
L_{39}	12	20	8	25	12	77	3-4	35-45
L_{40}	7	17	8	17	10	59	2-3	25-35
L_{41}	12	17	8	20	15	72	3-4	35-45
L_{48}	12	20	8	25	12	77	3-4	35-45
L_{49}	12	20	8	20	15	75	3-4	35-45
L_{50}	12	20	8	25	12	77	3-4	35-45
L_{51}	12	17	8	20	15	72	3-4	35-45
L_{42}	12	13	8	10	15	58	2-3	25-35
L_{43}	12	20	8	25	12	77	3-4	35-45
L_{44}	12	17	8	20	15	72	3-4	35-45
L_{47}	12	17	8	20	10	67	3-4	35-45
L_{45}	12	17	8	25	12	77	3-4	35-45
L_{46}	12	20	8	20	15	75	3-4	35-45

Locality No.	UCS	RQD	SP.	COD	GWC	RMR_B	C	ϕ
RIGHT BANK								
R_{13}	7	13	8	14	15	57	2-3	25-35
R_{14}	7	13	8	20	10	58	2-3	25-35
R_{15}	7	13	8	17	15	60	2-3	25-35
R_{16}	7	13	8	20	10	58	3-4	25-35
R_{17}	7	12	11	18	7	55	2-3	25-35
R_{18}	7	12	9	22	7	57	2-3	25-35
R_{19}	7	12	10	20	7	56	2-3	25-35
R_{21}	7	12	9	20	7	55	2-3	25-35
R_{22}	7	13	9	20	10	59	2-3	25-35
R_{23}	7	12	9	18	10	56	2-3	25-35
R_{24}	7	12	9	22	7	57	2-3	25-35
R_{20}	7	13	8	20	10	58	2-3	25-35
R_9	7	13	8	18	12	56	2-3	25-35
R_{10}	7	12	9	22	7	57	2-3	25-35
R_{12}	7	13	8	20	10	58	2-3	25-35
R_4	7	17	8	25	15	72	3-4	35-45
R_6	7	20	10	25	15	77	3-4	35-45
R_7	7	17	8	20	15	67	3-4	35-45
R_8	7	17	8	15	15	62	3-4	35-45
R_5	7	20	10	25	15	77	3-4	35-45
R_1	7	20	8	25	15	75	3-4	35-45
R_2	7	20	10	25	15	77	3-4	35-45
R_3	7	17	8	20	15	67	3-4	35-45
R_{38}	7	20	8	25	10	70	3-4	35-45
R_{41}	7	17	10	25	15	74	3-4	35-45
R_{37}	7	17	8	20	15	67	3-4	35-45
R_{47}	7	17	8	25	15	72	3-4	35-45
R_{48}	7	20	10	25	15	77	3-4	35-45
R_{49}	7	17	8	20	15	67	3-4	35-45
R_{51}	7	20	10	25	15	77	3-4	35-45
R_{52}	7	13	8	17	15	60	3-4	35-45
R_{53}	7	20	10	25	15	67	3-4	35-45
R_{54}	7	20	10	25	15	77	3-4	35-45
R_{55}	7	17	8	20	15	67	3-4	35-45
R_{56}	7	17	8	15	15	62	3-4	35-45
R_{57}	7	17	8	20	15	67	3-4	35-45
R_{58}	7	17	8	20	15	67	3-4	35-45

Locality No.	UCS	RQD	SP.	COD	GWC	RMR_B	C	ϕ
R_{59}	7	17	8	20	15	67	3-4	35-45
R_{60}	7	17	8	15	15	62	3-4	35-45
R_{61}	7	20	10	25	15	77	3-4	35-45
R_{62}	7	17	8	15	15	62	3-4	35-45
R_{72}	12	17	8	20	15	72	3-4	35-45
R_{73}	12	20	8	23	15	78	3-4	35-45
R_{74}	12	17	8	20	15	72	3-4	35-45
R_{75}	12	13	8	20	15	68	3-4	35-45
R_{76}	12	17	8	20	15	72	3-4	35-45
R_{69}	12	20	8	23	15	78	3-4	35-45
R_{70}	12	17	8	20	15	72	3-4	35-45
R_{71}	12	17	8	20	15	72	3-4	35-45
R_{80}	12	17	8	20	15	72	3-4	35-45
R_{81}	12	20	8	25	15	75	3-4	35-45
R_{82}	12	13	8	20	15	68	3-4	35-45
R_{83}	12	17	8	20	15	72	3-4	35-45

UCS = Uniaxial Compressive Strength; RQD = Rock Quality Strength;
SP. = Spacing Between Discontinuities; COD = Condition of Discontinuities;
GWC = Ground Water Condition; RMR_B = Rock Mass Rating (Basic);
C = Cohesion (Kg/cm^2); ϕ = Angle of Internal Friction(Degrees)

5.3 STABILITY ANALYSIS

The stability of the hill slopes, in the reservoir area, has been carried out to identify the unstable zones. The analysis has been carried out for the natural conditions, as well as, for conditions under reservoir impoundment. Besides, stability analysis has also been carried out for dynamic conditions to account for earthquake acceleration.

The collection of data is an important part of the stability analysis of reservoir slopes. The collection of field data has been done following the principle of "whole to part", where, the entire area has been surveyed initially and the potentially unstable zones have been identified, based on their field manifestations of instability, such as:

- presence of scarp faces on steep slopes,
- removal of toe support by river erosion,
- presence of evidences of slope distress, such as, development of cracks, bulging of slope face and other such features.
- presence of zones of excessive seepage

Initially, the geological mapping of the reservoir area on 1:15,000 scale has been carried out. Data pertaining to structural discontinuities, mainly joints, alongwith the data on RMR has been recorded from the entire reservoir rim area. A total 70 potentially unstable slopes from the reservoir area have been identified/selected (Fig.5.3) for the detailed stability analysis. The detailed study includes the following:

1. Preparation of geological cross sections across the potentially unstable slopes (Fig.5.4).

2. The potentially unstable slopes, identified in the reservoir area, are not found to have a uniform slope profile from the river bed to the hill top and so they have been further sub-divided into smaller segments. The boundaries of the subdivisions have been chosen so that the angle of the slope sections is more or less consistent within the segments. Thus, these 70 potentially unstable slope sections have been sub-divided into 204 segments (Fig.5.5). Later, the detailed stability studies have been carried out for all the slope segments.

3. The possible plane or wedge mode of failure in potentially unstable slopes in the reservoir area has been identified. The identification of the mode of failure in potentially unstable slopes has been discussed in detail later in this Chapter. Besides, the slope sections where the rock mass is heavily jointed, a rotational mode of failure is considered. The potentially unstable slopes do not contain deep seated soil materials and hence no rotational failure analysis involving soil slopes has been done.

4. The potentially unstable slopes, identified to have possible plane, wedge and rotational mode of failures have been further analysed for their factor of safety. For plane mode of failure, the calculation of factor of safety is based on the modified approach as discussed in Chapter III. But the factor of safety for wedge mode of failure has been obtained by Computer Programs ROSS and RWEDGE. The potentially unstable slopes having rotational mode of failure has been analysed using the computer program SARC.

5. Further, the maximum wave height generated by the possible slides in the reservoir has also been calculated by using Computer Program WAVE.

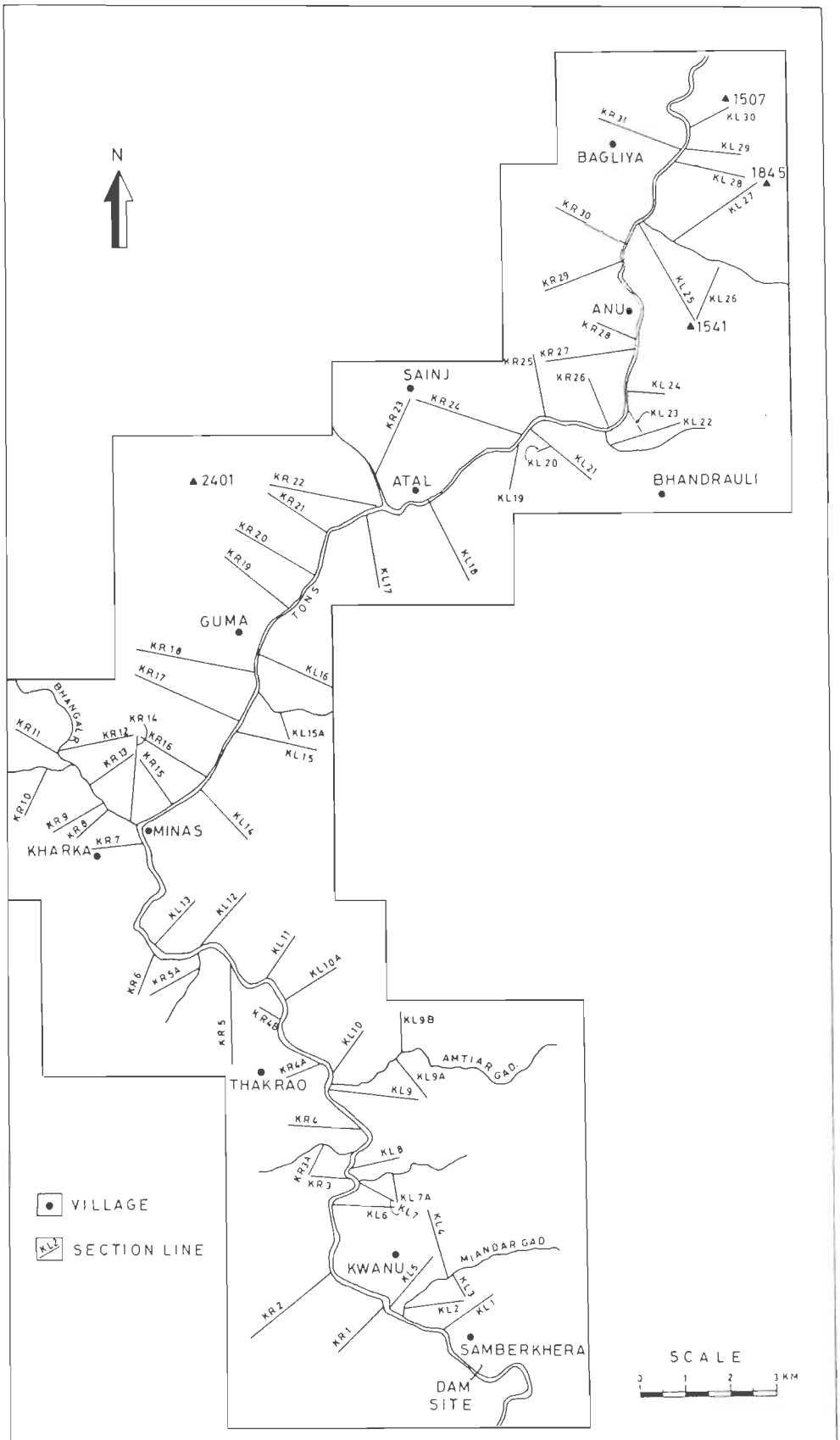

FIG:5.3 LOCATION OF SECTIONS FOR STABILITY ANALYSIS IN THE RESERVOIR OF KISHAU DAM.

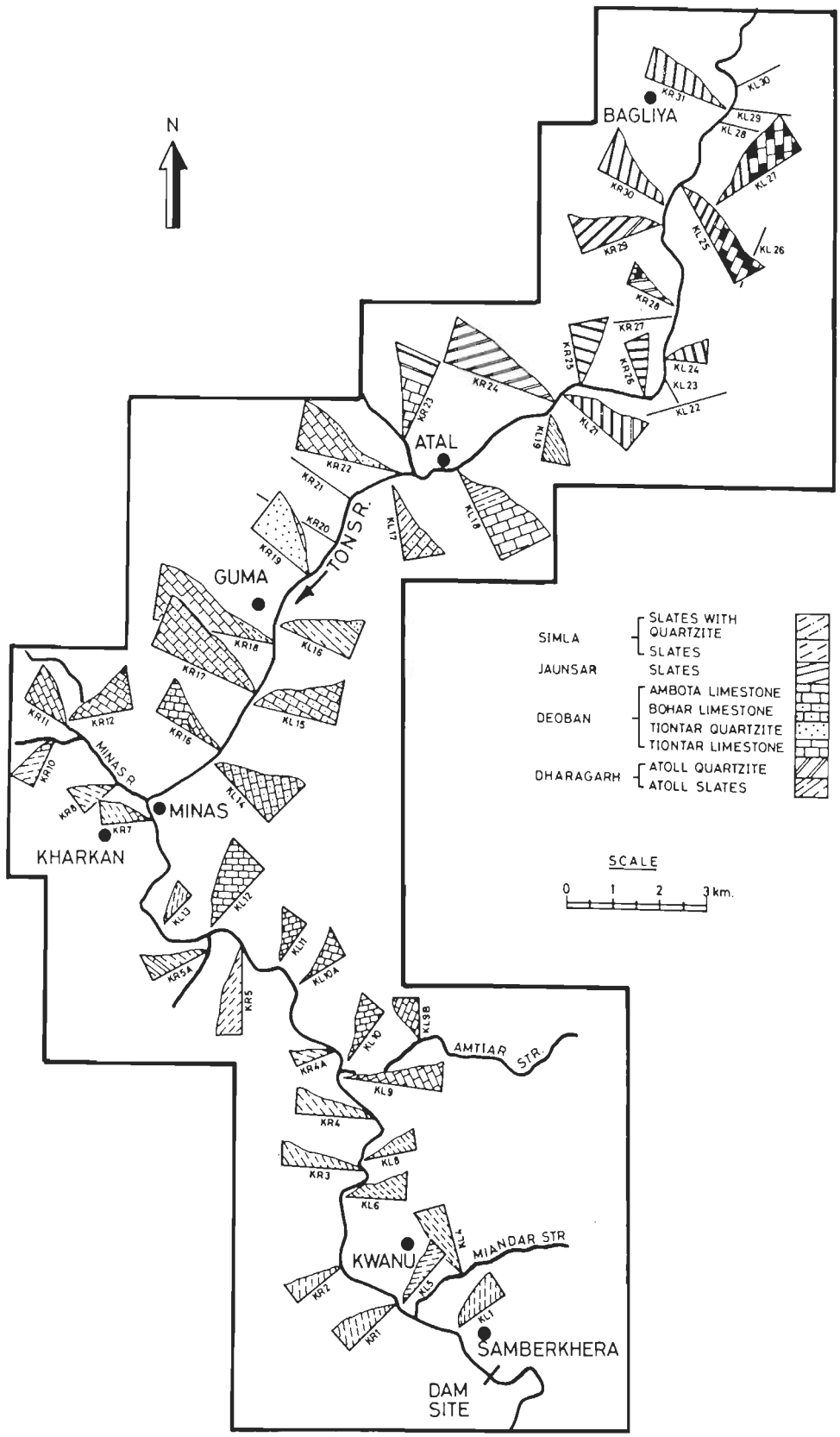

FIG. 5.4 GEOLOGICAL CROSS SECTIONS ACROSS THE POTENTIALLY UNSTABLE SLOPES IN THE RESERVOIR AREA

5.3.1 COMPUTER AIDED ANALYSIS

In order to analyse the stability of the rock slopes a computer program **ROSS** (**Rock Slope Stability Analysis**) has been prepared. The programme ROSS is basically designed to analyse the rock slope stability. It has the following facilities for the analysis

1. Identification of the possible mode of failure - plane and wedge failures.

2. Identification of the critical plane and wedge mode of failure.

3. Calculation of plunge and direction of the line of intersection of wedge forming planes

4. Calculation of Factor of Safety (FOS) under dry condition for the identified critical mode of failure.

For identifying the critical mode of failure in rock slopes, the program uses Markland test. The Markland test states that the following conditions should be satisfied for the failure to occur.

Markland Condition
For Plane Failure - $\alpha_f > \alpha_p > \phi$ For Wedge Failure - $\alpha_f > \alpha_i > \phi$
Where, α_f = Slope face inclination α_p = Failure plane inclination α_i = Plunge of line of intersection ϕ = Angle of internal friction

The detailed description of the program ROSS is given in Annexure II

In order to identify the possible modes of failures in 204 sub slope sections in the reservoir area, the program ROSS has been used. For that purpose, the input data required in the program includes discontinuity orientation, dip and dip direction of the slope face and angle of internal friction. The results of this analysis indicating the possible modes of failures in different sub-slope sections are presented in Table 5.4.

A perusal of the Table 5.4 indicates that out of 204 slope sections, only 17 sections are critical. Of these, 10 sections follow the wedge failure mode and the remaining 7 sections follow the plane mode of failure. Hence, further detailed studies have been carried out for calculating factor of safety for the critical sections.

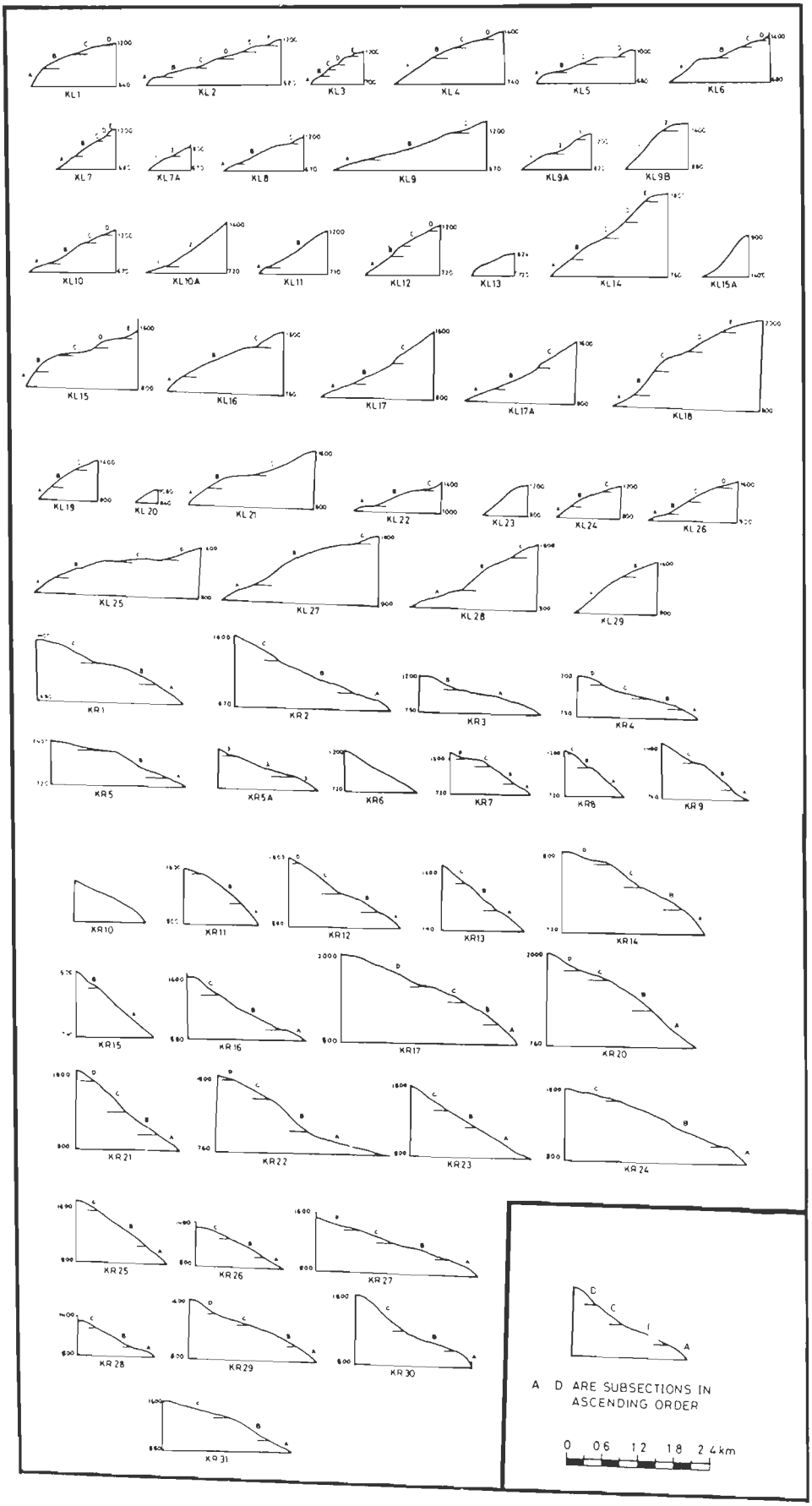

FIG.5.5 CROSS SECTIONS OF THE HILLSIDES FORMING THE RIM OF RESERVOIR

TABLE 5.4 POSSIBLE MODE OF FAILURE IN SLOPE SECTIONS IDENTIFIED BY PROGRAM ROSS

S.No.	Slope Section	Possible Mode of Failure	
		Wedge Failure	Plane Failure
1	KL1A	-	J_1^*
2	KL9B1	$(J_3,J_4)^*$	-
3	KL13A	-	J_1
4	KL15A	-	J_3
5	KL15D	-	J_3
6	KL19A	(J_2,J_3)	-
7	KR2A	(J_1,J_2)	-
8	KR3A1	-	J_1
9	KR5A	(J_1,J_2)	-
10	KR9B	(J_2,J_4)	-
11	KR14A	(J_3,J_4)	-
12	KR14C	(J_3,J_4)	-
13	KR15B	-	J_2
14	KR20A	(J_3,J_4)	-
15	KR21A	(J_3,J_4)	-
16	KR21C	(J_3,J_4)	-
17	KR30A	-	J_1

*(J_a,J_b) - Critical wedge formed by joint sets.
J_a - Plane failure along the joint set.
where a and b represents the joint set 1 to 4.

5.3.2 PLANE FAILURE ANALYSIS

The slopes having plane mode of failure have been analysed in dry, wet as well as in dynamic conditions. The analysis has been carried out for both natural and reservoir water impoundment conditions. The factor of safety for plane mode of failure has been obtained by a modified approach as discussed in Chapter III. The formula used for calculation of factor of safety for plane mode of failure, under static and dynamic conditions in Chapter III has been suitably modified for the conditions of reservoir impoundment.

Stability of the Slopes Having Plane Mode of Failure, Submerged in Water

The present analysis takes into consideration the effects of horizontal water force, produced by the standing reservoir water on the failure plane.

Determination of Water Pressure 'P'

Let `P' be the pressure generated by the standing reservoir water column of depth RL. This pressure `P' would be exerted horizontally on the failure plane dipping at an angle α_p.
The water pressure `P' would be

$$P = \tfrac{1}{2}\,\gamma_w\, RL^2\, \mathrm{cosec}^2\alpha_p \quad \ldots\ 5.1$$

where, γ_w is the density of water

This force `P' can be resolved along failure plane, into the components $P^*\mathrm{Cos}\alpha_p$ and $P^*\mathrm{Sin}\alpha_p$, as shown in Fig 5.6.

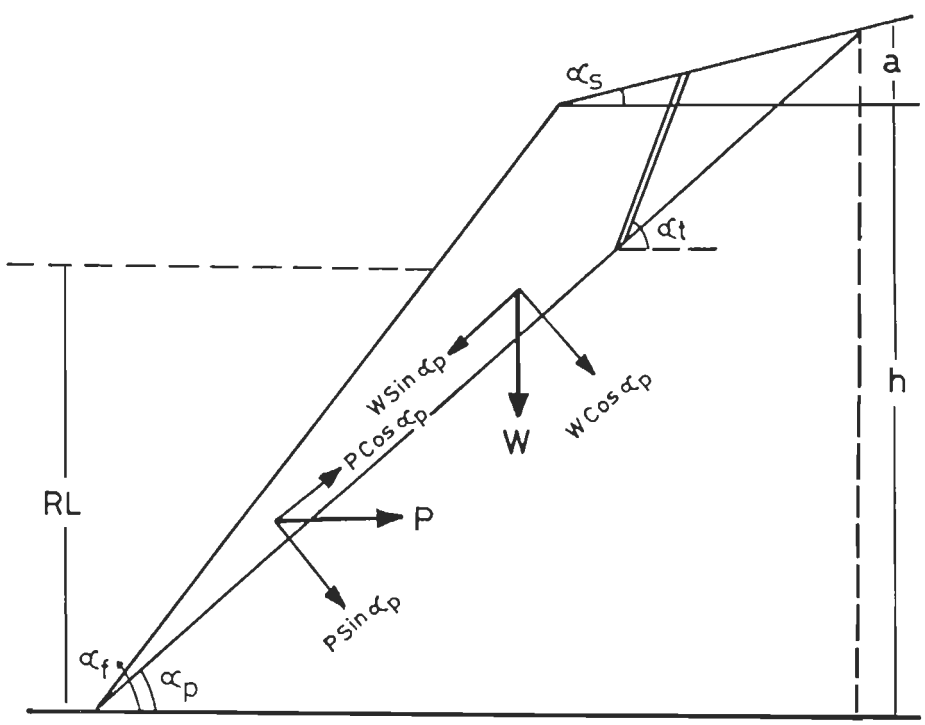

FIG. 5.6 RESOLUTION OF FORCE 'P' EXERTED ON THE FAILURE PLANE BY THE RESERVOIR WATER.

Thus, the following equation is obtained for calculating the factor of safety under static condition

$$F = \frac{CA + (W*Cos\alpha_p - U - V*Sin\alpha_p + P*Sin\alpha_p)* Tan\phi}{W*Sin\alpha_p + V*Cos\alpha_p - P*Cos\alpha_p} \quad \ldots 5.2$$

The Factor of Safety can also be calculated for dynamic condition by the following equation

$$F = \frac{CA + [W(Cos\alpha_p - \alpha*Sin\alpha_p) - U - V*Sin\alpha_p + P*Sin\alpha_p]*Tan\phi}{W(Sin\alpha_p + \alpha*Cos\alpha_p) + V*Cos\alpha_p - P*Cos\alpha_p} \quad \ldots 5.3$$

where P is the water pressure. Other symbols used in eq.5.2 & 5.3 have already been discussed in Chapter III.

In the reservoir area, as indicated in the previous section, seven slopes have been identified as kinematically unstable for plane mode of failure. For the stability analysis, the values of angle of internal friction have been obtained by Rock Mass rating (RMR). But, the values of cohesion have been obtained by back analysis of failed slopes in the same rock in the adjoining localities, where the plane failure has been identified along the same critical discontinuity. The geometry and other parameters of failed slopes used to calculate the cohesion values by back analysis are given in Table 5.5.

TABLE 5.5 GEOMETRY AND OTHER PARAMETERS OF FAILED SLOPES USED IN BACK ANALYSIS

Slope Section No.	Geometrical Parameters							γ T/m^3	ϕ Deg	C T/m^2
	α_f Deg	α_p Deg	α_s Deg	α_t Deg	H m	Z_L m	Z_W m			
KL1A	75	63	0	90	30	8.10	4.05	2.72	35	6.81
KL13A	70	50	10	70	10	4.20	2.1	2.50	35	4.68
KL15A	65	45	10	72	30	15.78	7.89	2.60	35	14.6
KR3A1	70	38	5	72	20	13.24	6.62	2.50	25	10.1
KR15B	70	42	5	80	10	5.35	2.67	2.60	35	3.00
KR30A	55	40	0	54	50	29.80	14.9	2.80	35	6.70
Factor of Safety = 1, Earthquake Horizontal Acc. = 0.15, Unit Wt. of Water = 1 T/m^3										

α_f = Slope face angle	Z_L = Depth of tension crack
α_p = Failure plane inclination	Z_W = Depth of water in tension crack
α_s = Upper slope angle	γ = Unit weight of rock
α_t = Tension crack angle	ϕ = Angle of internal friction
H = Total height of failed slope	C = Cohesion

Factor of Safety of Critical Slopes Having Plane Mode of Failure

The factors of safety of critical slopes have been determined for existing, as well as, for reservoir impoundment conditions. The factors of safety have also been determined for static and dynamic conditions. The effect of water in tension crack has also been taken into consideration.

Slope Section KL1A

This slope is located about 1.5 km upstream of dam site. The rocks exposed on this slope section are quartizites with minor slate bands. The bedding in general dips at 60°-65°, in Southwesterly direction. The slope is very steep and the slope direction is also Southwesterly. The distress due to instability of the slope is visibly noticed in the form of tension cracks on the slope. The calculated factor of safety is given in Table 5.6.

Slope Section KL15A & KL15D

These two sub-slope sections form the part of KL15 slope which is located on left bank, about 20 km upstream of dam site. The limestone of Bohar Formation is exposed on this slope section. The beds dip in Northeasterly direction and are traversed by four sets of joints (Fig.5.7). The factor of safety, as calculated for both the sections, separately, are given in Table 5.6.

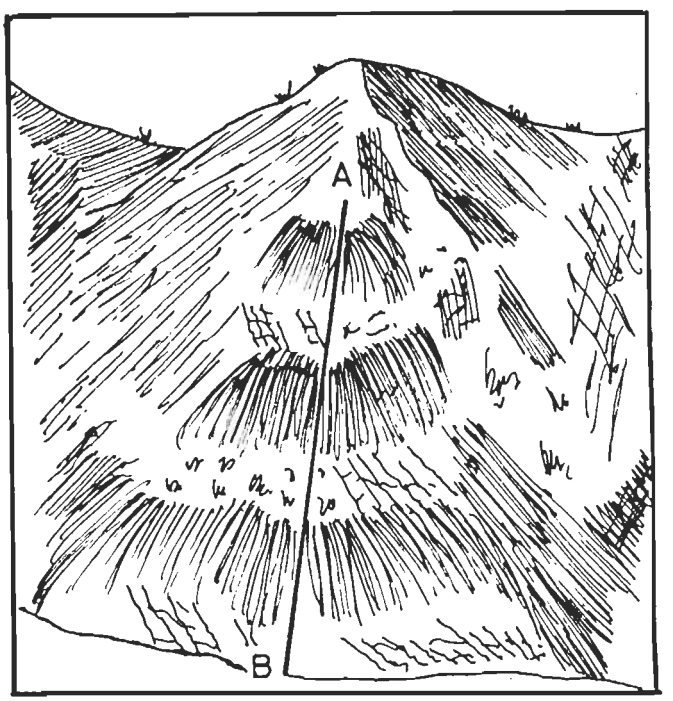

FIG. 5.7 A SKETCH OF KL15 SLOPE

Slope Section KR3A1

This slope section is located near Sarog village, about 6 km upstream of dam site (Fig.5.8). Slates of the Simla Group are exposed over this slope. The beds are dipping in Northeasterly direction and are traversed by four sets of joints. The calculated factor of safety for this slope section is given in Table 5.6.

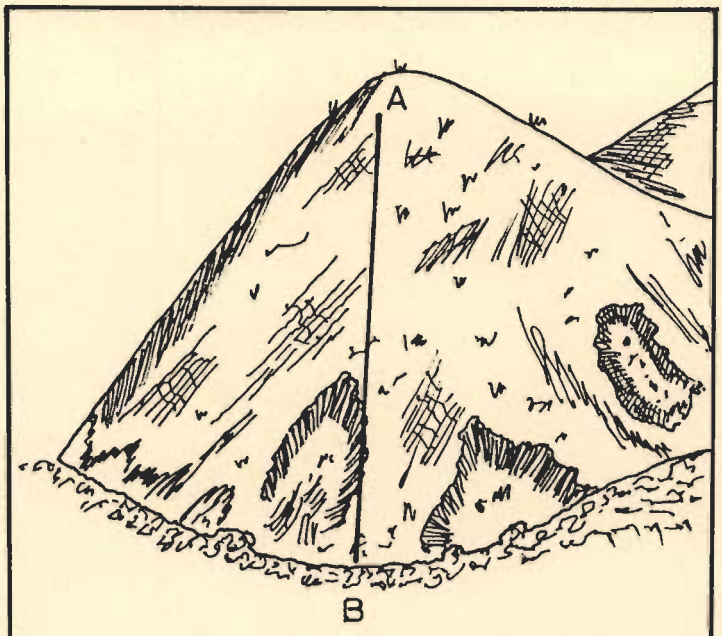

FIG. 5.8 A SKETCH OF KR3A SLOPE

Slope Section KL13A

The slope section is located on left bank about 15 km upstream of dam site. The quartzitic slates are exposed on this slope section. The bedding in general dips at 50°-55° in Southwesterly direction. The slope direction is also Southwesterly. Road construction has induced slope failure in the top portion of the slope section. The beds are dipping towards valley (Plate 5.1). Factors of safety as calculated for different conditions are given in Table5.6.

Slope Section KR15B

The slope section is located near Minas village, 20 km upstream of dam site (Plate 5.2). Massive limestone of the Ambota Formation is exposed on this slope section. The slope in general is dipping towards Northeasterly direction. The factor of safety, as calculated for different conditions are given in Table 5.6.

Slope Section KR30A

This slope section is located near Bagliya village, about 40 km of dam site (Plate 5.3). Quartzite of the Atoll Formation is exposed on this slope section. The slope, in general, is

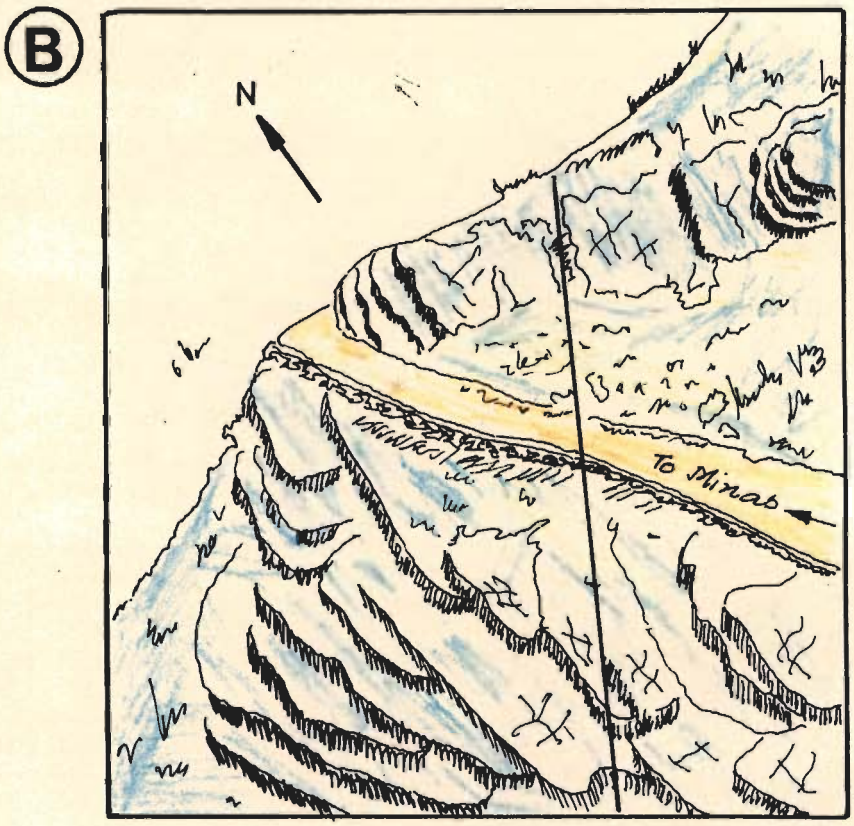

PLATE 5.1 A - PART OF SLOPE SECTION KL13A FAILED ALONG KWANU MINAS ROAD AT 14 KM MILESTONE
B - SKETCH OF KL13A SLOPE SECTION

dipping in Southeasterly direction (Fig.5.9).The factor of safety for different conditions is given in Table 5.6.

TABLE 5.6 FACTOR OF SAFETY OF SLOPES HAVING PLANE MODE OF FAILURE IN RESERVOIR RIM AREA

Input Data Sheet										
Slope Section	Geometrical Parameters						ϕ	C	γ	α
	α_f/β_f	α_p/β_p	α_s/β_s	α_t	H	RL				
KL1A	70/205	63/209	0	90	105	105	35	6.8	2.7	0.15
KL13A	60/223	50/220	30/223	72	104	104	35	4.6	2.5	0.15
KL15A	59/292	46/312	10/292	72	237	60	35	14.6	2.6	0.15
KL15D	55/292	46/312	5/292	72	140	0	35	14.6	2.6	0.15
KR3A1	48/29	38/22	10/29	72	177	0	25	10.1	2.5	0.15
KR15B	50/146	42/132	10/146	80	192	60	35	3.0	2.6	0.15
KR30A	50/128	40/140	20/128	54	252	60	35	6.7	2.8	0.15

α_f = Slope face angle (deg)
β_f = Direction of slope face inclination (deg)
α_p = Failure plane angle (deg)
β_p = Direction of failure plane inclination (deg)
α_s = Upper slope angle (deg)
β_s = Direction of upper slope inclination (deg)
α_t = Tension crack angle (deg)

H = Height of the slope (m)
RL = Height of reservoir standing water (m)
ϕ = Angle of internal friction (deg)
C = Cohesion (T/m^2)
γ = Unit weight of the rock (T/m^3)
α = Earthquake horizontal acceleration

Slope Section	FACTOR OF SAFETY											
	Static Condition						Dynamic Condition					
	Without Reservoir Water			With Reservoir Water			Without Reservoir Water			With Reservoir Water		
	A	B	C	A	B	C	A	B	C	A	B	C
KL1A	0.37	0.56	0.69	9.21	16.1	24.5	0.30	0.45	0.58	6.22	9.80	11.3
KL13A	0.35	0.52	0.65	12.3	35.1	41.3	0.20	0.37	0.49	4.91	7.61	9.60
KL15A	0.39	0.64	0.83	0.70	1.00	1.30	0.20	0.47	0.63	0.50	0.78	1.00
KL15D	0.67	0.91	1.10	0.67	0.90	1.10	0.50	0.70	0.87	0.51	0.70	0.80
KR3A1	0.48	0.66	0.80	0.48	0.60	0.80	0.30	0.50	0.61	0.36	0.50	0.60
KR15B	0.51	0.69	0.84	0.95	1.20	1.40	0.30	0.50	0.63	0.67	0.87	1.00
KR30A	0.45	0.69	0.87	0.69	1.03	1.28	0.31	0.50	0.65	0.48	0.74	0.90

A - Tension crack is completely filled with water
B - Tension crack is half filled with water
C - Tension crack is dry

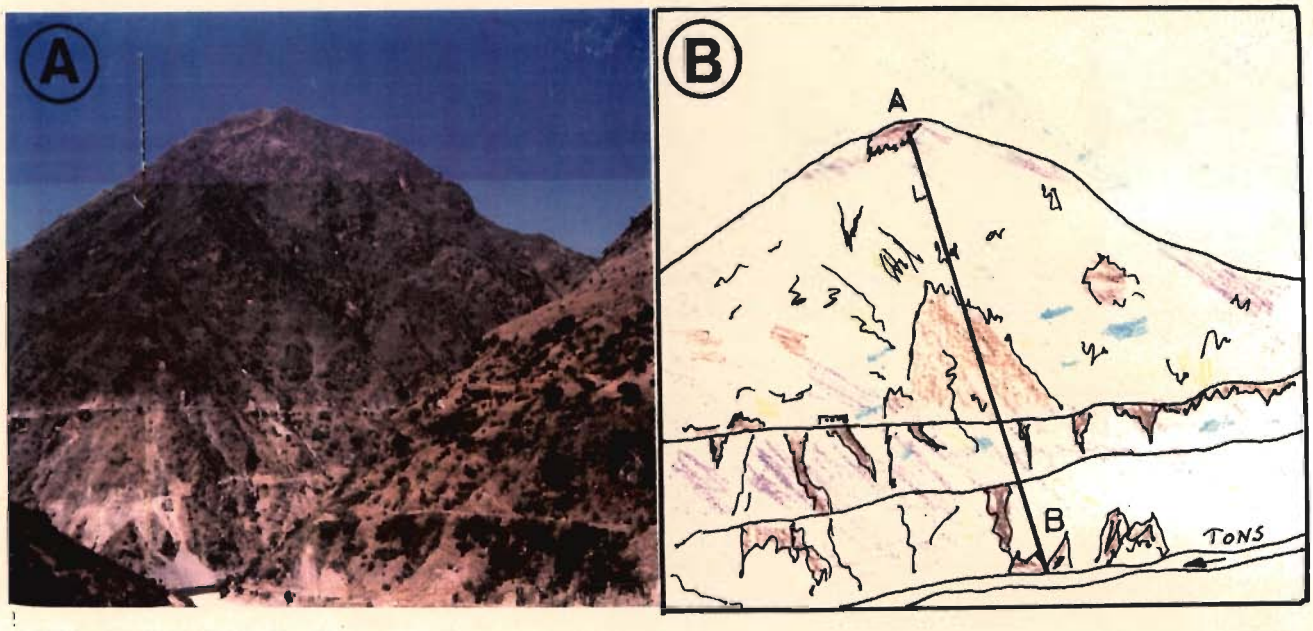

PLATE 5.2 A - A VIEW OF THE SLOPE KR15
B - SCHEMATIC VIEW OF THE SLOPE

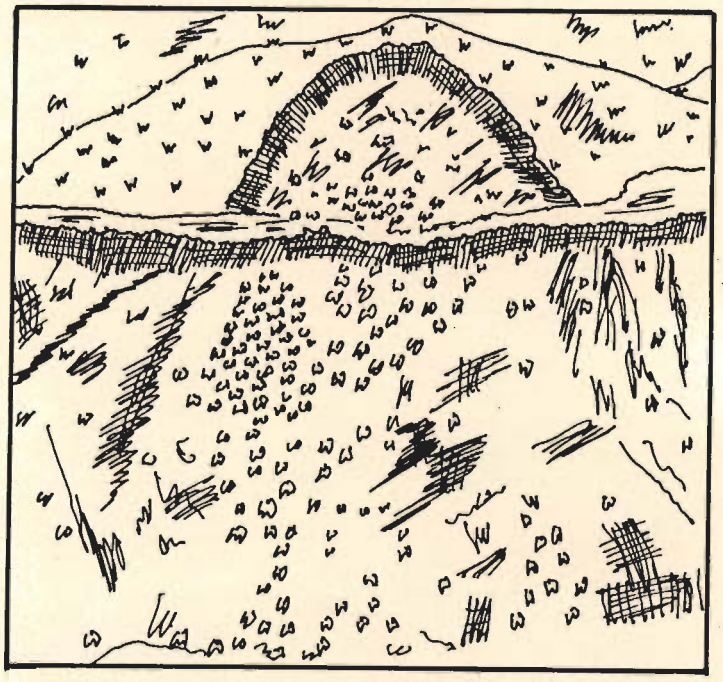

FIG. 5.9 A SKETCH OF KR30A SLOPE

PLATE 5.3 A PART OF KR30A SLOPE SECTION FAILED ALONG ATAL TIUNI ROAD

Discussion

Stability of the Slopes Without Reservoir Water Level

In the present analysis, the factor of safety has been obtained for conditions dry, half -filled and fully-filled tension crack. However, during rains the seepage water may be guided through inter-connected joints present in the rocks. Hence, it is reasonable to presume the slopes to have half filled tension crack, as the adverse condition (AC). Further, if an earthquake occurs during rains, it is anticipated that the slopes at the most may have an anticipated adverse condition (AAC) of half filled tension crack, in addition to earthquake loading. These conditions have been assumed when there is no water impoundment in the reservoir. A perusal of Table 5.6 showing results of plane failure analysis indicates the following.

All the slopes having plane mode of failure are unstable for dry, as well as, other anticipated conditions. Only slope KL15D under static and dry conditions has got a factor of safety very close to unity (1.1).

Stability of the Slopes with Reservoir Water Level

After the impoundment of reservoir, the slopes in the rim area would be submerged upto the maximum reservoir level. A lateral force due to the standing water will be exerted on the slopes and, thereby, resist the sliding of the slopes. The factors of safety calculated for reservoir impoundment conditions have been given in Table 5.6. It has been noticed that the factors of safety of all the slopes have improved remarkably, when they are submerged in reservoir water (Fig.5.10). However, the slope sections KL15D and KR3A1 are located above the maximum reservoir level.

It may be noted that all the slopes are stable in static condition. However, for dynamic condition, slope section KL15A, KR15B and KR30A become unstable.

Hence, it may be safely concluded that the slopes in the reservoir area having plane mode of failure are unstable in the adverse conditions. After reservoir impoundment, these slopes would be stabilised. But, under earthquake loading, some of these slopes would be unstable, even after the reservoir impoundment.

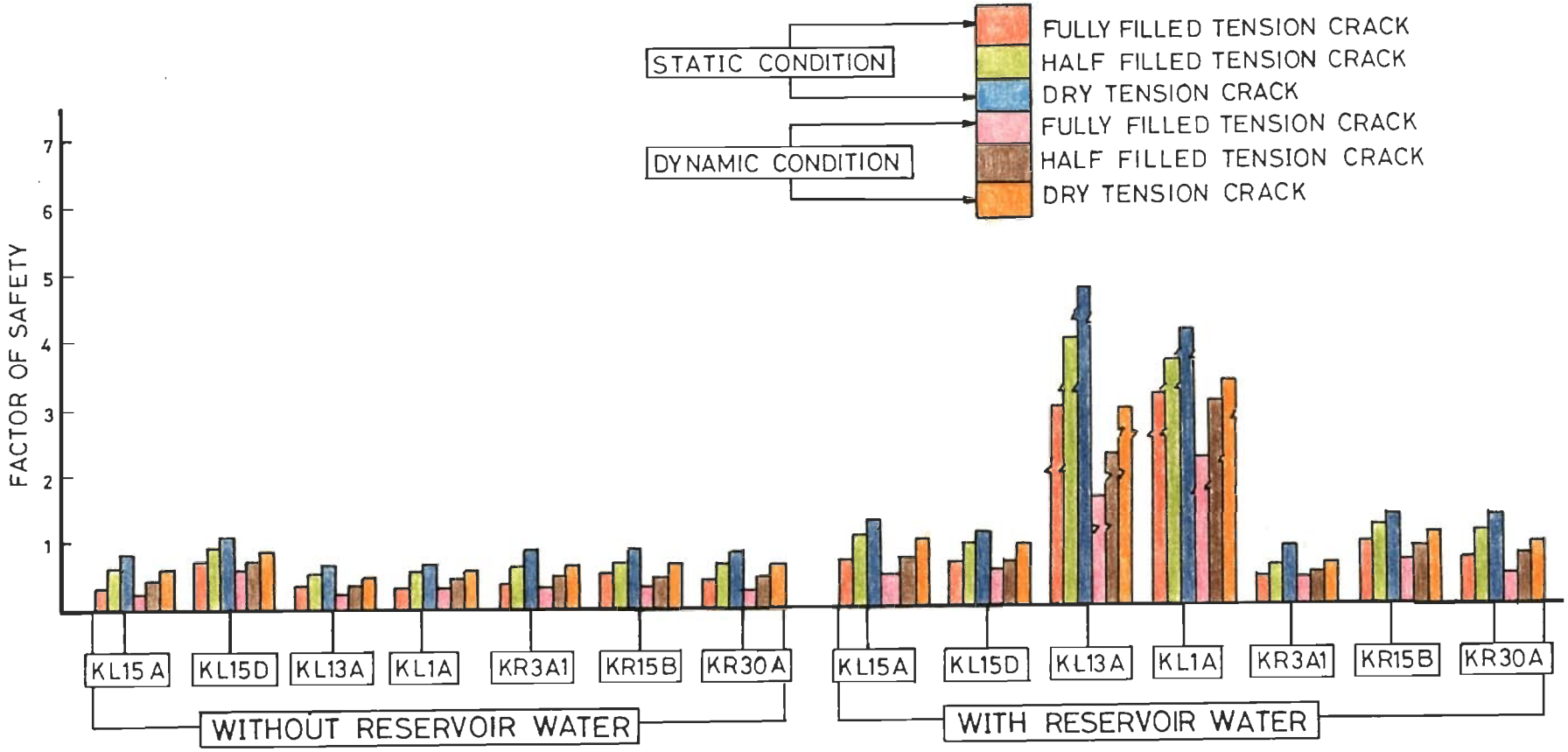

FIG. 5.10 'FACTOR OF SAFETY' OF SLOPES HAVING PLANE MODE OF FAILURE IN THE RESERVOIR AREA.

5.3.3 WEDGE FAILURE ANALYSIS

The slopes having wedge mode of failure have been analysed for existing natural as well as for the water impoundment conditions. The analysis has been carried out in dry, wet and dynamic conditions. To calculate the factors of safety of critical slopes having wedge mode of failure, the program ROSS has been used. This program can calculate factor of safety only for natural conditions (without reservoir impoundments).

For calculating the factor of safety under reservoir impoundment conditions, the formula for wedge mode of failure has been suitably modified, as below:

Stability of Slopes Having Wedge Mode of Failure, Submerged in Standing Water.

The `Factor of Safety' can be defined as the ratio of the total force available to resist sliding to the total force tending to induce sliding. In the present analysis, the forces which are being produced by the reservoir standing water on the planes of a wedge have been incorporated and, subsequently, the equation to calculate factor of safety have been derived.

Forces Due to Reservoir Standing Water

Let `P' be the force due to water pressure acting horizontally on the wedge. PA and PB are the components of force `P' acting perpendicularly on plane `A' and Plane `B' of wedge respectively (Fig.5.11).

Let P_A is represented by ON and P_B by OM, Angles NOC and COM be represented by angles β_1 and β_2 respectively.

Where $\beta_1 = 90-(\alpha_a - \alpha_i)$ ... 5.4

and $\beta_2 = 90-(\alpha_i - \alpha_b)$ ... 5.5

α_a and α_b are the dip directions of plane A and B of the wedge

α_i is the dip direction of line of intersection of plane A and B of the wedge

Further, CM and NC are drawn parallel to ON and OM respectively. Thus, the required component of `P' are OM and ON.

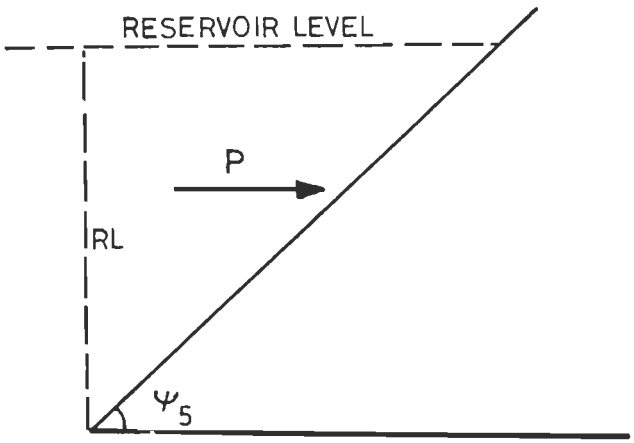

WATER PRESSURE EXERTED ON WEDGE BY RESERVOIR STANDING WATER

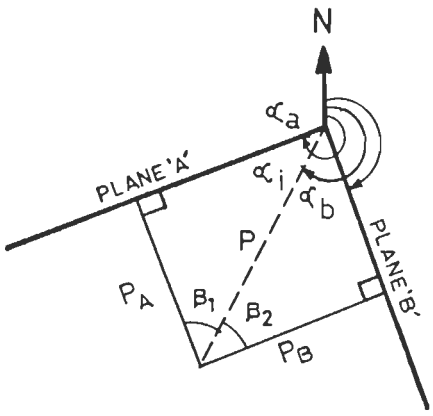

DIFFERENT ANGLES INVOLVED IN THE RESOLUTION OF FORCE 'P'

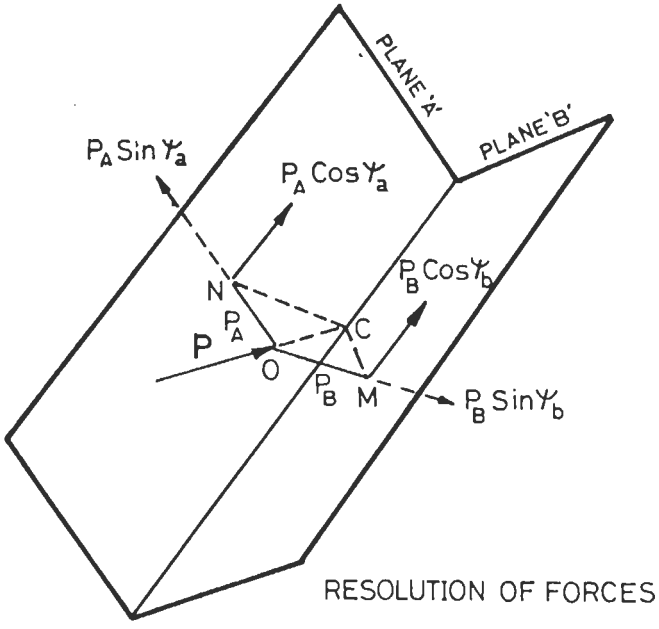

RESOLUTION OF FORCES

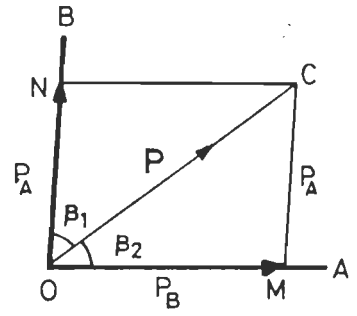

DIFFERENT FORCE VECTORS

FIG. 5.11 FORCES DUE TO WATER PRESSURE EXERTED ON THE WEDGE SUBMERGED IN RESERVOIR

Since, MC and ON are parallel, we have

$$OCM = \beta_1$$

$$\text{also, } OMC = 180° - CMA = 180° - (\beta_2 - \beta_1) \quad \text{(Fig.5.11)}$$

Since , the sides of the triangle OMC are proportional to the sines of opposite angles, we have,

$$OM/\sin OCM = MC/\sin MOC = OC/\sin OMC$$
$$\text{or } OM/\sin \beta_1 = MC/\sin \beta_2 = P/\sin(\beta_1+\beta_2)$$
$$\text{or} \quad OM = P^*\sin \beta_1/\sin(\beta 1+\beta 2)$$
$$\text{and} \quad MC = P^*\sin \beta_2/\sin(\beta 1+\beta 2)$$

Therefore, pressure exerted on Plane A of the wedge would be

$$P_A = P^*\sin \beta_2/\sin(\beta 1+\beta 2) \quad \ldots 5.6$$

and on Plane B

$$P_B = P^*\sin \beta_1/\sin(\beta 1+\beta 2) \quad \ldots 5.7$$

Further, the resolved components of P_A along Plane A will be

$$P_A \cos \Psi_a \text{ and } P_A \sin \Psi_a$$

Similarly, components resolved along Plane B will be:

$$P_B \cos \Psi_a \text{ and } P_B \sin \Psi_b$$

Where Ψ_a & Ψ_b are the dip angles of Plane A & B respectively.

Determination of Water Pressure 'P'

Let `P' be the pressure generated by the standing water column of reservoir of depth RL. It is assumed that this pressure `P' will be exerted along the line of intersection of the planes forming the wedge (Fig.5.11). If the line of intersection dips at an angle, then this water pressure `P' would be:

$$P = \tfrac{1}{2}\, \gamma_w\, RL^2 \operatorname{cosec}^2 \Psi_5 \quad \ldots 5.8$$
where, γ_w is the density of water

Equation For Factor of Safety

Hoek and Bray (1977) gave an analytical solution for wedge failure analysis. This approach accounts for those slopes only in which they are not subjected to any external force. The factor of safety as given in analytical solution of Hoek & Bray (1977) is:

$$F = \frac{C_A{*}A_A + C_B{*}A_B + (q{*}W + r{*}V - U_A){*}\tan\phi_A + (x{*}W + y{*}V - U_B){*}\tan\phi_B}{m_{W.5}{*}W + m_{V.5}{*}V} \quad \ldots 5.9$$

where,

$q = (m_{na.nb}{*}m_{W.nb} - m_{W.na})/(1-m^2_{na.nb})$
$r = (m_{na.nb}{*}m_{V.nb} - m_{V.na})/(1-m^2_{na.nb})$
$x = (m_{na.nb}{*}m_{W.na} - m_{W.nb})/(1-m^2_{na.nb})$
$y = (m_{na.nb}{*}m_{V.na} - m_{V.nb})/(1-m^2_{na.nb})$

$m_{na.nb} = \sin\Psi_a * \sin\Psi_b * \cos(\alpha_a-\alpha_b) + \cos\Psi_a * \cos\Psi_b$
$m_{W.na} = -\cos\Psi_a$, $m_{W.nb} = -\cos\Psi_b$, $m_{V.na} = \cos\Psi_a$
$m_{V.nb} = \cos\Psi_b$, $m_{W.5} = \sin\Psi_5$, $m_{V.5} = -\sin\Psi_5$

Also, W = Weight of the wedge
U_A & U_B = Uplift water forces on plane A & B
A_A & A_B = Area of plane A & B
C_A & C_B = Cohesion of plane A & B
ϕ_A & ϕ_B = Angle of Internal Friction of plane A & B

In the present approach the resolved components of 'P' are taken into account and the equation, given by Hoek & Bray (1977) have been modified. Thus, by using the above derived equations (Eq nos. 5.6 to 5.8), equation for calculation of factor of safety has been derived.

$$F = \frac{C_A{*}A_A + C_B{*}A_B + (q{*}W + r{*}V + \mathbf{t{*}P} - U_A){*}\tan\phi_A + (x{*}W + y{*}V + \mathbf{d.P} - U_B){*}\tan\phi_B}{m_{W.5}{*}W + m_{V.5}{*}V - \mathbf{m_{p.a}{*}P} - \mathbf{m_{p.b}{*}P}} \quad \ldots 5.10$$

where,

$P = \frac{1}{2}\gamma_w RL^2 \operatorname{cosec}^2\Psi_5$
$t = \cos(\alpha_i-\alpha_b){*}\sin\Psi_a/\sin(\alpha_a-\alpha_b)$
$d = \cos(\alpha_a-\alpha_i){*}\sin\Psi_b/\sin(\alpha_a-\alpha_b)$
$m_{p.a} = \cos(\alpha_i-\alpha_b){*}\cos\Psi_a/\sin(\alpha_a-\alpha_b)$
$m_{p.b} = \cos(\alpha_a-\alpha_i){*}\cos\Psi_b/\sin(\alpha_a-\alpha_b)$

The eq. 5.9 has been modified by incorporating the components shown in **bold faces**

Using above equation, the factor of safety of slopes having wedge mode of failure submerged in reservoir standing water has been calculated. Moreover, the factor of safety of slopes for dynamic condition has been calculated by using computer program RWEDGE, in addition to calculate factor of safety for saturated slopes. A brief description of program RWEDGE is given in Annexure II.

The input data required to obtain factor of safety of slopes, having wedge mode of failure, in the reservoir area is given in Table 5.7 while the results are shown in Table 5.8.

Discussion

A perusal of Table 5.8 on the results of wedge failure analysis indicates the following:

Stability Analysis Without Reservoir Water

The slopes having wedge mode of failure are stable in dry condition, even when, they are subjected to earthquake loading, except one slope (KR2A), whose factor of safety is less than unity (0.76). However, when the slopes are one fourth saturated, sections KL19A, KR2A, KR5A and KR21A become unstable even in static condition. Further, from the results, it may be noted that on increasing the saturation of slopes, the instability of the slopes increases.

When the slopes are 50% saturated, all slopes, except KL9B1 and KR9B, become unstable in static, as well as, in dynamic conditions. The anticipated adverse condition (AAC) that could affect the slopes having wedge mode of failure in the reservoir area, may be represented by a combination of 50% saturated slopes with earthquake loading. For these conditions all the slopes, except KL9B1 and KR9B, becomes unstable.

Stability Analysis with Reservoir Standing Water

As discussed in the previous section, the slopes generally show improvement in the factor of safety with reservoir water impoundment. All the slopes attain stability under reservoir impoundment conditions (Fig.5.12) except KR2A section, under dynamic condition. When slopes are saturated to one fourth of their height, all the slopes are stable in static, as well as, in dynamic conditions except slope section KR2A. However, under the anticipated adverse conditions, slope sections KL9B1, KL19A, KR2A,KR20A, KR21A and KR21C become unstable.

Thus, from the above discussion it may be concluded that all the slopes, having wedge modeof failure in the reservoir area are unstable in the natural condition. Only two slopes, namely, KL9B1 and KR9B are stable. But under the anticipated adverse condition, all the slopes except KR9B, would be unstable. Further, after reservoir impoundment, slopes KL9B1, KL19A, KR2A, KR20A, KR21A and KR21C would be unstable.

PLATE 5.4 WEDGE MODE OF FAILURES IN RESERVOIR AREA

TABLE 5.7 INPUT DATA SHEET FOR CRITICAL WEDGE FAILURE ANALYSIS OF THE SLOPES AROUND RESERVOIR

S.No	Slope Section	Plane A	Plane B	Upper Slope	Slope Surface	Friction Angle	Cohesion (T/m^2)		Unit Wt. of Rock	Ht. of the Slope	Ht. of Water above Toe
		α_A/β_A (Deg)	α_B/β_B (Deg)	α_U/β_U (Deg)	α_S/β_S (Deg)	ϕ (Deg)	C_A	C_B	γ (T/m^3)	H (m)	RL (m)
1	KL9B1	N110/42	N240/80	N190/8	N190/50	25	25	20	2.4	333	0
2	KL19A	N142/72	N31/72	N60/10	N60/65	25	25	30	2.8	162	64
3	KR2A	N22/38	N287/84	N20/10	N20/48	25	10	12	2.5	244	200
4	KR5A	N22/38	N287/84	N0/16	N0/40	25	10	12	2.5	119	119
5	KR9B	N102/52	N310/52	N62/11	N62/40	25	20	30	2.5	329	35
6	KR14A	N178/54	N300/64	N195/11	N195/50	36	35	30	2.6	296	144
7	KR14C	N178/54	N300/64	N195/18	N195/48	36	35	30	2.6	281	144
8	KR20A	N200/52	N101/64	N130/15	N130/55	35	35	30	2.6	322	104
9	KR21A	N200/52	N101/64	N135/10	N135/50	38.5	35	30	2.6	177	64
10	KR21C	N200/52	N101/64	N135/10	N135/54	41	36	30	2.8	318	0

TABLE 5.8 FACTOR OF SAFETY OF SLOPES HAVING WEDGE MODE OF FAILURE IN RESERVOIR RIM AREA .

Without Reservoir Water											
S.No	Slope Section	Static Condition					Dynamic Condition				
		Dry	Wet				Dry	Wet			
			25%	50%	75%	100%		25%	50%	75%	100%
1	KL9B1	2.05	1.77	1.49	0.85	0.71	1.56	1.33	1.10	0.63	0.52
2	KL19A	8.06	0.00	0.00	0.00	0.00	6.87	0.00	0.00	0.00	0.00
3	KR2A	1.01	0.83	0.65	0.47	0.05	0.76	1.12	0.90	0.68	0.07
4	KR5A	5.01	0.00	0.00	0.00	0.00	4.02	0.00	0.00	0.00	0.00
5	KR9B	3.22	2.85	2.48	2.12	1.75	2.13	1.87	1.61	1.35	1.09
6	KR14A	3.80	3.14	0.76	0.50	0.32	3.08	2.53	0.58	0.40	0.00
7	KR14C	5.58	1.17	0.63	0.00	0.00	4.50	0.93	0.53	0.00	0.00
8	KR20A	2.73	1.08	0.72	0.00	0.00	2.25	0.86	0.56	0.00	0.00
9	KR21A	11.1	0.00	0.00	0.00	0.00	9.18	0.00	0.00	0.00	0.00
10	KR21C	2.76	2.15	0.85	0.00	0.00	2.26	0.96	0.64	0.00	0.00
With Reservoir Water											
1	KL9B1	2.05	1.77	1.49	0.85	0.71	1.56	1.33	1.10	0.63	0.52
2	KL19A	8.23	2.28	0.00	0.00	0.00	6.99	1.95	0.00	0.00	0.00
3	KR2A	1.09	1.01	1.02	1.03	1.03	0.78	0.76	0.75	0.74	0.73
4	KR5A	7.75	5.47	6.05	6.79	7.75	5.55	4.31	4.64	5.05	5.55
5	KR9B	3.22	2.89	2.57	2.24	1.91	2.13	1.90	1.67	1.43	1.20
6	KR14A	3.91	3.56	3.32	3.06	0.85	3.14	2.88	2.67	2.45	0.65
7	KR14C	6.23	5.56	5.53	5.50	5.47	4.89	4.46	4.41	4.35	4.30
8	KR20A	2.76	2.39	1.02	0.79	0.55	2.26	1.95	0.81	0.61	0.00
9	KR21A	11.3	4.57	0.00	0.00	0.00	9.30	3.80	0.00	0.00	0.00
10	KR21C	2.76	2.15	0.85	0.00	0.00	2.26	0.96	0.64	0.00	0.00

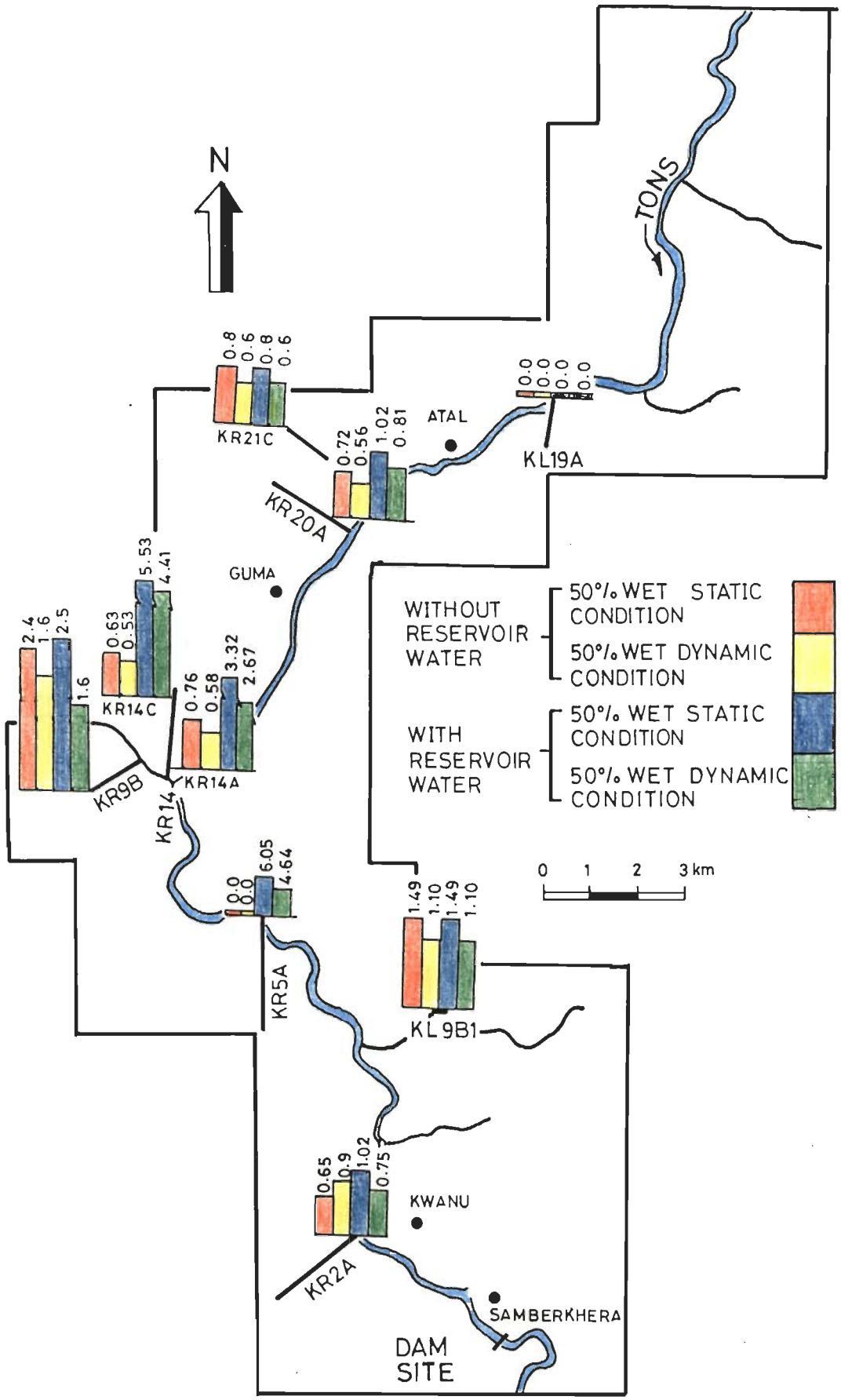

FIG. 5.12 FACTOR OF SAFETY OF SLOPES HAVING WEDGE MODE OF FAILURE IN THE RESERVOIR AREA

5.3.4 ROTATIONAL FAILURE ANALYSIS

Rotational or circular mode of failure are usually found in soils, highly weathered or crushed rocks. In such slope materials, failure occurs along a surface which attains a circular shape. Circular failures are common in rock masses, where the material is so intensely fractured that it may be considered as randomly jointed and isotropic.

In the entire reservoir rim area, the conditions discussed above have been observed to prevail only on four slope sections. They are KR1B,KR2B, KR5A3 and KR6B. The rocks exposed on these slope sections are slates. The Tons thrust, a major tectonic structure, is passing through these slope section, which has resulted into intense jointing and crushing of the exposed rocks. Hence, the stability analysis of these slope sections, have been carried out by computer program "SARC" for rotational mode of failure. A brief description of program SARC is given in Annexure II.

To obtain the representative shear strength values for these slope materials, the computer program BASC has been used. A brief note on BASC program is given in Annexure II.

The computer program `BASC' can analyse any surface profile and determines one of the representative shear strength parameters, cohesion (C) and angle of internal friction (ϕ). For that purpose, a judicially chosen values of angle of internal friction (ϕ) are provided as input to obtain corresponding value of cohesion (C). For the present study, the back analysis of KR2B slope section has been carried out. The shear strength values for KR2B slope section, as determined from back analysis, are taken as the representative values for other slope sections also. This has been done, because the nature and type of the rock material on all the four slopes are same . The input data required by the program to determine the value of Cohesion of KR2B slope is shown in Table 5.9.

The output results, shown in Table 5.9 reveal, that for all values of internal friction, the slip circle is critical. The values of cohesion corresponding to ϕ = 30,35 and 40 are negative, therefore, these values have been neglected. It may be noted that the values of Cohesion corresponding to ϕ = 20 and 25 are 6.9 and 3.0 respectively. However, keeping in view the general condition of the slope material, the value of 25° of angle of internal friction and the corresponding value of cohesion (3 T/m^2) has been considered for the stability analysis.

TABLE 5.9 BACK ANALYSIS FOR SHEAR STRENGTH PARAMETERS OF KR2B SLOPE SECTION

INPUT DATA SHEET			
Parameter	Value	GAMA (T/m^3) = 2.5 BBAR = 0.1 ZWR = 0.0 AH = 0.0 NFS = 1.0 NX = 5.0 DELX = 1.0 ENTX = 0.0	GAMAW (T m^{-3}) = 1.0 ZC (m) = 0.0 RWL (m) = 0.0 AV = 0.0 FS = 1.0 NY = 5.0 DELY = 1.0 ENTY = 0.0
NPHI	5		
PHI (I) I = 1 to NPHI	20,25, 30,35,40		
ROCK (m)	0.0		
XCUT (m)	100		
XHILL (m)	230		
CX,CY (m)	0.5, 146.21		

NPHI = Number of Phi Values
PHI = Angle of Internal Friction
ROCK = Elevation of Hard Strata w.r.t river bed level
XCUT = X-coordinate of a point before which 10 slices should be there for proper accuracy
XHILL = X-coordinate of top of the slope
GAMA = Unit weight of rock/soil
GAMAW = Unit weight of water
BBAR = Pore water pressure/ gama*Av.ht of slices
ZC = Depth of tension crack
ZWR = Depth of water in tension crack/ZC

RWL = Reduced level of reservoir w.r.t. river bed level
AH = Horizontal component of earthquake acceleration
AV = Vertical component of earthquake acceleration
NFS = No. of sets of factor of safety
FS = Factor of safety
NX,NY = No. of center points in X and Y direction (in array)
DELX,DELY = Increment in center in X and Y direction
CX,CY = Coordinates of center of slip circle
ENTX,ENTY = X and Y coordinate of entry point of circle

RESULTS FOR CRITICAL SLIP CIRCLE	
Angle of Internal Friction, ϕ	Cohesion, C
20	6.9
25	3.0
30	-1.0
35	-5.6
40	-10.9

The program SARC identifies the various slip surfaces along which failure may take place. Also, it calculates the radius and center of the slip circle, for which, the factor of safety is

minimum. The factor of safety is computed by using Bishop's equation (1955). The program also computes dynamic displacement utilising correlation given by Lavania et.al (1987). The required input data for the stability analysis of the slopes, having rotational mode of failure, in the reservoir rim area is given in Table 5.10.

TABLE 5.10 INPUT DATA SHEET FOR SLOPES HAVING ROTATIONAL MODE OF FAILURE

Parameter	SLOPE SECTION				
	KR1B	KR2B	KR5A3	KR6B	
N	21	23	20	18	ROCK=0.0, RWL=0.0, XS=0.0 WI=0.0, ZC=0.0, ZWR=0.0, C=3.0, PHI=25, GAMA=2.5, GAMAW=1.0, BBAR=0.0-0.2, AH=0.15, AVR=0.5, EQM=6, NENP=1.0, ENTX=0.0, ENTY=0.0
XEXITI	65	106	70	20	
XEXITL	100	226	150	29	
GAP	10	20	10	5	

N = Number of profile coordinates (<50)
ROCK = Reduced level of hard strata w.r.t. river bed level (m)
RWL = Reduced level of GWT/reservoir water w.r.t river bed level (m)
XS = X-coordinate of point from where surcharge starts (m)
WI = Uniform surcharge intensity (T)
ZC = Depth of tension crack (m)
ZWR = Depth of water in tension crack/ZC
C = Cohesion of soil/rock (T/m^2)
PHI = Angle of internal friction of soil/rock (deg)
GAMA = Unit weight of rock (T/m^3)
GAMAW = Unit weight of water (T/m^3)
AH = Horizontal component of earthquake acceleration
AVR = Vertical component of earthquake acceleration/AH
EQM = Corresponding earthquake magnitude on Richter scale
NENP = Number of entry points of slip circles (<10)
ENTX = X-coordinate of entry point of slip circle (m)
ENTY = Y-coordinate of entry point of slip circle (m)
NOPT = 0, When only minimum factor of safety is required
= 1,when factor of safety of all slip circles is required
NEP = Number of exit points (<50)
= 0,when no individual point is given
XEXITI = X-coordinate of first exit point of slip circle (m)
XEXITL = X-coordinate of last exit point of slip circle (m)
GAP = Horizontal distance between consecutive exit points (m)
XEXIT = X-coordinate of exit point of slip circle (m)

The stability analysis of the slopes having rotational mode of failure, have been carried out for static, as well as, for dynamic conditions. Besides, the analysis has also been carried out for water charged conditions. The results are given in Table 5.11.

TABLE 5.11 RESULTS OF STABILITY ANALYSIS OF SLOPES HAVING ROTATIONAL MODE OF FAILURE

Factor of Safety							
S.No	Slope Section	Static Condition			Dynamic Condition		
		Dry	Wet (BBAR =)		Dry	Wet (BBAR =)	
			0.1	0.2		0.1	0.2
1.	KR1B	1.23	1.11	0.99	0.90 **0.13**	0.81 **3.22**	0.71 **46.2**
2.	KR2B	1.03	0.92	0.81	0.77 **17.9**	0.68 **46.2**	0.59 **46.2**
3.	KR5A3	0.95	0.85	0.74	0.71 **46.2**	0.63 **46.2**	00.54 **46.2**
4.	KR6B	1.28	1.17	1.06	0.90 **0.16**	0.88 **0.36**	0.79 **9.22**
The figures in **Bold Faces represents** the Dynamic Displacement of the Slope							

A perusal of Table 5.11 shows that all the slope sections are stable, in static and dry conditions except KR5A3 section, which has a factor of safety very close to unity. However, with earthquake loading all the slope sections are unstable in dry, as well as, in wet conditions. The probable slip circles for all the four slope sections having minimum factor of safety are shown in Fig. 5.13.

It is reasonable to presume the anticipated adverse conditions to be represented by BBAR = 0.1 with earthquake loading. Under this condition, all the four slope sections are unstable.

5.4 HEIGHT OF WAVE GENERATED IN RESERVOIR DUE TO POSSIBLE LANDSLIDES

Sudden failure of slopes around the reservoir would generate water waves in the reservoir. These waves will propagate in all directions (Fig. 5.14). The distance, upto which these waves would travel depends mainly upon the Kinetic energy involved in it. Other factor, which influence the wave propagation is the shape of the reservoir. The waves generated due to landslide in a sinuously shaped reservoir would dissipate completely, but in a straight, narrow canyon of a funnel shaped reservoir, such waves would travel a longer distance. A sufficiently massive slide from the rim slopes could cause overtopping of a dam, either by wave action, or simply by raising the water surface faster than the Spillway could discharge.

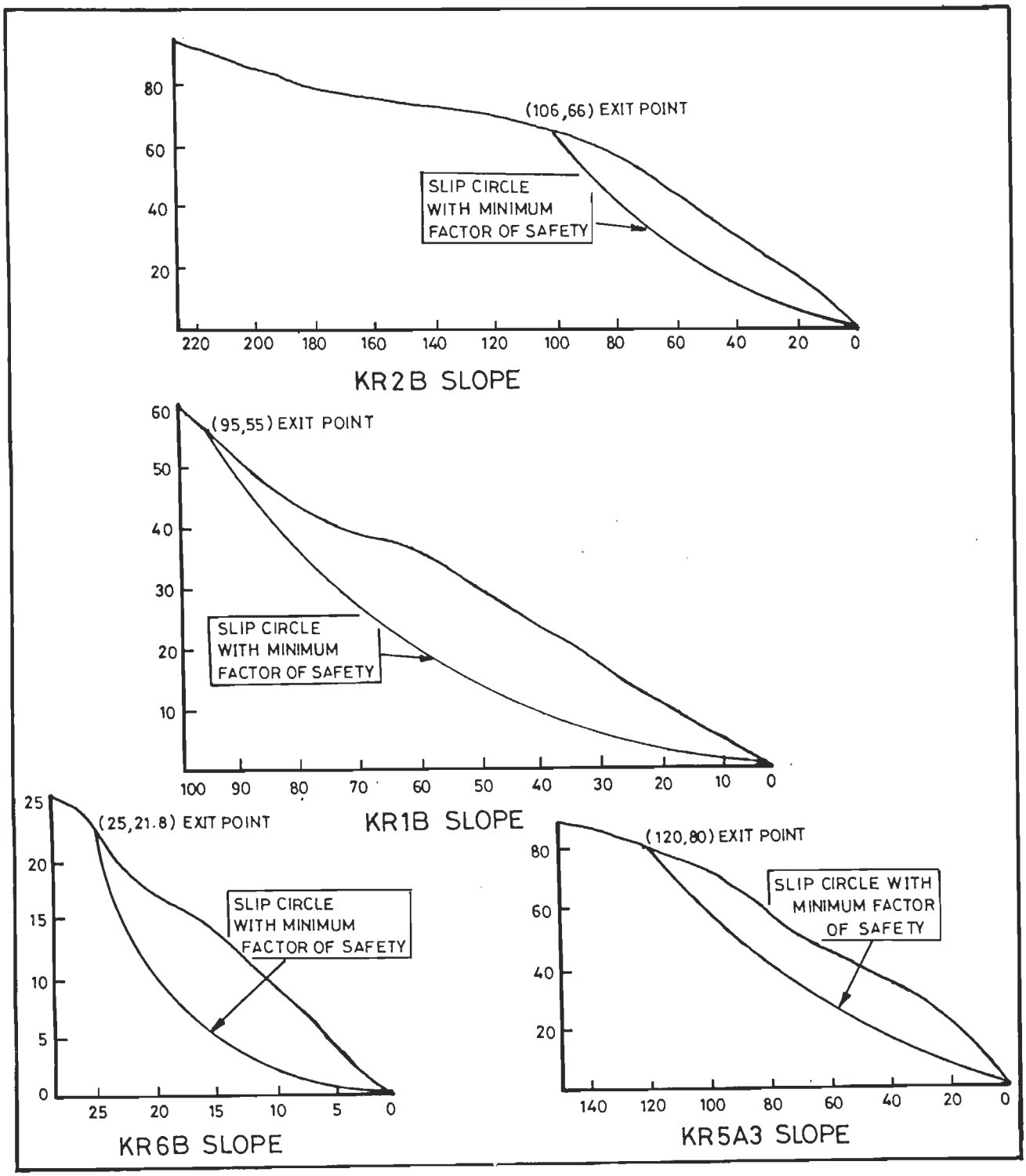

FIG.5.13 CROSS SECTION OF SLOPES HAVING ROTATIONAL MODE OF FAILURE.

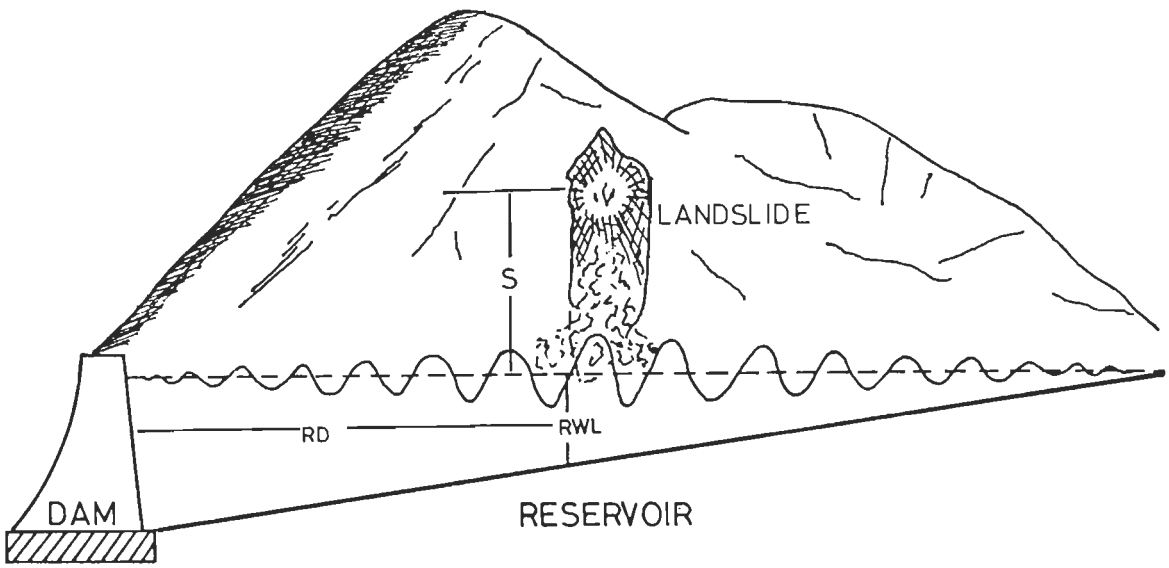

FIG. 5.14 WAVE GENERATION IN RESERVOIR DUE TO LANDSLIDE

In the reservoir area ten slope sections have been identified as critical, and they may fail under the anticipated adverse condition after the reservoir impoundment (Fig. 5.15). In the present analysis, an attempt has been made to calculate the wave height generated by the possible slides in the reservoir area. Besides, the kinetic energy involved in a possible slide has also been computed. For this purpose, Computer Program `WAVE' has been used. This program, not only calculates the maximum wave height at the impact point, but it also calculates the height of the wave near to the dam body. A brief description of WAVE program is given in Annexure II. The program WAVE is applicable to those slopes only which are submerged partially or completely in the reservoir water. The input data required to calculate the wave height, generated by the possible slides in the reservoir rim area, is shown in Table 5.12 and the results are given in Table 5.13.

A perusal of Table 5.13 reveals that the maximum wave height, due to possible slides for the reservoir rim slope, varies from 0.42 m to as high as 20.3 m. Moreover, waves generated by all the possible slides would die out before they reach the dam body. Only the wave generated

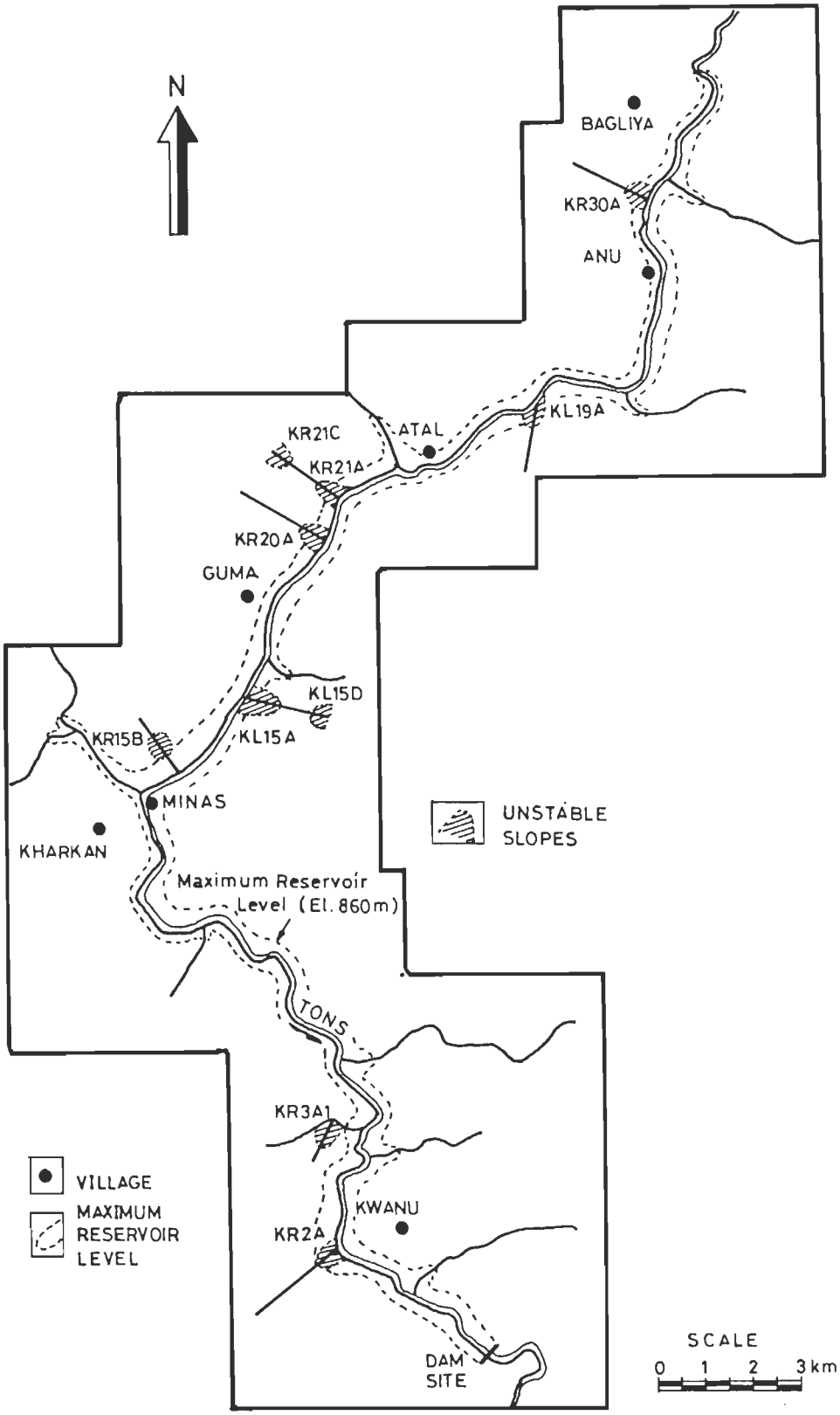

FIG. 5.15 UNSTABLE SLOPES IN THE RESERVOIR AREA (After reservoir impoundment-under anticipated adverse conditions)

TABLE 5.12 INPUT DATA SHEET TO CALCULATE THE WAVE HEIGHT GENERATED BY THE POSSIBLE SLIDES IN THE RESERVOIR AREA

Acceleration due to gravity = 9.8 m/s^2
Unit weight of water = 1 T/m^2

Slope Section	FOS_r	ϕ_r	W	H	α_L	S	RL	D
KL15A	0.18	17.5	27665.49	237	59	185.24	60	22800
KR15B	0.26	17.5	15537.69	192	50	167.92	60	20700
KR30A	0.26	17.5	47723.30	252	50	220.40	60	40000
KL19A	0.10	12.5	8627.00	162	65	119.76	64	27000
KR2A	0.19	12.5	28100380	244	48	219.98	200	4650
KR20A	0.22	17.5	715503.0	322	55	263.36	104	27150
KR21A	0.28	19.0	12205.00	177	50	154.80	64	28050

FOS_r=Residual factor of safety
ϕ_r=Residual angle of friction (deg)
W=Weight of the wedge (tons)
H=Height of the slope (m)
α_L=Dip of Landslide face (deg)
S=Distance of slope movement (deg)
RL=Height of water above toe (m)
D=Distance of slope from dam (m)

TABLE 5.13 RESULTS SHOWING HEIGHT OF WAVE AND KINETIC ENERGY OF POSSIBLE LANDSLIDE IN THE RESERVOIR AREA

Slope Section	Maximum Wave Height Due to Landslide (mtr)	Height of Wave (m)	At Distance from the Dam (m)	Maximum Velocity of Landslide (m/s)	Kinetic Energy of Landslide
KL15A	1.34	0.01	22800	50.25	0.27
KL15B	0.71	0.008	20700	43.08	0.11
KR30A	1.93	0.01	40000	49.35	0.45
KL19A	0.42	0.004	27000	43.69	0.05
KR2A	20.30	3.49	4650	50.66	2.29
KR20A	5.96	0.09	27150	57.43	1.02
KR21A	0.49	0.004	28050	40.67	0.06

by KR2A slope would reach the dam body with a height of 3.49 m . The maximum velocity by which the debris and the rock material of these possible slides would fall into the reservoir

varies from 40.67 m/s to 57.43 m/s.

However, the Kinetic energy of these slides varies from 0.05 to 2.29. Hence, it can safety be concluded that the waves generated by the slopes, identified to be critical in the reservoir rim area, would not endanger the safety of the dam. Only slope KR2A, if failed, would generate 20m high wave at the impact area, which would close to a height of 3.49 meters near to the dam body. In view of the fact that the free board of 8m is already provided in the dam design, the waves generated will have no impact on the stability of the dam.

CHAPTER VI

CONCLUSIONS

The Kishau dam project envisages the construction of a 236m high concrete gravity dam, across the Tons river, near village Samberkhera, (30° 39' 39" : 77° 46' 55"), and a surface power house with an installed capacity of 600 MW of peak power. The dam is planned to be founded over the quartzitic slates and quartzites of Simla Group. The Engineering geological appraisal of Kishau dam project has been carried out under three broad heads. The findings of the present research study are summarised below:

6.1 ENGINEERING GEOLOGICAL EVALUATION OF FOUNDATION CONDITION

1. In the river section of the foundation of the dam, quartzitic slates with interbands of purple quartzites are present. Purple quartzites and white quartzites are present on the dam abutment.

2. The rocks at the dam area are folded into an upright asymmetrical anticline and the dam base would rest on the hinge zone of this fold.

3. The Tons thrust is present on the right abutment ridge, dipping 15° to 25° in Southwesterly direction into the adjoining Meera river valley. The Tons thrust is present between El. 845 m to 850 m, close to the dam axis . The thrust, close to the dam axis,

would be submerged under the maximum reservoir level of 860 m.

4. The lateral depth of weathering ranges from 20 to 34 m on the left abutment and this range varies from 16 to 24 m on the right abutment. However, the rocks on the right abutment are badly sheared upto a lateral depth of 20 to 45 m along the drift. Hence, the lateral depth of stripping for left and right abutments has been estimated to be 22 to 34m and 25 to 45 m, respectively.

5. The fluvial overburden in the river bed section ranges from 3.65 m to 11.88 m and the bed rock is available at El. 635.2 m. In the river bed section the alternating bands of grey quartzitic slate and purple quartzite are present. The foundation rocks are highly fractured due to folding.

6. On the basis of limited water pressure test data, it is estimated that the foundation rocks are semipervious to pervious in nature.

7. The stability analysis of abutments has revealed that the left abutment slope is stable while the right abutment slope is kinematically unstable for plane mode of failure. The plane failure analysis for right abutment slope has been carried out by modifying the Hoek& Bray (1981) analytical technique where the effects of inclined upper slope surface and tension crack have been incorporated. The analysis shows that the right abutment slope is unstable for anticipated adverse conditions i.e. tension crack half filled with water and earthquake loading.

8. The few shear zones, ranging in thickness 0.5 m to 2 m may get exposed at the foundation grade during foundation stripping. In order to improve the foundation strength, control the seepage and to make the abutment slopes more stable the following foundation treatments are suggested:

i) Based on the stability analysis a safe cut slope design for both the abutments have been proposed. Besides, the abutment slopes should be cut in terraced design by maintaining 5 m wide benches. To avoid any local failures near the humps of individual benches, it is suggested to provide two rows of grouted anchors to a depth of 5 m, at about 45° into the slope at 3 m centre to centre.

ii) The shear zones, likely to be encountered at the foundation level during the foundation stripping should be removed by dental treatment, using the Shasta's formula.

iii) A grout curtain upto a depth of 100 m is necessary to control the seepage in the heel portion of the dam. This grout curtain shall increase the path of percolation of seepage water. Besides, in order to intercept the seepage water which may find its way through the grout curtain, two to three rows of drainage holes, drilled from the drainage gallery, should also be provided.

iv) To improve the physical properties of the foundation rocks and to make the foundation rocks monolithic, consolidation grouting is suggested. In the river bed area it should be carried out to a depth of 15 m and on abutments to a depth of 5 to 10 m. Besides, an extension of consolidation grouting upto 57 m beyond the heel and 76 m beyond the toe of the dam should also be carried out.

v) To control the seepage through the Tons thrust, a 0.75 m wide and 150 m long diaphragm is proposed. This diaphragm is proposed to be founded over the competent white quartzite and the top of the diaphragm will be extended upto El. 860 m.

6.2 ENGINEERING GEOLOGICAL EVALUATION OF POWER HOUSE SITE

For housing the power units, a terrace (22 x 70 m) has to be created by excavating the adjoining hill slopes. For that purpose, an engineering geological evaluation of the site has been carried out, which includes the following:

1. The stability analysis of the slopes adjoining the power house indicates that two slopes, SR1A and SR2A, have been identified as critical on the basis of friction only case analysis.

2. Both these slopes indicate that they are possibly kinematically unstable for plane mode of failure. Hence the plane failure analysis of these slopes has been carried out for static and dynamic conditions.

3. The detailed analysis using the limit equilibrium method indicates that the factor of safety for SR1A and SR2A slope sections are 3.71 and 2.26 respectively, for possible

adverse conditions (half-filled tension crack), whereas for anticipated adverse conditions (half filled tension crack with earthquake loading) the FOS for SR1A and SR2A are 3.06 and 1.83 respectively.

4. From the friction only case technique, a safe cut slope angle of 34° has been found to be adequate for a stable cut slope. Hence it is proposed that the slopes must be excavated in a terraced design by maintaining an overall cut slope angle of 34°. A height of 4 m and width of 2 m have been proposed for individual benches.

5. Although the cut slopes would remain stable with the proposed cut slope design, the slopes may be subjected to continuous vibrations during the operation of power house which may tend to destabilise the slopes. Therefore, some suitable additional stability measures have been suggested.

i) Two layers of shotcreting on a chainlink wiremesh, leaving 25 percent surface area for drainage has been suggested for preventing surface erosion and to improve the stability condition.

ii) Perfo-anchors of 6 m length at 3 m spacing in staggered fashion may be provided.

iii) Lined catch water drains towards the hill side end of benches with proper gradients may be provided.

6. Though the site will be stable with the proposed cut slope design, the site incidently falls on a location where a minor perennial Jamar stream flows in the middle of the site. One of the most important problems anticipated at this site is that a safe and permanent diversion has to be provided for Jamar stream.

7. The Jamar stream course can be avoided completely by shifting the power house site towards East in the down stream direction by about 75 m.

8. At this site, the slopes are gentle and hence the quantum of excavation is less for creating the terrace.

9. The stability analysis of the slopes adjoining the alternative site indicates that it is stable slope. The cut slope design and other remedial measures suggested for the

earlier site are also applicable for this site which has minimum engineering geological problems.

6.3 STABILITY ANALYSIS OF HILL SLOPES IN THE RESERVOIR AREA

1. The reservoir area has been mapped on 1:15,000 scale. The rocks belonging to Dharagad Group, Deoban Group, Simla Group and Jaunsar Group are exposed in the reservoir area.

2. In the entire reservoir area, a total 70 potentially unstable slopes have been identified. For the stability analysis, these slopes have been further subdivided into 204 smaller segments.

3. A compute program `ROSS' (Rock Slope Stability) has been developed to analyse the stability of these slope segments. The results indicate that 17 slope segments are critical. Of these, 10 accounted for wedge and 7 accounted for plane modes of failure.

4. The plane failure analysis has been carried out for dry, wet as well as for dynamic conditions. The analysis has been carried out for both natural and water impoundment conditions. The results indicate that for the natural conditions (without reservoir impoundment) all the slopes having plane mode of failure are unstable for the adverse conditions (half filled tension crack and static condition) and the anticipated adverse conditions (half filled tension crack and earthquake loading). But, under reservoir impoundment conditions, all the slopes would be stable under adverse conditions, except KL15D and KR3A1. However, under anticipated adverse conditions, all the slopes are unstable, except KL1A and KL13A slope sections.

5. The slopes having wedge mode of failure have been analysed by using computer programs ROSS and RWEDGE. The results indicate that for the natural conditions (without reservoir impoundment) all the slope sections are stable in dry conditions even when they are subjected to earthquake loading, except slope KR2A, whose FOS is 0.76. Under anticipated adverse condition, represented by a combination of 50% water saturation and earthquake loading, all the slopes, except KL9B1 and KR9B, are unstable. However, after reservoir impoundment, the slopes KL9B1, KL19A, KR2A, KR20A, KR21A and KR21C would be unstable.

6. In the entire reservoir area four slope sections have been identified to have the circular mode of failure. All the slopes lie above the maximum reservoir level. The stability analysis of these slope sections has been carried out by computer program 'SARC'. The results show that the slope sections are stable in static and dry conditions, except KR5A3 section, which has a factor of safety 0.95. However, all the four sections are unstable under earthquake loading in dry and as well as in wet conditions.

7. An attempt has been made to calculate the possible height of the waves to be generated by the unstable slopes, if the failure occurs. The analysis has been carried out by using computer program WAVE. The results indicate that the maximum wave height varies from 0.4 m to as high as 20.3 m. However, the study shows, that most of the waves would die out before they reach the main dam. Only the wave to be generated by KR2A slope may reach the main dam with a height of 3.49 m. But the chances of overtopping the dam is remote as 8 m free board has already been provided.

6.4 CONCLUDING REMARKS

The Engineering Geological evaluation of the Kishau dam project has been carried out using geological mapping, surface and subsurface investigations as well as detailed stability analysis of abutments. The foundation of the Kishau dam, though has some minor engineering geological problems, can be rendered stable and competent to withstand the loads, to be imposed by the dam after adequate foundation treatments.

In view of the envisaged engineering geological problems with the proposed power house site, an alternate site has been identified. The suggested cut slope and the other slope treatment will make the site stable after construction.

The stability studies of reservoir slopes show that most of the slopes are stable, except for a few slopes, which have been identified as critical. Though the reservoir impoundment may stabilise some of the critical slopes, ten numbers of slopes still have the problems of stability. But in case of failure, they are not likely to affect the safety of the dam.

In view of the above it can be safely concluded that the Kishau dam project is technically sound with minimum engineering geological problems. The project if completed in time will

help to ease the power crises being faced by Uttar Pradesh State which in addition would help in solving the drinking problem of Delhi, the capital of India.

REFERENCES

Agarwal, C.K., Mehrotra, V.K. and Mitra, Subash 1991 Need of long term evaluation of rock parameters in the Himalayas Proc. 7th Int.Cong.Rock.Mech., Aachen, Germany.

Anbalagan, R. 1986 Geotechnical Study and Environmental Appraisal of a Water Resource Development Project in Kumaun Himalaya, U.P. Unpublished Ph.D. Thesis, Kumaun University, Nainital, pp.126

Anbalagan, R. 1990 Appraisal of Environmental Impact of the construction of Jamrani Dam in Nainital District, Kumaun Himalaya, Jour.Geol.Soc.Ind.,V.36,pp 307-316

Anbalagan, R., Singh, B. and Sharma, S. 1993 Some aspects of environmental impacts of dam reservoirs in Himalayan region, Proc.Int.Conf.Env.Manage., Geo-water and Engg. aspects, Ed. Chowdhury,. R.N. and Sivakumar, M., Australia, pp.735-739

Anbalagan, R., Sharma, S. and Raghuvanshi, T.1995 Engineering Geological Appraisal of Jamrani Dam across Gaula river in Kumaun Himalaya, India, Engineering Geology (In Press)

Auden, J.B. 1934 The Geology of Krol Belt, Rec. Geol.Surv.India, V.67, pp. 357-454

Azmi, R.J. and Joshi, M.N. 1983 Conodont and other Biostratigraphic evidences on the age and evolution of Krol Belt, Him.Geol., V.11, pp. 198-223

Barton, N. 1973 Review of a new shear strength criteria for rock joints, Engg. Geol., V.7, pp. 287-330

Barton, N. and Choubey, V. 1977 The shear strength of rock joints in theory and practice, Rock Mech., V.10, pp.1-54

Bhargava, O.N. 1972 A reinterpretation of the Krol Belt Him.Geol., V.2, pp.47-82

Bhargava, O.N.1976 Geology of the Krol Belt and associated formations : A reappraisal, Geol. Surv.Ind. Misc. Publ., No.34, pp.168-229

Bieniawski, Z.T. 1976 Rock mass classification in rock engineering, Proc. Symp. Exploration for rock engineering (Ed. Z.T. Bieniawski), V.1., pp.97-106

Bieniawski, Z.T. 1978 Determining rock mass deformability experiences from case histories, Int. J. Rock Mech Min. Sci., & Geomech. Abstr., V.15, pp.237-247

Bieniawski, Z.T. 1979 The geomechanics classifiacation in rock engineering applications, Proc. 4th Int.Cong.Rock.Mech.,Montreux., V.2, pp.41-48

Bieniawski, Z.T. 1979 Tunnel design by rock mass classification, Technical report GL-79-19, U.S. deptt. of commerce pp 1-67.

Bieniawski, Z.T. 1989 Engineering rock mass classifications, John Willey & Sons, New York, pp.251

Creager, W. P., Justin, and Hinds, J. 1968 Engineering for dams, V.II, Concrete dams, Wiley Eastern Pvt. Ltd., new Delhi, pp. 247-260.

Dube, M. D. 1987 Hydroelectric project in Himalaya - Their necessity and environmental aspects, Proc. 2nd National Convention of Environmental Engineers and National Seminar on Impact of Environmental Protection on Future Development of India, pp.69-70.

Dubey, M. D., Rajvanshi,.U. S. and Sharma, C. P. 1989 Geotechnical problems in Himalaya with special refernce to Ganga and Yamuna valley projects, Proc. Nat. Symp.- App. of Rock Mech. in River Valley Projects, Roorkee, pp. I-6 to I-12.

Dutta, K.K. and Kumar, G. 1964 Geology of the Dehradun-Mussorie-Chakrata area, guide to excursion No.s Au and C3, 22nd Int. Geol. Cong., New Delhi (Unpublished)

Ewert, F.K. 1985 Rock Grouting with emphasis on dam sites, Springler Verlag, Berlin, pp.141-369

Ganesan, T.M. and Verma, R.N. 1974 Geology of a part of Simla District, H.P. and Dehra Dun district, U.P., with special reference to copper mineralisation, Indian Minerals, V.28, pp.47-60

Ganesan, T.M. and Thussu, J.L. 1978 Geology of a part of Tons valley, Garhwal Himalaya with special reference to old fold trends, Jour. Geol.Soc.India, V.19,pp.285-291

Ganesan, T.M. and Verma, R.N. 1981 The Deoban structural belt of the Garhwal Himalaya, Jour.Geol.Soc.India, V.22, pp.201-215

Gansser, A. 1964 Geology of the Himalaya, Inter Science, New York, pp.299

Golze, A.R. 1977 Hand book of Dam engineering, Van Nostrand Reinhold Company, New York, pp.793

Hanna, F. W. and Kennedy, R. C. 1938 The design of dams, Mcgraw-Hill Book Company, London, pp. 37-44.

Hoek, E., Bray,J.W. and Boyd, J.M. 1973 The stability of a rock slope containing a wedge resting on two intersecting Discontinuities, Quarterly J.Engg. Geol., V.6, No.1

Hoek, E. 1976 Rock slopes, Rock Engineering for foundation and slopes, V.1, pp.157-171

Hoek, E. and Bray, J.W. 1981 Rock slope engineering (3rd edition), Institution of Mining and Metallurgy, London, pp. 358.

Houlsby, A.C. 1976 Routine interpretation of the Lugeon water pressure test, Quart. J.Engg. Geol., V.9, pp.303-313

Jain, A.K. 1987 Kinematics of the transverse lineaments, regional tectonics and Holocene stress fields in the Garhwal Himalaya, Jour.Geol.Soc.India, V.30, pp.169-186

Kumar, G., Sinha, Roy. S and Ray, K. K. 1989 Structure and tectonics of the Himalaya, Geology and Tectonics of the Himalaya, special publication 26, Geol. Surv. India, pp 1-50.

Lavania, B.V.K., Basu, S., Srivastava, L.S. and Singh, A.K. 1987 A simplified approach for evaluation of earthquake induced displacements, Proc.All India Seminar on Earth and Rock Fill dams Theme D, pp.D21

Mistry, J. F. 1983 Recent trends in foundation evaluation and treatment of dam foundation in Gujarat, Jour. Engg. Geol., India, V.12, pp.9-27.

Oldham, R.D. 1883 Note on the geology of Jaunsar and the Lower Himalaya Rec. Geol. Surv. India, V.16, pp.193-198

Palmstörm, A. 1982 The volumetric joint count - a useful and simple mesure of the degree of jointing . IV Int. Cong., IAEG, New Delhi, India, pp. V 221-V 228.

Profile of the power industry, March, 1993, Chartered Financial analyst, pp.54-55.

Serafim. J. L. and Pereira, J. P. 1983 Considerations of the Geomechanical classifiacation of Bieniawski, Proc. Int. Symp. Engg.Geol. Underground construction, Boston, pp.33-43

Shankar, K. 28th June, 1993 Darkness shrouds power sector scenario, The Hindustan Times, pp. 4

Shankar, R., Kumar, G., and Saxena. S. P. 1989 Stratigraphy and sedimentation in Himalaya: A reappraisal, Geology and Tectonics of the Himalaya, special publication 26, Geol. Surv. India, pp 1-50.

Sharma, H. D. 1981 Concrete Dams, Metropolitan Book Co. New Delhi, pp.537

Sharma, S., Raghuvanshi, T. K. and Anbalgan, R. 1995 Plane failure analysis rock slopes Geotech. Geolog. Engg., V.13 pp. 105-111

Sharma, S. 1995 Geotechnical investigations of Lakhwar dam, Garhwal Himalaya, Uttar Pradesh, India, Unpublished Ph.D. Thesis, University of Roorkee, Roorkee, India.

Sharma, V.M. 1992 Special lecture on geotechnical problems of water reservoirs development in the Himalayan region, Ind. Geotech. Soc. Delhi Chapter, pp. 1-38

Shome, S. K., Rawat, U. S. and Kaistha, G. K. 1987 Geotechnical evaluation of sites for a high rockfill dam on the river Tons, District Dehradun, Uttar Pradesh, Proc. Sem. on Earth and Rockfill Dams, Lucknow, pp.A 93 to A 101.

Singh, B. 1995 Development of water resources in Ganga Brahmaputra basin, Jour. Ind. Water Res. Soc., V.1, pp.1.

Slingerland, R. L. and Voight, B. 1979 Occurence, properties and predictive models and landslide generated waves, Rock slide avalavches, Dev. Geotech. Engg. Series, V. 14B.

Srikantia,S.V. and Sharma,R.P. 1971 Simla Group - a reclassifiacation of the 'Chail Series', 'Jaunsar Series' and 'Simla Slates' in the Simla Himalaya, Jour.Geol.Soc.India,V.12 pp.234-240

Srikantia,S.V. and Bhargava,O.N. 1974 The Jaunsar problem in the Himalaya - a critical analysis and evaluation, Jour.Geol. Soc.India, V.12 pp.115-136

Valdiya, K. S. 1987 Environmental Geology: Indian Context, Tata Mcgraw-Hill Pub. Co. New Delhi.

Water resources hydro power development in India, 1991 Central Water Commission, Govt. of India, pp. 1-53.

ANNEXURE I

SUMMARISED LOGS OF DRILL HOLES

LOG OF DRILL HOLE NO. DH - 1

Location : Left Abutment (Dam axis) Elevation : 656.8 m	Angle : 60° Bearing : S34°W
Depth (m)	Description
0 - 9.85	Quartzitic slates, occasionally phyllitised. B.P. 30° to 35°. Percentage core recovery 33.3 to 100
9.85 -12.57	Purple quartzites. B.P. 50° to 60°. Percentage core recovery 40 to 100
12.57 - 19.50	Quartzitic slates. B.P. 50° to 60°. Percentage core recovery 21.2 to 100
19.50 - 22.33	Purple quartzite. Percentage recovery 41.54 to 95
22.33 - 48.15	Grey coloured quartzitic slates grading into quartzite. B.P. 40° to 60°. Percentage core recovery nil to 97.57
48.15 - 58.82	Purple quartzitic slates.B.P. 40° to 65°.Percentage core recovery 14 to 100
58.82 - 83.36	Grey quartzitic slates. B.P. 20° to 25°.Percentage core recovery nil to 83.3
83.36 - 90.55	Purple quartzite. B.P. 55°.Percentage core recovery vary from 24.1 to 73.9
90.55 - 98.07	Grey Quartzitic slates grading into quartzite. B.P. 50° to 55°. Percentage core recovery 34.21 to 68.66

LOG OF DRILL HOLE NO. DH - 2

Location : Right Abutment (Dam axis) Angle : 60°
Elevation : 657.3 m Bearing : N 34° E

Depth (m)	Description
0 - 2.89	Purple quartzite. B.P. 50°. Percentage core recovery 17.5 to 50
2.89 - 3.35	Dark grey quartzite. Percentage core recovery 33.3 to 37.5
3.35 -10.20	Purple quartzite. Percentage core recovery nil to 95
10.20 - 12.80	Grey quartzitic slates. B.P. 50°. Percentage core recovery 72.2 to 95.3
12.80 - 18.28	Purple quartzite. Percentage core recovery nil to 91.6
18.28 - 33.83	Grey slaty quartzite. B.P. 40°. Percentage core recovery nil to 97.5
33.83 - 43.43	Purple quartzite. B.P. 40° to 50°. Percentage core recovery nil to 100
43.43 - 65.53	Grey slaty quartzites, quartzitic slates. B.P. 55° to 65°. Percentage core recovery nil to 75
65.53 - 73.45	Purple quartzite. Percentage core recovery nil to 55.6
73.45 - 74.97	Grey quartzitic slates. Percentage core recovery 26.1
74.97 -76.49	Purple quartzite. Percentage core recovery 55.0
76.49 - 96.01	Grey slaty quartzite/quartzitic slate. B.P. 40° to 50°. Percentage core recovery nil to 100

LOG OF DRILL HOLE NO. DH - 3

Location : Left Abutment (100 m d/s of dam axis) Angle : 60°
Elevation : 650.5 m Bearing : S34° W

Depth (m)	Description
0 - 39.1	Grey quartzitic slates with specks of pyrite. B.P. 40° to 52°. Percentage core recovery nil to 83.3
39.11 - 51.51	Purple quartzite. B.P. 35° to 45°. Percentage core recovery 17.0 to 44.6
51.51 - 66.52	Grey quartzitic slates.B.P. 55° to 60°.Percentage core recovery 31 to 100
66.52 - 68.88	Purple quartzite. Percentage core recovery 47.65 to 63.3
68.88 - 91.57	Grey quartzitic slates. Percentage core recovery 11.5 to 53.85

LOG OF DRILL HOLE NO. DH - 4

Location : River Bed Elevation : 647.1 m	Angle : 90°
Depth (m)	Description
0 - 11.88	Comprising of boulders of limestone, pink white quartzite and slate
11.88 - 18.28	Grey quartzitic slates.B.P. 50°to 65°.Percentage core recovery 10 to 58.3
18.28 - 23.16	Purple quartzite. B.P. 50° to 70°. Percentage core recovery 25 to 75
23.16 - 25.60	Grey quartzitic slates. B.P. 60°. Percentage core recovery 57.1 to 72.2
25.60 - 32.16	Purple quartzite. B.P. 50°. Percentage core recovery nil to 75
32.16 - 34.13	Grey quartzitic slate.. B.P. 70°. Percentage core recovery 21.9
34.13 - 35.95	Purple quartzite traversed by quartz vein. B.P. 70°. Percentage core recovery 33.3 to 77.8
35.95 - 91.74	Grey quartzitic slate grading into quartzite phyllitised along bedding plane. Traversed by quartz vein. B.P. 40° to 60°. Percentage core recovery 3.3 to 91.7

LOG OF DRILL HOLE NO. DH - 5

Location : Right Abutment (100 m u/s of dam axis) Elevation : 647.9 m	Angle : 60° Bearing : N 51°E
Depth (m)	Description
0 - 2.65	Overburden comprising of quartzitic slate and white quartzite
3.65 - 14.63	Grey quartzitic slate. B.P. 40° to 65°.Percentage core recovery 7.1 to 66

ANNEXURE II

A BRIEF OUTLINE OF COMPUTER PROGRAMS

The Computer Programs, namely RWEDGE, BASC, SARC & WAVE, are prepared by Prof. Bhawani Singh, Department of Civil Engineering, University of Roorkee, Roorkee. The author of this research work is highly grateful to him, for allowing to use these programs. However, the Computer Program ROSS (Rock Slope Stability) has been developed by the author along with his colleagues, Mr. S. Sharma and Mr. S. Maheshwari, under the guidance of Dr. R. Anbalagan.

Many Geologists, Civil Engineers and Mining Engineers have used the programs of Prof. Bhawani Singh over the last 15 years for stability studies of assessment of dam abutment and dam reservoir slopes, wave height in reservoir due to possible slides, design of rail and road side cut slopes, site development for building complexes, landslide control and planning of eco-development in seismic hilly areas.

USE OF COMPUTER PROGRAMS (RWEDGE, BASC, SARC & WAVE)

The programs (X) are written in Fortran 77 and EXE files work in DOS environment. The user's manual is also included as IX. NEW for preparation of input data files. Further, typical input data files are also given as IX.DAT beginning with I. The corresponding output files OX.DAT are added, beginning with O.

The typical computer commands are

```
 NE IX.DAT  - To open Input File
NE OX.DAT - To open output File
         X  - Name of Computer Program
    IX.DAT  - Input File Name
   OX.DAT  - Output File Name
            2  -  For Execution
            1  -  For Help menu
NE OX.DAT - For seeing output file OX.DAT
```

The capability of each program, used in this research work, is described below:

RWEDGE

This program is used for the computation of factor of safety of tetrahedral wedge formed by the intersection of two discontinuities, the slope face and the upper surface. The program automatically chooses a pair of discontinuities from the given set of data and it checks whether such planes do forms surface along which the rock wedge could slide. The influence of tension crack is included in the program. The program also allows for different strength parameters on the two planes of weakness and different water conditions on the slope face i.e. no crack and dry condition, wet slope with no crack, presence of crack with water and presence of crack with no water.

The special feature of this program is to compute the factor of safety under earthquake loading. Moreover, the program also calculates the dynamic displacement of slope by utilising the correlation developed by Lavania et al. (1987).

BASC

Computer program BASC facilitates the back analysis of slopes to determine the strength parameters cohesion (C) and angle of internal friction (ϕ) of a rock/soil slope with probable circular mode of failure. As already discussed in Chapter V, only one of the two shear strength parameter can be determined by the back analysis. Hence, for judicially chosen values of angle of internal friction, the values of cohesion is calculated by the program BASC.

This program analyses any general surface profile and considers the effect of pore water pressure, tension crack at the top of the slope and earthquake loading to determine the shear strength parameters.

SARC

This program facilitates to compute the factor of safety with circular failure surface emerging at the toe. It analyses any general profile of the slope surface and for various forces i.e. pore water pressure, depth of tension crack at the top of the slope, depth of water in tension crack and earthquake force. In the first step, it draws the various slip surfaces along which failure can take place. Then it calculates the radius and centre of each slip surface.

In the next step, the factor of safety is computed using Bishop's equation for various slip surfaces until a minimum factor of safety is obtained. The analysis evaluates critical acceleration for slopes with factor of safety less than unity and compute dynamic displacement utilising correlation developed by Lavania et al. (1987).

WAVE

This program is used for the calculation of wave height, generated due to a possible slide in the reservoir area. Besides, it also facilitates to calculate the velocity and the kinetic energy involved in a possible slide. The distance to which the wave will propagate is also calculated. This program utilises the relation given by Slingerland and Voight (1979).

The input data required for WAVE program is listed below:

AV = Coefficient of vertical earthquake acceleration
AH = Coefficient of horizontal earthquake acceleration
AI = Dip of plane or intersection of joint planes
= Average dip of circular wedge
FS = Static residual factor of safety of the slope during landslide (c= 0.0 & $\phi_R = \phi/2$)
G = Acceleration due to gravity
GAMAW = Unit weight of water
H = Height of slope
PHI = Angle of sliding friction
RWL = Mean depth of reservoir
RD = Distance of landslide from dam
S = Distance of movement of landslide

The limitation of WAVE program is that it is applicable to those slopes only which are submerged partially or completely in the reservoir.

ROSS

The Computer Program ROSS has been developed for carrying out the stability analysis of slopes having wedge or planar mode of failure. This program has been written in Basic language. The user's friendly program ROSS facilitates the following analysis:

1. Identification of all possible wedge and plane failure.
2. Identification of critical wedge and plane failure.
3. Calculation of Plunge and direction of line of intersection of wedge forming planes.
4. Calculation of factor of safety (FOS) for wedge and plane failure.

WEDGE FAILURE ANALYSIS

The program ROSS facilitates the stability analysis of tetrahedral wedge formed in a rock mass by interlocking discontinuities. A pair of discontinuities are selected from the given set of data and it checks whether such planes do form such surface along which the rock wedge could slide, if separates from the rock mass. It works out the geometry of such wedges taking into account the dip amount and direction of slope face and calculates the plunge of the line of intersection of bounding planes along which sliding could occur. For all wedges, thus formed, Markland test is applied. Wedges which satisfies Markland test are considered as critical and are further analysed to calculate the factor of safety. The formulation to calculate

the factor of safety is taken from the analytical solution of Hoek & Bray (1977).

PLANE FAILURE ANALYSIS

The program also identifies the possible plane mode of failure. If the Markland test is satisfied, the program automatically indicate such case as a critical one. To identify the critical plane mode of failure, the required input data is:

1. Dip amount and dip direction of all the discontinuities.
2. Angle of internal friction.
3. Slope inclination.

The program can analyses three cases

1. Slope without tension crack
2. Slope having tension crack on the upper slope surface.
3. Slope having tension crack on the slope face.

The formulation to calculate the factor of safety of plane failure is taken from the analytical solution of Hoek & Bray (1977).